

***Diastereoselective Alkylation of Bi- and
Tricyclic Lactimethers as a Pathway to
Biologically Relevant Diketopiperazines***

Von der Fakultät Chemie der Universität Stuttgart zur Erlangung der
Würde eines Doktors der Naturwissenschaften (Dr. rer. nat.) genehmigte
Abhandlung

vorgelegt von

Daniela Hendea

aus Zalău (Rumänien)

Hauptberichter:

Prof. Dr. Sabine Laschat

Mitberichter:

Prof. Dr. Stephen Hashmi

Tag der mündlichen Prüfung:

12. Juni 2007

Institut für Organische Chemie Universität Stuttgart

2007

Eidesstattliche Erklärung zur eingereichten Dissertation

Hiermit erkläre ich, dass ich die vorliegende Dissertation "*Diastereoselective Alkylation of Bi- and Tricyclic Lactimethers as a Pathway to Biologically Relevant Diketopiperazines*" selbständig und ohne fremde Hilfe bzw. unerlaubte Hilfsmittel angefertigt, andere als die angegebenen Quellen und Hilfsmittel nicht benutzt und die den benutzten Quellen wortlich oder inhaltlich entnommenen Stellen als solche kenntlich gemacht habe.

“The universe is full of magical things patiently waiting for our wits to grow sharper.”

~Eden Phillpotts, *A Shadow Passes*

“Love hides in molecular structures”

~The Doors – *Love hides*

To my grandmother Ana,
the most amazing woman I know

Danksagung

Mein besonderer Dank gilt Frau Professor Dr. Sabine Laschat für die Überlassung des interessanten und vielseitigen Themengebietes, für die Betreuung und für die hervorragenden Arbeitsbedingungen. Ich bedanke mich ganz herzlich für die zahlreichen Möglichkeiten an Konferenzen und Lehrgängen teilzunehmen und ihr Vertrauen in meine selbstständigen Arbeitsweise,

Herrn Professor Dr. Stephen K. Hashmi bedanke ich mich für seine Tätigkeit als Mitberichter und Herrn Professor Dr. Emil Roduner danke ich für seine Bereitschaft, die Doktorprüfung abzunehmen.

Frau Angelika Baro gilt mein herzlicher Dank für ihr Falkenauge beim intensive Korrekturlesen, für die moralische Unterstützung und für viele Ratschläge im Kampf gegen Word®. Danke für die investierte Zeit und dass Sie offen ihre Meinung gesagt haben.

Nelli Steinke, ich danke dir für deine Bereitschaft unendliche NMR Spektren zu interpretieren und für die unglaublichen Augen bei der identifizierung der NMR-Signale zu (dddddddddddddd...). Ich hatte die Chance "aus erster Hand" mit ein NMR-Expertin zu arbeiten.

Für das Erledigen der NMR-, Massen- und Elementar-Analysen möchte ich allen Mitarbeitern des Institutes für Organische Chemie herzlich Dank sagen. Den Mitarbeitern der Analyseabteilung J. Rebell N. Böres, A. Pikulski (auch für die Unterhaltungsmöglichkeit in meiner Muttersprache!), J. Trinkner, F. Bender, C. Lauxmann, L. Müller, D. Göhringer danke ich für sorgfältige Messungen.

Ein ganz besonderer Dank geht an Herrn Dr. Wolfgang Frey für die Einkristallstrukturuntersuchungen, immer wenn er meine Tage gerettet hat als er eine Röntgenstruktur vorbeibrachte.

Für die entgegenkommende Hilfe bei Anträgen und Bestellungen bin ich den Mitarbeitern U. Henn, A. Schwarzkopf, P. Schüle, H.-J. Bräuner, R. A. Linderer und R. Anagnostou sehr dankbar.

Allen Mitgliedern des AK Laschat möchte ich für die ausgelassene, freundliche, tolle Arbeitsatmosphäre Danke sagen.

In chronologischer Reihenfolge, ich danke Nicolai Cramer für die Ermutigung am Anfang meiner Doktorarbeit (WHAT the heck are you doing there?!) und für die super und stinkende (Skatol war doch seine Idee!) Synthese-Ratschläge. Ich danke Armand Becheanu und Roxana Judele, meine Landsleute, für die Hilfe in meinen erste Monate in Deutschland. Ich danke Nelli Steinke, dass sie mit mir nur Deutsch sprechen wollte. Ich danke Christof Gastl für seine Bereitschaft zahlreiche GC-MS zu messen und zu interpretieren und für sein Interesse an meiner Arbeit ("Wie geht's dein' Chemie?"). Mein ganz besonderer Dank gilt Eli Kapatsina, die beste Laborkollegin und Vorbild in wissenschaftlicher Arbeit. Steffen Pachali und Sven Sauer danke ich für das lockere und äußerst angenehme Arbeitsklima und die Erinnerung an meine Arbeitskreisaufgaben (Daniela, die PE Destille!!!!)

Ich danke Alina Schreivogel, Lena Affolter, Yana Galeyeva für das Korrekturlesen und Deutschübersetzungen.

Ferner gilt mein Dank André Hätzelt für die Vorarbeiten, die zu dieser Dissertation führten.

Meinen besonderen Dank bekunde ich Regina Schweizer und Julia Zug für ihre engagierte Arbeit während der Forschungspraktika.

Meiner Familie danke ich herzlich für die Unterstützung während all der Jahren, die ich fern von ihr war.

Meiner zweiten Familie, meinen Freunden von IBC Stuttgart, bin ich dankbar für ihre ehrliche Freundschaft und die Ermutigung immer mein Bestes zu geben.

Und ich danke dem EINEN, der die Welt der Chemie geschaffen hat - voller Geheimnisse, die nur darauf warten von Wissenschaftlern entdeckt zu werden.

Lebenslauf

Name	Daniela Monica Hendea
Geburtsdatum	08.10.1975 in Zalau, Rumänien
Abitur	1994 / Zalau, Rumänien
Studium	<p>1994 – 1999 Chemie Ingenieur Diplom / Technische Universität Gh. Asachi Iasi, Rumänien</p> <p>Diplomarbeit in der Abteilung Organische Technische Chemie der Technischen Universität "Gh. Asachi" Iasi, Rumänien, unter Leitung von Prof. Dr. Corneliu Oniscu mit dem Thema: <i>"Die Synthese von Anesthezin"</i></p> <p>1999 – 2000 Masters in Biotechnologie / Technische Universität Gh. Asachi Iasi, Rumänien</p> <p>Mastersarbeit in der Abteilung Biotechnologie der Technischen Universität "Gh. Asachi" Iasi, Rumänien, unter Leitung von Prof. Dr. Dan Cascaval mit dem Thema: <i>"Trennungsmethoden für Produkte der Biosynthese"</i></p> <p>2000 – 2002 Wissenschaftliche Hilfskraft in der Abteilung Organische Technische Chemie der Technischen Universität "Gh. Asachi" Iasi, Rumänien</p>
Promotion	<p>09 / 2002 – 06 / 2007 am Institut für Organische Chemie der Universität Stuttgart unter Leitung von Prof. Dr. Sabine Laschat mit dem Thema: <i>"Diastereoselective Alkylation of Bi- and Tricyclic Lactimethers as a Pathway to Biologically Relevant Diketopiperazines"</i></p>

Partial results from this Ph.D. Thesis presented in:

Journals: D. Hendea, S. Laschat, A. Baro, W. Frey "*Diastereoselective Alkylation of a Proline-Derived Bicyclic Lactim Ether*", *Helv. Chim. Acta* **2006**, 89, 1894–1909.

Conferences:

Posters on Asymmetric Alkylation of Lactimethers:

German Chemical Society Annual Conference (GDCh) 2003,
München

German Chemical Society Annual Conference (GDCh) 2005,
Düsseldorf

ORCHEM 2004, Bad Nauheim

ImSat 2005 (Iminiumsalt Conference), Bartholomä

Table of Contents

List of abbreviations	xi
1. Introduction	1
2. Motivation and Approach	11
3. General part	12
3.1 The diketopiperazines in nature.....	12
3.1.1 Bicyclic diketopiperazines.....	12
3.1.2 Tricyclic diketopiperazines.....	17
4. Retrosynthetic analysis and strategy	22
4.1 Tryprostatins: structure analysis and previous syntheses in the literature.....	22
4.2 Retrosynthetic strategy for tryprostatin B 20b via stereoselective alkylation...	33
4.2.1 The synthesis of the 2,4-diketopiperazine fragment 73	36
4.2.2 The synthesis of the indole fragment 66	39
4.3 Alkylation studies on bicyclic lactim ether 63	40
4.3.1 Diastereoselective alkylation of lactim ether 63 with various electrophiles.....	40
4.3.2 Configuration determination by synthesis of diketopiperazines 48a,d,e,h from the corresponding amino acids.....	45
4.4 Synthesis of tryprostatin B 20b	50
4.4.1 Alkylation of lactim ether 63 with indole derivative 66	50
4.4.2 Alkylation of indole lactim ether <i>cis</i> - 79 with isoprenyl derivative 46	52
4.5 Quinocarcin ring system: structure analysis and previous synthesis in the literature.....	54
4.6 Retrosynthetic strategy for the quinocarcin precursor via stereoselective alkylation.....	65
4.6.1 Synthesis of the tricyclic lactim ether fragment 129	66
4.6.2 Synthesis of (<i>E</i>)-4-bromo-2-butenyltrimethylsilane fragment 128	68

4.7	Alkylation studies of bicyclic lactim ether 129	69
4.7.1	Diastereoselective alkylation of tricyclic lactim ether 129 with various electrophiles.....	69
5.	Experimental section	73
6.	X-Ray data analysis	148
7.	Summary	193
8.	Zusammenfassung	201
9.	References	209

List of abbreviations

abs.	absolute
AcOEt	ethyl acetate
AcOH	acetic acid
AIBN	azoisobutyronitril
4-AMP	4-(aminomethyl)-piperidine
ATR	attenuated total reflectance
Boc	tert-butyloxycarbonyl
BOPCl	bis(2-oxo-3-oxazolidinyl)phosphinic chloride
Bn	benzyl
<i>i</i> Bu	<i>iso</i> -butyl
<i>n</i> Bu	<i>n</i> -butyl
<i>n</i> BuLi	<i>n</i> Butyllithium
<i>t</i> -BuOK	potassium <i>tert</i> -butanolate
Cbz	benzyloxycarbonyl
Conv.	conversion
COSY	correlation spectroscopy
m-CPBA	m-chloroperbezoic acid
DBU	1,8-diazabicyclo[5.4.0]undec-5-ene
DCC	N,N'-dicyclohexylcarbodiimide
DEPC	diethylcyanophosphonate
DEPT	distortionless enhancement by polarization transfer
DMAP	dimethylaminopyridine
DMAPP	dimethylallyl pyrophosphate
DME	dimethoxyethan
DMF	dimethylformamid
DMSO	dimethylsulfoxid
DNA	deoxyribonucleic acid
EDC	1-(3-dimethylaminopropyl)-3-ethylcarbodiimide hydrochloride
ET-743	ecteinascidin 743
Fmoc	fluorenylmethyloxycarbonyl
FT-IR	Fourier transform infrared spectroscopy
GC	gas chromatography

GC-MS	gas chromatography coupled with mass spectrometry
GlyOEt	glycine methyl ester
HOBT	1-hydroxybenzotriazol
HMPA	hexamethylphosphoramide
HPLC	high pressure liquid chromatography
HRMS	high resolution mass spectra
IC ₅₀	50% inhibition concentration
KHMDS	potassium bis(trimethylsilyl)amide
LAH	lithium aluminum hydride
LDA	lithiumdiisopropylamide
LHMDS	lithium bis(trimethylsilyl)amide
Me	methyl
MeCN	acetonitrile
MeOH	methanole
MOM	methyloxymethyl
MS	mass Spectrometry
NaHMDS	sodium bis(trimethylsilyl)amide
NBS	N-bromosuccinimide
NCI	National Cancer Institute
NEt ₃	triethyl amine
NMR	nuclear magnetic resonance
NOE	Nuclear Overhauser effect
NOESY	Nuclear Overhauser effect spectroscopy
NPSP	<i>N</i> -phenylselenophthalimide
ORTEP	Oak Ridge Thermal Ellipsoid Plot
PCC	pyridinium chlorochromate
PE	petrolether
Ph	phenyl
Phth	phthalimido
PPTS	pyridinium <i>p</i> -toluenesulfonate
<i>i</i> Pr	<i>iso</i> -propyl
<i>i</i> Pr ₂ NH	diisopropylamine
L-Pro	L-proline
quant.	quantitative

RNA	ribonucleic acid
rt	room temperature (21°C)
sat.	saturated
TBAB	tetrabutylammoniumbromid
TBAF	tetrabutylammoniumfluoride
TESCI	triethylchlorosilane
<i>tert</i>	tertiary
Tf	trifluoromethanesulfonyl
TFA	trifluoro acetic acid
TFE	2,2,2-trifluoroethanol
THF	tetrahydrofuran
TLC	thin layer chromatography
TMS	tetramethylsilane
TMSCN	trimethylsilylacetonitrile
TMSI	trimethylsilyliodid
Troc	trichloroethoxycarbonyl
L-Trp	L-tryptophan
Ts	p-toluene sulfonyl
TsOH	p-toluenesulfonic acid

1 Introduction

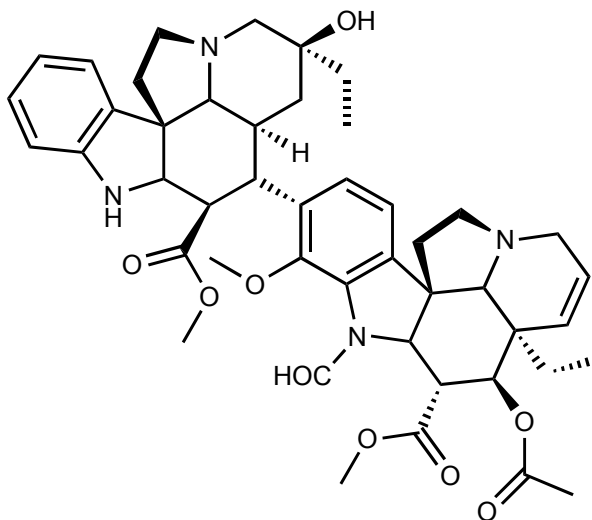
The legend says that a long time ago, in the part of the world that is now known as Peru, a raging storm felled a giant tree that came to rest in a pool of stagnant water. Eventually, a native passed that way. He was extremely ill, burning with fever, having what we call today malaria. His fever had caused intense thirst and he drank from the pond. Shortly after, a miracle occurred and his fever vanished.

From the dawn of history, people turned to nature in the attempt to cure diseases. Primitive people discovered that cinchona bark cured intermittent fever, the coca leaves numbed the tongue and reduced the appetite, the latex from the capsule of the opium poppy allayed pain. Extensive lists of these natural products have survived from antiquity and they are of considerable interest, because of the many well-known products they contain. The Chinese Pen Ts'ao, written in 2800 B.C. lists 366 plant drugs, among them the familiar Ephedra. The Egyptian Papyrus Ebers, dating from 1550 B.C., mentions opium and aloes, among others. The economy of these ancient cultures depended on the commerce with natural products, being considered ones of the most expensive products at that time. The Greek and Romans traded them widely and the European colonial expansion was influenced by the discovery of rich territories in natural products.

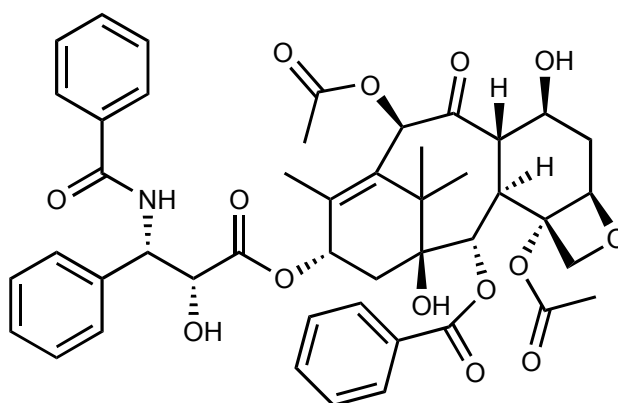
For more than fourteen centuries, the natural products extracted from plants reigned supremely in medicine, but then a Swiss pharmacist, known as Paracelsus (around year 1500) introduced a new dimension to drug therapy. He advocated the use of chemical therapy and he challenged the alchemists to prepare medicines, not gold. Although the field was slow to develop, medicinal chemistry was born with Paracelsus.

Conventional therapy with the plant drugs continued almost unchanged for three more centuries. Then, around year 1800, a small-town pharmacist in Germany attempted and succeeded the isolation of the active principle of opium, which he called morphine after Morpheus, the Greek god of dreams. He found the chemical alkaline in character, the first of a compound class later called alkaloids. The search for alkaloids continued well into the twentieth century. The most famous compounds

extracted from plants in the treatment of tumors are vinca alkaloids (Vincristine, **1**), from the *Catharanthus roseus* (Madagascar periwinkle)^{[1],[2]} and taxane (Taxol®, **2**), isolated the compound from the bark of the Pacific yew tree *Taxus brevifolia*.^{[3],[4]}



1 Vincristine



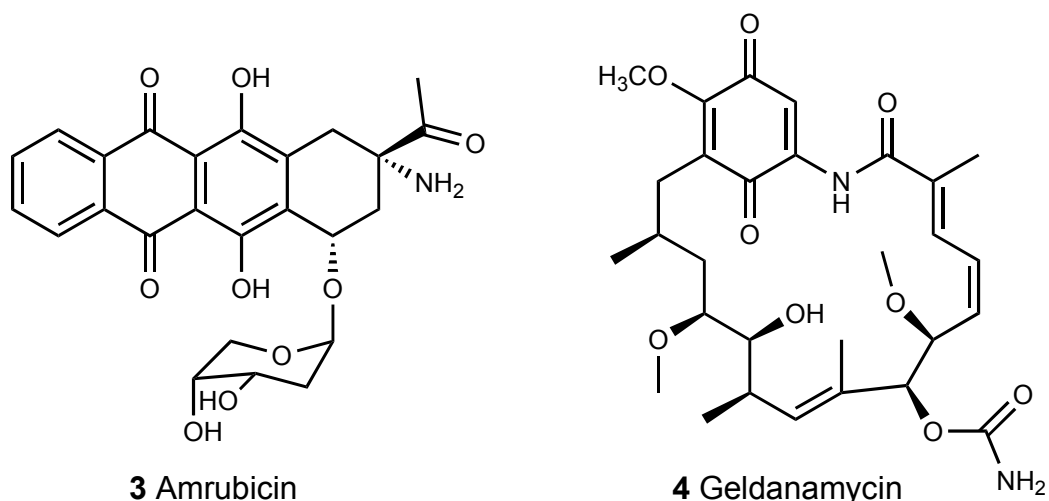
2 Paclitaxel (Taxol)

Scheme 1

It was not until 1870s, however, that Tyndall, Pasteur and Roberts separately observed the antagonistic effects of one microbe upon another. Pasteur, with his characteristic foresight, suggested the therapeutic potential of the phenomenon. For the next half-century, various microbial preparations were tested as medicines, but they were either too toxic or inactive. Finally, in 1929, Fleming published his historic observation that a contaminating mold, identified as *Penicillium notatum* killed his bacterial culture of *Staphylococcus aureus*. He named the active substance penicillin.

The importance of Fleming's discovery was that it led to the first successful chemotherapeutic agent produced by a microbe, thus initiating the golden age of antibiotics. Soil microbiologists succeeded in isolating many new antibiotics from soil-inhabiting bacteria, i.e. actinomycetes, of which the best known is streptomycin, the first active antibiotic against tuberculosis. One such member of this group, actinomycin D was used to combat a certain kidney tumor in children.^[5]

By 2002, over 22,000 bioactive compounds have been discovered from microbes. Of the actinomycete antibiotics about 80% are made by members of the genus *Streptomyces*. Two of the compounds with anti tumor activity, isolated from *Streptomyces* and involved in clinical trials are amrubicin **3**, isolated from *Streptomyces peucetius*, and geldanamycin **4**, isolated from *Streptomyces hygroscopicus*.^[6]



Scheme 2

Soil has the largest population of microbes of any habitat, but only about 0.3% of soil microbes are cultivable with current techniques. Cultured soil microbes have been an incredibly productive source of drugs for cancer chemotherapeutics. Unfortunately, the current yield of new drugs of soil microbes is low due to repeated cultivation of the same small fraction of cultivable microbes.^[7]

This problem is being studied and some success has been achieved by using one or more of the following strategies:

1. very low nutrient concentration,
2. signaling molecules,
3. inhibitors of undesired microbes,
4. long periods of incubation,
5. growth conditions resembling the natural environment,
6. protection of cells from exogenous peroxides,
7. addition of humic acid,
8. hypoxic or anoxic atmospheres,
9. encapsulation of cells in gel microdroplets and detection of microcolonies by flow cytometry,
10. high CO₂ concentration along with high throughput polymerase chain reaction technology.

Chemists on a worldwide basis have paid attention toward the potential of marine microorganisms as an alternative source for isolation of novel metabolites with interesting biological and pharmaceutical properties. The world oceans do indeed represent a microbial broad and microbiologically diverse resource of huge dimension but about which we know relatively little. As it is estimated that less than 5% of marine bacterial and fungal species are known, it is clear that the microbial diversity of oceans is still poorly understood. In the area of natural products chemistry, only a few early reviews have covered the small number of metabolites derived from marine fungi.^[8]

Marine microorganisms continue to be the subject of vigorous chemical investigation, although the studies of marine bacteria might be decreasing in comparison with those of other microorganisms. Studies of marine fungi appear to be expanding at a much faster rate than those of other unicellular organisms.^[9]

A statistic analysis of the National Cancer Institute shows that marine flora prove to be a very effective source for cytotoxic compounds. Their percentage is with 2%

significantly higher than terrestrial plants (approximately 0.3%), although they have been explored three times more.^[10]

With several marine-derived now in clinical trials and others on the way, ocean products may be outstripping land-based plants and microorganisms as promising sources of potential anti tumor drugs.^[11]

The explanation for the fact that the marine habitat is the place for interesting bioactive materials is very simple: the conditions that dominate the aquatic environment differentiate themselves seriously from the terrestrial counterpart. The influence of the seawater conditions - density, viscosity and high specific heat, pressure, salt content (specific pressure), lighting conditions (high irradiation at the surface, obscurity in the depth – create different properties in the marine organisms. The oceans cover more than two thirds of the earth's surface, include 90% of the biosphere and therefore represent the biggest habitat of our planet, with a high level of composition diversity. This diversity includes a high number of sessile invertebrate organism, for example sponges (*poriferans*), corals (*cnidaria*), moss organisms (*bryozoans*). Their lifestyle is facilitated by the marine currents that supply them with all necessary nutrients, still being subject to a competitive rivalry, including shortage of space, nutrition, natural cover and predators. Having a sedentary and an impossibility of changing their location, they have developed effective chemical defense mechanisms that lead to the desired marine secondary metabolites with their multitude of pharmacological properties, among which the cytotoxic ones have a special meaning. Because of the diluting effect of seawater, the effect has to be exquisitely potent.

This enormous interest in potential cytostatics is based on the fact that one from three persons of the first world would eventually develop cancer at one point in their lives. Taking the family and friends in consideration, the number of people affected increases dramatically. Although not every case leads to death, still in year 2000 alone there were about 10 million incidences of malign tumors of which 6.2 million fell prey to it. In Europe, the percentage is about a third, meaning 2.8 millions new patients and 1.7 millions deaths. Taking in consideration the current trend of an aging population, the unhealthy lifestyle, the World Health Organization estimated that in

the next 20 years the figures would increase with 50%, meaning 10 million people. In the last couple of years in some developed countries, the mortality rate decreased due to a better diagnostic and medication. In the search for new effective and innovative active substances, the marine biological resources have been strongly taken into consideration. With the development of modern analysis methods, thousands of substances from the entire flora and fauna have been tested for pharmacological activity, by high-throughput screening. When an active substance is identified by screening and proved to meet the expectations, bigger quantities of the compound are necessary. This aspect is associated with significant problems, because of the small concentration in the host organism and often the extremely complicated chemical structure. Serious shortcomings can be encountered on the market launch, despite successful medical studies. For the approval of a medicine, besides the successful medical studies, a sufficient provision of the active substance is necessary (approximately one kilogram is necessary before any medical studies, depending on the effectiveness of the substance). In order to overcome this obstacle, an economically meaningful and efficient method of fabrication or isolation has to be developed. In the industrial production, the following possibilities are conceivable in principle:

1. The exploitation of the natural resources,
2. the cultivation of marine organisms and microorganisms, respectively (aquaculture, fermentation),
3. *in vitro* in cell cultures of the organism,
4. production by genetically modified third organisms like, for example, *E. coli* or giant hamster cells,
5. synthesis of bioactive molecules in the laboratory.

The advantages for each of these methods preponderate differently. For a conclusion, exact knowledge of population dynamic and ecology are necessary. The cultivation in the laboratory is problematic for many organisms that often produce the desired active agent only under certain conditions. An open aquaculture in offshore-waters is connected with a total loss risk. Both pure biotechnological methods are still in the incipient phase of development and still struggling with children's diseases that will be illustrated in the following examples. A real alternative for the biological and

biotechnical methods is offered by the chemical synthesis. The more complicated the molecule is, the more unlikely is a synthesis to be proven valuable in the laboratory. An additional possibility is the synthesis of analogues with the same efficacy spectrum, simpler in their structure, with a better pharmacological profile in the same time, translated in a higher efficacy and reduction of side effects.^[12]

Recently, the attention is oriented not only at the microorganism, but also at the genes within it that make a specific compound. For example, the genes responsible for the synthesis of patellamides, cytotoxic cyclic peptides from a tunicate, have been cloned. To produce these peptides, the researchers inserted the cloned patellamide genes into *E. coli*. As *E. coli* reproduced, it also produced patellamide. Developing genetic engineering approaches may be the next step in moving drug discovery and development forward. Chemists may be able to use these genetic techniques in tandem with chemical synthesis to make complicated molecules with fewer steps.^[11]

The first modern marine-derived drugs date back more than 50 years. Among the first bioactive compounds from marine sources, spongouridine and spongothymidine from the Caribbean sponge (*Cryptotheca crypta*) were isolated serendipitously in the early 1950s.^[13]

They were approved as an anti-cancer drug (cytosine arabinoside, Ara-C) and an anti-viral drug (adenine arabinoside, Ara-A), respectively, 15 years later. Ara-C was approved for the treatment of certain leukemias in 1969, making it the first such approved marine-derived drug for use in cancer chemotherapy. The secondary metabolites of marine organisms have been studied extensively over the past 30 years. Drug discovery research from marine organisms has been accelerating and now involves interdisciplinary research including biochemistry, biology, ecology, organic chemistry and pharmacology.^{[14], [15]}

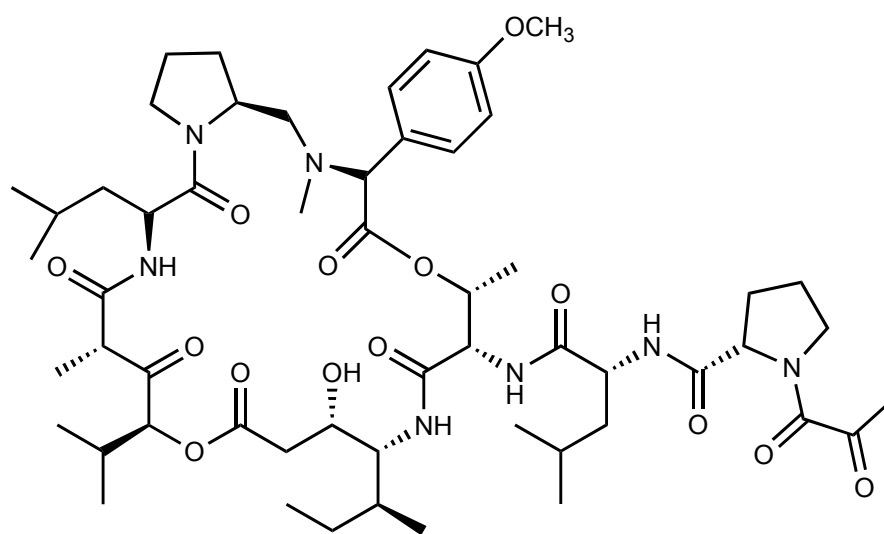
Structurally unique secondary metabolites have been isolated and identified from marine organisms and, consequently, compounds based on new chemical templates have been developed and involved in clinical trials.^[16]

The Caribbean tunicate *Trididemnum solidum* was the source organism for a family of novel marine compounds called didemnins. Initial evaluation of the bioactivity led to the selection of one of the derivatives, didemnin B, as the most promising drug candidate, being one of the first marine natural product placed in clinical trials. Phase I trials looked promising, but larger phase II trials reported poorer response at low doses and excessive toxicity when dosage was increased. Another derivative of the didemnins family, aplidine (**5**) (Scheme 3) was isolated from the Mediterranean tunicate, *Aplidium albicans* and has shown activity against certain tumor types and is present in the phase II of clinical trials. It has been reported to inhibit the secretion of the vascular endothelial growth factor related to angiogenesis and to arrest the cell cycle and is currently obtained by total synthesis.^[17]

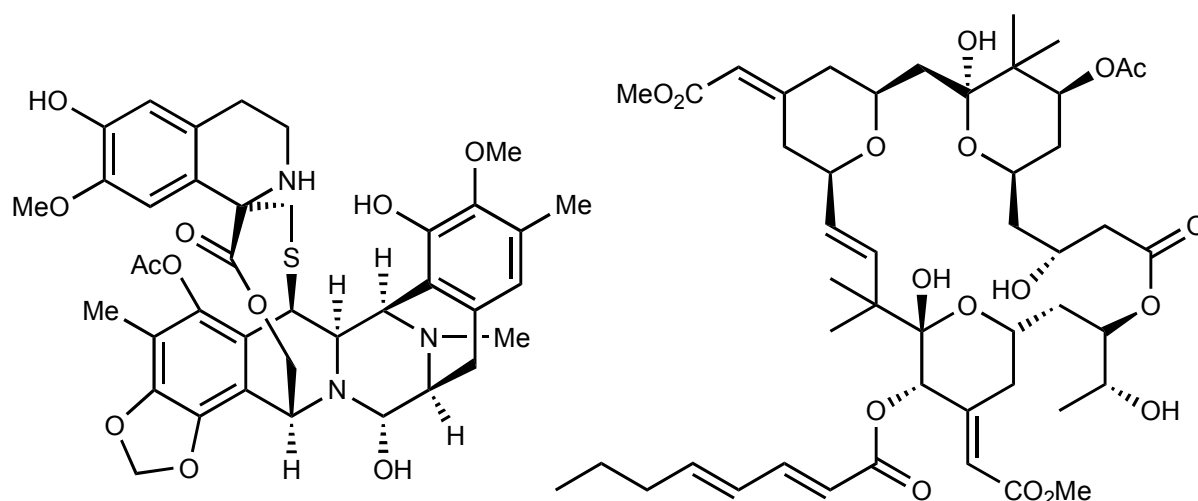
Another very efficient cytostatic is bryostatin I **7** (Scheme 3), isolated from a California population of the fouling community bryozoan *Bugula neritina*. Although *Bugula neritina* is spread worldwide in the tropical regions only very few population in the Gulf of California and around produce bryostatin I. Also in this case, a ton of the species is needed to obtain one gram of active substance (1 kg costs approximately 3.750.000 US\$).^{[4], [18]}

The laboratory cell cultures covered only around 5% of the natural concentration of bryostatin I.^[19] When the cell culture was placed in the open waters, the concentration reaches the natural level very quickly. The laboratory synthesis was difficult and the total synthesis was possible only in 70 steps.^[20] Recently, significant steps forward have been made and the pharmaceutical industry relies on a fabrication process.

Another example is ecteinascidin 743 (ET-743, **6**)^[21] (Scheme 3) that was isolated from a Caribbean mangrove tunicate species, *Ectenaiscidia turbinata*. The relative abundance and the ease of collection of *E. turbinata* also played a role in selection of this natural product as a drug development candidate. The special advantage of this compound is the absence of the common side effects in chemotherapy. ET-743 is currently obtained through aquaculture of the tunicates and semi-synthetically. A gram of pure substance can be isolated from a ton of wet mass containing the active substance.

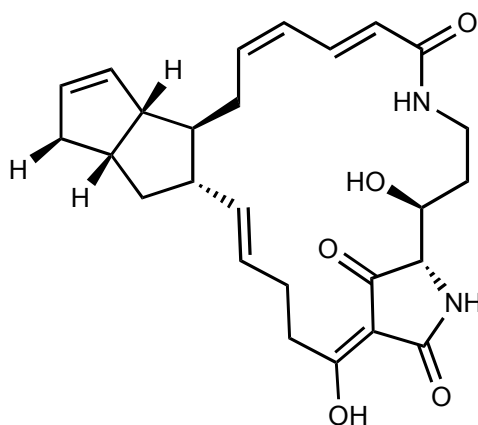


5 Aplidine



6 Ecteinascidin 743 (ET-743)

7 Bryostatin I



8 Cylindramid

Scheme 3

Along with these previous natural products, there is another cytotoxic substance, cylindramide **8** (Scheme 3), still at the beginning of the long development phase. Cylindramide was isolated in 1993 from the species *Halichondria cylindrata*, one of the sponges found in the coast waters of Japan. After extraction of a kilogram of wet mass, 70 mg of the pure substance were isolated, representing a very small percent. The potent toxicity against B 16 melanoma cells and its molecular architecture was the motivation beyond the first total synthesis of cylindramide **8**,^[22] achieved by Nicolai Cramer.

2 Motivation and approach

The present work aims to study a new pathway to already known anti-tumor alkaloids, tryprostatins A **20a** and B **20b** and quinocarcin **30**, as biological relevant diketopiperazine-derived structures.

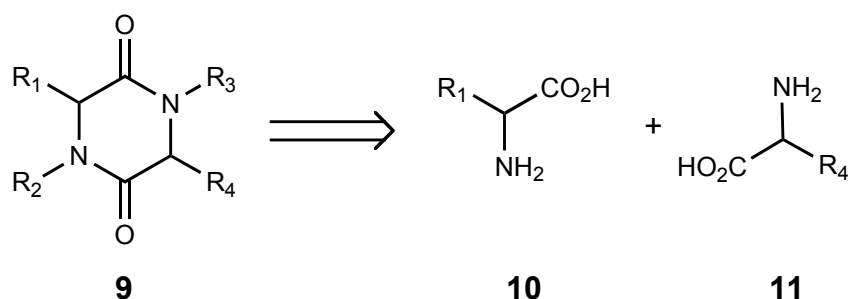
Some of the difficulties encountered in the previous syntheses of anti-tumor compounds are the number of steps and quantity of starting material necessary to obtain a significant amount of active substance.

The objective is motivated by the necessity of discovering new and affordable strategies to synthesize compounds proven to be effective against cancer. The alkylation of the lactim ethers derived from bi- and tricyclic diketopiperazines contained in tryprostatins and quinocarcins provides a fast, elegant and affordable method toward a multi-gram synthesis of these alkaloids.

3 General Part

3.1 The diketopiperazines in nature

Diketopiperazines represent an important class of natural products, many of which are known to exhibit a wide range of biological activity. They occur widely throughout nature and are generally biosynthesized from proteinogenic L- α -amino acids **10**, **11**, where cyclization of a L,L-dipeptide affords the core skeleton of the diketopiperazine **9** (Scheme 4).^[23] Further enzymatic functionalization of this diketopiperazine template may then occur to afford more complex natural products. As a consequence of their biosynthetic origin from two L- α -amino acids, most naturally occurring diketopiperazines are *cis*-configured.^[24]



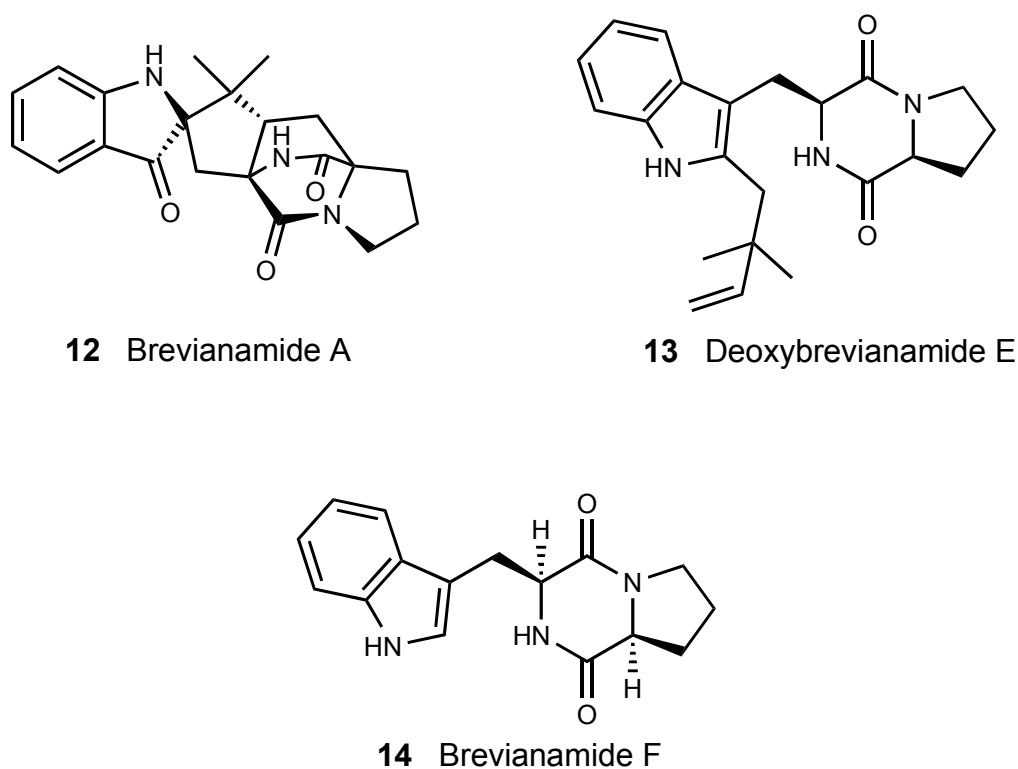
Scheme 4

3.1.1 Bicyclic diketopiperazines

A number of structurally interesting natural alkaloids have been isolated from various fungi that contain the unique bicyclo[2.2.2]octane ring system constituted mainly from tryptophane, proline and substituted proline derivatives where the olefinic unit of the isoprene moiety has been formally oxidatively cyclized across the α -carbon atoms of a cyclic dipeptide (a piperazinedione or a diketopiperazine). The family of alkaloids that shares this unusual core includes the brevianamides, fumitremorgins, cyclotryprostatins, tryprostatins.^[25]

The brevianamides **12** - **14** constitute a small but structurally interesting family of indole alkaloids constituted from tryptophan, proline and one isoprene unit (Scheme 5). Brevianamide A **12** was originally isolated from cultures of *Penicillium*

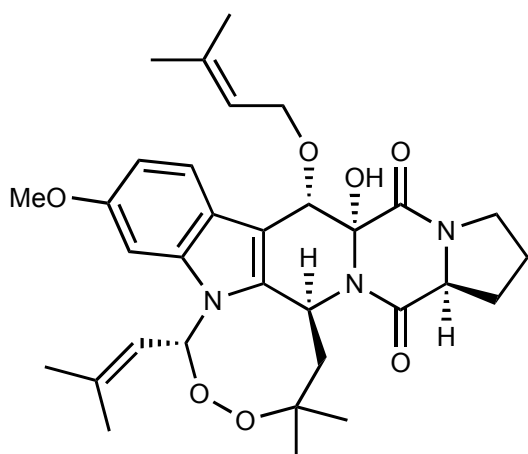
brevicompactum, being the main fluorescent metabolite, found also in cultures of *Penicillium viridicatum*^[26] and *Penicillium ochraceum*^[27]. A logical biosynthetic sequence was postulated: the coupling of L-proline and L-tryptophan → brevianamide F (**14**) → deoxybrevianamide E (**13**) → brevianamide A (**12**) (Scheme 5).^[28]



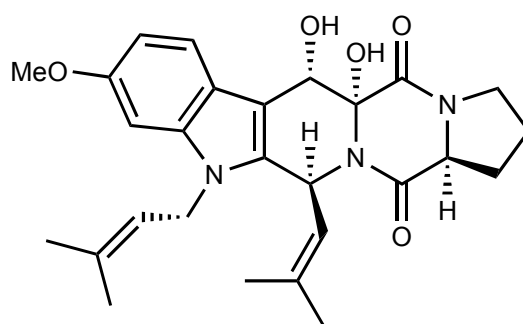
Scheme 5

Fumitremorgins A (**15**) and B (**16**) were isolated from cultures of *Aspergillus fumigatus*^[29] and are mycotoxic alkaloids that are capable of eliciting a sustained tremoring response in vertebrates and has been the subject of investigation of animal neurological disorders. These substances are fashioned from L-tryptophan, L-proline, L-methionine and one or more isoprene moieties (Scheme 6).^[30]

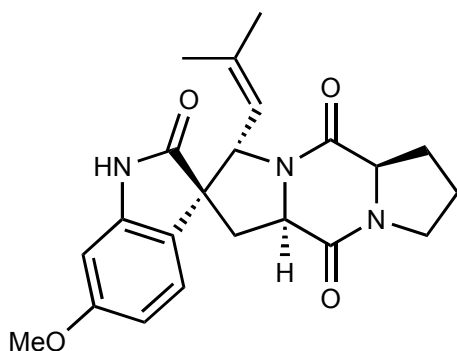
Spirotryprostatins^[31] A (**17**) and B (**18**) and cyclotryprostatins^[32] **19** were also isolated from *Aspergillus fumigatus* and have been shown to be mammalian cell cycle inhibitors interfering with the cell cycle at the G₂/M phase (Scheme 6).^[33]



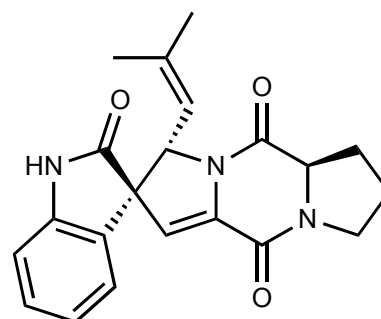
15 Fumitremogin A



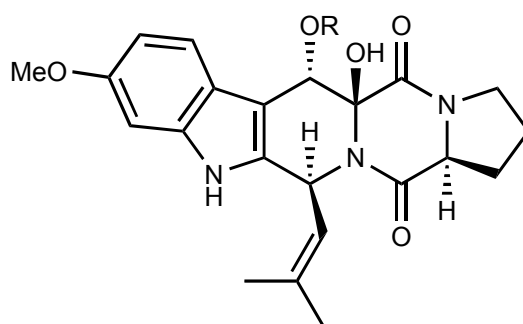
16 Fumitremogin B



17 Spirotryprostatin A



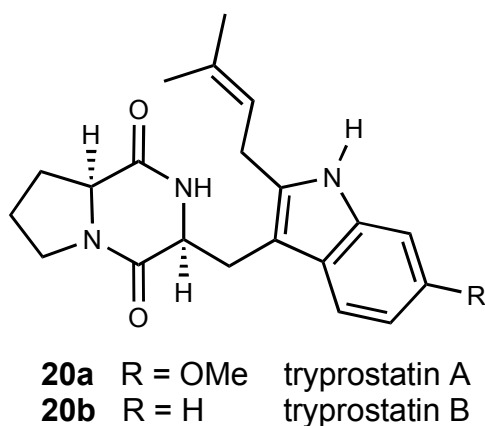
18 Spirotryprostatin B



19a R = H cyclotryprostatin A
19b R = Me cyclotryprostatin B

Scheme 6

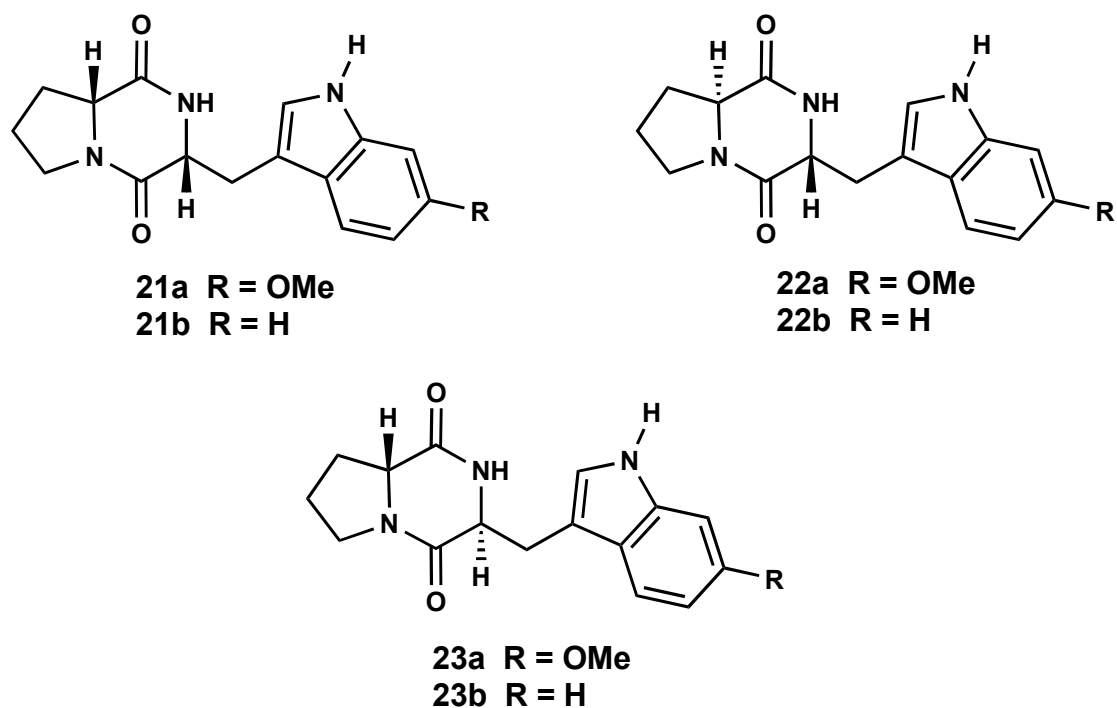
Among the active substances isolated from a marine source tryprostatin A **20a** and B **20b** (Scheme 7) constitute the focus of the first part of this work. Tryprostatin A **20a** and B **20b** have been isolated as secondary metabolites from the fermentation broth of a marine fungal strain of *Aspergillus fumigatus* BM939. They completely inhibit cell cycle progression at a final concentration of 50 $\mu\text{g/mL}$ of **20a** and 12.5 $\mu\text{g/mL}$ of **20b**, respectively.^[34] Structurally, tryprostatins A and B contain a 2-isoprenyltryptophan moiety and a proline residue, the latter of which is fused to the diketopiperazine unit.



Scheme 7

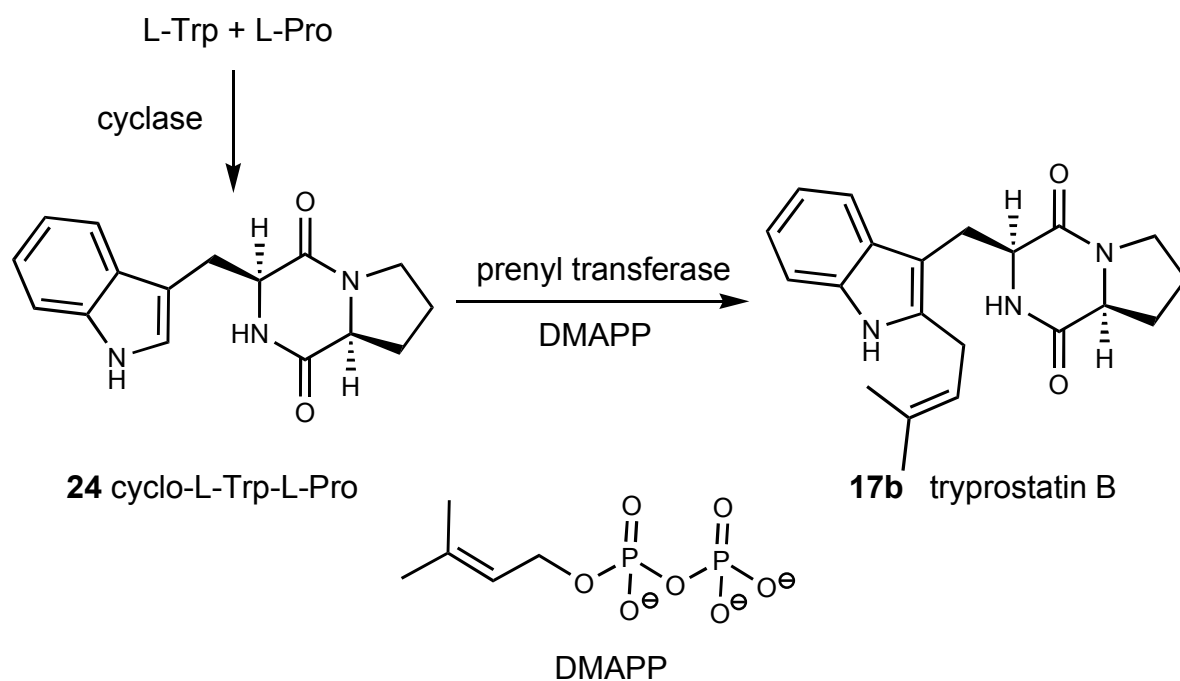
The biological activity of these alkaloids has stimulated research on their total synthesis. In order to assess the effect of the stereochemistry of the diketopiperazine structure on the biological activity, the enantiomers **21a**, **21b** and the diastereomers **22a** to **23b** (Scheme 8) were evaluated for their ability to inhibit topoisomerase II (G_2 phase) or tubulin binding protein (M phase), in order to shed light on the mechanism of action of the tryprostatins and employ this knowledge to design agents active against human carcinoma cells.

The growth inhibition properties of all eight diastereomers were studied on three human cancer cell lines: breast, prostate and lung. The diastereomer **23b** exhibited potent cytotoxic activity against all three cancer cell lines. This indicated that (1) the L-tryprostatin unit was required since none of the other tryprostatins (**21a**, **21b**, **22a**, **22b**) which contain the D-tryprostatin unit exhibited activity; (2) the presence of 6-methoxy group on **23a** nearly eliminated the activity; (3) the stereochemistry of **23b** is novel for the unnatural proline residue and may retard the metabolism *in vivo* and may provide an agent with a very long half-life (Scheme 8).^[34]



Scheme 8

The biosynthesis of tryprostatin B **20b** has been suggested to start with coupling of L-tryptophan (L-Trp) and L-proline (L-Pro) giving the cyclic dipeptide **24**, that is subjected to prenylation with dimethylallyl pyrophosphate (DMAPP) in the C-2 position of the indole moiety yielding the intermediate tryprostatin B **20b** (Scheme 9).^[35]

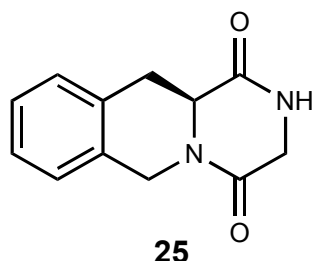


Scheme 9

The postulated prenyltransferase represents an interesting enzyme, since different brevianamide F prenyltransferases probably act as branching enzymes in the biosynthetic pathways of indole alkaloids derived from cyclo-L-Trp-L-Pro. Prenylation of brevianamide F by a 'regular' prenyltransferase at position C-2 of the indole nucleus is considered to be an initial step in the biosynthesis of tryprostatins, cyclotryprostatins, spirotryprostatins and fumitremorgins. Prenylation of brevianamide F at the same position by a "reverse" prenyltransferase leads to formation of the brevianamides.

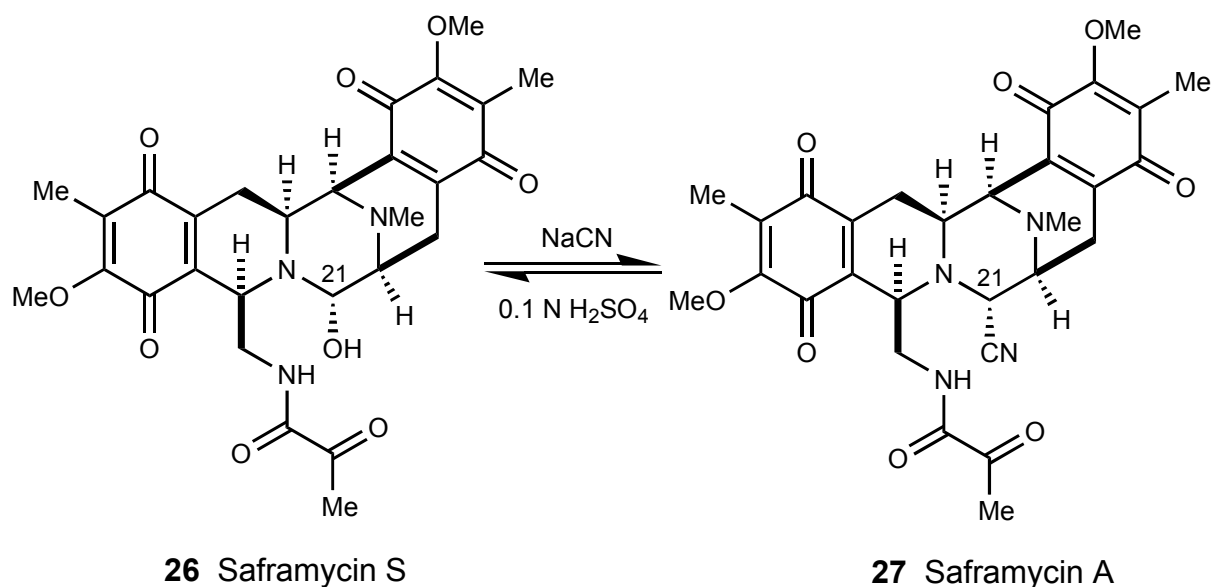
3.1.2 Tricyclic diketopiperazines

The tetrahydroisoquinoline-related tricyclic diketopiperazine **25** (Scheme 10) serves as a building block for quinocarcin and quinocarcin-related structures, as antitumor antibiotics belonging to the tetrahydroisoquinoline family.



Scheme 10

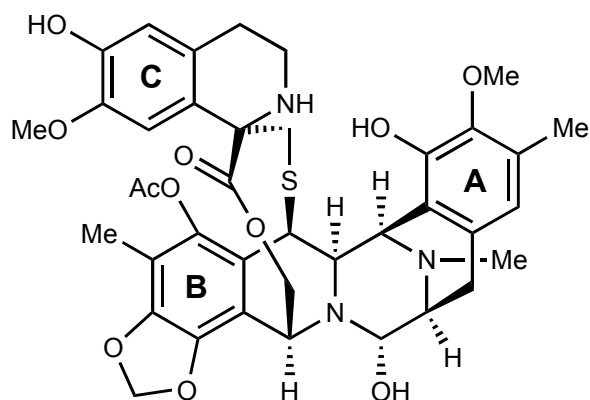
Saframycins were isolated from *Streptomyces lavendulae*^[36], of which Saframycin S **26** display the most potent antitumor activity. Saframycin A **27** had been shown to inhibit RNA synthesis at 0.2 $\mu\text{g}/\text{mL}$, while DNA synthesis was inhibited at a higher concentration. The presence of either a nitrile or a hydroxyl group at C-2 allows for the formation of an electrophilic iminium species that alkylates DNA in the minor groove (Scheme 11).



Scheme 11

The characteristics of DNA binding by the saframycins appear to be a two-step process where reversible noncovalent binding of the drug to the minor groove of DNA is immediately followed by the formation of a covalent bond with DNA within the minor groove. The cytotoxicity of saframycins is not exclusively due to DNA alkylation, but also due to DNA cleavage under aerobic conditions, this being consistent with the well-known capacity of quinines to reduce molecular oxygen to superoxide.

Ecteinascidins have the most potent biological activity by a significant margin relative to that of any of the tetrahydroquinoline antitumor antibiotics. The activity of ecteinascidin 743 (ET-743) **28** (Scheme 12) is orders of magnitude more potent than saframycin A against B16 melanoma. The exciting aspect of ET-743 **28** is that it appears to have a unique mode of action, thus constituting a new subclass of antitumor agent and is currently in phase II human clinical trials in United States. The similar structure to that of saframycins indicates that the DNA alkylation takes place in the minor groove, as does the alkylation with saframycins. The alkylated DNA substrate exhibits a bend of the minor groove, presumably due to the C-subunit of ecteinascidins. The C-subunit, which is perpendicular to the rest of the molecule make the ecteinascidins unique from saframycins, which are fairly flat.

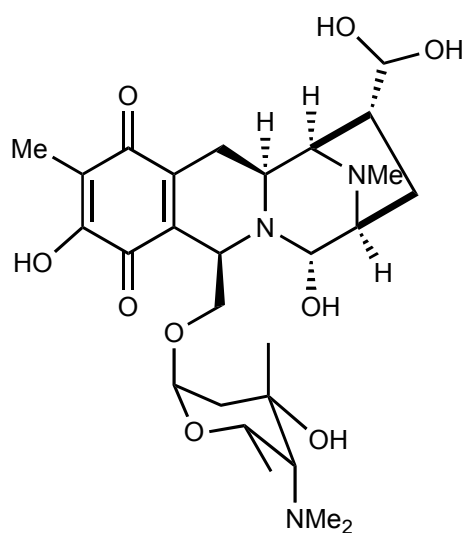


28 Ecteinascidin 743 (ET-743)

Scheme 12

It has been postulated that this bend in DNA disrupts DNA-protein binding and may be, in part, the source of the enhanced biological activity of ecteinascidins.

A unique compound structurally related is lemonomycin **29**. Lemonomycin **29** was isolated from *Streptomyces candidus*^[36] 40 years ago, but its structure was not determined until 2000. Lemonomycin **29** contains an unusual 2,6-dideoxy-4-amino sugar and is the only member in the family of tetrahydroisoquinoline antibiotics to bear a sugar residue (Scheme 13).



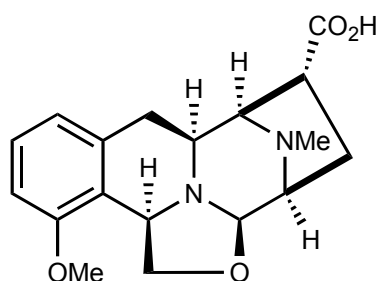
29 Lemonomycin

Scheme 13

Lemonomycin exhibits *in vitro* activity against the human colon cell line and its biological mechanism is still to be clarified.

The tetrahydroisoquinoline family of antitumor antibiotics constitutes a small yet growing and increasingly important family of chemotherapeutic agents. Nature has taken the relatively simple and innocuous tetrahydroisoquinoline ring system and endowed this heterocycle with a rich array of functionality and stereochemistry that has generated a bewildering manifold of biochemical and cellular reactivity. The known biochemical manifolds include: (1) DNA alkylation, (2) DNA cross-linking, (3) oxidative nucleic acid damage, (4) topoisomerase inhibition, (5) superoxide formation, (6) inhibition of protein synthesis.^[36]

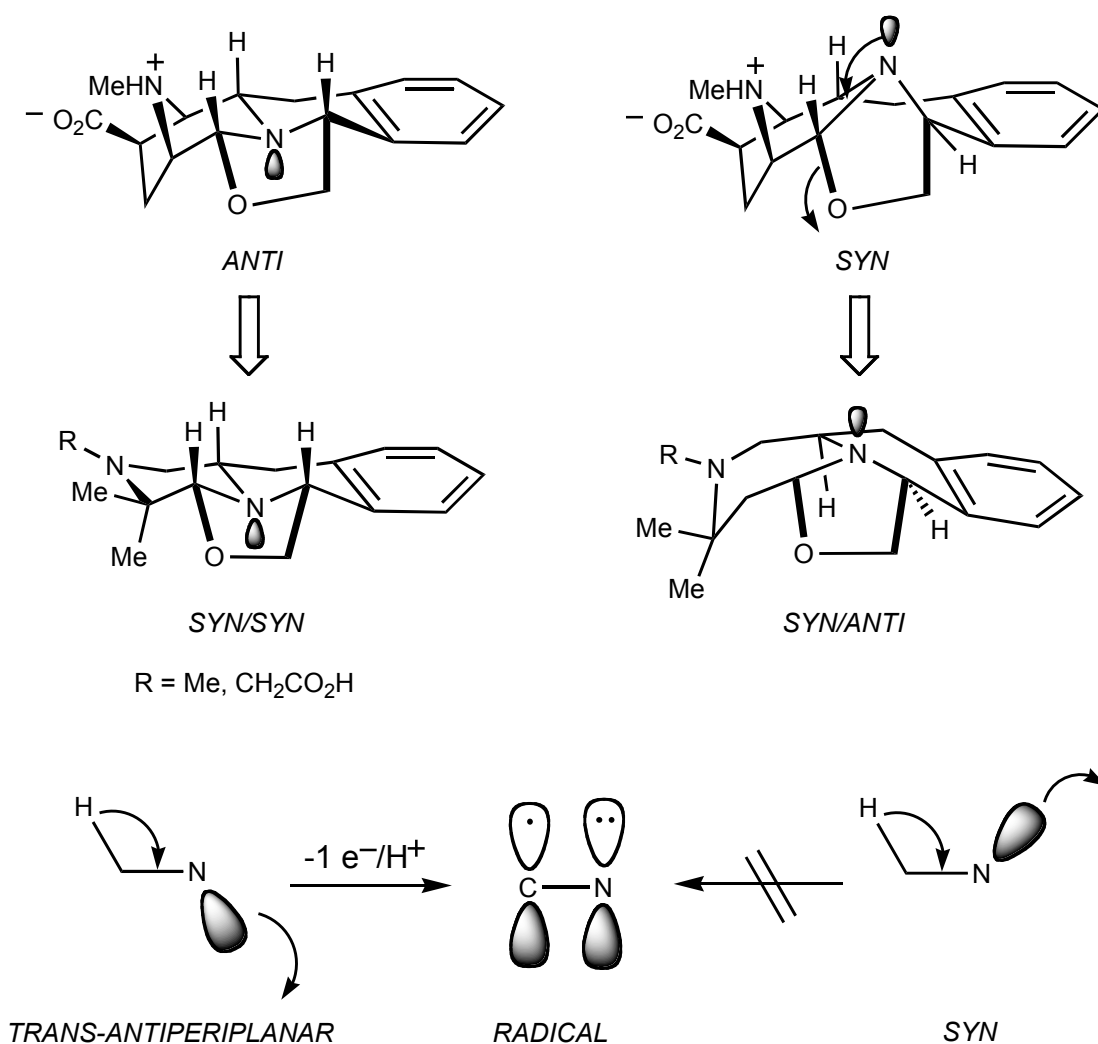
Quinocarcin **30** (Scheme 14), a tetrahydroisoquinoline antitumor antibiotic, that represents the focus of the second part of this work, was isolated from *Streptomyces melanovinaceus* and has shown potent antitumor activity against several tumor cell lines including gastric carcinoma, human colon carcinoma, human mammary carcinoma and leukemia.



30 Quinocarcin

Scheme 14

Quinocarcin **30** has been reported to mediate oxidative cleavage of DNA and was found to be due to the formation of superoxide. It was found that *syn*-analogues mediate superoxide production at rates comparable to that for quinocarcin, but the *anti*-analogues were dormant in aerated water.



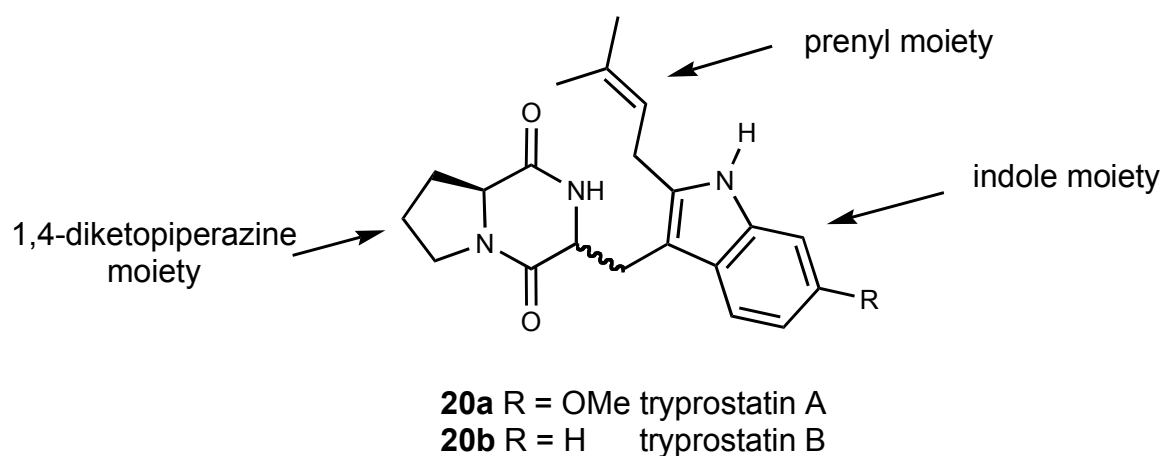
Scheme 15

This observation was explained by the fact that the *anti*-analogues assume a conformation in which the nonbonded electron pair at nitrogen is disposed *trans-antiperiplanar* to the methine hydrogen of the oxazolidine ring (Scheme 15), allowing for the formation of a carbon centered oxazolidinyl radical. This stereoelectronic arrangement is obligatory for the concomitant loss of the methine proton and a single non-bonded electron from nitrogen to form the oxazolidinyl radical. In contrast, the *syn*-analogues do not form a corresponding oxazolidinyl radical due to *syn-clinal* arrangement of the nonbonded electron pair on nitrogen relative to the methine hydrogen.^[35]

4 Retrosynthetic analysis and strategy

4.1 Tryprostatins: structure analysis and previous syntheses in the literature

Tryprostatin B **20b** is a complex natural product that can be divided in three major fragments (Scheme 16). The diketopiperazine structural motif in these natural products provides both stereocenters and determines the sterical orientation. Based on previous research, the L-configuration of the tryprostatin was required, since none of the derivatives that contain the D-configured tryprostatin unit exhibited biological activity.^[37] This aspect reinforces the effect on the stereochemistry of the diketopiperazine structure on the biological activity. The structural relationship with the essential amino acid tryptophane requires the presence of the indole fragment in the molecule. Tryptophan constitutes a key primary metabolite from which countless secondary metabolic indole alkaloids and related nitrogenous substances are biosynthesized. In nature, a particularly fascinating array of structurally diverse and interesting natural alkaloids has been created, through sequestering and adorning the basic tryptophan core with isoprenic building blocks. The rich nucleophilic chemistry of the indole ring wherein all positions of this heterocyclic nucleus are susceptible to electrophilic attack has been extensively exploited.^[25]



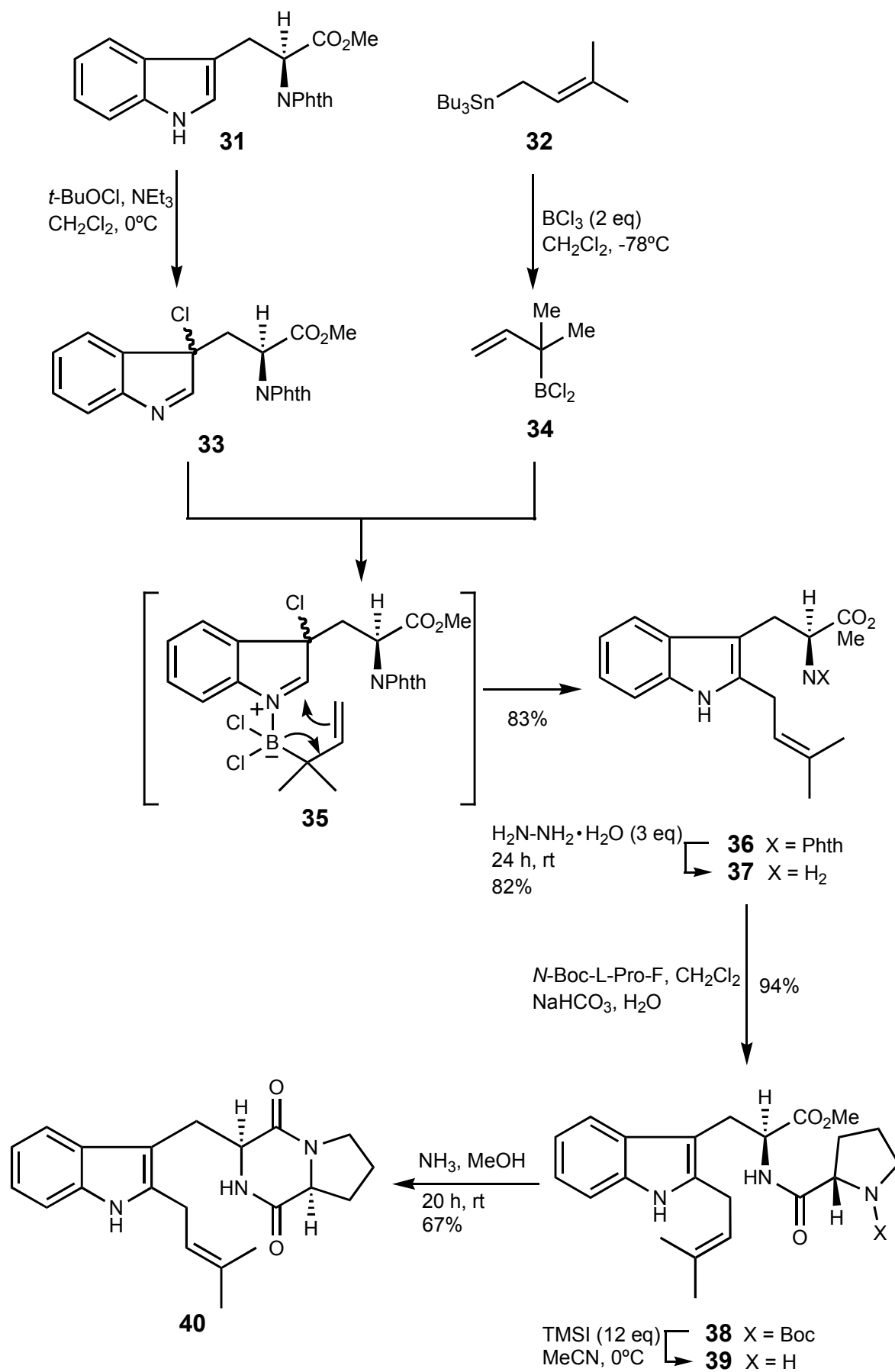
Scheme 16

The transformation into monolactim ether allows the stereoselective introduction of the indole fragment via alkylation of the desired 3-position of the diketopiperazine moiety. The third fragment, the isoprenyl moiety, introduced by nucleophilic prenylation, completes the structure of tryprostatin A (**20a**) and B (**20b**).

All syntheses of tryprostatins published to date rely mostly on the preparation of a suitable 2-prenylindole intermediate. Regarding tryprostatin B **20b**, three total syntheses have been published. The one due to Danishefsky^[38] is based on the preparation of a 2-prenyltryptophan derivative **37** by attack of a nucleophilic species generated from tributylprenylstannane **32** and boron trichloride onto an unstable 3-chloroindolenine **33**, obtained from a suitably protected tryptophan derivative **31** (Scheme 17). Thus, a simple method to introduce a prenyl function at the 2-position of a 3-substituted indole is now available.

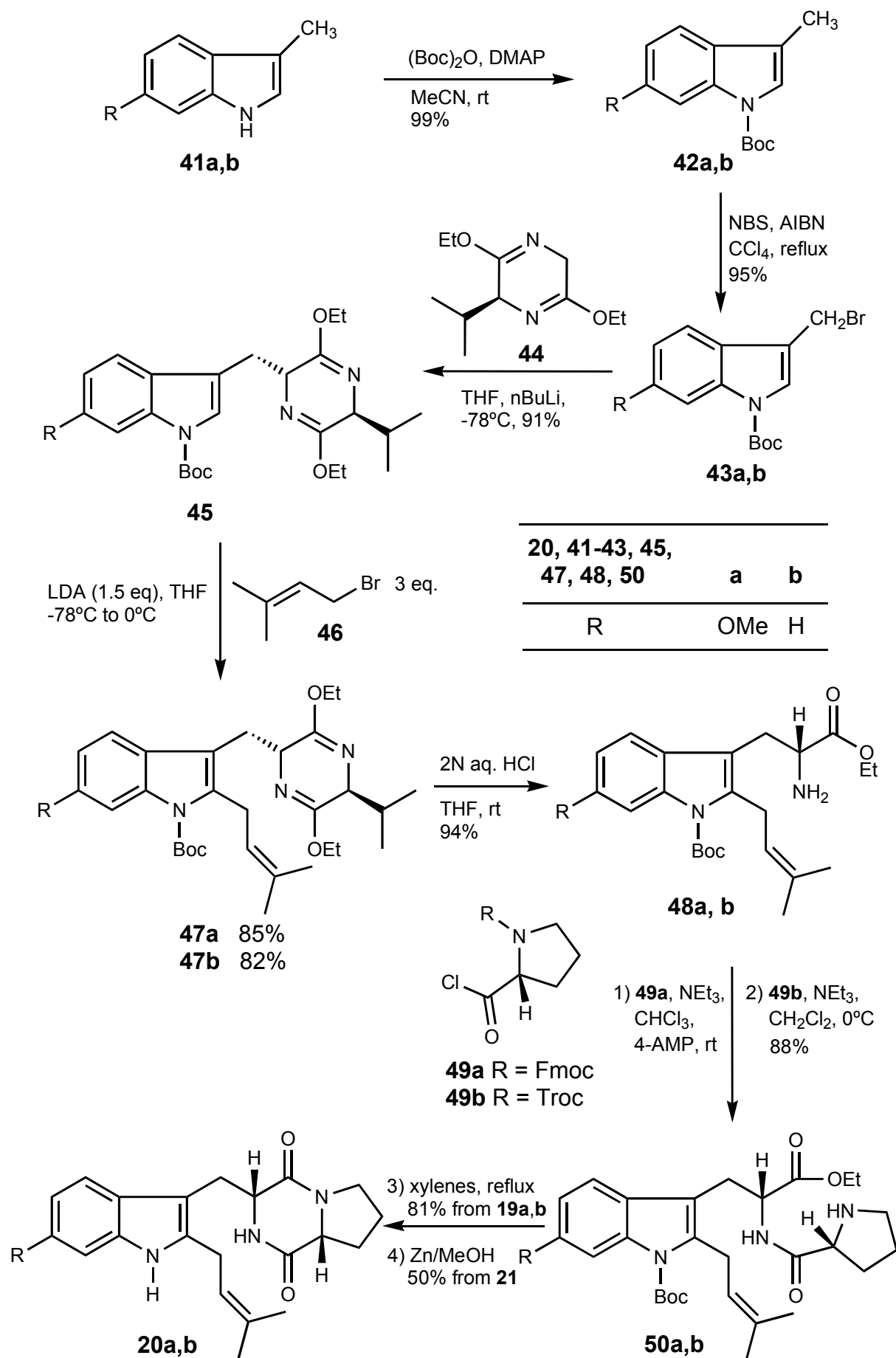
According to Scheme 17, *N*-phthaloyl-L-tryptophan methyl ester **31** on treatment with *tert*-butyl hypochlorite cleanly generated 3-chloroindolenine **33** at 0°C. This solution in CH₂Cl₂ was cooled to -78°C and treated with stannane **32** followed by rapid addition of 2 eq of BCl₃. Upon workup the desired product **36** was obtained in 83% yield. The reaction of **29** with BCl₃ generates **34**, wherein reaction with chloroindolenine **33** led to the “ate”-like structure **35**. Intramolecular delivery of the prenyl function culminated in the formation of **36**. The cleavage of the *N*-phthaloyl group was followed by coupling of the resultant amino acid ester **37** with *N*-Boc-L-proline acid fluoride, to afford **38**. Further deprotection led to **39** and then, by diketopiperazine formation, to **40**, in 67%.

The synthesis developed by Cook^[39c] is also based on the preparation of a 2-prenyltryptophan derivative **45**, in this case by directed *ortho* lithiation of a *N*-Boc-indolylmethyl derivative with the Schöllkopf chiral auxiliary **44**, followed by alkylation and hydrolysis of the pyrazine moiety (Scheme 18). A stereospecific total synthesis of the enantiomers of tryprostatins **20a** and **20b** was accomplished via alkylation of the corresponding 2-lithioindole derivatives. The synthesis starts with indoles **41a** and **41b** which were available on large scale via a Japp-Klingmann/Fischer-indole protocol followed by hydrolysis and Cu/quinoline mediated decarboxylation.^[39b]



Scheme 17

Indole **41a** or **41b** was reacted with di-*tert*-butyl dicarbonate in the presence of DMAP, to give *N*-Boc-protected indoles **42a** or **42b** in 99% yield. The protected 3-methylindole **42a** or **42b** was then treated individually with NBS in the presence of AIBN to provide the 3-(bromomethyl)indole **43a** or **43b**, as illustrated in Scheme 18. The Boc moiety not only promoted the regioselectivity of the bromination sequence but it also provided the protected indole system necessary for alkylation with the Schöllkopf chiral auxiliary **44**. When bromides **43a,b** were coupled with the anion of the chiral auxiliary **44**, the desired *trans* diastereomers **45a** and **45b** were obtained exclusively. These diastereomers are required for the synthesis of the antipodes of tryprostatin A **20a** and B **20b** and are available by the transfer of the electrophile from the opposite direction relative to the isopropyl group, via the chiral auxiliary **44**. In order to introduce the isoprenyl group at the indole C-2 position of **45b**, LDA was employed to form the anion. When **45b** was treated with LDA at -78°C and this was followed by addition of isoprenyl bromide **46**, 2-isoprenylpyrazine **47b** was obtained. Consequently, the 6-methoxy analogue **47a** was later prepared by the same method. Since the Schöllkopf chiral auxiliary can tolerate strongly alkaline conditions, it served as a protective group for the amino acid functionality to prevent racemization. The pyrazine moiety was removed from **47a** and **47b** under acidic conditions (aqueous HCl, THF) in 94% yield to provide L-valine ethyl ester, which can be recycled and the 2-isoprenyl tryptophan **76a** and **76b**, respectively. When 2-isoprenyltryptophan **76a** and **76b** was stirred with *N*-Fmoc-D-prolyl chloride **49** in the presence of triethylamine in CHCl₃ at room temperature, followed by removal of the Fmoc protecting group by addition of 4-(aminomethyl)-piperidine (4-AMP) to the solution, the desired dipeptide **50a** or **50b** was obtained. Formation of the diketopiperazine unit as well as removal of the Boc protecting group from the indole functionality were achieved when dipeptide **50a** or **50b**, according to reaction conditions 3 in Scheme 18, was heated individually in refluxing xylenes, giving the compounds **20a** and **20b**, respectively (Scheme 18).^[39c]



Scheme 18

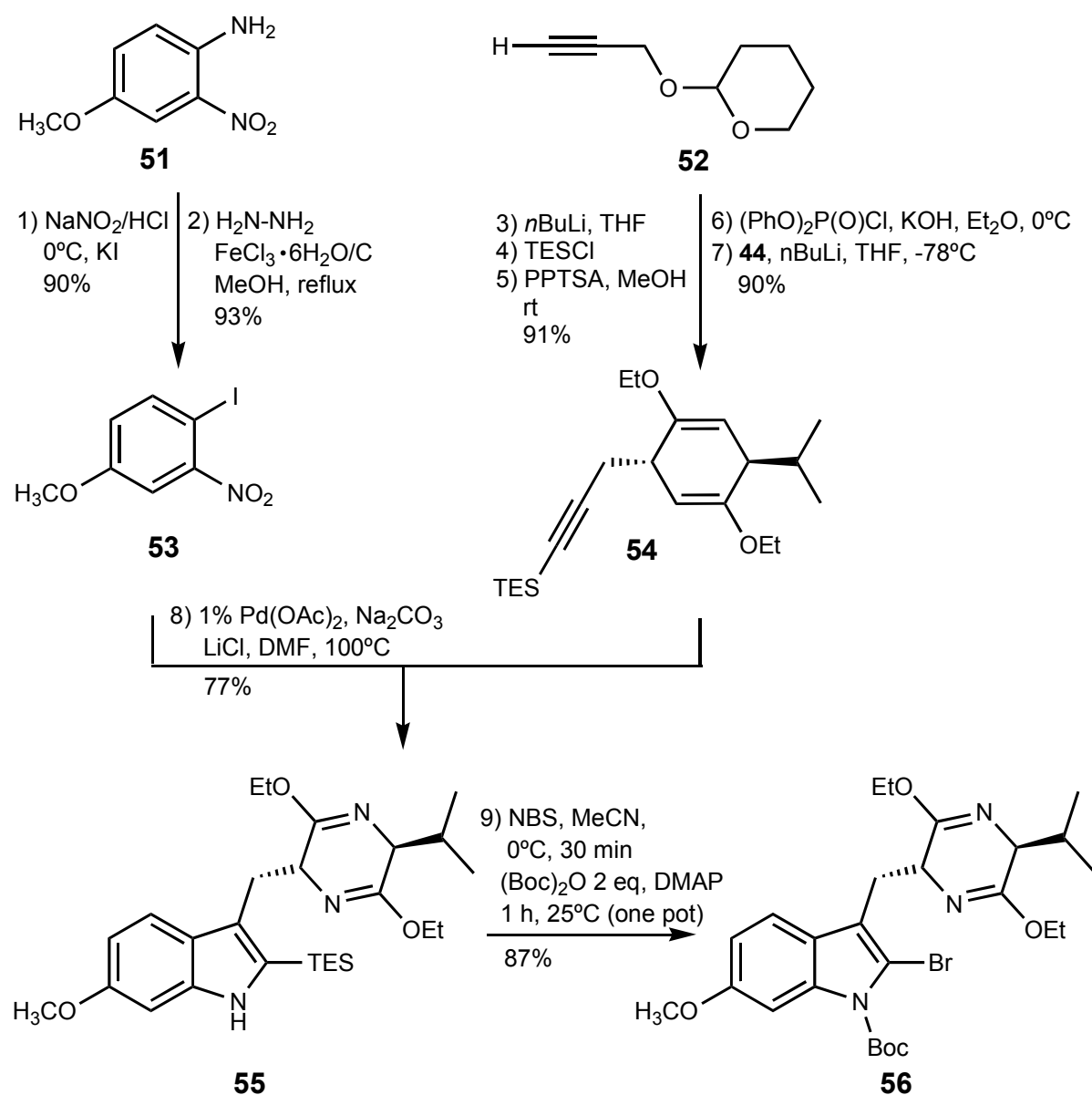
An alternative way of obtaining the tryprostatin enantiomers (+)-**20a** (A) and (+)-**20b** (B) started with the reaction of the tryptophan ethyl ester intermediate **76** with trichloroethoxycarbonyl (Troc)-L-prolyl chloride **49b** in the presence of triethylamine in CH₂Cl₂ at 0°C, to give **50** (Scheme 18). The resulted proline substituted intermediate **50** was heated with Zn dust in refluxing MeOH, followed by heating at 160°C (neat) to yield tryprostatin A **20a** in 50% overall yield from **50**.^[39a]

The advantages of this method consists in the ability to prepare either antipode of the Schöllkopf chiral auxiliary **44** on a large scale and facile preparation of 6-methylindole **41** via the Japp-Klingmann/Fischer-indole protocol.

Also relevant are the alternative syntheses of tryprostatin A **20a** and B **20b** developed by Cook where the tryptophan derivatives were obtained via palladium-mediated heteroannulation reaction (Scheme 19).^[39d] The palladium-catalysed heteroannulation is short, practical and versatile in operation because of the variety of iodoanilines. The synthesis starts with a large scale-preparation of the 5-methoxy-2-iodoaniline **53**. The commercially available 2-nitro-3-methoxyaniline **51** was diazotized under standard conditions, followed by treatment of the diazonium ion with KI to give the iodo derivative in 90% yield. Reduction of the nitro group was effected with hydrazine in the presence of a catalytic amount of FeCl₃ on charcoal in refluxing methanol to give the desired *ortho* iodoaniline **53** in 93% yield (100 g scale) (Scheme 19).

With *o*-iodoaniline **53** in hand, the diastereoselective preparation of the internal alkyne **54** was addressed (Scheme 19). The protected propargylic alcohol **52** was treated with *n*BuLi, followed by quenching with TESCl to give the TES derivative in 95% yield. Hydrolysis of the THP group was effectuated with a catalytic amount of PPTS (pyridine *p*-toluenesulfonic acid) in methanol to afford the TES-protected propargylic alcohol in 95% yield. Activation of the hydroxyl group by the diphenyl chlorophosphate moiety was achieved in 90% yield. The diphenyl phosphate that resulted was then stirred with the anion of the Schöllkopf auxiliary **54** at -78°C to provide the alkyne **54** in 90% yield and greater than 96% *de*. With both the TES-substituted alkyne **54** and iodoaniline **53** readily available, the annulation was carried out in the presence of only 1% Pd(OAc)₂ to afford the desired indole **55** in 77% yield

(300 g scale). No racemization of the chiral center was observed under these conditions.



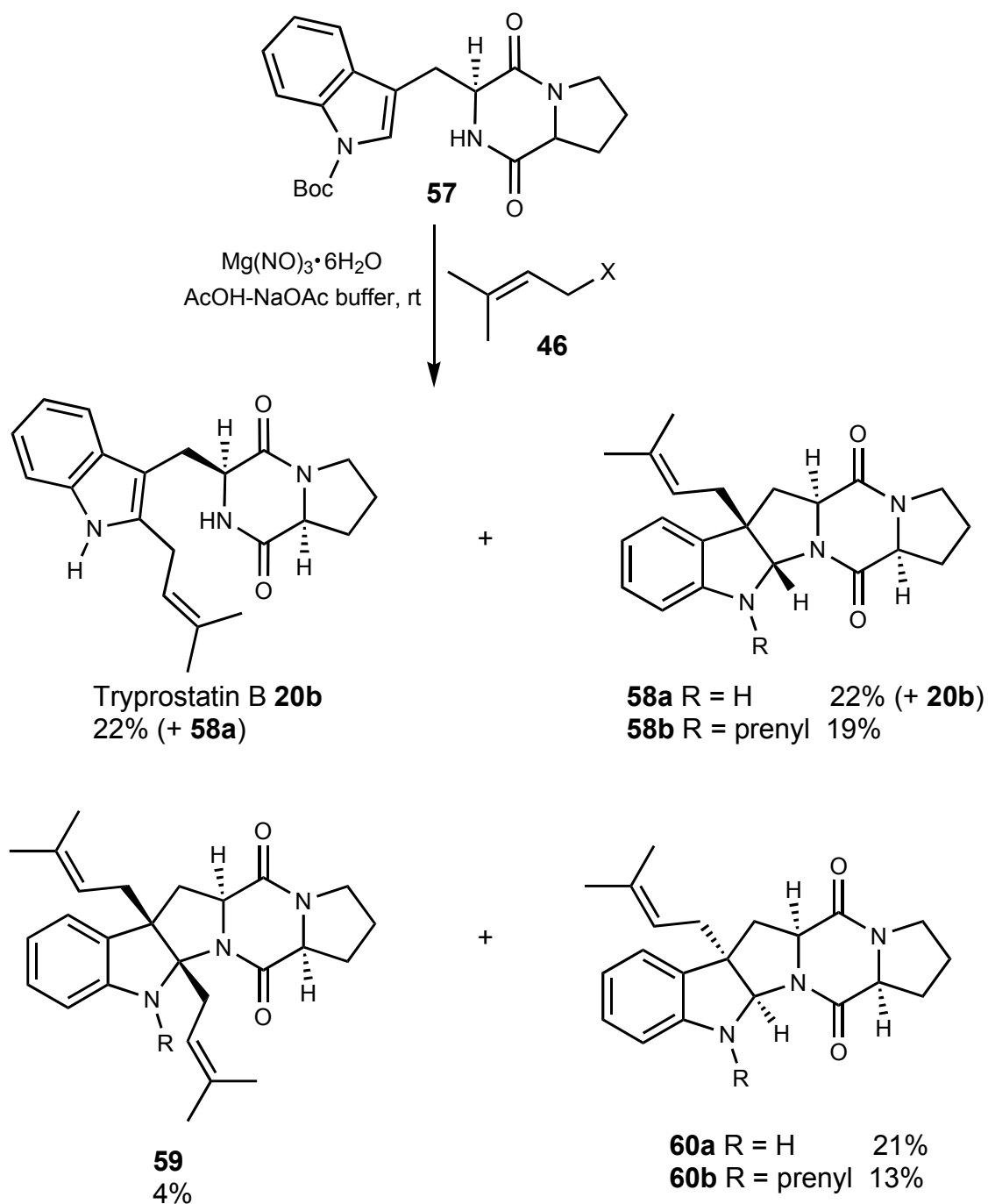
Scheme 19

This first enantiospecific total synthesis of tryprostatin A^[39a,b] **20a** includes the bromide **56** as a synthetic intermediate. With the chemistry developed above, the bromide **56** could be synthesized from the readily available indole derivative **55**. As shown in Scheme 19, the 2-silyl indole **55** which was synthesized via a palladium-catalyzed annulation, was treated with NBS in acetonitrile for 30 min, until analysis by TLC indicated complete reaction. Subsequent addition of 1 eq of di-*tert*-butyl

dicarbonate to the same reaction vessel gave the desired Boc-protected 2-bromoindole **56** in only 40% yield while about half of the starting material remained unreacted. Analysis of the reaction course suggested that the reaction byproduct (N-silylsuccinimide) might consume 1 eq of di-*tert*-butyl dicarbonate, thus resulting in the insufficiency supply of di-*tert*-butyl dicarbonate for the desired transformation. Consequently, 2 equiv of di-*tert*-butyl dicarbonate were needed to completely convert **55** to **56**. As indicated in Scheme 19, *N*-Boc-2-bromoindole **56** was prepared in 87% yield in a one-pot fashion via treatment of **55** with NBS and 2 equiv of di-*tert*-butyl dicarbonate. Conversion of **56** to tryprostatin A **20a** can be executed following the route described in Scheme 18, starting from **45**. Therefore, an improved total synthesis of tryprostatin A **20a** has been accomplished via a palladium-catalyzed heteroannulation process.

The most recent strategy for the synthesis of tryprostatin B **20b** is based on the preparation of the fused pentacyclic compound from cyclo-(L-Trp-L-Pro) **57**, followed by rearrangement of the prenyl chain with concomitant ring opening and rearomatization of the indole system (Scheme 20).

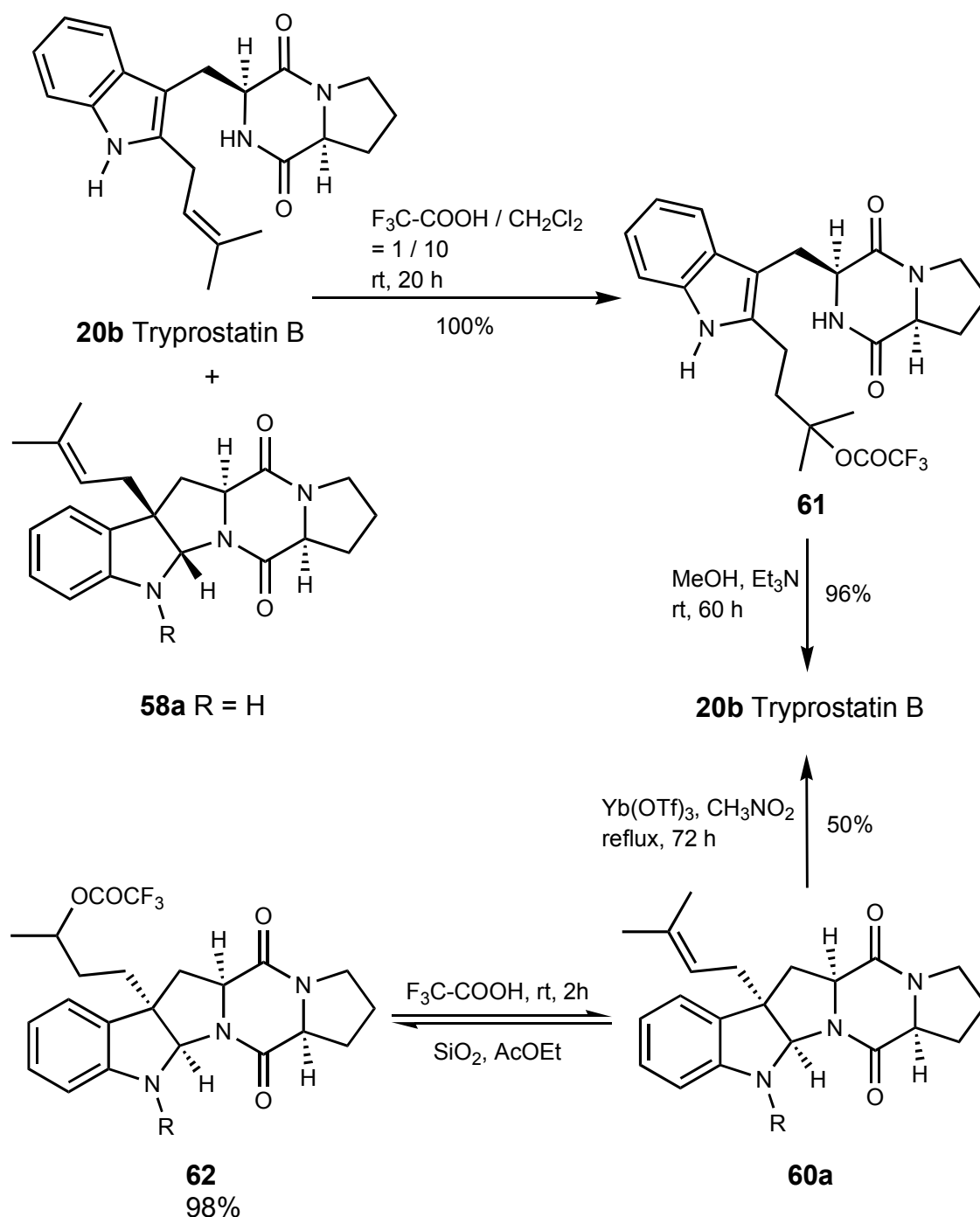
As shown in Scheme 20, slow addition of prenyl bromide **46** to a solution of *cyclo*-(L-Trp-L-Pro) **57** and magnesium nitrate in acetate buffer gave a mixture of diastereomers (**58a**, **60a**) arising from the alkylation of the indole ring at C-3 and subsequent cyclization by nucleophilic attack of the neighboring piperazinedione nitrogen, together with their prenylated derivatives **58b**, **60b**. The reaction also gave an inseparable mixture of compound **58a** and tryprostatin B **20b** and a trace (4%) of the diprenylated pentacyclic derivative **59**, arising from C-3 prenylation/cyclization of tryprostatin B **20b**. Since even C-3 substituted indoles are normally alkylated at C-3 preferably to C-2, the formation of tryprostatin B **20b** observed can in principle be explained by acid-catalyzed rearrangement of **58a** or **60a** under the reaction conditions, although direct alkylation at C-2 cannot be completely be excluded and rearrangement of **60a** can be discarded.



Scheme 20

To trigger the desired rearrangement of the prenyl chain of compound **58a**, a number of acidic conditions were assayed, involving various trifluoroacetic acid concentrations and reactions times, leading always to mixtures of compound **61** and tryprostatin B **20b** (Scheme 21). Since it was not possible to prevent the addition of trifluoroacetic acid to the double bond of **20b**, a relatively concentrated acid solution was used and a long reaction time in order to ensure the isolation of **61** as the only

reaction product and then transform it into the target compound **20b** by base-catalysed elimination.



Scheme 21

Thus, in Scheme 21, the mixture of **58a** and **17b** was exposed to 1:10 trifluoroacetic acid-dichloromethane for 20 h, giving a quantitative yield of trifluoroacetate **61**. Finally, exposure of compound **61** to NEt_3 in methanol gave tryprostatin B **20a** in

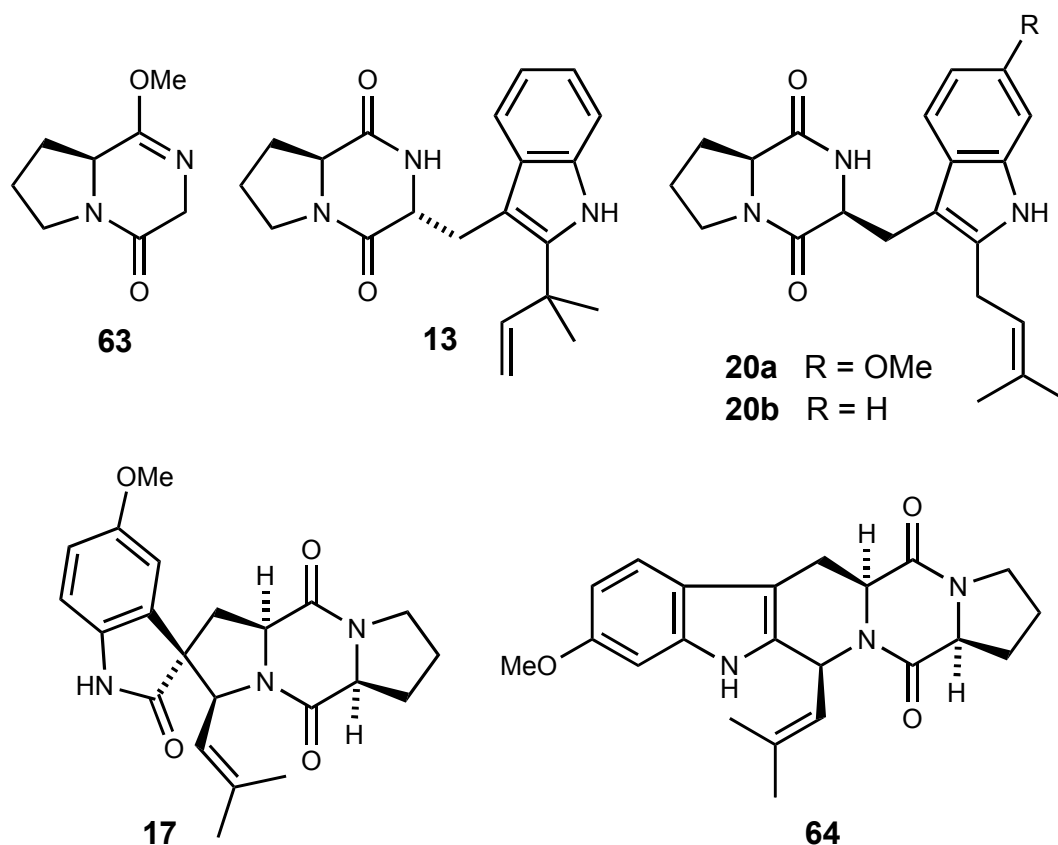
96% yield (Scheme 21). It was expected that compound **60a** could also be transformed into tryprostatin B **20b** by similar rearrangement of its prenyl chain. However, its treatment with several trifluoroacetic acid-dichloromethane mixtures gave only the starting material and forcing conditions (neat trifluoroacetic acid) led to compound **62** from addition of trifluoroacetic acid to the prenyl double bond, which upon attempted silica gel chromatography, reverted to the starting material. Despite this drawback, it was found that **60a** could also be transformed into tryprostatin B **20b** in 50% yield by prolonged treatment with ytterbium triflate in nitromethane, thus raising the overall yield of the route to 32% (Scheme 21). Ytterbium triflate is a well-known Lewis acid that promotes the addition of nucleophiles to aldehydes^[40] and has also found application in the deprotection of prenyl ethers,^[41] but there is no literature precedent on its use for promoting a rearrangement similar to **60a** → **20b** transformation. The preparation of tryprostatin B **20b** described above opened the way for the synthesis of analogues by replacing proline by other amino acids, although the practical realization of this modification might not be completely trivial since the presence of an additional NH group in the starting diketopiperazine creates a potential site for competitive alkylation.

The methods presented encounter difficulties in separation of stereoisomers and although over all the yields are high they require an increased number of steps and expensive reagents.

4.2 Retrosynthetic strategy for tryprostatin B via stereoselective alkylation

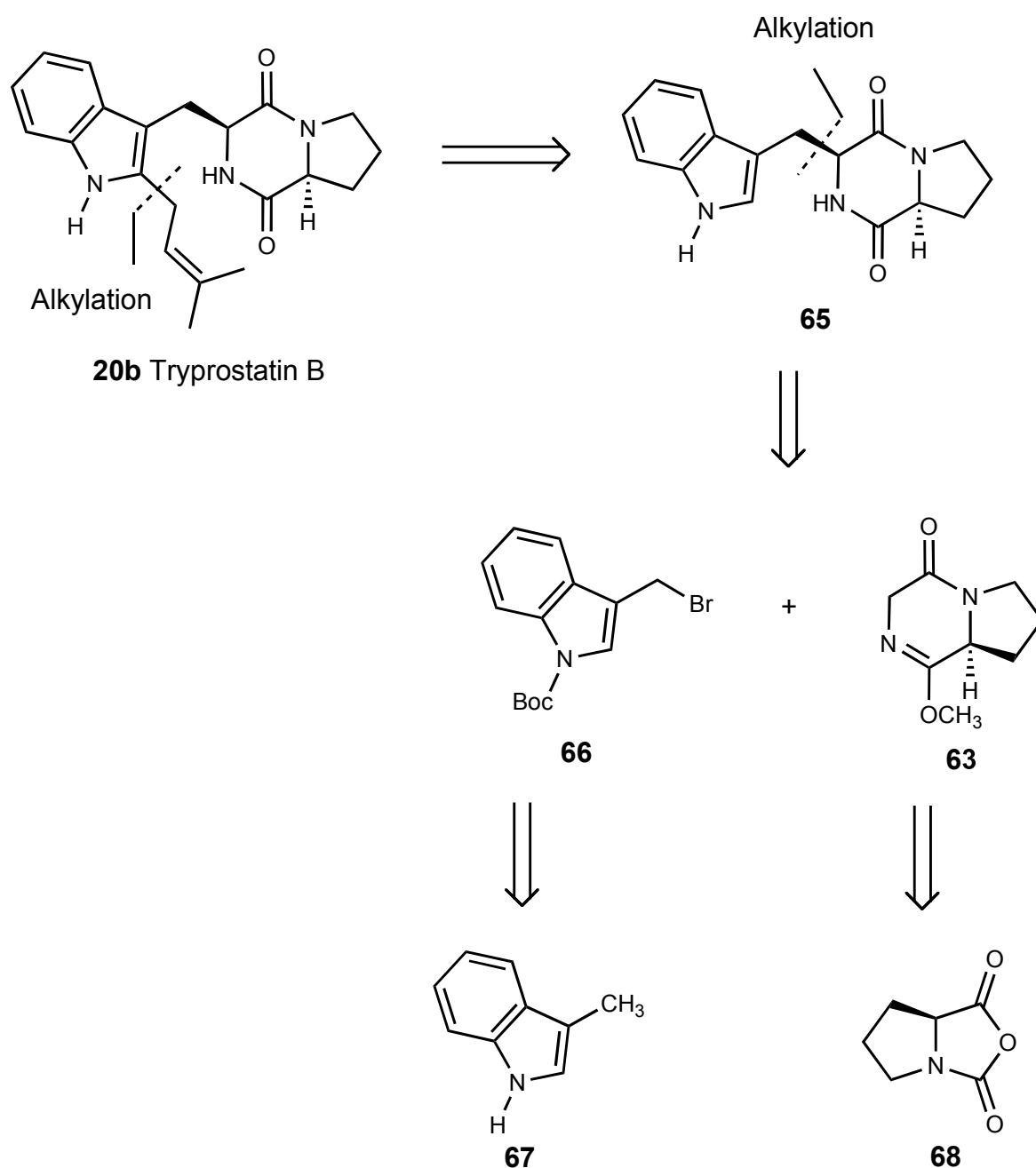
A new strategy for the synthesis of biologically relevant diketopiperazines, in particular tryprostatin B **20a** and quinocarcin **30**, via stereoselective alkylation is presented in this work.

In contrast to the well-known Schöllkopf bislactim ether method for the synthesis of α -amino acids^[39d,42-44] the alkylation of monolactim ethers is rarely reported in the literature.^[45-47] Recently, the preparation of tricyclic diketopiperazines with an annulated tetrahydroisoquinoline moiety via diastereoselective alkylation of the corresponding monolactim ethers and subsequent hydrolysis^[48] has been published.



Scheme 22

Several secondary metabolites of microorganisms with interesting biological properties such as deoxybrevianamide E **13**,^[49] tryprostatin A and B **20**,^[50] spirotryprostatin A **17**,^[51] and fumitremorgin C **64**^[52] (Scheme 22) contain a proline-derived diketopiperazine as part of their molecular skeleton. Furthermore, this type of compound has been found in the bitter flavor of roasted coffee.^[53] The diketopiperazine structural motif in these natural products was prepared in most cases by cyclocondensation.^[49-52,54,55]



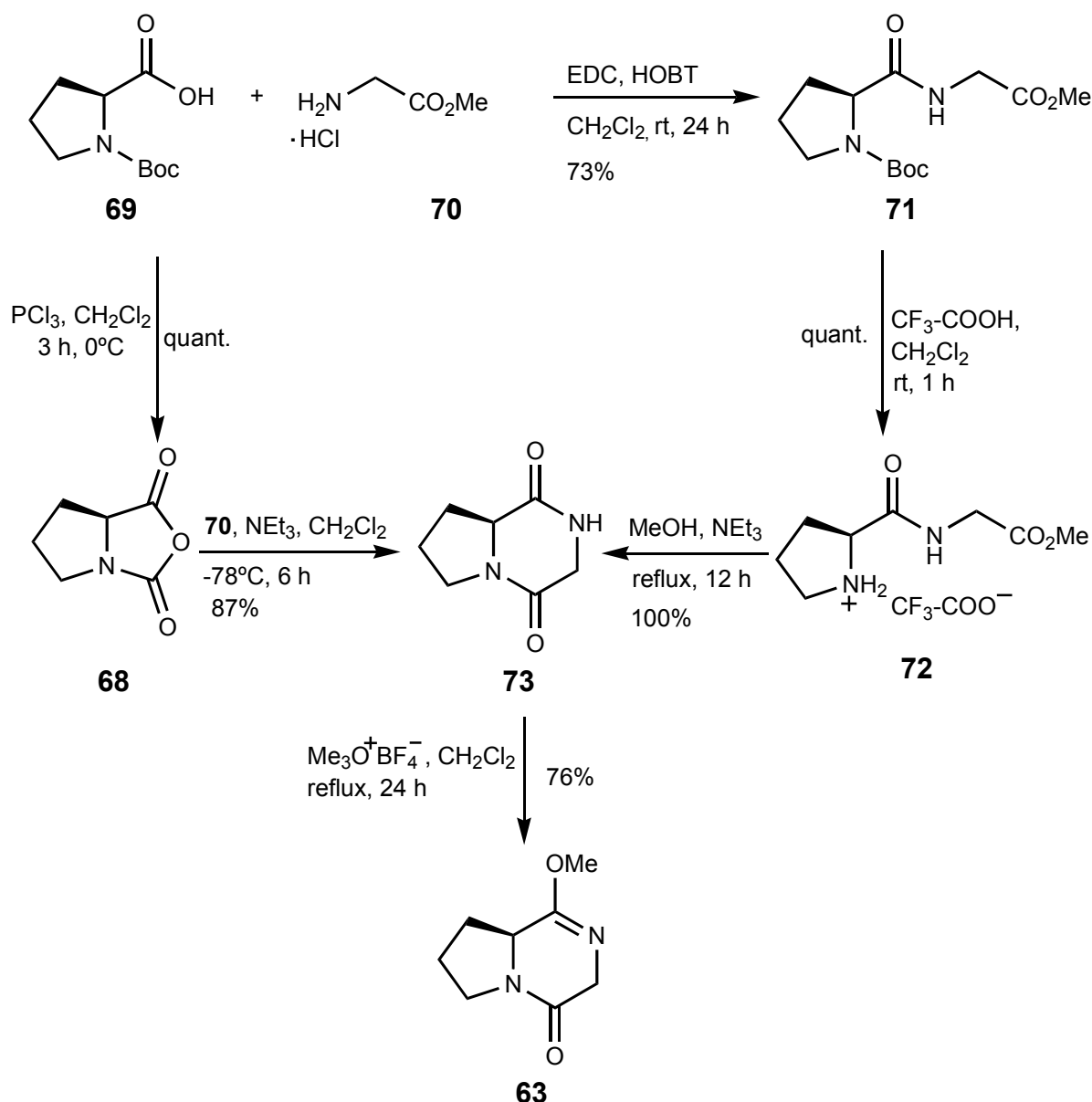
Scheme 23

However, we were interested to synthesize related proline-based diketopiperazines via alkylation of bicyclic lactim ether **63** followed by acidic hydrolysis (Scheme 23). This synthetic route should allow a novel access to diketopiperazine indole-related alkaloids.

The retrosynthetic strategy described in this work (Scheme 23) approaches tryprostatin B **20b** by introduction of the prenyl side chain at C-2 position of the indole moiety in the compound **65**, under basic conditions and low temperature. The indole-derived diketopiperazine **65** was obtained by direct diastereoselective alkylation at the C-3 of the lactim ether **63**, (related to the 2,4-diketopiperazine moiety) under basic conditions and low temperature, with bromo indole derivative **66**, obtained by *N*-Boc protection, followed by regiospecific bromination under free radical conditions from 2-methyl indole **67**. The lactim ether **63** resulted from the anhydride **68** that treated with glycine methyl ester hydrochloride, at low temperature. Further reflux in H₂O, in the presence of NEt₃ gave the 2,4-diketopiperazine unit that led to the lactim ether **63** by treatment with Me₃O⁺BF₄⁻.

4.2.1 The synthesis of the 2,4-diketopiperazine fragment (73)

Synthetically, the 2,4-diketopiperazine fragment is accessible by two methods.^{[56],[57]} The first procedure involves cyclisation of the dipeptide **71** from amino acids L-(*tert*-butoxycarbonyl)-proline **69** and glycine methylester hydrochloride **70**. The second procedure is carried out by treating the L-(*tert*-butoxycarbonyl)-proline-derived anhydride **68** with glycine methylester hydrochloride **43** (Scheme 24).^[48]



Scheme 24

As shown in Scheme 24, the coupling of L-(*tert*-butoxycarbonyl)-proline **69** and glycine methylester hydrochloride **70** in the presence of 4-hydroxybenzotriazole

monohydrate (HOBT), as an agent which is known to suppress racemization, and 1-[3-(dimethylamino)propyl]-3-ethylcarbodiimide hydrochloride (EDC), in dichloromethane as a solvent, for 24 h, afforded the dipeptide **71**, as a crystalline solid, with 73% yield. The Boc-deprotection of dipeptide **71** with F₃C-COOH followed by evaporation of the solvent gave the corresponding salt **72** in quantitative yield. Neutralization of salt **72** by partitioning with aqueous NaHCO₃ / CHCl₃ or treatment with excess NEt₃ in MeOH at reflux afforded the 2,4-diketopiperazine **73** quantitatively.^[56]

In addition to the classic peptide coupling reagents (EDC, HOBT) a few other possibilities have been explored. In the presence of carbonyl diimidazole and N-ethylmorpholine^[58] the yield increased significantly (100%), while the use of isobutyl chloroformate and N-methylmorpholine^[59] has been accompanied, besides increased yield (78%), by shorter reaction time (14 h). The optimal procedure has proven to be the one using diethyl phosphorcyanidate and dimethylformamide, with 1 h reaction time and 80% yield. The variation of the peptide coupling reagents have led to improved reaction conditions and yields, as well as availability of low cost starting materials.

Scheme 24 describes a new alternative to the methods via dipeptide that involves the reaction of the proline-derived anhydride **68** with glycine methyl ester hydrochloride **70**, at -78°C in CH₂Cl₂, in the presence of NEt₃. As shown in Scheme 24, the treatment of L-(*tert*-butoxycarbonyl)-proline **69** with phosphorus trichloride, in CH₂Cl₂ for 3 h at room temperature provided the anhydride **68** in quantitative yield. Reaction of anhydride **68** with glycine methyl ester hydrochloride **70** in the presence of NEt₃, followed by reflux in H₂O provided the ring closure, affording the 2,4-diketopiperazine **73** in 87% yield.^[57]

A comparison of both procedures shows that the second route via proline-derived anhydride **68** offers less reaction time, as a result of a reduced number of steps and high yields, while requiring affordable starting materials. The only problem encountered has been the handling and purification of the anhydride **68**, which had to be used without further purification, not affecting the following steps and yield of the final product.

An X-ray crystal structure analysis of diketopiperazine **73** revealed the presence of hydrogen bridges in the solid state (Figure 1). The bond length of N1–H \cdots O2 is 2.8 Å and the bridge angle is 175.18°.

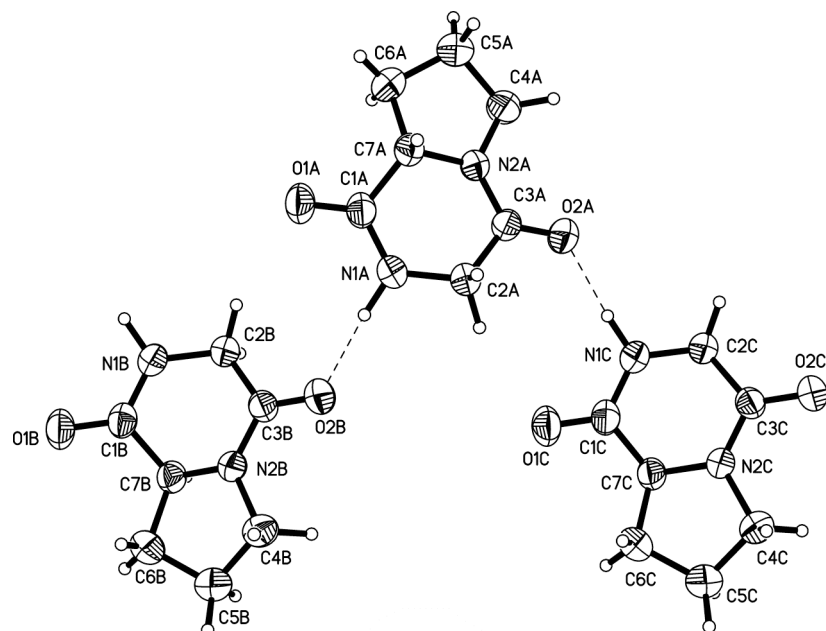
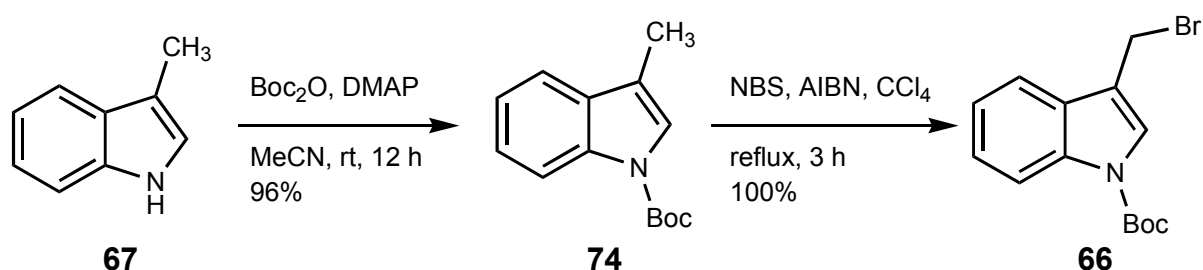


Figure 1. Molecular structure of diketopiperazine **73** in the solid state (ORTEP presentation)

Since the competing alkylation of the secondary amide group would interfere with the alkylation at C-3 position, this function was protected by preparing the O-methyl derivative **63**, which can be formed by reaction of 2,4-diketopiperazine **73** with trimethyloxonium tetrafluoroborate (Meerwein's salt) (Scheme 24).

4.2.2. The synthesis of the indole fragment (66)

According to a procedure by Cook,^[39b] the preparation of the desired *N*-(*tert*-butoxycarbonyl)-3-bromomethyl indole **66** was based on the regiospecific bromination at C-3 of the *N*-Boc-protected derivative of 3-methyl indole **74** (Scheme 11). When 2-methyl indole **67** was stirred with di-*tert*-butyl dicarbonate in the presence of DMAP, *N*-Boc protected indole **74** was obtained in 96% yield. The protected 3-methyl indole **74** was treated with *N*-bromosuccinimide (NBS) in the presence of azobisisobutyronitrile (AIBN) to provide the 3-(bromomethyl) indole **66**, in quantitative yield, as shown in Scheme 25.



Scheme 25

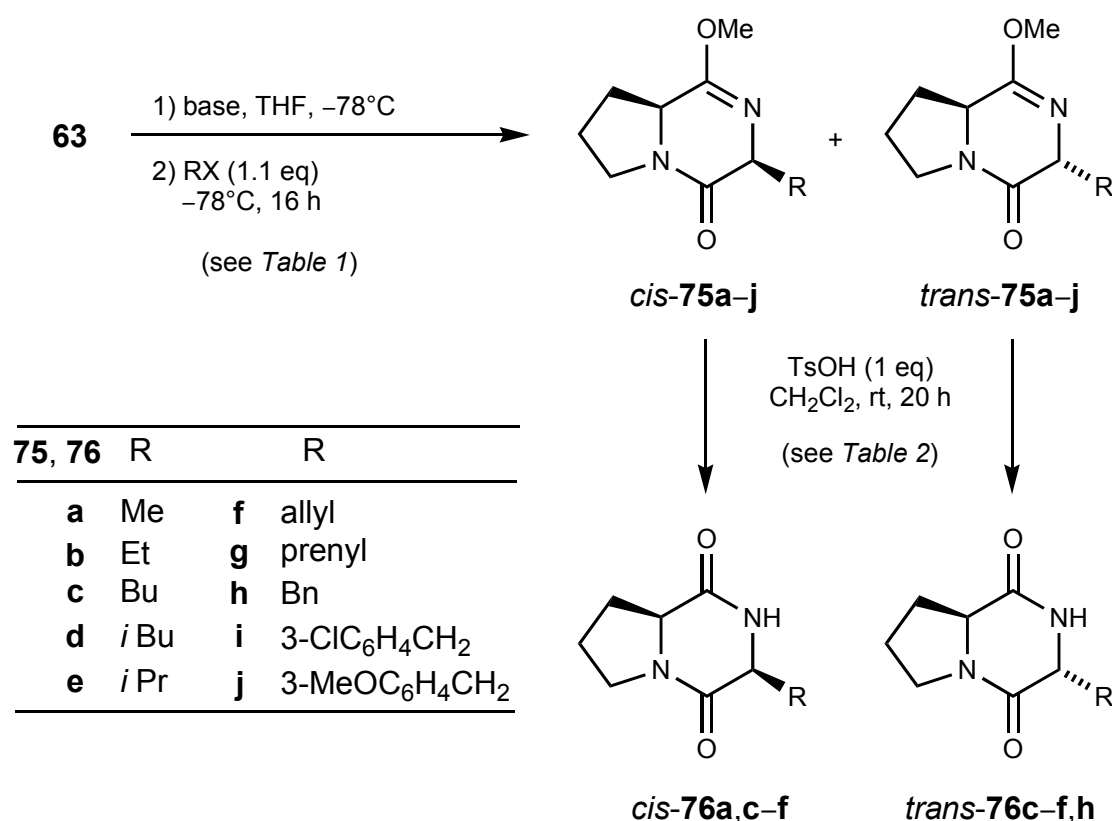
Regiospecific bromination of 3-methyl indoles can be controlled by judicious choice of the reaction conditions and the choice of the protecting group at the *N*-1 position. Since the Boc group can be removed under different conditions and facilitate the free radical bromination at the 3-methyl group by its electron-withdrawing effect, it has been preferred to other *N*-protective groups. The presence of the radical initiator AIBN is required, in order to eliminate the competition of the free radical substitution versus electrophile one, at C-2 position.

The 3-bromomethyl indole **66** was not very stable to chromatographic purification. Therefore, it has been dried and used without further purification. Small samples have been purified by crystallization from hexane, for analysis purpose, affording the product as colorless crystals, in 100% yield.

4.3 Alkylation studies of lactim ether (63)

4.3.1 Diastereoselective alkylation of lactim ether (63) with various electrophiles

In order to find the optimal conditions for the coupling of lactim ether **63** with bromo indole derivative **66**, the alkylation of lactim ether **63** with different electrophiles was investigated (Scheme 26, Table 1).^[57] Since LDA and LHMDS were previously found to be most promising with regard to yields and diastereoselectivities in case of tricyclic lactim ethers,^[48] both bases were used for the deprotonation step.



Scheme 26

Treatment of lactim ether **63** with LDA followed by addition of methyl iodide and aqueous workup after 16 h gave the crude products **75a** in an excellent diastereoisomeric ratio *cis* : *trans* = 98 : 2. The mixture was separated by flash chromatography, yielding the major diastereoisomer *cis*-**75a** in 94% (entry 1). Similar results were obtained with LHMDS (entry 2). The alkylation of **63** with ethyl iodide

also favored the formation of the corresponding *cis*-**75b** (entry 3). However, for electrophiles with either longer alkyl chains or more bulky alkyl groups the *cis/trans*-selectivity decreased remarkably (entries 4–12).

Table 1. Alkylation of lactim ether **63** to compounds **75**^{a)}

Entry	R	X	Base	Product	Conv. ^{b)}	Yield ^{c)}	Ratio ^{b)}
					[%]	[%]	<i>cis</i> : <i>trans</i>
1	Me	I	LDA	75a	100	94	98 : 2
2	Me	I	LHMDS	75a	80	75	95 : 5
3	Et	I	LDA	75b	70	60	96 : 4
4	<i>n</i> Bu	I	LDA	75c	81	33 ^{d)}	50 : 50
5	<i>n</i> Bu	I	LHMDS	75c	80	–	50 : 50
6	<i>i</i> Bu	I	LDA	75d	96	–	29 : 71
7	<i>i</i> Bu	Br	LDA	75d	65	48	30 : 70
8	<i>i</i> Bu	Br	LHMDS	75d	56	–	40 : 60
9	<i>i</i> Pr	Br	LDA	75e	86	67	60 : 40
10	<i>i</i> Pr	I	LDA	75e	67	–	68 : 32
11	<i>i</i> Pr	I	LHMDS	75e	39	–	50 : 50
12	<i>i</i> Pr	Br	LHMDS	75e	85	–	50 : 50
13	Allyl	Br	LDA	75f	99	–	33 : 67
14	Allyl	I	LDA	75f	90	35 ^{d)}	33 : 67
15	Allyl	I	LHMDS	75f	35	–	12 : 88
16	Allyl	Br	LHMDS	75f	51	–	30 : 70
17	Prenyl	Br	LDA	75g	69	7 ^{e)}	15 : 85
18	Bn	Br	LDA	75h	77	71	4 : 96
19	Bn	Br	LHMDS	75h	61	–	<1 : 99
20	3-ClC ₆ H ₄ CH ₂	Br	LDA	75i	68	6 ^{e)}	12 : 88
21	3-MeOC ₆ H ₄ CH ₂	Br	LDA	47j	76	66	12 : 88

a) Cf. Scheme 26. ^{b)} Conversion and diastereomeric ratios were determined by capillary GC of the crude products. ^{c)} Yields refer to isolated yields. ^{d)} Difficult chromatographic purification caused loss of yields. ^{e)} Yield of minor *cis*-diastereoisomer, the *trans*-diastereoisomer was hydrolyzed to the corresponding diketopiperazine **76** during chromatography.

While *n*-butyl iodide gave an equimolar mixture of *cis*-**75c** and *trans*-**75c** (entries 4,5), isobutyl (**75d**) and isopropyl derivatives (**75e**) were obtained in ratios *cis* : *trans* = 29 : 71 and 68 : 32, respectively (entries 6, 10). The situation changed remarkably, when electrophiles with additional π -systems were applied (entries 13–21). In these cases, a pronounced preference of *trans*-products *trans*-**75f–j** was observed. The best selectivity of *cis* : *trans* = <1 : 99 was obtained for the benzylated product **75h** with LHMDS as base (entry 19).

It should be noted that in some cases the yields of the isolated products **75** were considerably decreased due to difficult chromatographic purification of the diastereoisomers. Furthermore, the *trans*-diastereoisomers of prenyl- and 3-chlorobenzyl-substituted lactim ethers **75g,i** turned out to be more prone to hydrolysis than their *cis*-congeners. Upon prolonged chromatographic purification the *trans*-diketopiperazines *trans*-**76g,i** were isolated rather than the corresponding lactim ethers *trans*-**75g,i**, whereas the *cis*-lactim ethers *cis*-**75g,i** were obtained without any problem.

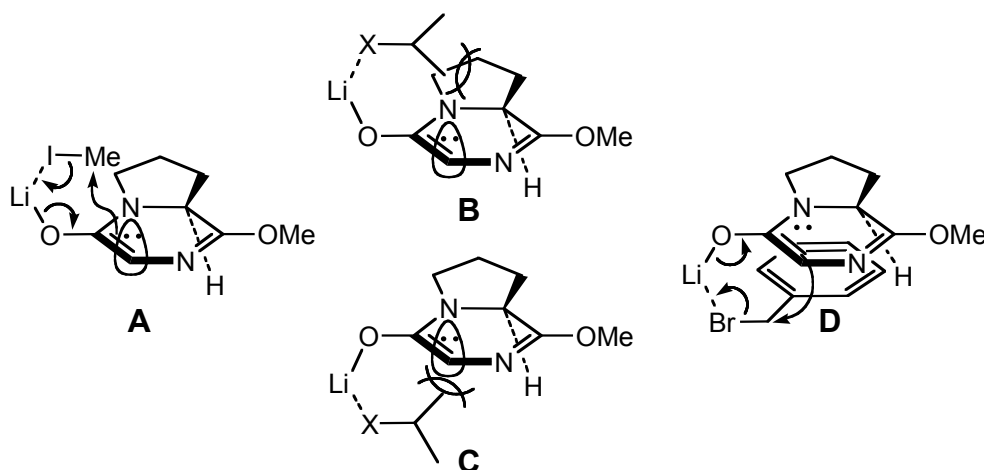
Table 2. Hydrolysis of separated lactim ethers *cis*- and *trans*-**75** to give the corresponding diketopiperazines *cis*- and *trans*-**76**^{a)}

Entry	Reactant	R	Product	Yield [%]
1	<i>cis</i> - 75a	Me	<i>cis</i> - 76a	81
2	<i>cis</i> - 75c	<i>n</i> Bu	<i>cis</i> - 76c	81
3	<i>trans</i> - 75c	<i>n</i> Bu	<i>trans</i> - 76c	quant.
4	<i>cis</i> - 75d	<i>i</i> Bu	<i>cis</i> - 76d	quant.
5	<i>trans</i> - 75d	<i>i</i> Bu	<i>trans</i> - 76d	quant.
6	<i>cis</i> - 75e	<i>i</i> Pr	<i>cis</i> - 76e	quant.
7	<i>trans</i> - 75e	<i>i</i> Pr	<i>trans</i> - 76e	94
8	<i>cis</i> - 75f	allyl	<i>cis</i> - 76f	70
9	<i>trans</i> - 75f	allyl	<i>trans</i> - 76f	60
10	<i>trans</i> - 75h	Bn	<i>trans</i> - 76h	83

a) Cf. Scheme 12.

Finally, some of the isolated pure *cis*- and *trans*-lactim ethers **75** were treated with TsOH (1 eq) at room temperature in CH₂Cl₂ to give the corresponding diketopiperazines *cis*- and *trans*-**76** (Scheme 26, Table 2).

From the results of alkylation reactions the following mechanistic rationale may be deduced (Scheme 27).

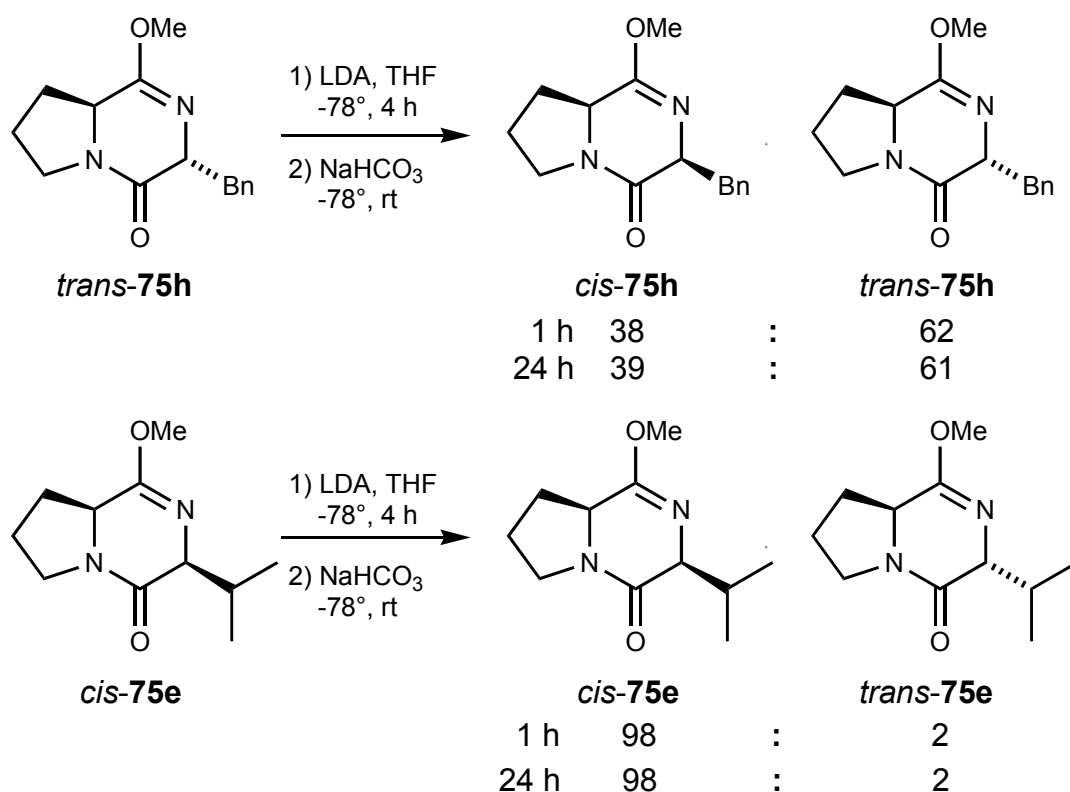


Scheme 26

Assuming a Li-mediated attack of the electrophile, four different geometries **A–D** are conceivable. Small electrophiles such as methyl or ethyl iodide are preferably delivered from the top face (*Si* face) of the carbanion (**A**), because attack from the bottom face interferes with the lone pair at N(5). In the case of the more bulky *i*-propyl and *i*-butyl electrophiles, two competing geometries are possible, which, however, suffer either from steric hindrance between the alkyl moiety of the electrophile and the pyrrolidine ring (**B**) or from the lone pair repulsion between the leaving halogen and N(5) (**C**), thus resulting in poor selectivities. For benzyl, allyl and prenyl halides bearing a π -system a favorable π - π -interaction between the electrophile and the carbanion is possible in geometry **D**^[60]. As described recently in the literature,^[60] the aromatic-prolyl interaction was proposed to be stabilized by a CH- π interaction, in which the aromatic ring donates electron density to the relatively electron-deficient C-H. This description suggests that electron-rich aromatic residues should stabilize this interaction and promote *cis* conformation. In contrast, electron-

deficient aromatic residues should yield a less favorable aromatic-prolyl interaction and relatively favor the *trans* conformation.

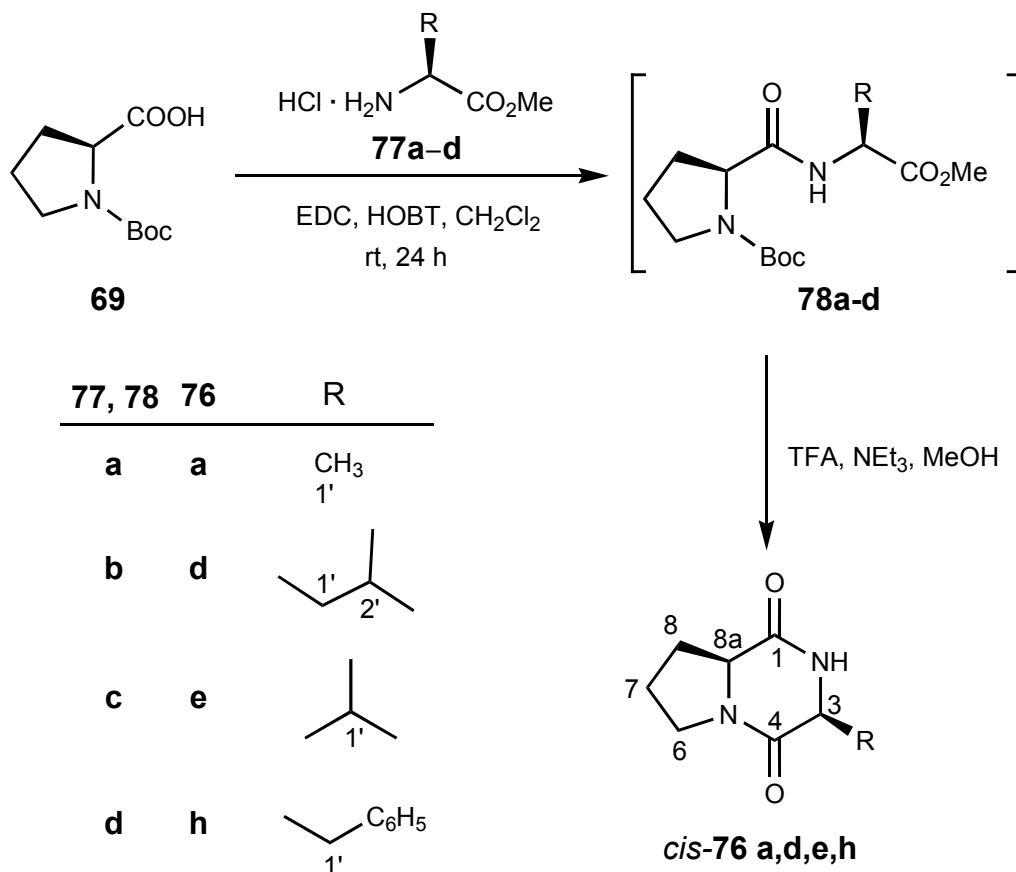
In order to control whether the diastereoisomeric ratio in the alkylation step is caused by epimerization, the isolated benzyl- and isopropyl-substituted lactim ethers *cis*-**75e** and *trans*-**75h** were treated with LDA in THF at -78°C for 4 h followed by quenching with aqueous NaHCO_3 (Scheme 26). At given time intervals, aliquots were taken from the reaction mixture and directly analyzed by capillary GC (**75h**) or HPLC (**75e**). In the case of the benzyl derivative *trans*-**75h**, a significant amount of the *cis*-congener was detected after 1 h (*cis* : *trans* = 38 : 62), remaining nearly constant after 24 h. Thus, the excellent *trans*-selectivity found in the alkylation step is probably due to kinetic control. In contrast, the isopropyl compound *cis*-**75e** epimerized only to a small extent, resulting in a diastereoisomeric ratio *cis* : *trans* = 98 : 2 after 24 h (Scheme 28).



Scheme

28

4.3.2 Configuration determination via synthesis of the diketopiperazines (76a,d,e,h) starting from the corresponding amino acids



Scheme 29

In order to confirm the preliminary stereochemical assignment of the lactim ethers **75** and the corresponding diketopiperazines **76** based on NMR and NOE experiments, the *cis*-diketopiperazines *cis*-**76a,d,e,h** derived from methyl L-alaninate (**77a**), L-leucinate (**77b**), L-valinate (**77c**) and L-phenylalaninate (**77d**) were prepared as outlined in Scheme 29. Following a procedure by de Costa,^[56] L-proline derivative **69** was condensed with the amino acid esters **77** in the presence of EDC and HOBT to give intermediate dipeptides **78a-d** which were immediately cyclized to the diketopiperazines *cis*-**76** (Scheme 29).

NMR data (Table 3) and optical rotation values together with an X-ray crystal structure analysis of methyl-substituted diketopiperazine *cis*-**76a** derived from L-alanine (Figure 2) confirm the *cis*-diastereomer assignment. Further support gave the X-ray crystal structures of the isobutyl-substituted diketopiperazines *cis*-**76d** and *trans*-**76d** (Figures 3a, b) isolated via the alkylation route after chromatographic separation, and prenyl-substituted diketopiperazine *trans*-**76g** obtained via hydrolysis on silica gel (Figure 4).

Table 3. The comparison of ^{13}C -NMR chemical shifts [δ (ppm)] for *cis*-diketopiperazines **76a,e,d,h** via alkylation (**1**) and cyclisation (**2**)

	<i>cis</i> - 76a	<i>cis</i> - 76e	<i>cis</i> - 76d	<i>cis</i> - 76h
^{13}C	1 / 2	1 / 2	1 / 2	1 / 2
CH ₃	-	16.0 / 16.0	21.2 / 21.2	-
CH ₃	-	19.3 / 19.3	23.3 / 23.3	-
C-7	22.7 / 22.1	22.4 / 22.4	22.8 / 22.8	22.5 / 21.7
C-8	28.1 / 28.1	28.3 / 28.3	28.1 / 28.1	28.3 / 29.0
C-1'	15.9 / 16.0	28.5 / 28.5	38.5 / 38.5	36.8 / 40.7
C-2'	-	-	24.6 / 24.6	-
C-6	45.4 / 45.5	45.1 / 45.1	45.5 / 45.5	45.4 / 45.2
C-3	51.2 / 51.2	58.8 / 58.8	53.4 / 53.4	56.2 / 57.8
C-8a	59.3 / 59.3	60.4 / 60.4	58.9 / 58.9	59.1 / 59.2
C-1	166.5 / 166.5	164.9 / 164.9	166.3 / 166.3	165.1 / 162.5
C-4	170.7 / 169.3	170.0 / 170.0	170.4 / 170.4	169.4 / 169.0

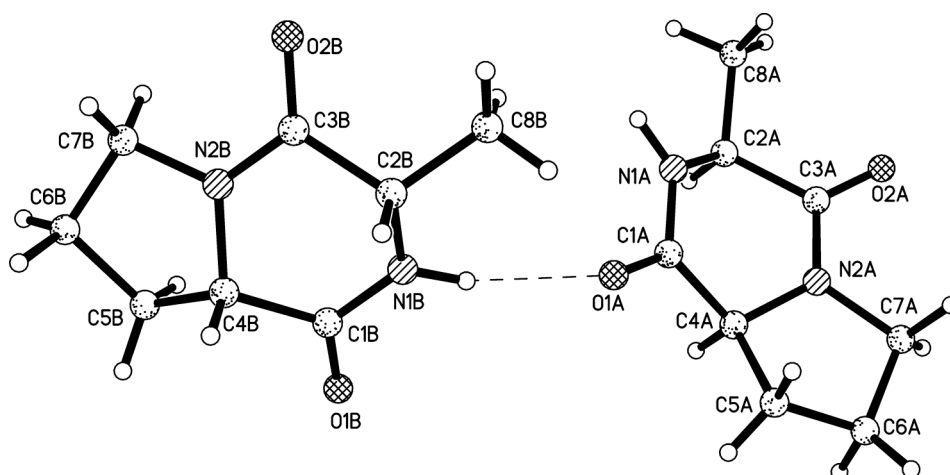


Figure 2. Molecular structure of diketopiperazine *cis*-76a (ORTEP presentation)

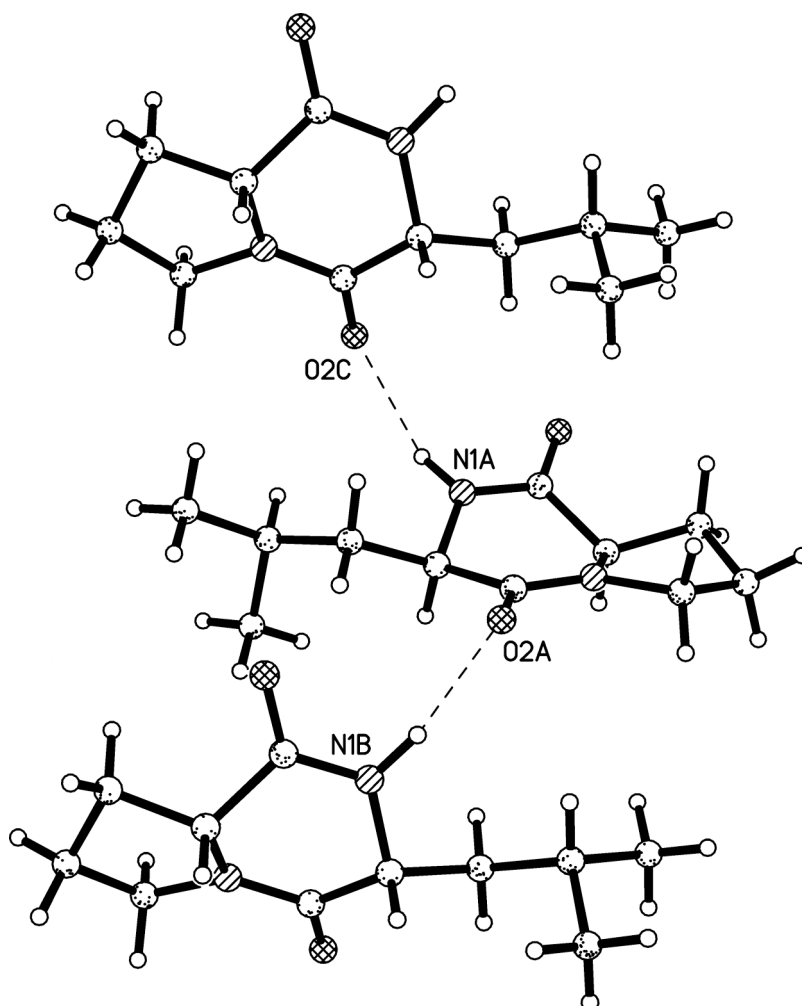


Figure 3. Molecular structure of diketopiperazine *cis*-76d (ORTEP presentation)

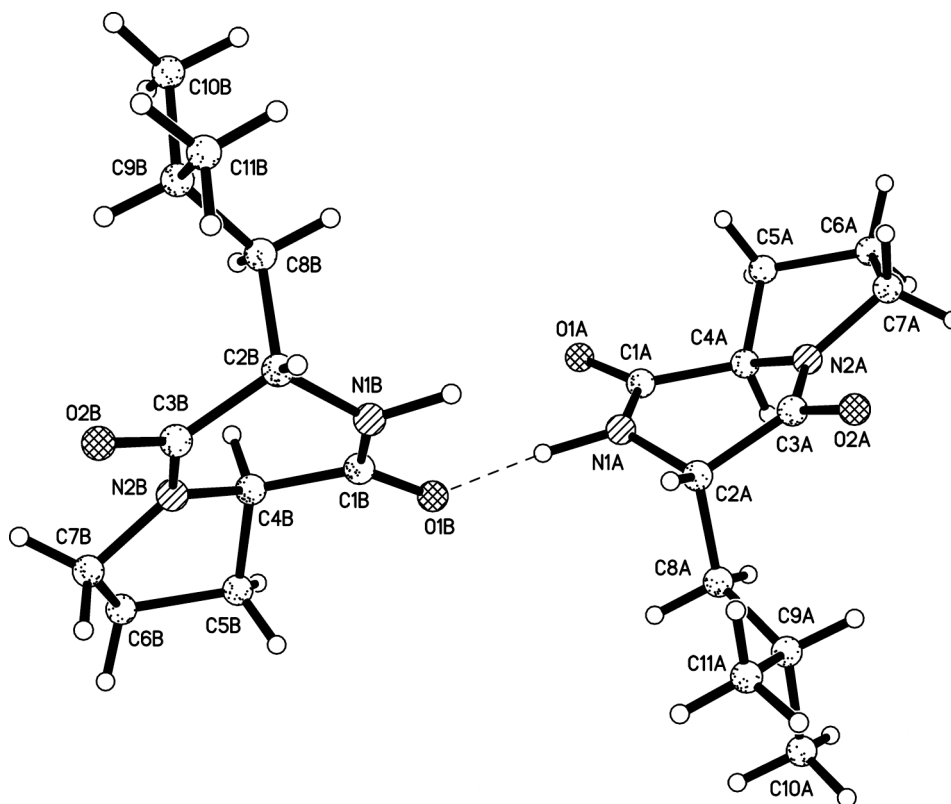


Figure 4. Molecular structure of diketopiperazine *trans*-76d (ORTEP presentations)

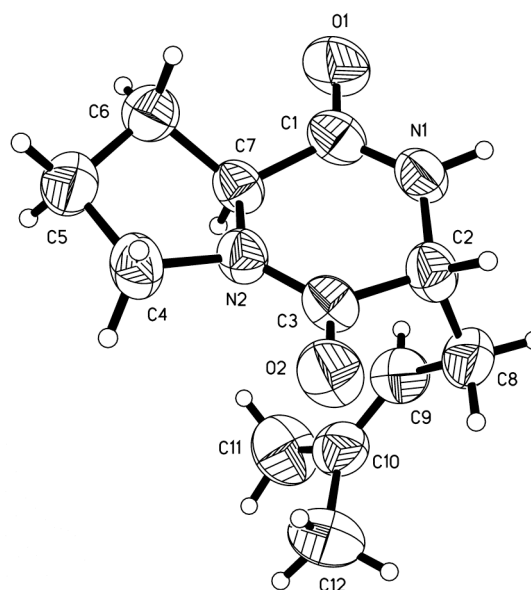


Figure 5. Molecular structure of diketopiperazine *trans*-76g (ORTEF presentation)

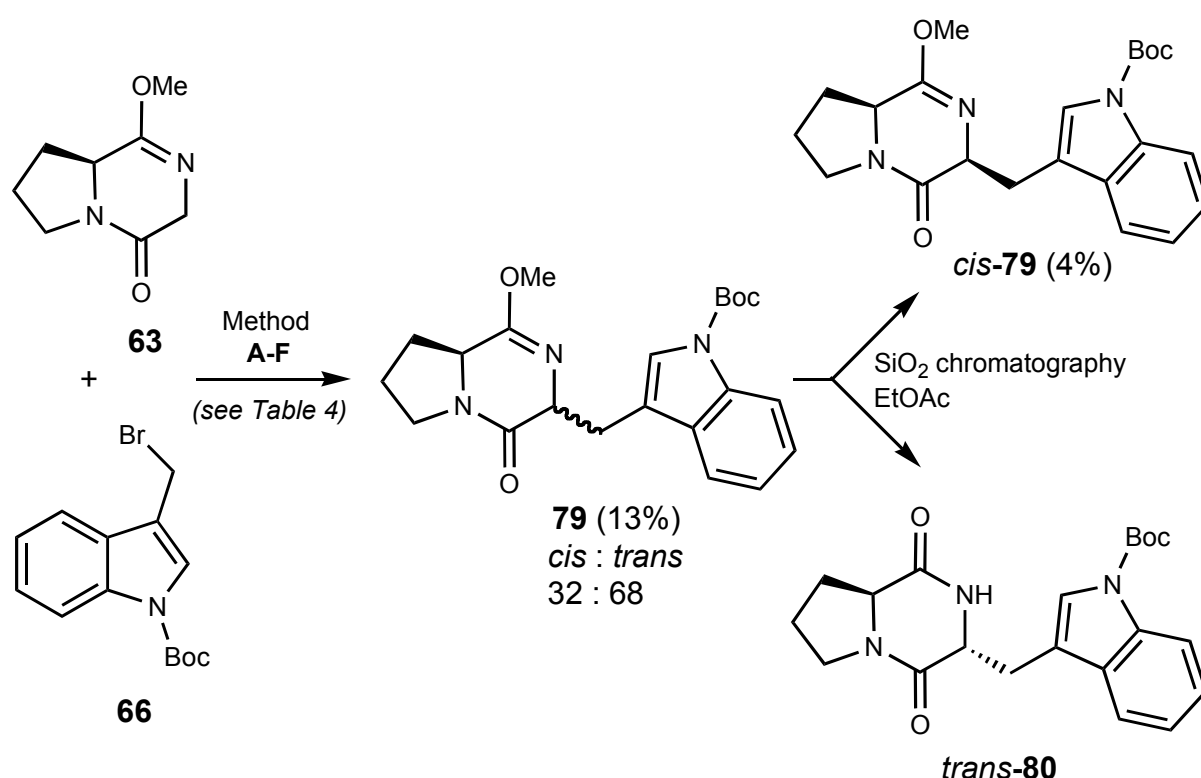
The compounds **70** and **76** crystallized from *i*-propanol in chiral space groups as pure enantiomers. In all cases the determination of the absolute configuration by X-ray analysis was not possible due to lack of atoms with evident anomalous scattering parts (see crystal structures of **76d** in Figure 3, 4). Nevertheless, the data of X-ray analysis unambiguously confirm the discussed *cis/trans* configuration of the diastereoisomers **76**. In the solid state compounds **76** are stabilized by strong intermolecular hydrogen bridges between the N–H donor and oxygen of the carbonyl functions. This hydrogen bridge is nearly linear with the exception of *cis*-**76d** (Figure 3), where the N–H · · · O bridge angle is 145°.

Also a comparison of NMR data (Table 3) and optical rotation values of L-phenylalanine-derived *cis*-**76h** and *trans*-**76h** indicate correct assignment of the diastereomers. At this point, it should be mentioned that the hydrolysis of lactim ethers **75** to **76** did not affect the center of chirality at C(3). Isolated *cis*- and *trans*-lactim ethers **75** gave in each case a single diketopiperazine **76** with the same configuration at C(3) and C(8) when treated with TsOH.

4.4 Synthesis of tryprostatin B (20b)

4.4.1 The alkylation of lactim ether (75) with the indole derivative (66)

Based on the alkylation experiments of the lactim ether **63** with various electrophiles described in chapter 6, the alkylation reaction with the indole derivative **66** was carried out under similar reaction conditions (Scheme 30, Table 4).



Scheme 30

According to the procedure used in the alkylation with different electrophiles, lactim ether **63** was treated with LDA at -78°C in THF for 20 h and the indole derivative **66** was added in a 1:1 molar ratio (Method A). Because the desired alkylated product resulted only in traces identified by GC-MS, the reaction conditions were adjusted. However, variation of the base in different equivalent ratios (1-6 eq) and the temperature (-78° to -20°C) gave the desired alkylated product only in traces (by GC-MS) (Table 4).

Table 4. Reaction conditions for the alkylation of lactim ether **63** with bromo indole derivative **66**

Method	Base	Solvent	Temp.	Yield	<i>cis/trans</i>
A	LDA (1 eq)	THF	-78°C	-	-
B	<i>n</i> BuLi (1 eq)	THF	-78°C	-	traces
C	LDA(1 eq)	THF	-78°C to -20°C	-	traces
D	LDA (6 eq)	THF	-78°C	-	traces
E	K ₂ CO ₃	MeCN	rt	8%	38:62
F	LDA (1 eq)	THF/ HMPA	-78°C	13%	32:68

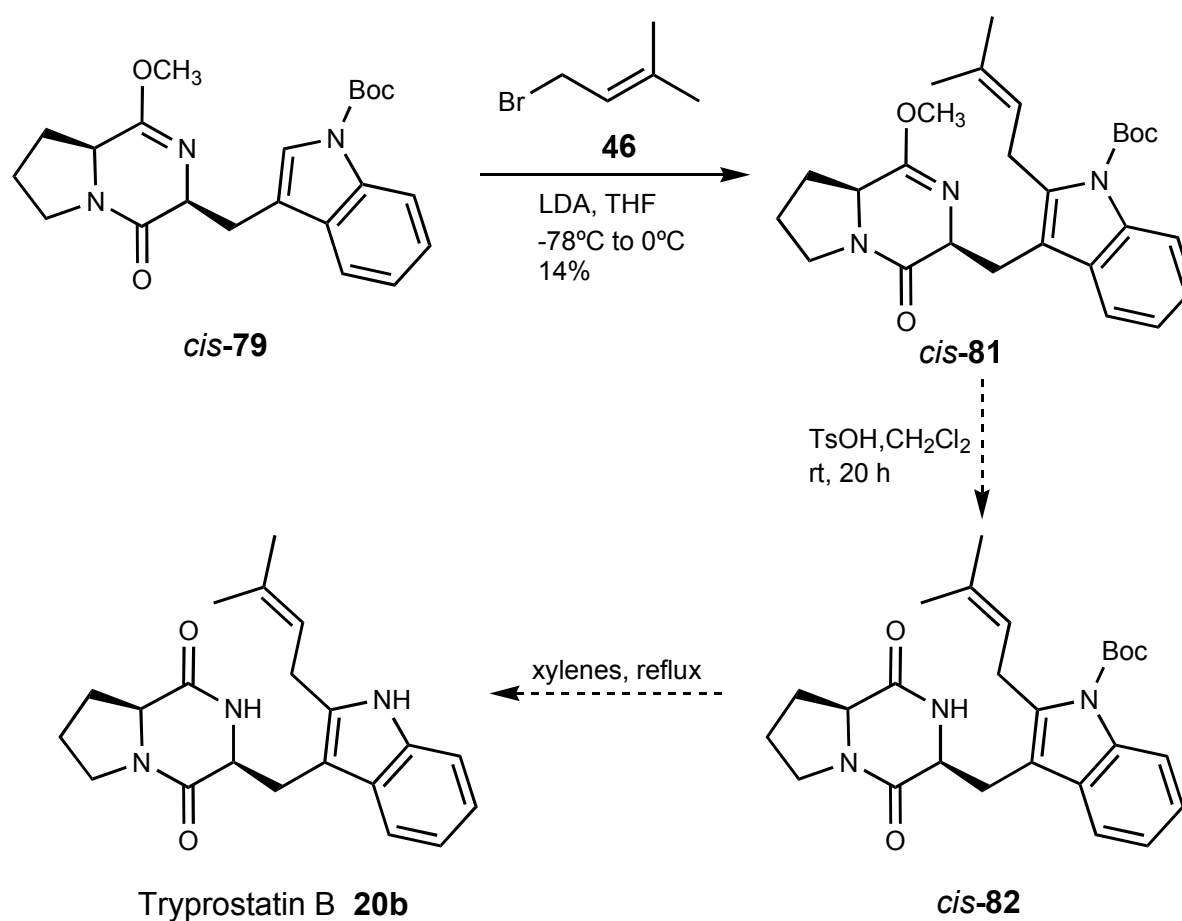
Another route has been taken^[62], when the alkylation was performed under very mild phase transfer catalysis conditions employing potassium carbonate in acetonitrile and tetra-*n*-butylammonium bromide (TBAB, 10 mol%) as catalyst. Unfortunately, this method led to very small amounts of desired alkylated products, with a conversion of 5% and 3%, respectively, identified with GC. When hexamethylphosphoramide (HMPA) was used as a co-solvent, in the presence of LDA in THF as a base, the reaction conditions proved to be successful. The lactim ether **63** was deprotonated with LDA for 4 h, at -78°C then HMPA was added and the reaction mixture was stirred for 45 min, at the same temperature. A solution of the indole derivative **63** in THF was added and the reaction mixture was kept over night at -78°C, leading to a mixture of diastereomers in 13% yield and a ratio of *cis* : *trans* = 32 : 68. During purification by flash chromatography on silica gel with ethyl acetate as eluent, the diastereomer *trans*-**79** hydrolysed to the corresponding diketopiperazine **80**.

The treatment of LDA dimer with HMPA, a dipolar aprotic solvent with excellent ability of forming cation-ligand complexes, causes sequential solvation of the Li cation, increasing the reactivity through cation coordination. Furthermore, the same pattern as in the case of *trans*-diastereoisomers of prenyl- and 3-chlorobenzyl-substituted lactim ethers **75g,I** has been observed, as the *trans*-diastereomer turned

out to be more prone to hydrolysis than the *cis*-congener. Upon prolonged chromatographic purification the *trans*-diketopiperazine *trans*-80 was isolated rather than the corresponding lactim ethers *trans*-79, whereas the *cis*-lactim ethers *cis*-79 was obtained without any problem.

4.4.2 The alkylation of indole lactim ether (*cis*-79) with isoprenyl derivative (46)

For the total synthesis of tryprostatin B **20b**, the 2-isoprenyltryptophan derivative was required. To introduce the isoprenyl group at the indole C-2 position, the substrate *cis*-79 was deprotonated using LDA as a base, in THF at -78°C , to form the corresponding anion. This step was followed by addition of pure isoprenyl bromide **46**, to yield the alkylated product *cis*-81 in 14% yield (Scheme 31).



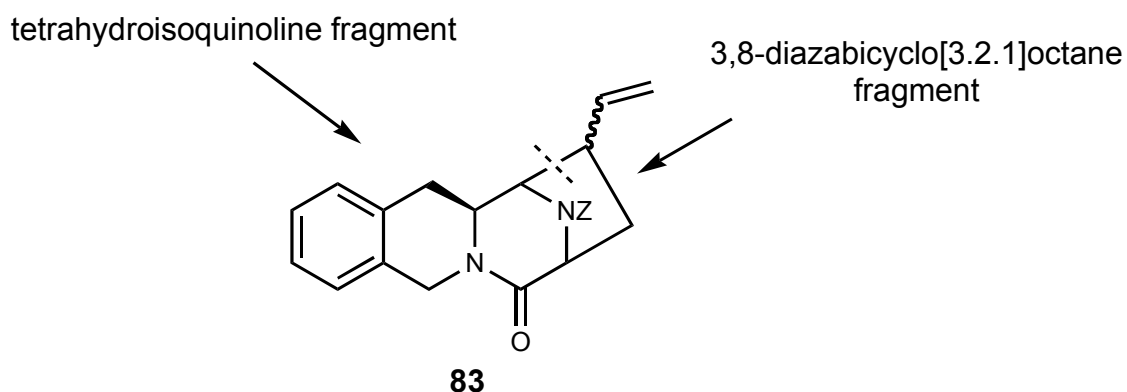
Scheme 31

According to the literature,^[48] the compound *cis*-**81** would be treated with TsOH (1 eq) at room temperature in CH₂Cl₂ to give the corresponding diketopiperazine *cis*-**82** (Scheme 31). The Boc group removal, by refluxing in xylenes,^[37] would complete the synthesis of tryprostatin B **20b**.

Although the yields of the alkylation reactions are modest, these are the first attempts toward the total synthesis of tryprostatin B **20b** and the synthesis method has great potential for optimization.

4.5 Quinocarcin ring system: structure analysis and previous synthesis in the literature

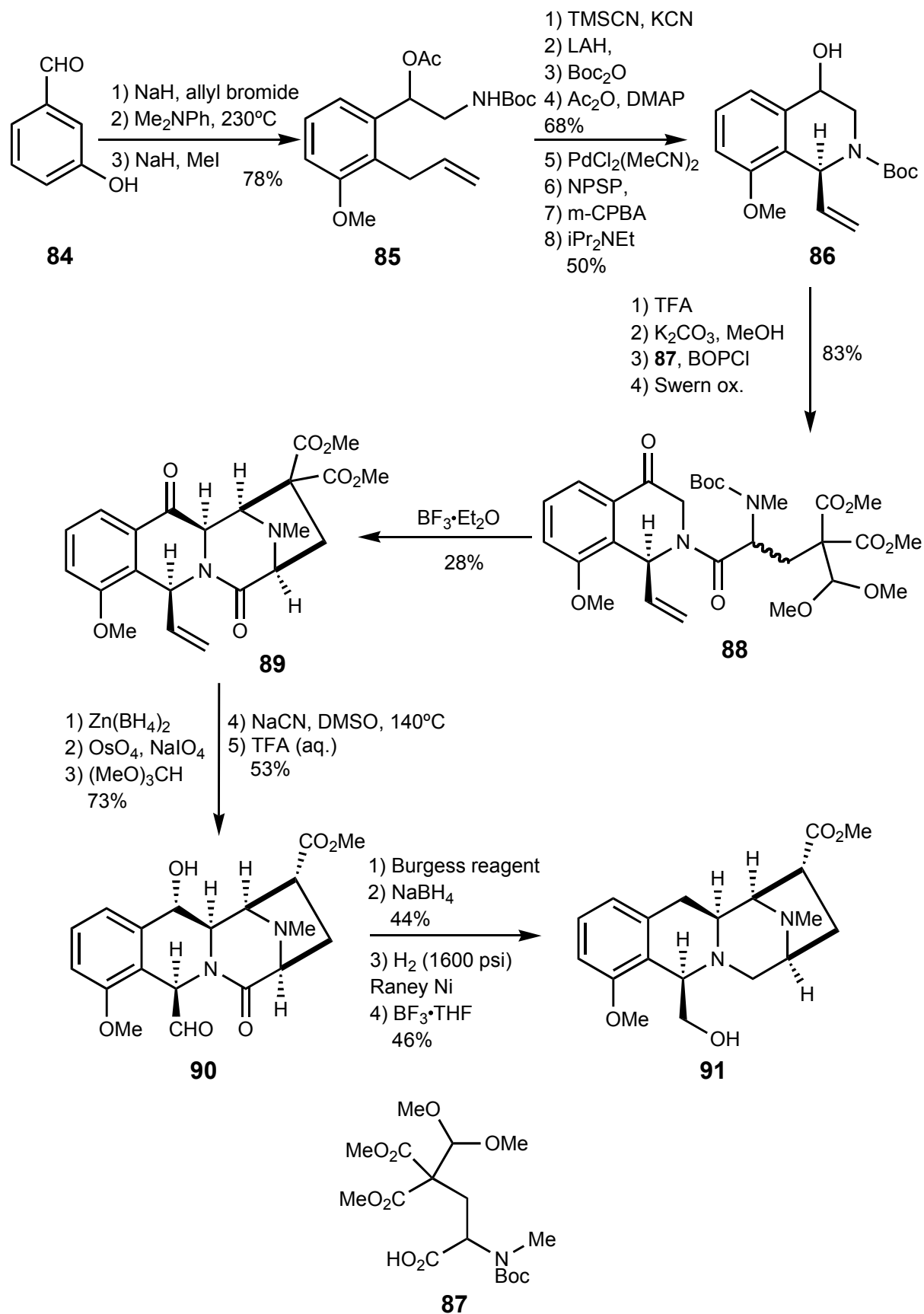
The quinocarcin ring system is divided in two major fragments (Scheme 32). The first fragment is represented by the isoquinoline structural motif, which by transformation into tricyclic diketopiperazine, provides the first three rings of the quinocarcin precursor molecule. The congruence of the isoquinoline segment of the quinocarcin system with other natural products indicated that this substructure is critical for biological activity. The apparent potent activity of the quinocarcins tends to suggest that the hexahydroiminoazepinoisoquinoline ring system may house much of the antibiotic function.^[63] The fourth ring is formed by introduction of a side chain in the tricyclic diketopiperazine fragment, followed by cyclization.



Scheme 32

Due to the promising antibiotic and antitumor activities displayed by the class of compounds that share the quinocarcin ring system, interest in the total synthesis of biological active structural analogues has attracted considerable attention.^[64-67]

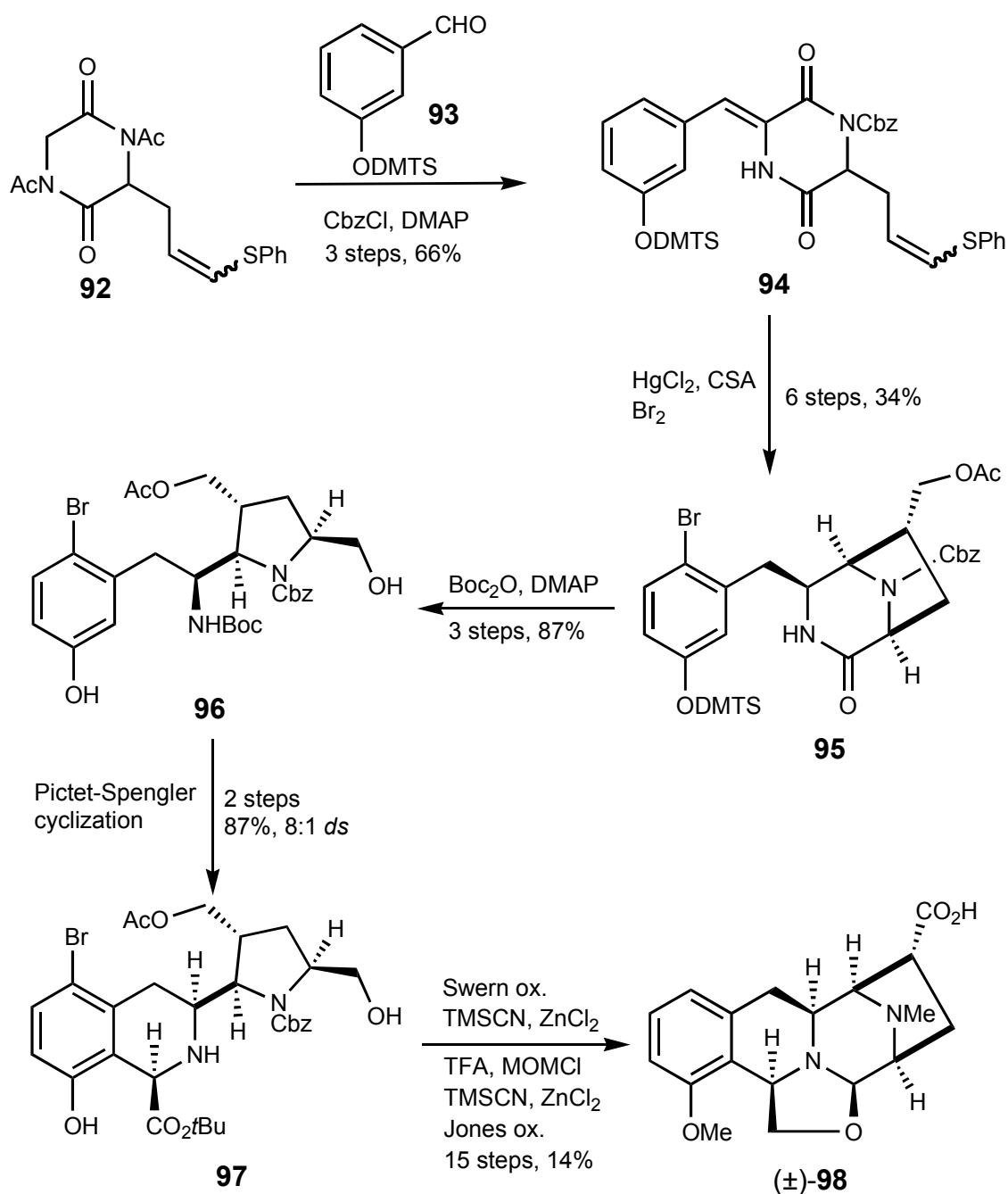
One of the first quinocarcin derivatives, quinocarcinol methyl ester **90** was synthesized by Danishefsky and co-workers in 1985 (Scheme 33).^[63] Their interest in the quinocarcin class evolved from a long term pursuit directed to the total synthesis of a related antibiotic.



Scheme 33

Starting with the aromatic aldehyde **84**, in Scheme 33 the phenol was allylated followed by Claisen rearrangement and methylation of the phenol. Conversion of the aldehyde to cyanohydrin was followed by reduction of the nitrile using Lithium aluminium hydride (LAH). Protection of the amine and alcohol provided **85**, which was followed by treatment of the allyl group with $\text{PdCl}_2(\text{MeCN})_2$ complex to afford a mixture of *E* : *Z* benzylic olefins. Further treatment with *N*-phenylselenophthalimide (NPSP) in the presence of camphorsulfonic acid followed by treatment with *m*-CPBA and Hünig's base, then removal of the Boc and acetate protecting groups afforded the secondary amine **86** which was coupled with the amino acid **87** using BOPCl. Further Swern oxidation afforded the ketone **88** in 83% yield and treatment with $\text{BF}_3 \cdot \text{Et}_2\text{O}$ afforded the tetracycle **89** in 28% yield, only one from the possible four diastereomers. Reduction of the benzylic ketone was followed by oxidative cleavage of the olefin to the corresponding aldehyde, which was protected as dimethylacetal. Diastereoselective decarbomethoxylation was accomplished using sodium cyanide in DMSO at 140°C. The acetal was then cleaved to afford the aldehyde **90** and the elimination of the hydroxyl group in **90** was accomplished using the Burgess reagent followed by reduction of the aldehyde. The final steps to quinocarcinol methyl ester **91** were the reduction of the benzylic olefin using high pressure hydrogenation over Raney-nickel followed by reduction of the amide to the amine using borane in THF.

The first total synthesis of (\pm)-quinocarcin was achieved by Fukuyama and Nunes^[64] in 1988. Starting with diethyl malonate, diketopiperazine **92** was synthesized in seven steps in 39% overall yield (Scheme 20). Aldol condensation with aromatic aldehyde **93**, followed by selective protection of one of the lactam nitrogen atoms afforded diketopiperazine **94**. Reduction of the activated lactam carbonyl was followed by an acyliminium ion-mediated cyclization using HgCl_2 and camphorsulfonic acid. Reduction of the resultant aldehyde and the benzylic olefin from the least hindered face was followed by re-protection of the secondary amine as a benzyl carbamate. Subsequent acylation of the incipient alcohol afforded **95**. Ring opening was accomplished via activation of the lactam followed by treatment with sodium borohydride to afford the pyrrolidine **96**, after silyl ether cleavage. TFA cleavage of the Boc carbamate was followed by a Pictet-Spengler cyclization to afford tetrahydroisoquinoline **97** in 86% yield as a 8 : 1 mixture of diastereomers.

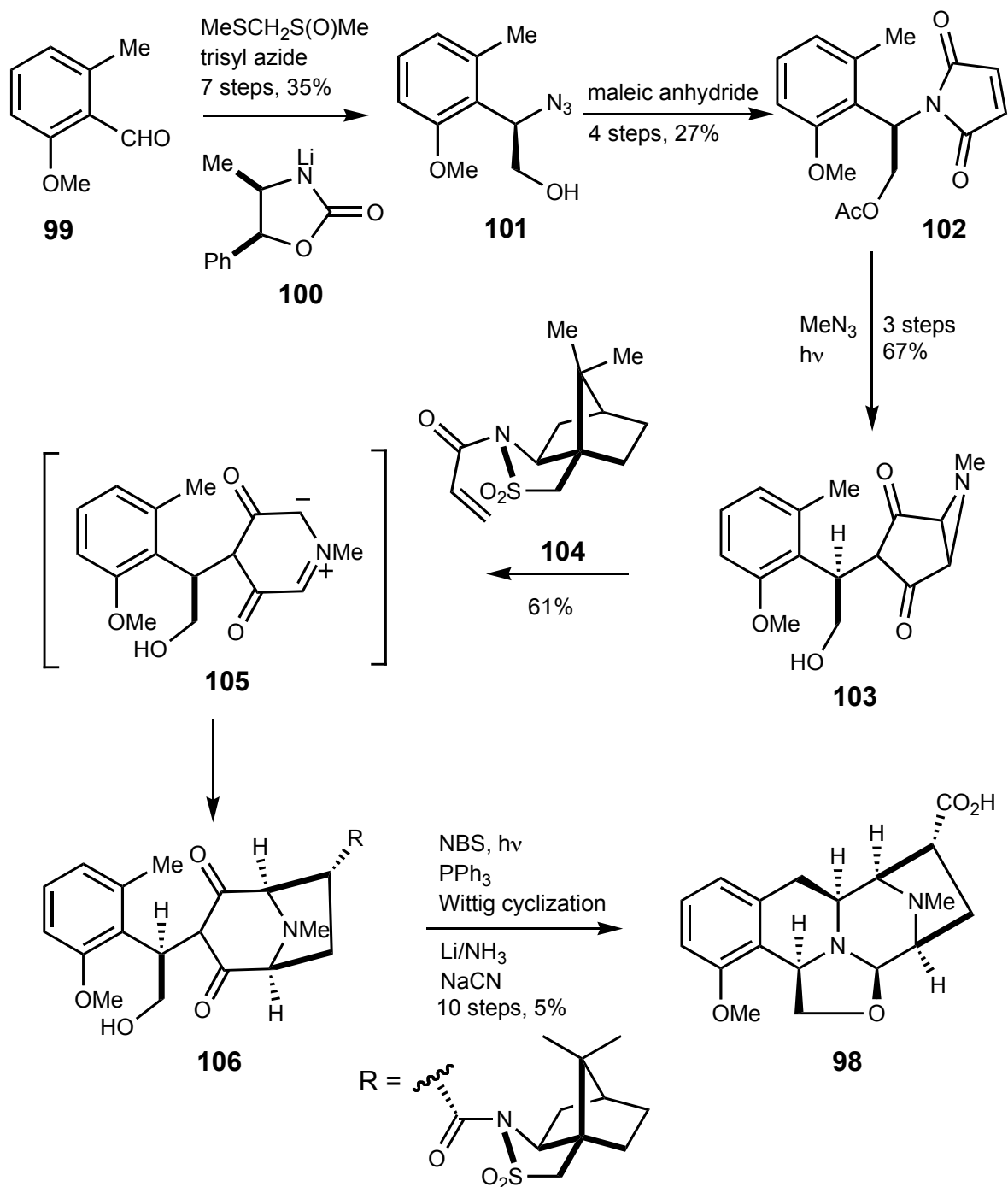

Scheme 34

Following Scheme 34, selective phenol acylation was followed by Swern oxidation of the primary alcohol. Treatment of the resultant amino aldehyde with TMS cyanide and zinc chloride afforded the tetracyclic core. Cleavage of the phenolic acetate was followed by phenol methylation and radical cleavage of the bromide. Cleavage of the *tert*-butyl ester and subsequent reduction of the carboxylic acid was followed by alcohol protection as the methoxymethyl ether. Removal of the acetate and Cbz groups was followed by *N*-methylation and oxidation of the alcohol to the carboxylic acid to afford the MOM-protected derivative. The final steps in the total synthesis

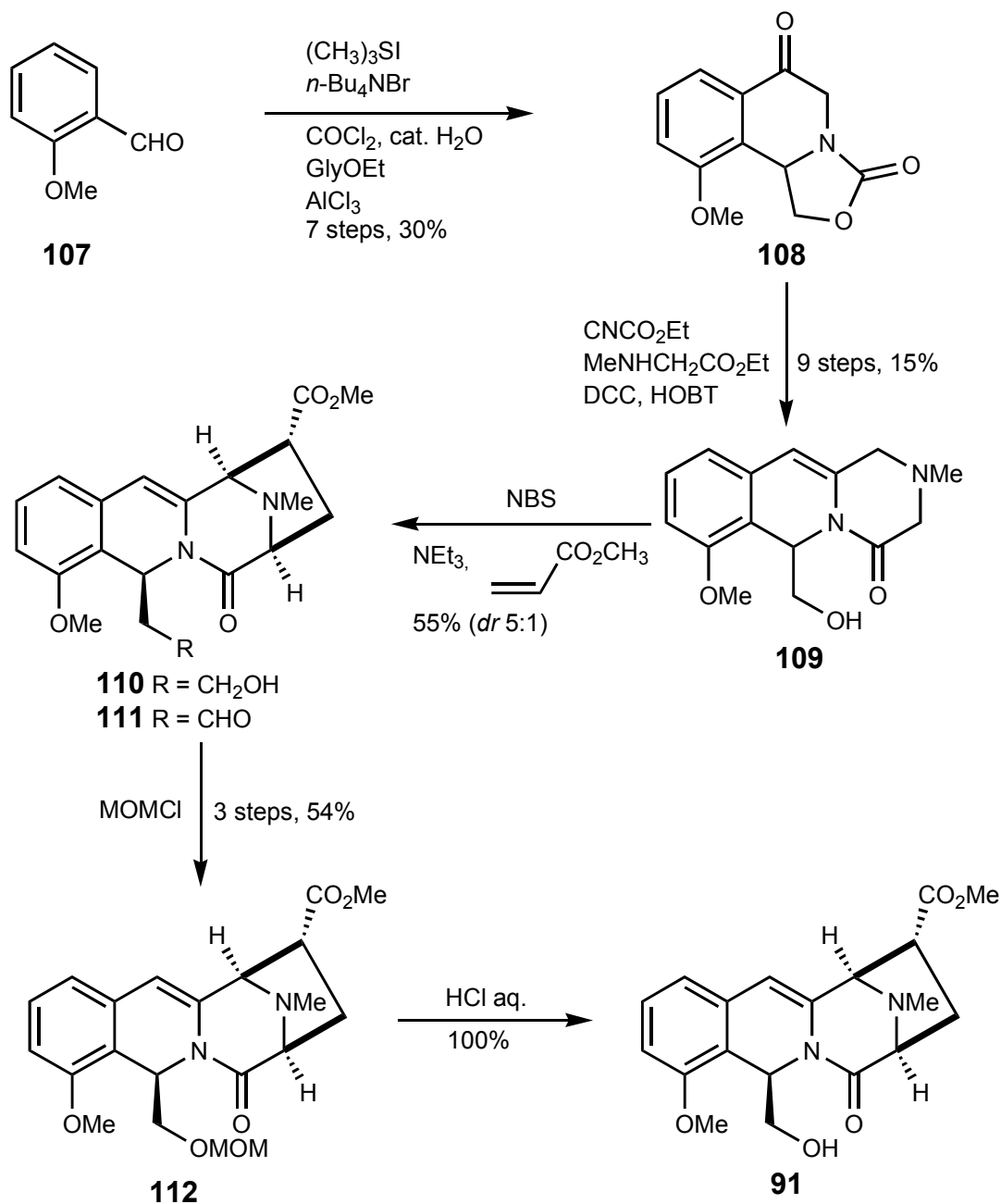
were the removal of the MOM group using TMSI in situ and the closure of the oxazolidine ring using silver nitrate to afford (\pm)-quinocarcin **98** in 70% yield for the final two steps.

Further approaches to the asymmetric synthesis of the quinocarcin ring system are oriented toward dipolar cycloadditive strategy.^[65-68]

In 1992, Garner published the first asymmetric synthesis of (-)-quinocarcin.^[66, 77] The key step involved an intermolecular 1,3-dipolar cycloaddition, as shown in Scheme 35. Starting with aldehyde **99**, the optically active azido alcohol **101** was obtained over 7 steps. Treatment of **99** with methylsulfinylmethyl sulfide in the presence of Triton B and acidic hydrolysis afforded a carboxylic acid. Formation of the mixed anhydride and treatment with the chiral auxiliary **100**, followed by deprotonation and treatment with trisyl azide and reductive cleavage provided the azido alcohol **101** in an overall yield over 7 steps of 35% along with the recovery of the chiral auxiliary **100** in 96%. Hydrogenolysis of the azide was followed by treatment with maleic anhydride. Cyclization to form the maleimide was accomplished using acetic anhydride to form **102** as the major product. Hydrolysis of the acetate **102** was followed by treatment with methyl azide. Irradiation using a high-pressure Hg lamp extruded nitrogen, affording aziridine **103** in high yield. The azomethine ylide **105** was formed via irradiation of aziridine **102** and the ylide was then trapped with Oppolzer's sultam **104** to afford the desired bicyclic cycloadduct, via an *exo-si* attack on the olefin. Protection of the alcohol group was followed by benzylic bromination with NBS. Conversion to the phosphonium salt was followed by deprotonation to form the ylide, which suffered intramolecular Wittig cyclization. High pressure reduction of the benzylic olefin was followed by hydrolysis of the sultam. High pressure hydrogenation provided a 1 : 1 mixture of the desired compound along with the product of reduction of the sultam imide to a primary alcohol. Partial reduction of the amide was accomplished by using a dissolving metal reduction, followed by trapping of the carbinolamine with sodium cyanide to provide the stable aminonitrile. The final two steps, as in Fukuyama's synthesis, were the cleavage of the MOM group and closing of the oxazolidine ring to afford (-)-quinocarcin **68** (Scheme 35).


Scheme 21

In 1995, Flanagan and Williams published the synthesis of (\pm)-quinocarcinamide **91** (Scheme 36). A late stage intermediate intersected Garner's total synthesis of quinocarcin, thus making this a formal total synthesis of D,L-quinocarcin. The key step in this synthesis was an intermolecular azomethine ylide using NBS to oxidize an allylic amine was developed.

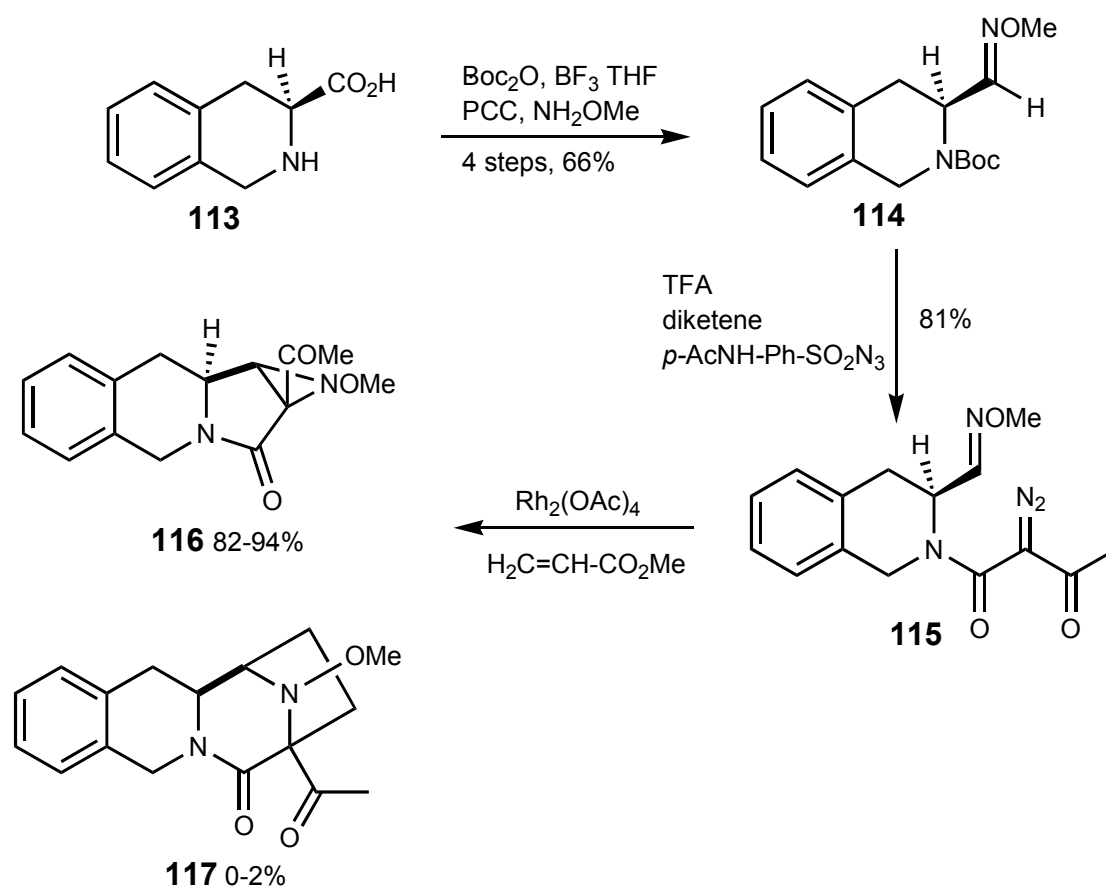


Scheme 36

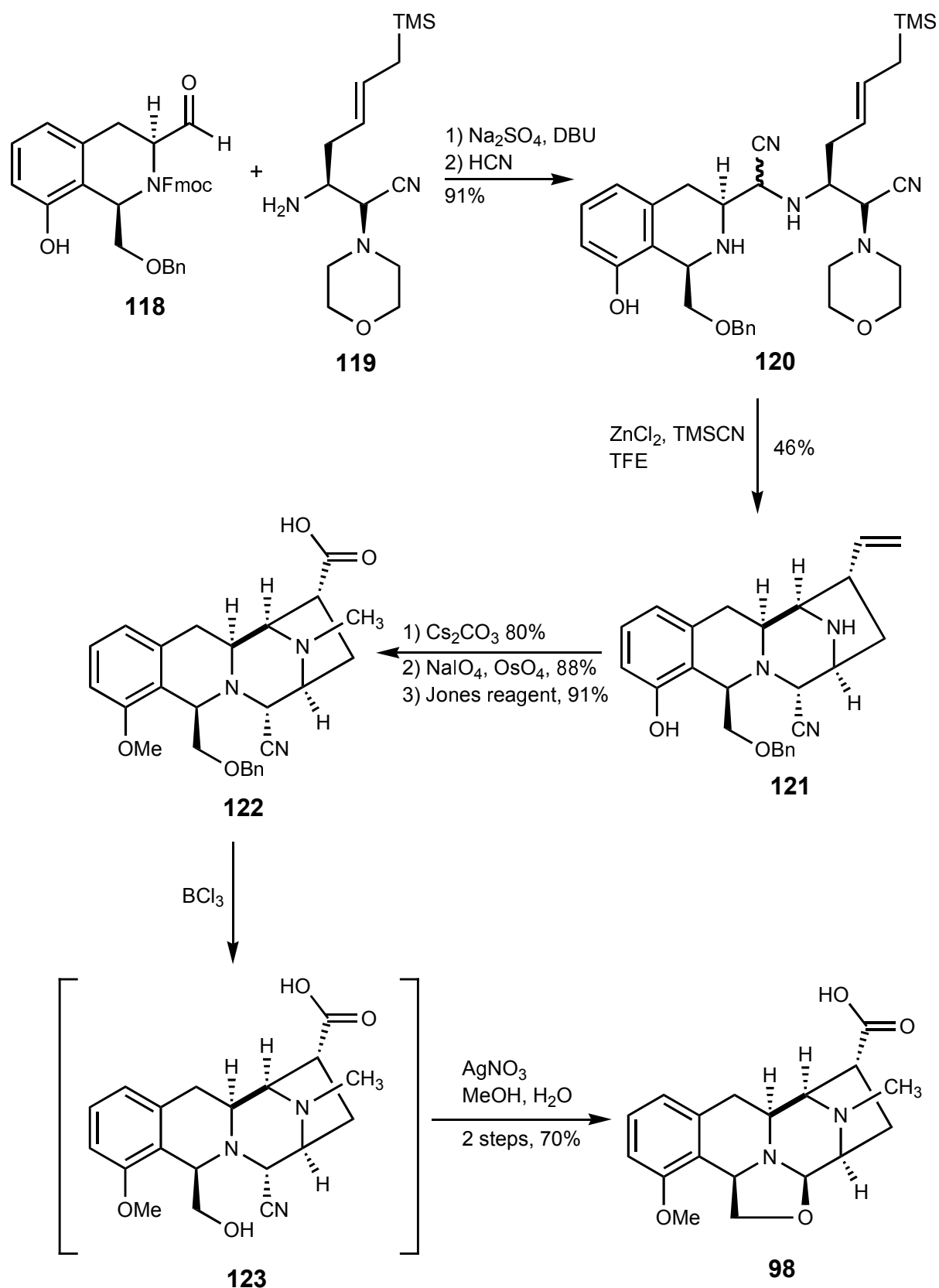
Treatment of *o*-anisaldehyde **107** with trimethylsulfonium iodide under phase-transfer conditions afforded the benzylic epoxide which was opened with phosgene to form the chloroformate. Conversion to the carbamate was accomplished via treatment with glycine ethyl ester. Cyclization afforded the oxazolidinone, which upon saponification yielded the carboxylic acid, which was converted to the corresponding acid chloride. An intramolecular Friedel-Crafts acylation provided isoquinolone **108** in 30% overall yield.

Treatment with LDA and ethyl cyanofornate followed by reduction of the ketone afforded the β -hydroxy ester, that was converted to the allylic alcohol. Formation of the allylic chloride was followed by treatment with sarcosine ethyl ester to afford the allylic amine. Hydrolysis of the oxazolidinone was followed by coupling of the secondary amine upon the resultant acid to afford the tricyclic compound **109**. NBS oxidation of the allylic amine afforded a dark green solution of the incipient iminium salt, which upon deprotonation using triethylamine resulted in a dark blue solution of the azomethine ylide. Treatment of this substance with methyl acrylate afforded 5 : 1 ratio of cycloadducts. Unfortunately, the desired diastereomer **110** was the minor product of the cycloaddition. The major product was efficiently epimerized to **110** via three steps sequence of oxidation to aldehyde, epimerization using DBU and final reduction of aldehyde to the alcohol **111**. Protection of the alcohol as the MOM ether (**112**) was followed by high-pressure reduction of the benzylic olefin. Saponification of the ester and removal of the MOM group afforded (\pm)-quinocarcinamide (**91**).

In 1996, McMillis attempted to form an azomethine ylide similar to the Garner and Williams intermediates via rhodium-catalyzed carbene cyclization (Scheme 37). Conversion of commercially available **113** to the oxime **114** was accomplished via a four-step sequence in 66% overall yield. Removal of the Boc group from **114** was followed by α -diazoamide formation using Davies protocol to afford **115**. Unfortunately, upon treatment of **115** with the rhodium catalyst, the desired tetracycle **117** could only be detected in very small amounts. Aziridine **116** was the major product in all attempts using both rhodium and copper catalysts.


Scheme 37

One of the most recent asymmetric synthetic routes to (-)-quinocarcin involves the direct condensation of C- and N-protected α -amino aldehyde derivatives (Scheme 38). The major bond formations were achieved using simple condensation reactions of α -amino aldehyde derivatives.^[69] The synthetic sequence to (-)-quinocarcin developed is illustrated in Scheme 38 and employs as starting materials the N-protected α -amino aldehyde **118**, comprising the A and B ring of the target and the C-protected α -amino aldehyde **119**. Condensation of **118** and **119** in dichloromethane in the presence of sodium sulfate afforded the corresponding imine. Without isolation, the imine intermediate was treated with 1,8-diazabicyclo[5.4.0]undec-7-ene (DBU, 1.1 eq), cleaving the fluorenylmethoxycarbonyl (Fmoc) protective group and to the resulting product was added methanolic hydrogen cyanide (prepared *in situ*), leading to Strecker addition.

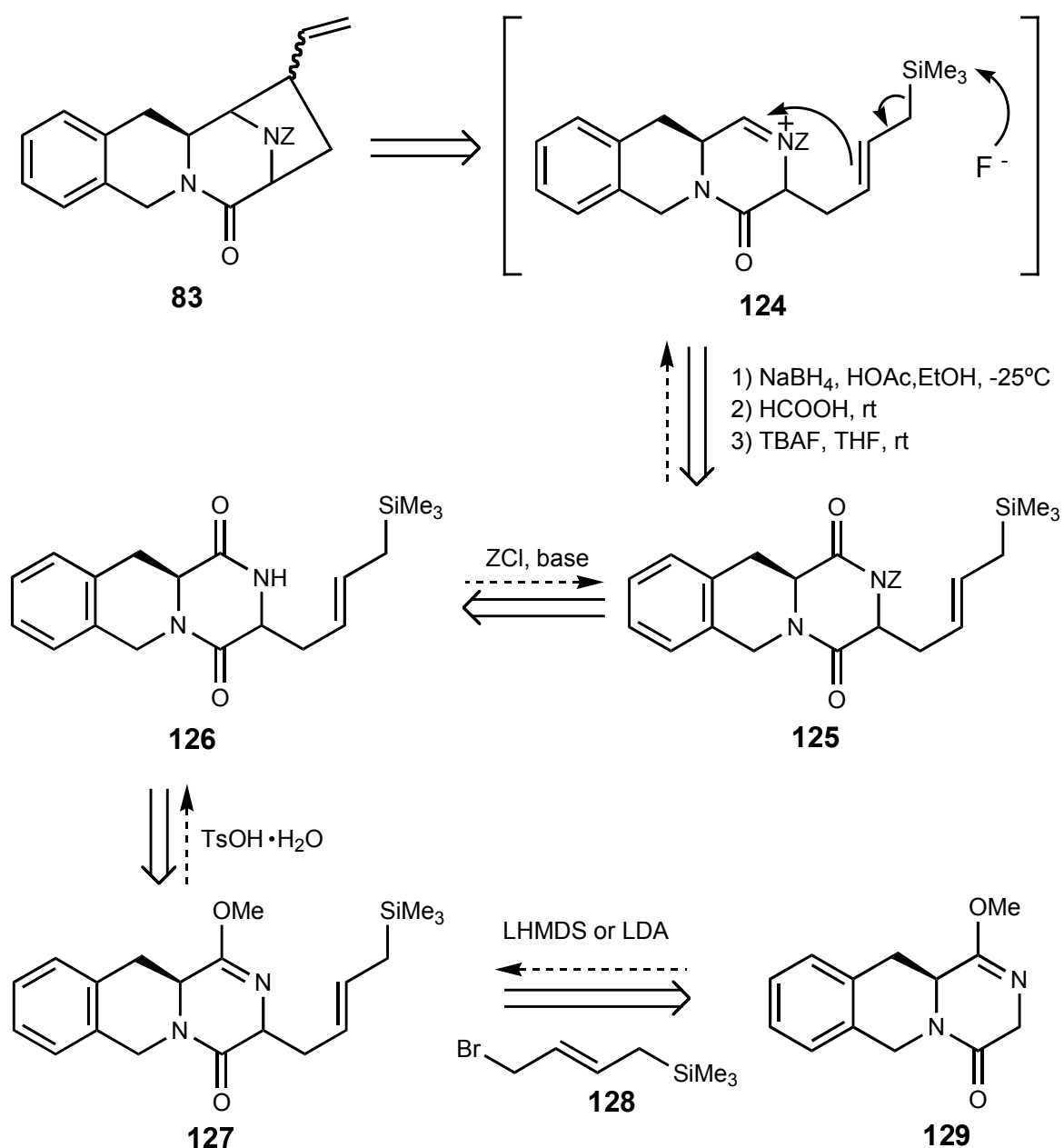


Scheme 38

This sequence conducted as one operation, afforded the bis-amino nitriles **118** as a mixture of diastereomers, as indicated, in 91% yield after flash-column chromatography. In the key transformation of the synthetic route, the mixture of diastereomers **120** was warmed in 2,2,2-trifluoroethanol (TFE) in the presence of trimethylsilyl cyanide and zinc chloride, forming the tetracyclic ring system of quinocarcin in the form of cyanopiperazine intermediate **121** (46% from **120**). This process which forms two of the four rings of the target and three of its six stereocentres, proceeds by initial cyclization of the C-ring in an intramolecular amino nitrile exchange and then by closure of the D-ring in an allyl silane-imine addition reaction. This proves to be critical to achieving proper stereochemistry of the D-ring. To complete the synthesis of the quinocarcin, the tetracyclic cyanopiperazine intermediate **121** was bis-methylated and the olefinic side chain of the resulting product was subjected to oxidative cleavage. The aldehyde formed was oxidized with Jones reagent in acetone to furnish the intermediate **122** (64% over three steps). Debenzylation of **122** with boron trichloride produced quinocarcin **98** and a small amount of its noncyclized precursor **91** also known as DX-52-1. By treating the crude mixture with silver nitrate in aqueous methanol, complete conversion to quinocarcin **98** was achieved (70% yield, two steps).

4.6 Retrosynthetic strategy for the quinocarcin precursor via stereoselective alkylation

The retrosynthesis strategy attempted in this work proceeds with the building of the quinocarcin ring system, following an allylsilane addition to the iminium ion in the derivative **124**. The piperazine **124** should be obtained from the tricyclic diketopiperazine **125**, by reduction with NaBH_4 and acetic acid, in EtOH at -25°C , followed by treatment with HCOOH at room temperature and *tert*-butylammonium fluoride (TBAF) in THF at room temperature.



Scheme 3

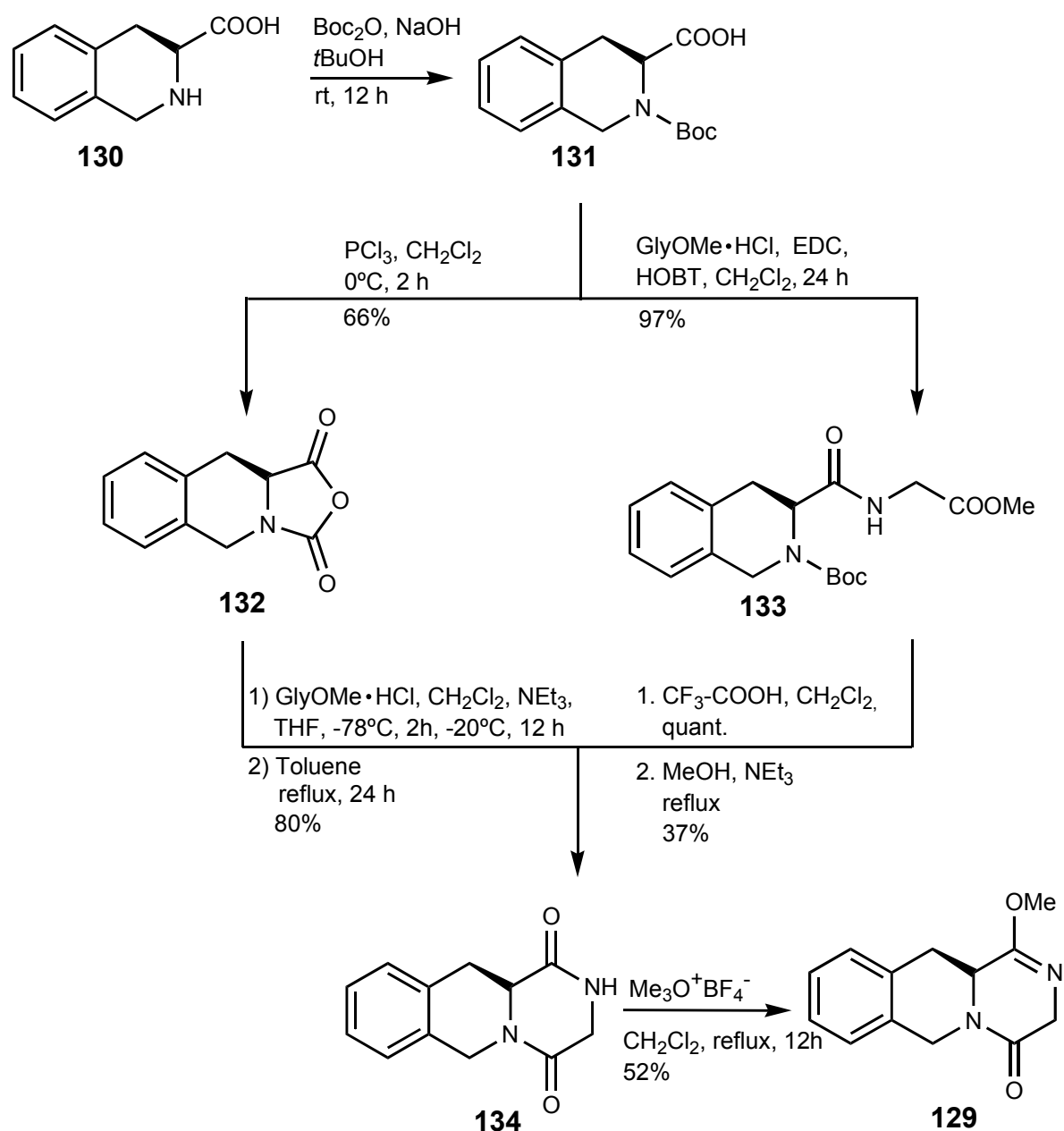
The *N*-protected tricyclic diketopiperazine **125** can be obtained from the tricyclic diketopiperazine **126**, by treatment with ZCl in the presence of a base. The tricyclic diketopiperazine **126** is obtained from the lactim ether **127**, by hydrolysis with TsOH•H₂O. The key transformation of the synthetic route is the alkylation of the tricyclic lactim ether **129** with the olefinic halogenide **128**, in the presence of LHMDs or LDA in THF, at -78°C, in order to incorporate the olefin in the molecule, that would react with the iminium ion functionality, to generate the quinocarcin ring system **83**. The tricyclic lactim ether **129** was obtained from tetrahydroisoquinoline carboxylic acid and L-phenylalanine by Pictet-Spengler cyclization and then treatment with Meerwein's salt, affording the first three rings present in the quinocarcin ring system (Scheme 39).

4.6.1 Synthesis of the tricyclic lactim ether fragment (129)

The tricyclic lactim ether fragment was synthesized via two methods^[48,56] and illustrated in Scheme 40. Enantiomerically pure L-tetrahydroisoquinoline carboxylic acid **130** obtained from L-phenylalanine by Pictet-Spengler cyclization,^[70] was converted into the known *N*-Boc-protected derivative **131**.^[71] Further treatment with phosphorus trichloride^[48] provided the anhydride **132** in 66% overall yield from **130**. Reaction of compound **132** with glycine methyl ester hydrochloride in the presence of triethylamine, followed by heating in toluene,^[44] afforded the tricyclic dioxopiperazine **134** in 80% yield.

The second method involves peptide coupling, between Boc-protected L-tetrahydroisoquinoline carboxylic acid **131** and glycine methyl ester hydrochloride, in the presence of 1-[3-(dimethylamino)propyl]-3-ethylcarbodiimide hydrochloride EDC and 1-hydroxybenzotriazole monohydrate HOBT leading to the corresponding peptide **133**, in 97%. Boc-deprotection with F₃C-COOH afforded the corresponding salt that was further refluxed in MeOH, with NEt₃ as a base, providing the cyclisation to diketopiperazine **134**.

The recrystallization from *i*-PrOH afforded the crystalline product, in 37% yield. Upon treatment of the diketopiperazine **134** with Meerwein's salt, the desired mono lactim ether **129** was obtained in 52% yield (Scheme 40).

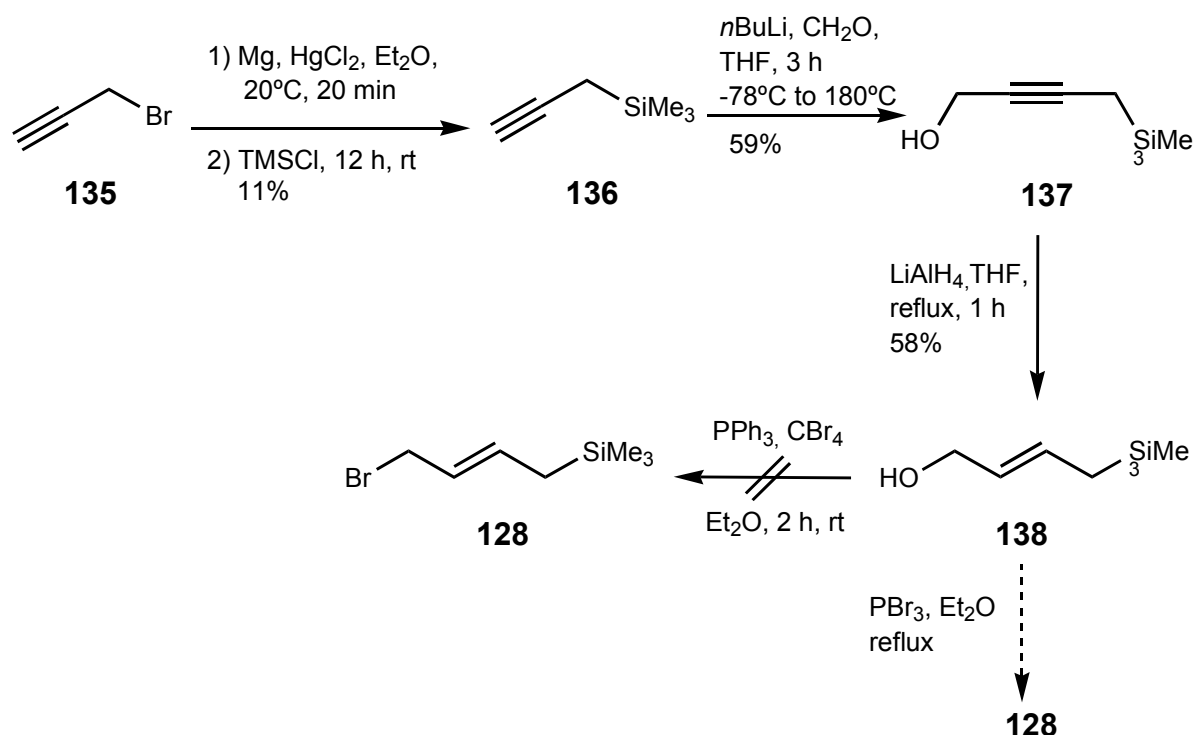


Scheme 40

4.6.2 Synthesis of (*E*)-4-bromo-2-butenyltrimethylsilane fragment (128)

The synthesis of the (*E*)-4-bromo-2-butenyltrimethylsilane fragment followed a known procedure^[72,73] (Scheme 41), starting from propargyl bromide **135** that, transformed in a Grignard reagent in the presence of Mg and diethyl ether, with HgCl₂, as a catalyst, reacts with trimethylsilyl chloride, affording propargyltrimethylsilane **136** in 11% yield. Propargyltrimethylsilane **136** is treated with gaseous formaldehyde, generated by depolymerization of paraformaldehyde, leading to 1-(trimethylsilyl)-2-butyn-4-ol **137** in 59% yield. The reduction of the triple bond to the double bond was performed using LiAlH₄ in THF under reflux, affording the corresponding alkene **138** in 58% yield. The synthesis of the brominated alkene **128** proved to be unsuccessful when triphenylphosphane and carbon tetrabromide (CBr₄) were used, as reagents.

The method that seems promising in substituting the alcohol group in the alkene **138**, to lead to the desired product **128**, involves phosphorus tribromide in diethyl ether, under reflux.^[74]

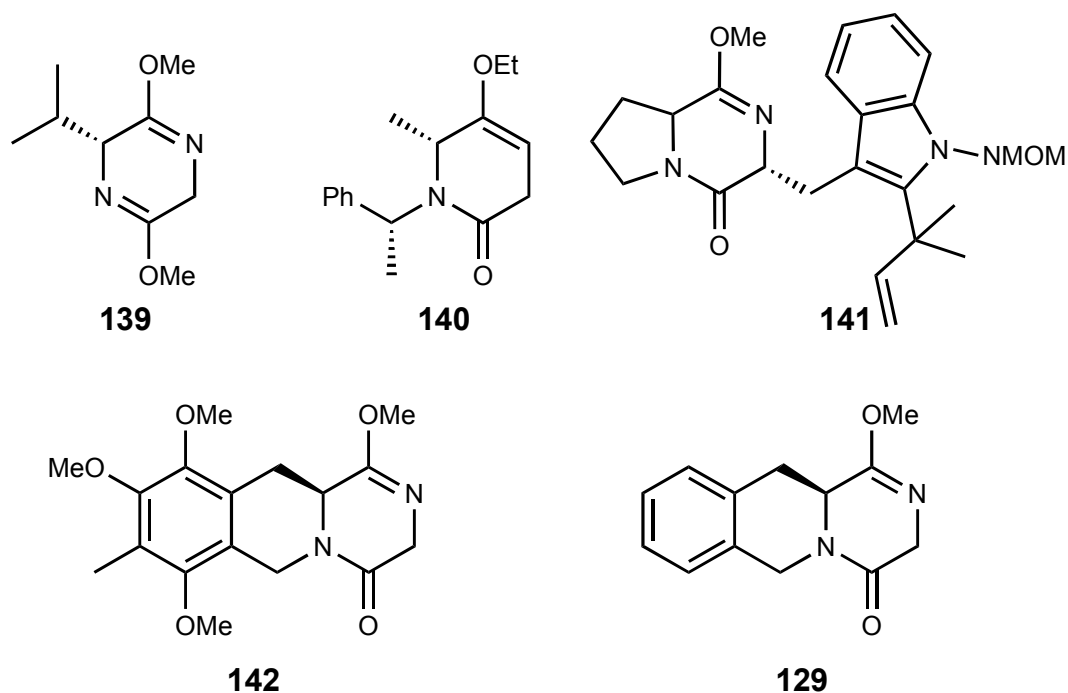


Scheme 41

4.7 Alkylation studies of tricyclic lactim ether (129)

4.7.1 Diastereoselective alkylation of tricyclic lactim ether (129) with various electrophiles

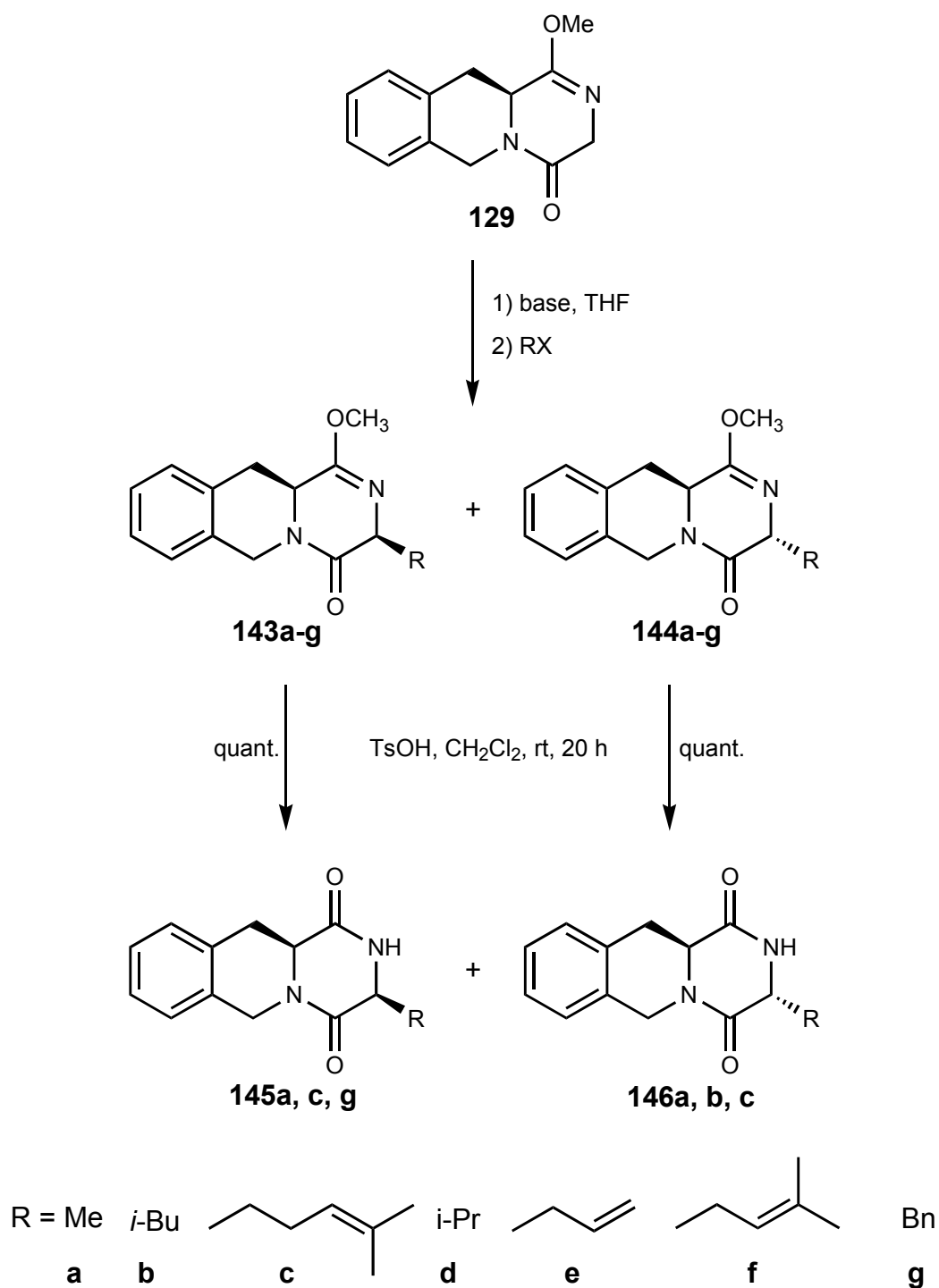
Since its introduction in 1981 the Schöllkopf bis(lactim ether) **107** has proved to be a powerful chiral auxiliary for the synthesis of α -amino acids (Scheme 42). Deprotonation of the bis(lactim ether) and subsequent reaction with various electrophiles afforded the corresponding 5-substituted 2,5-dihydro-3,6-dimethoxypyrazines **140** with high diastereoselectivities.^[44]



Scheme 42

In contrast, the reactions of carbanions derived from mono(lactim ethers) have received much less attention. Sammes, for example, reported the conjugate addition of allylic sulfones to *N*-benzyl lactim ethers in studies towards the synthesis of the antibiotic dioxopiperazine bicyclomycin.^[45] However, no details concerning diastereoselectivity were given. Sandri studied mono- and dialkylations and also aldol reactions of carbanions derived from lactim ethers **140**.^[46] Although Williams utilized the *epi*-deoxybrevianamide E derivative **141** in the biomimetic total synthesis of the alkaloid UM 55599, the starting material **142** was prepared by cyclocondensation

from tryptophan precursors rather than diastereoselective alkylation of a cyclic lactim ether.^[49c-f]



Scheme 43

Fukuyama observed the formation of a single *trans* diastereomer upon alkylation of tricyclic lactim ether **142**. This lack of information about bi- and tricyclic lactim ethers prompted the study of their alkylation more systematically.

Thus, tricyclic lactim ether **129** was used as a model system for the study of such alkylations by Hätzelt^[48] and the results are presented in this chapter (Scheme 43).

In order to investigate the diastereoselectivity of the alkylation reaction, lactim ether **129** was deprotonated with various bases in THF at -78°C. Various electrophiles were then added. Irrespective of the base, primary alkyl halides such as methyl iodide and isobutyl bromide displayed almost no selectivity. The same was true for 4-methyl-pent-3-enyl bromide. A slight increase of the selectivity was observed for isopropyl bromide, depending on the base. While KO^tBu led to a slight preference for the *trans* diastereomer **144d** (**144d** / **143d** = 58 : 42), LDA and LHMDS resulted in the preferred formation of the *cis* diastereomer **143d** (**144d** / **143d** = 42 : 58). It was anticipated that the use of different leaving groups might improve the selectivity. However, in contrast to a recent report by Cook^[39d] the use of alkyl tosylates or alkyl diphenylphosphates instead of corresponding alkyl halides gave very poor conversions and low selectivities and thus this approach was not pursued further. Fortunately, the reaction with allylic and benzylic halides turned out to be more selective. For allyl bromide, LDA was found to give best diastereoselectivity (**144e** / **143e** = 80 : 20). The amount of *trans* isomer slightly decreased when *n*BuLi or LHMDS were used instead. For 3-methylbut-2-enyl bromide a variety of bases were screened: *n*BuLi, LDA, LHMDS, NaHMDS, KHMDS. The highest degree of diastereoselectivity (**144f** / **143f** = 92 : 8) was observed for LHMDS. All other bases gave lower *cis/trans* ratios. When LDA was used in combination with DMPU, the selectivity was even lower than for LDA alone. In the case of benzyl bromide, LDA was the base of choice, giving the products **143g**, **144g** with exceptional diastereoselectivity (**144g** / **143g** = 97 : 3).

Next, the conversion of the lactim ethers **143**, **144** into the corresponding dioxopiperazines **145**, **146** was attempted. While treatment of unsubstituted lactim ether **129** with dilute HCl did not give any conversion, the use of TsOH resulted in clean conversion into the starting dioxopiperazine **134** within 1 d. Thus, diastereomeric alkylation products **143a-c** and **144a, c, g** were treated with 1 eq of TsOH in CH₂Cl₂ at room temperature overnight and the corresponding dioxopiperazines **145a-c** and **146a, c, g** were isolated quantitatively.

From the above results, the following conclusions can be drawn. In alkylations of tricyclic lactim ether **129**, steric constraints are not sufficient to achieve useful discrimination between diastereotopic faces of the carbanion. However, alkylations using allylic and benzylic halides capable of π -stacking interactions with the tetrahydroisoquinoline moiety result in improved diastereoselectivity.

5 Experimental section

5.1 Instrumentation and material

NMR Spectroscopy: ^1H -NMR spectra were measured at 250, 300, 500 MHz, $\{^1\text{H}\}^{13}\text{C}$ -NMR spectra respectively at 62.5, 75, 125 MHz, on *AC 250*, *ARX 300*, *Avance 300*, *ARX 500* and *Avance 500* spectrometers of Bruker Comp. The signals were assigned by COSY, NOESY, as well as DEPT measurements. Unless otherwise mentioned, all the measurements were performed in CDCl_3 , at room temp. The chemical shifts δ are given in ppm, using tetramethylsilane (TMS) as an internal standard or/and were referred to the rest signals of the corresponding solvents. *J*-coupling constants are given as frequencies, in Hertz (Hz). Signal multiplicities are abbreviated as follows: *s* (singlet), *d* (doublet), *t* (triplet), *q* (quartet), *m* (multiplet), as well as *br* for broad signals.

IR Spectroscopy: Infrared spectra were measured based on ATR technique on a FT-IR spectrometer *Vektor22* of Bruker Comp. with *MKII Golden Gate Single Reflection Diamant ATR System*. The position of the absorption band is given in wavelength figures (cm^{-1}). The intensity of the bands are characterized by the following abbreviations: *vs* (very strong), *s* (strong), *m* (medium), *w* (weak).

Mass spectrometry: The determination of the fragment ions and exact masses have been measured on a *MAT 95* of *Finnigan* Comp. under chemical ionization (CI) with methane as reagent gas and on a *MAT 711* of *Varian* Comp. under EI conditions at 70eV. GC-MS spectra have been measured on a *GC HP 5890 Series II* with a *HP-5 MS* (30 m, $\varnothing = 0.25$ mm) column of *Hewlett-Packard* Comp. and a *Trace DSQ GS-MS Unity* of *Thermo-Finnigan* Comp. with an *Optima-5-MS* column (30 m, $\varnothing = 0.25$ mm) of *Macherey-Nagel* Comp. The relative intensities are given as percent of the corresponding base peaks.

Polarimetry: The specific optical rotation values $[\alpha]$ (in $\text{kg grad}^{-1} \text{dm}^{-1}$) have been determined on a *Polarimeter 241* of *Perkin Elmer*, using the Na-D/line (589 nm), at room temp. The solvent and concentration are also mentioned.

Melting points: Melting points have been measured on a differential scanning calorimeter DSC822[®] of *Mettler-Toledo* Comp.

Elemental analysis: CHN Analysis have been measured on a *Carlo Erba Strumentazione Elemental Analyser Modell 1106*.

X-Ray structure analysis: The data have been determined on diffractometers *P3* and *P4* of Fa. *Nicolet* with Cu-K_α and Mo-K_α-radiation and graphite monochromators in ω-scan-modus and undergone a Lorenz- and polarization correction. The structure determination have been refined based on the least square error. The measurement have been performed at 293(2) K.

Analysis of diastereomers: Diastereomeric excesses were measured by gas chromatography on a GC HRGS MEGA 8560 of *Fisons* Comp., respectively on a Trace GC Ultra of *Thermo-Finnigan*. The utilized columns, instrument parameters and retention times are mentioned. In addition, the diastereomeric excesses have been determined with HPLC, with a PU980 pump of *Jasco* Comp. and a variable wavelength detector 875-UV of *Jasco* Comp .

Flash column chromatography: For the flash column chromatography, silica gel of *Fluka* Comp. (Typ 60, grain diameter 40 to 63 μm) and basic and neutral aluminium oxide of *Merck* Comp. (Alox 90, grain diameter 63 – 200 μm, activity level I) have been used. The eluents are given.

Thin layer chromatography: For the thin layer chromatography, TLC plates silica gel 60 F254 and aluminum oxide 60 F254 type E of *Merck* Comp., aluminum foil and glass with fluorescence indicator 254 have been used. The eluent is given in relation with the corresponding *R_f* value. The detection was performed with UV light of 254 nm wavelength. In the case of non UV active substances, the chromatogram was immersed in iodine recipient or a different dying reagent, followed by heating:
“Phosphomolybdc acid reagent” (PMA): 12 g phosphomolybdc acid hydrate, 250 mL ethanol,

“Permanganate reagent”: 3 g potassium permanganate, 20 g potassium carbonate, 5 mL 5% NaOH, 300 mL water.

High pressure liquid chromatography: For the analytical HPLC, a PU980 pump of *Jasco Comp.* was used. For semi-preparative HPLC, a pump of *Knauer Comp.*, provided with a preparative pump head and an unmodified silica gel column (250 mm, $\varnothing = 25$ mm, 10 μm) of *Knauer Comp.* or a *RP-18 AB* phase (250 mm, $\varnothing = 21$ mm, 7 μm) of *Macherey-Nagel Comp.* was used. The detection takes place at 254 nm, with a variable wavelength detector of *Knauer Comp.*

Gas chromatography: For reaction monitoring and control of the purity of the products, gas chromatographs HP 6890 with a DB-5MS column (30 m, $\varnothing = 0.32$ mm) of *Hewlett-Packard Comp.* and *Trace GC Ultra* of *Macherey-Nagel Comp.*, according to the following program (if not mentioned otherwise), were used: starting temp. 80 °C, heating rate 16 °C/min, final temp. 280°C, min.

5.2 Solvents and procedures

Unless otherwise mentioned, the chemicals have been used as provided from the suppliers. The solvents for the reactions have been purified by standard methods: the solvents for chromatography, petrol ether (30-75 °C), methanol, diethyl ether and ethyl acetate have been distilled, the latter over K_2CO_3 . The solvents for HPLC have been used as “gradient HPLC/grade”. Water has been purified with a Milli-Q-Equipment of *Millipore Comp.* Solvents were dried by using the following methods:

- THF and DME over potassium/benzophenone,
- diethyl ether over sodium/benzophenone,
- methylene chloride, benzene, toluene, triethylamine, pyridine, diisopropyl amine over calcium hydride,
- *n*-pentane over lithium aluminum hydride
- methanol over magnesium
- ethanol over sodium

and freshly distilled prior to use. Dry DMF, DMSO and acetonitrile have been used as provided by *Aldrich Comp.*

Oxidation and moisture sensitive substances and reactions were handled under nitrogen or argon atmosphere in carefully heated glassware, using the standard Schlenk techniques.

5.3 Products and reagents known in the literature

The preparation of the products and reagents known in the literature has been carried out according to the following references:

- (3*S*, 8*aS*)-3-Benzylhexahydropyrrolo[1,2-*a*]pyrazine-1,4-dione *cis*-**75h**^[56]
1-(*tert*-butoxycarbonyl)-3-bromomethyl indole **66**^[75]
1-(*tert*-butoxycarbonyl)-3-methyl indole **74**^[75]
(*S*)-(-)-*N*-(*tert*-butoxycarbonyl)-prolylalanine methylester **78a**^[56]
(*S*)-(-)-*N*-(*tert*-butoxycarbonyl)-prolylglycine methylester **71**^[56]
(*S*)-(-)-*N*-(*tert*-butoxycarbonyl)-prolylisoleucine methylester **78d**^[56]
(*S*)-(-)-*N*-(*tert*-butoxycarbonyl)-prolylphenylalanine methylester **78h**^[56]
(*S*)-(-)-*N*-(*tert*-butoxycarbonyl)-prolylvaline methylester **78e**^[56]
(*S*)-(-)-*N*-(*tert*-butoxycarbonyl)-1,2,3,4-tetrahydroisoquinoline-3-carboxylic acid **131**^[70]
(*S*)-(-)-*N*-carboxy-1,2,3,4-tetrahydroisoquinoline-3-carboxylic acid anhydride **132**^[48]
(*S*)-1,4-Dioxo-1,3,4,6,11,11*a*-hexahydro-pyrazino[1,2-*b*]isoquinoline **134**^[48]
(*S*)-Hexahydropyrrolo[1,2-*a*]pyrazine-1,4-dione **73**^[56]
(3*S*, 8*aS*)-3-Isobutylhexahydropyrrolo[1,2-*a*]pyrazine-1,4-dione **75d**^[56]
(3*S*, 8*aS*)-3-Isopropylhexahydropyrrolo[1,2-*a*]pyrazine-1,4-dione **75e**^[56]
Lithium diisopropylamide^[76]
Lithium hexametyldisilazide^[77]
(3*S*, 8*aS*)-3-Methylhexahydropyrrolo[1,2-*a*]pyrazine-1,4-dione **75a**^[56]
1-Methoxy-3,6,11,11*a*-tetrahydro-4*H*-pyrazine-[1,2-*b*]isoquinolin-4-one **129**^[48]
Propargyltrimethylsilane **136**^[72]
(*S*)-Tetrahydro-1*H*-pyrrolo[1,2-*c*][1,3]oxazole-1,3-dione **68**^[48]
1-(Trimethylsilyl)-2-buten-4-ol **138**^[72]
1-(Trimethylsilyl)-2-butyne-4-ol **137**^[72]

5.4 General procedures (GP)

General procedure for the synthesis of bi- and tricyclic diketopiperazines (GP1)

A mixture of peptide **71** (9.00 mmol) and trifluoroacetic acid (10.0 mL, 15.3 g, 134 mmol) was dissolved in CH₂Cl₂ (10 mL) and the solution was stirred at room temp. for 1 h. The solvent was removed and the residue was dissolved in MeOH (50 mL) and treated with triethylamine (5.00 mL, 36.4 g, 36.0 mmol). The reaction mixture was kept under reflux overnight. The solvent was removed under reduced pressure and the oily residue was redissolved in isopropanol to give the diketopiperazine **73** as colorless crystals.

General procedure for the synthesis of bi- and tricyclic lactimethers (GP2)

A mixture of diketopiperazine **73** (1.35 g, 8.75 mmol) and trimethyloxonium tetrafluoroborate (1.55 g, 10.5 mmol) were grounded together in a mortar, suspended in dry CH₂Cl₂ (50 mL) and refluxed for 12 h. Then further trimethyloxonium tetrafluoroborate was added (809 mg, 5.46 mmol) and the suspension was stirred for further 12 h. With vigorous stirring the mixture was slowly poured into an ice-cold saturated NaHCO₃ solution (pH >8), the layers were separated and the aqueous layer was extracted with CH₂Cl₂ (3 × 20 mL). The combined organic layers were dried (Na₂SO₄), evaporated and purified on silica gel to give the lactim ether **63**.

General procedure for the alkylation of mono-lactimether (GP3)

A solution of lactimether **63** (100 mg, 0.59 mmol) in THF (2 mL) was added dropwise to a cooled solution of the respective base (0.63 mmol) in THF (3 mL) at –78°C. LDA in THF was freshly prepared from *n*BuLi (393 μL solution 1.6 M in pentane, 0.630 mmol) and diisopropyl amine (63.7 mg, 88.4 μL, 0.63 mmol). LHMDs was freshly prepared from *n*BuLi (393 μL solution 1.6 M in pentane, 0.63 mmol) and

hexamethyldisilazane (140 μL , 107 μg , 0.66 mmol). After stirring for 4 h at -78°C , the respective freshly distilled alkyl halide (0.65 mmol) was added, and the reaction mixture stirred for further 16 h. Then it was warmed to room temp. and hydrolyzed with a saturated NaHCO_3 solution (20 mL). The layers were separated and the aqueous layer was extracted with CH_2Cl_2 (3×20 mL). The combined organic layers were dried (Na_2SO_4), evaporated and purified by flash chromatography on silica gel to give the alkylated lactim ethers **75a-j**. GC temperature program for determination of diastereomeric ratios: initial temp. 80°C , heating rate 8°C min^{-1} until 180°C , 1°C min^{-1} until 220°C , then $16^\circ\text{C min}^{-1}$ until 300°C .

General procedure for the hydrolysis of lactim ethers *cis*- and *trans*-**29** (GP4)

A solution of *cis*-**75** or *trans*-**75** (1.00 mmol) in CH_2Cl_2 (10 mL) was treated with *p*- $\text{TsOH} \cdot \text{H}_2\text{O}$ (190 mg, 1.00 mmol), and the mixture was stirred at room temp. for 20 h. Then a saturated NaHCO_3 solution (20 mL) was added and the mixture extracted with CH_2Cl_2 (5×100 mL). The combined organic layers were dried (MgSO_4), evaporated and purified by flash chromatography on silica gel with EtOAc to give the *cis*- or *trans*-diketopiperazines **76**.

General procedure for the synthesis of the intermediate peptides (GP5)

To a stirred mixture of (*S*)-(-)-*N*-(*tert*-butoxycarbonyl)-proline **69** (5.00 g, 23.0 mmol), aminoacid methylester hydrochloride (23.0 mmol), 1-[3-(dimethylamino)propyl]-3-ethylcarbodiimide hydrochloride (5.34 g, 28.0 mmol) and 1-hydroxybenzotriazole monohydrate (3.77 g, 28.0 mmol) triethylamine (6.50 mL, 4.71 g, 46.6 mmol) was added and the reaction mixture was stirred for 24 h at room temp. The solvent was removed under reduced pressure and the residue was taken up in ethyl acetate (200 mL), and washed successively with water (200 mL), 5% aqueous citric acid solution (4×60 mL) and 10% aqueous K_2CO_3 solution (2×100 mL) and the solvent was removed under reduced pressure to give the peptides **78a-d** as colorless crystalline solids.

General procedure for the preparation of lithium diisopropylamide (LDA) (GP6)

To a cooled solution of diisopropylamine (88.0 μ L, 63.0 mg, 0.63 mmol) in THF (2 mL) at -78°C *n*BuLi (0.43 mL 1.6 M solution in pentane, 0.68 mmol) was added dropwise under nitrogen and the mixture was allowed to warm to room temp. for 20 min.

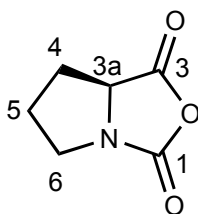
General procedure for the preparation of lithium hexamethyldisilazide (LHMDS) (GP7)

To a cooled solution of *n*BuLi (0.39 mL, 0.63 mmol, 1.6 M in pentane) at 0°C hexamethyl disilazane (0.14 mL, 107 mg, 0.66 mmol) was added drop wise over 10 min. The solution was then stirred for 15 min at room temp. Pentane was removed and replaced with THF.

5.5 Experiments to chapter 4.2.1

(S)-Tetrahydro-1H-pyrrolo[1,2-c][1,3]oxazole-1,3-dione (68)

To a suspension of (S)-(-)-*N*-(*tert*-butoxycarbonyl)-proline **69** (10.9 g, 50.0 mmol) in dry CH₂Cl₂ (50 mL) PCl₃ (5.21 mL, 8.20 g, 60.0 mmol) was added drop wise at 0°C and the resulting mixture was stirred for 3 h at 0°C. The solvent was removed under vacuum, and the residue was washed with *n*-hexane (5 × 20 mL) and dried under high vacuum in a desiccator over P₂O₅ to give **68** as a colorless solid (7.06 g, 50.0 mmol, 100%). The product was used without further purification.



M.p. = 50–52°C.

¹H-NMR (300 MHz, DMSO): δ = 1.90–2.34 (*m*, 4H, 4-H, 5-H), 3.28–3.36 (*m*, 1H, 6-H_b), 3.72–3.81 (*m*, 1H, 6-H_a), 4.33 (*t*, *J* = 8.4 Hz, 1H, 3a-H) ppm.

¹³C-NMR (75 MHz, DMSO): δ = 23.1 (C-5), 27.9 (C-4), 45.1 (C-6), 58.6 (C-3a), 154.9 (C-1), 170.4 (C-3) ppm.

¹H-NMR data were in accordance with the literature.^[78]

(S)-(-)-*N*-(*tert*-butoxycarbonyl)-prolylglycine methylester (71)

Method A:

Preparation according to GP5

Stoichiometry: 5.00 g, 23.0 mmol (S)-(-)-*N*-(*tert*-butoxycarbonyl)-proline

Yield: 4.80 g, 16.8 mmol, 73%
Purity: >90% (GC, ¹H-NMR)
R_f = 0.32 (EtOAc : PE = 1 : 1, Permanganate)
GC: t_R = 10.54 min.
Colorless crystalline solid

Method B:^[58]

To a stirred solution of (S)-(-)-N-(*tert*-butoxycarbonyl)-proline **69** (4.30 g, 20.0 mmol) in dry THF (40 mL) carbonyl diimidazole (3.20 g, 20.0 mmol) was added under nitrogen. After 30 min a solution of glycine methylester hydrochloride **70** (2.50 g, 20.0 mol) and *N*-ethylmorpholine (9.00 mL, 8.00 g, 70.0 mmol) were added, under stirring. The resulting mixture was stirred at room temp. for 24 h under nitrogen. After the hydrochloride salts were filtered off, the solvent was removed under reduced pressure. The residual oil was redissolved in ethyl acetate (40 mL) and the solution was washed with aqueous 1N HCl solution (20 mL), brine (20 mL), dried over MgSO₄ and the solvent was removed under reduced pressure to afford the product as a colorless solid. (5.80 g, 20.0 mmol, 100%).

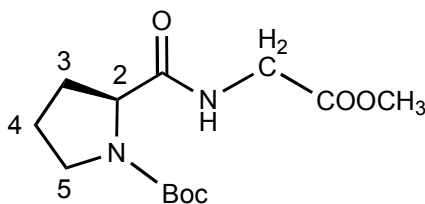
Method C:^[59]

A solution of (S)-(-)-N-(*tert*-butoxycarbonyl)-proline **69** (25.3 g, 116 mmol) and *N*-methylmorpholine (13 mL, 12.0 g, 116 mmol) in dry THF (200 mL) was cooled at -15°C and isobutyl chloroformate (15.5 mL, 16.2 g, 114 mmol) was added with stirring. After 2 min a solution of glycine methylester hydrochloride **70** (14.6 g, 116 mmol) and *N*-methylmorpholine (13.0 mL, 12.0 g, 116 mmol) in THF (100 mL) and DMF (26 mL) was added in one portion to the stirred suspension. The reaction mixture was allowed to warm to room temp. over 2 h and left standing overnight. The hydrochloride salts were filtered off and the solvent removed under reduced pressure. The residual oil was redissolved in ethyl acetate (500 mL) and the solution was washed with aqueous 0.5 M HCl solution (2 x 300 mL), 5% aqueous NaHCO₃ solution (3 x 300 mL) and brine (300 mL). The solution was dried (MgSO₄) and the

solvent was removed under reduced pressure to afford the product as a colorless solid (26.0 g, 90.5 mmol, 78%).

Method D.^[79]

To a stirred mixture of (S)-(-)-*N*-(*tert*-butoxycarbonyl)-proline **69** (215 mg, 1.00 mmol), glycine methylester hydrochloride (138 mg, 1.10 mmol) and diethyl phosphorcyanidate (147 μ L, 158 mg, 1.10 mmol) in DMF (2 mL), triethylamine (147 μ L, 106 mg, 1.05 mmol) was added over 10 min at 0°C. The mixture was stirred at 0°C for 30 min and then at room temp. for 1 h, then diluted with ethyl acetate (25 mL) and benzene (13 mL) and successively washed with 5% aqueous HCl solution (5 mL), water (5 mL), saturated NaHCO₃ solution (5 mL) and brine (5 mL) to yield 230 mg (800 μ mol, 80%) of a colorless solid.



M.p. = 70-71°C

¹H-NMR (500MHz, CDCl₃): δ = 1.46 [s, 9H, C(CH₃)₃], 1.74-2.41 (*m*, 4H, 4-H, 3-H), 3.47 (*m*, 2H, 5-H), 3.73 (s, 3H, OCH₃), 4.05 (*d*, *J* = 5.6 Hz, 2H, NH-CH₂), 4.32 (*br s*, 1H, 2-H), 6.53 (*br s*, 1H, CONH) ppm.

¹³C NMR (125 MHz, CDCl₃): δ = 23.7 (C-3), 24.5 (C-4), 28.3 [C(CH₃)₃], 31.0 (C-3), 41.2 (C-5), 47.2 (NH-CH₂-COOCH₃), 52.3 (OCH₃), 59.9, 61.1 (C-2), 80.6 (C(CH₃)₃), 155.9 (N-CO), 170.2 (CO-NH), 172.5 (COOCH₃) ppm.

Experimental data are in accordance with the literature.^[56]

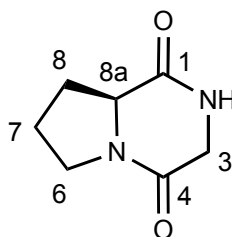
(S)-Hexahydropyrrolo[1,2-a]pyrazine-1,4-dione (73)

Method A:

At -78°C , the anhydride **68** (7.28 g, 51.0 mmol) was slowly added over 1-1.5 h to a cooled solution of glycine methylester hydrochloride (8.80 g, 70.0 mmol) and triethylamine (20 mL, 14.4 g, 142 mmol) in CH_2Cl_2 (50 mL). After stirring for further 6 h at -78°C , the mixture was filtered through Celite and washed with CH_2Cl_2 (50 mL). The yellowish oil obtained after removal of the solvent was dissolved in H_2O and refluxed for 24 h. The solvent was removed under reduced pressure and the precipitate was purified by crystallization from isopropanol to give **73** as colorless crystals (6.80 g, 44.4 mmol, 87%).

Method B:

Procedure	according to GP1
Stoichiometry	2.60 g, 9.00 mmol (S)-(-)- <i>N</i> -(<i>tert</i> -butoxycarbonyl)-prolylglycine methylester 71
Yield:	1.38 g, 9.00 mmol, 100%
Purity	>95% (GC, $^1\text{H-NMR}$)
Colorless crystalline solid	



M.p. = 216–217 $^{\circ}\text{C}$.

$[\alpha] = -171$ ($c = 2.0$, CHCl_3).

$^1\text{H-NMR}$ (500 MHz, CDCl_3): $\delta = 1.76$ - 1.92 (*m*, 1H, 7- H_b), 1.92 - 2.07 (*m*, 2H, 7- H_a , 8- H_b), 2.26 - 2.36 (*m*, 1H, 8- H_a), 3.45 - 3.62 (*m*, 2H, 6-H), 3.88 (*ddd*, 1H, $J = 16.4, 4.5, 0.9$

Hz, 3-H_b), 3.99 (*dd*, *J* = 1.8, 0.9 Hz, 8a-H), 4.03-4.06 (*m*, 1H, 3-H_a), 6.89 (*br s*, 1H, *NH*) ppm.

¹³C-NMR (125 MHz, CDCl₃): δ = 22.8 (C-7), 28.8 (C-8), 45.7 (C-6), 47.0 (C-3), 58.9 (C-8a), 163.9 (C-4), 170.4 (C-1) ppm.

FT-IR (ATR): ν = 3161 (*m*), 2876 (*m*), 1674 (*s*), 1639 (*vs*), 1453 (*s*), 1293 (*s*), 1110 (*m*), 1103 (*m*), 778 (*vs*) cm⁻¹.

CHN Analysis: C ₇ H ₁₀ N ₂ O ₂ (154.17):	calc: C 54.54,	H 6.54,	N 18.17
	found: C 54.42,	H 6.53,	N 18.09

(S)-1-Methoxy-6,7,8,8a-tetrahydropyrrolo[1,2-a]pyrazin-4-(3H)-one (63)

Procedure: according to GP2

Stoichiometry 1.35 g, 8.75 mmol (S)-hexahydropyrrolo[1,2-a]pyrazine-1,4-dione
73
 2.36 g, 16.0 mmol trimethyloxonium tetrafluoroborate
 CH₂Cl₂ (50 mL)

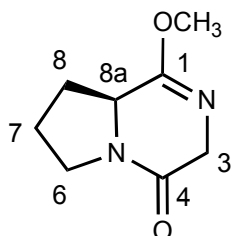
Eluent: EtOAc

Yield: 1.13 g, 6.65 mmol, 76%

Purity: >95% (GC, ¹H-NMR)

R_f = 0.33 (EtOAc, Permanganate)

Colorless oil



¹H-NMR (500 MHz, CDCl₃): δ = 1.76-1.93 (*m*, 2H, 8-H_b, 7-H_b), 2.02-2.08 (*m*, 1H, 7-H_a), 2.30-2.34 (*m*, 1H, 8-H_a), 3.40-3.50 (*m*, 1H, 6-H_b), 3.65-3.70 (*m*, 1H, 6-H_a), 3.74

(s, 3H, OCH₃), 4.02-4.06 (m, 1H, 8a-H), 4.08 (dddd, 1H, $J = 19.5, 4.5, 0.9, 0.9$ Hz, 3-H_b), 4.20 (dd, 1H, $J = 19.5, 1.6$ Hz, 3-H_a) ppm.

¹³C-NMR (125 MHz, CDCl₃): $\delta = 22.3$ (C-7), 29.4 (C-8), 44.3 (C-3), 52.7 (C-6), 53.3 (OCH₃), 56.6 (C-8a), 161.9 (C-4), 166.4 (C-1) ppm.

FT-IR (ATR): $\nu = 3455$ (w), 2947 (m), 2847 (m), 1640 (vs), 1436 (s), 1315 (s), 1255 (s), 1019 (s), 748 (m) cm⁻¹.

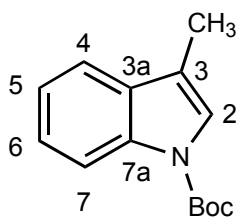
HRMS (EI): calc. for C₈H₁₂N₂O₂ 168.0899; found: 168.0902 [M⁺].

$[\alpha] = -138$ (c = 1.0, CH₂Cl₂).

5.6 Experiments to chapter 4.2.2

1-(*tert*-Butoxycarbonyl)-3-methylindole (**74**)

A solution of 3-methyl indole **67** (50.0 g, 381 mmol) in acetonitrile (500 mL) was stirred under nitrogen at room temp. with di-*tert*-butyl-dicarbonate (86.0 g, 0.40 mmol) and dimethyl aminopyridine (2.30 g, 2.00 mmol) for 12 hours. Then, the solvent was removed under reduced pressure and the residue was dissolved in ethyl acetate (500 mL), washed with aqueous 1N HCl solution (2 x 150 mL) and brine (250 mL) and dried with NaSO₄. The removal of the solvent under reduced pressure, yielded 1-(*tert*-butoxycarbonyl)-3-methyl indole **74** as a light yellow oil. (85.0 g, 366 mmol, 96%).



R_f = 0.69 (EtOAc : PE = 1 : 6, Permanganate)

¹H-NMR (300 MHz, CDCl₃): δ = 1.69 [s, 9H, C(CH₃)₃], 2.20 (d, J = 1.3 Hz, 3H, CH₃), 7.19 (ddd, J = 7.7, 7.2, 1.1 Hz, 1H, H_{aryl}), 7.25-7.31 (m, 1H, H_{aryl}), 7.32 (br s, 1H, H_{aryl}), 7.41 (ddd, J = 7.7, 1.4, 0.7 Hz, 1H, H_{aryl}), 8.14 (br d, J = 7.7 Hz, 1H, 2-H) ppm.

¹³C-NMR (125 MHz, CDCl₃): δ = 9.3 (CH₃), 82.7 [C(CH₃)₃], 114.9 (C-7), 116.0 (C-3), 118.6 (C-4), 122.0 (C-6), 122.5 (C-2), 123.9 (C-5), 131.2 (C-3a), 135.3 (C-7a), 149.5 (C=O) ppm.

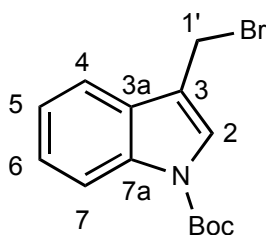
FT-IR (ATR): ν = 2977 (m), 1725 (vs), 1450 (s), 1345 (vs), 1249 (s), 1221 (m), 1149 (vs), 1084 (vs), 1017 (s), 856 (m), 739 (vs) cm⁻¹.

GC: t_R = 8.11 min.

Experimental data are in accordance with the literature^[75].

***N*-(*tert*-Butoxycarbonyl)-3-bromomethylindole (66)**

A solution of 1-(*tert*-butoxycarbonyl)-3-methyl indol **74** (10.0 g, 43.0 mmol) in CCl₄ (200 mL) was heated to reflux, then a mixture of *N*-bromosuccinimide (8.00 g, 45.0 mmol) and azobisisobutyronitrile (182 mg, 1.10 mmol) was carefully added portionwise, over 5 min. After the completion of the addition, three portions of azobisisobutyronitrile (3 x 72.0 mg, 1.30 mmol) were added, one each 30 minutes. After 3 h, the mixture was cooled to room temp. and the resulted succinimide was filtered off and washed with CCl₄ (3 x 10 mL). The solvent was removed under reduced pressure, to yield a brown solid. Further crystallization from Et₂O afforded *N*-(*tert*-butoxycarbonyl)-3-bromomethylindole **66**, as colorless crystals (13.3 g, 43.0 mmol, 100%.)



R_f = 0.58 (EtOAc : PE = 1 : 1, Permanganate)

M.p. = 100°C

¹H-NMR (500 MHz, CDCl₃): δ = 1.66 [s, 9H, C(CH₃)₃], 4.68 (d, *J* = 0.7 Hz, 2H, 1'-H), 7.30 (ddd, *J* = 7.7, 7.3, 1.1 Hz, 1H, H_{aryl}), 7.34-7.38 (m, 1H, H_{aryl}), 7.67-7.69 (m, 2H, H_{aryl}), 8.14 (d, *J* = 7.3 Hz, 1H, 2-H) ppm.

¹³C-NMR (125 MHz, CDCl₃): δ = 28.1 (C-1'), 84.1 [C(CH₃)₃], 115.4 (C-7), 117.1 (C-3), 119.3 (C-4), 122.88 (C-6), 124.9 (C-2), 125.0 (C-5), 128.7 (C-3a), 135.7 (C-7a), 149.3 (C=O) ppm.

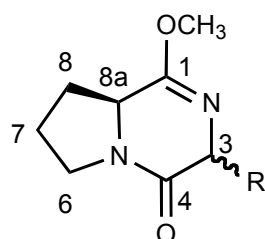
CHN Analysis: C₁₄H₁₆BrNO₂ (310.18): calc: C 54.21, H 5.20, N 4.52;
found: C 54.02, H 5.15, N 4.49.

Experimental data are in accordance with the literature.^[39b]

5.7 Experiments to chapter 4.3

4.3.1 Alkylation of Lactim Ether 63

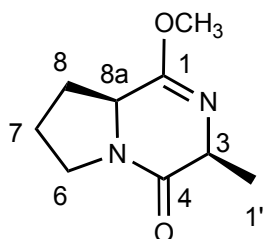
1-Methoxy-3-alkyl-6,7,8,8a-tetrahydropyrrolo[1,2-a]pyrazin-4(3H)-one (75)



75	R =				
a	CH ₃	e	i-C ₄ H ₉	i	CH ₂ (4-C ₆ H ₄ Cl)
b	C ₂ H ₅	f	C ₃ H ₅	j	CH ₂ (4-C ₆ H ₄ OMe)
c	C ₃ H ₇	g	C ₅ H ₉		
d	C ₄ H ₉	h	CH ₂ -C ₆ H ₅		

(3*S*,8*aS*)-1-Methoxy-3-methyl-6,7,8,8a-tetrahydropyrrolo[1,2-a]pyrazin-4(3*H*)-one (5a) (*cis*-75a)

Preparation	according to GP3
Stoichiometry	41.0 μ L, 92.7 mg, 0.65 mmol methyl iodide
Base:	LDA, LHMDS
Eluent	EtOAc : PE = 3 : 2
Yield	102 mg, 0.56 mmol, 94% (LDA) 76.0 mg, 0.45 mmol, 75% (LHMDS)
Purity	>90% (GC, ¹ H-NMR)
R _f	= 0.58 (EtOAc : PE = 4 : 1, Permanganate)
	Pale yellow oil



$^1\text{H-NMR}$ (500 MHz, CDCl_3): δ = 1.36 (*d*, 3H, J = 7.3 Hz, CH_3), 1.72–1.90 (*m*, 2H, 7- H_b , 8- H_b), 2.00–2.07 (*m*, 1H, 7- H_a), 2.28–2.33 (*m*, 1H, 8- H_b), 3.44 (*ddd*, J = 11.7, 9.2, 2.4 Hz, 1H, 6- H_b), 3.65–3.70 (*m*, 1H, 6- H_b), 3.74 (*s*, 3H, OCH_3), 4.02 (*ddd*, J = 11.0, 6.0, 1.7 Hz, 1H, 8a-H), 4.23 (*dq*, J = 1.7, 7.3 Hz, 3-H) ppm.

$^{13}\text{C-NMR}$ (125 MHz, CDCl_3): δ = 20.2 (C-1'), 22.5 (C-7), 29.9 (C-8), 44.8 (C-6), 53.6 (OCH_3), 56.4 (C-8a), 58.5 (C-3), 161.1 (C-4), 170.1 (C-1) ppm.

HRMS (EI): calcd. for $\text{C}_9\text{H}_{14}\text{N}_2\text{O}_2$ 182.0155; found: 182.0155 [M^+].

MS (CI, CH_4): m/z (%) = 183 (100) [$\text{M}^+\text{+H}$], 167 (2), 155 (11).

FT-IR (ATR): ν = 3246 (*m*), 2978 (*m*), 2948 (*m*), 2883 (*w*), 2198 (*w*), 1969 (*w*), 1637 (*vs*), 1436 (*s*) cm^{-1} .

α = -48.7 (c = 1.0, CH_2Cl_2).

GC: $t_{\text{R}}(\text{cis-75a})$ = 1.29 min.

GC: $t_{\text{R}}(\text{trans-75a})$ = 1.85 min.

GC: PS086, temp. program: 3 min. at 100°C , heating rate: $2.5^\circ\text{C min}^{-1}$ until 175°C , then $20^\circ\text{C min}^{-1}$ until 300°C .

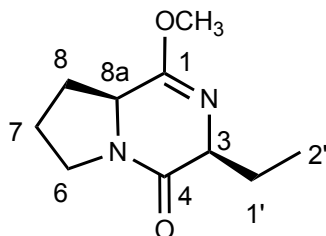
(3*S*,8*aS*)-3-Ethyl-1-methoxy-6,7,8,8*a*-tetrahydropyrrolo[1,2-*a*]pyrazin-4(3*H*)-one (cis-75b)

Procedure	according to GP3
Stoichiometry	52.0 μL , 102 mg, 0.65 mmol ethyl iodide
Base:	LDA
Eluent:	$\text{Et}_2\text{O} : \text{MeOH} = 8 : 1$
Yield:	70 mg, 0.36 μmol , 60%

Purity: >90% (GC, ¹H-NMR)

R_f = 0.58 (Et₂O : MeOH = 8 : 1, Permanganate)

Pale yellow oil



¹H-NMR (500 MHz, CDCl₃): δ = 0.96 (*t*, *J* = 7.4 Hz, 3H, CH₃), 1.68-1.87 (*m*, 4H, 1'-H, 8-H_b, 7-H_b), 1.98-2.04 (*m*, 1H, 7-H_a), 2.26-2.31 (*m*, 1H, 8-H_a), 3.42 (*ddd*, *J* = 11.8, 9.6, 2.3 Hz, 1H, 6-H_b), 3.62-3.71 (*m*, 1H, 6-H_a), 3.73 (*s*, 3H, OCH₃), 3.98 (*ddd*, *J* = 11.1, 6.0, 1.8 Hz, 1H, 8a-H), 4.12 (*ddd*, *J* = 7.2, 5.6, 1.8 Hz, 1H, 3-H) ppm.

¹³C-NMR (125 MHz, CDCl₃): δ = 9.6 (C-2'), 22.1 (C-1'), 27.8 (C-7), 29.7 (C-8), 44.5 (C-6), 53.3 (OCH₃), 56.5 (C-3), 63.5 (C-8a), 161.0 (C-4), 169.4 (C-1) ppm.

HRMS: calc. for C₁₀H₁₆N₂O₂ 196.1212; found: 196.1195 [M⁺].

MS (EI): *m/z* (%) = 196 (6) [M⁺], 181 (16) [M⁺ - CH₃], 168 (100) [M⁺ - CH₂CH₃], 153 (40) [M⁺ - CH₃, CH₃-CH₂], 139 (26), 126 (42), 112 (62), 96 (12), 83 (14), 70 (38), 60 (20).

FT-IR (ATR): ν = 2996 (*m*), 1683 (*vs*), 1655 (*vs*), 1438 (*s*), 1321 (*m*), 1253 (*s*), 1130 (*w*), 1033 (*w*), 1004 (*w*), 808 (*w*) cm⁻¹.

[α] = -54.0 (c = 1.0, CH₂Cl₂).

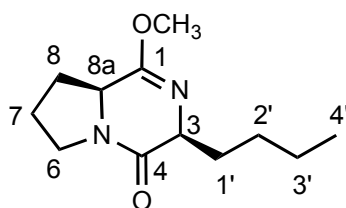
GC: t_R(*cis*-75b) = 11.67 min.

3-Butyl-1-methoxy-6,7,8,8a-tetrahydropyrrolo[1,2-a]pyrazin-4(3H)-one (75c)

Procedure according to GP3
 Stoichiometry: 74.0 μ L, 120 mg, 0.65 mmol *n*-butyl iodide
 Base: LDA
 Eluent: EtOAc

(3*S*,8*aS*)-isomer (*cis*-75c).

Yield: 22.0 mg, 98.0 μ mol, 16.5% (LDA)
 Purity: >90% (GC, ¹H-NMR)
 R_f = 0.49 (EtOAc, Permanganate)
 Pale yellow oil



¹H-NMR (300 MHz, CDCl₃): δ = 0.92 (*t*, J = 7.0 Hz, 3H, CH₃), 1.31-1.49 (*m*, 4H, 2'-H, 3'-H), 1.73-1.94 (*m*, 3H, 7-H, 8-H_b), 1.99-2.11 (*m*, 2H, 1'-H), 2.22-2.34 (*m*, 1H, 8-H_a), 3.39-3.47 (*m*, 1H, 6-H_b), 3.57-3.68 (*m*, 1H, 6-H_a), 3.72 (*s*, 3H, OCH₃), 3.88 (*dt*, J = 7.4, 4.2, 0.8 Hz, 1H, 3-H), 3.98-4.06 (*m*, 1H, 8a-H) ppm.

¹³C-NMR (75 MHz, CDCl₃): δ = 14.0 (C-4'), 20.0 (C-3'), 22.6 (C-7), 27.5 (C-2'), 29.1 (C-8), 31.8 (C-1'), 44.1 (C-6), 53.3 (OCH₃), 55.4 (C-8a), 59.1 (C-3), 165.8 (C-4), 172.9 (C-1) ppm.

HRMS (EI): calcd. for C₁₂H₂₀N₂O₂ 224.1525; found: 224.1525 [M⁺].

FT-IR (ATR): ν = 2951 (*m*), 2859 (*w*), 1653 (*vs*), 1431 (*s*), 1313 (*m*), 1255 (*w*), 1037 (*m*), 763 (*w*) cm⁻¹.

$[\alpha] = -62.6$ ($c = 1.0$, CH₂Cl₂).

GC: $t_R(\text{cis-75c}) = 14.48 \text{ min}$

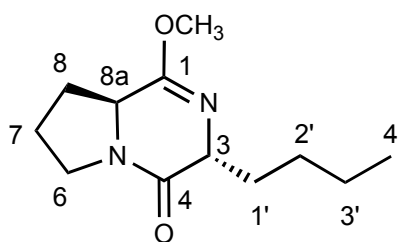
(3*R*,8*aS*)-isomer (*trans*-75c)

Yield: 23.0 mg, 100 μmol , 17% (LDA)

Purity: >90% (GC, $^1\text{H-NMR}$)

$R_f = 0.31$ (EtOAc, Permanganate)

Colorless solid



M.p. = 46–48°C

$^1\text{H-NMR}$ (300 MHz, CDCl_3): $\delta = 0.89$ (*t*, $J = 7.1 \text{ Hz}$, 3H, CH_3), 1.26-1.46 (*m*, 4H, 2'-H, 3'-H), 1.63-1.71 (*m*, 1H, 7- H_b), 1.72-1.80 (*m*, 2H, 7- H_a , 8- H_b), 1.80-1.91 (*m*, $J = 12.3$, 1H, 8- H_a), 1.99-2.06 (*m*, 1H, 1'- H_b), 2.27-2.32 (*m*, 1H, 1'- H_a), 3.44 (*ddd*, $J = 11.8$, 9.4, 2.3 Hz, 1H, 6- H_b), 3.67-3.72 (*m*, 1H, 6- H_a), 3.74 (*s*, 3H, OCH_3), 4.00 (*ddd*, $J = 11.0$, 6.0, 1.8 Hz, 1H, 8*a*-H), 4.15 (*ddd*, $J = 7.4$, 5.7, 1.7 Hz, 1H, 3-H) ppm.

$^{13}\text{C-NMR}$ (75 MHz, CDCl_3): $\delta = 14.0$ (C-4'), 22.1 (C-3'), 22.6 (C-7), 27.7 (C-2'), 29.7 (C-8), 34.4 (C-1'), 44.6 (C-6), 53.3 (OCH_3), 56.4 (C-8*a*), 62.5 (C-3), 160.9 (C-4), 169.6 (C-1) ppm.

HRMS (EI) calcd. for $\text{C}_{12}\text{H}_{20}\text{N}_2\text{O}_2$ 224.1525; found: 224.1525 [M^+].

FT-IR (ATR): $\nu = 3232$ (*w*), 2953 (*m*), 2871 (*w*), 1675 (*vs*), 1651 (*vs*), 1436 (*s*), 1323 (*w*), 1253 (*w*), 1013 (*w*), 742 (*w*) cm^{-1} .

$[\alpha] = -61.3$ ($c = 1.0$, CH_2Cl_2).

GC: $t_R(\text{trans-75c}) = 14.54$ min.

3-Isobutyl-1-methoxy-6,7,8,8a-tetrahydropyrrolo[1,2-a]pyrazin-4(3H)-one (75d).

Procedure according to GP3
 Stoichiometry: a) 71.0 μL , 89.5 mg, 0.65 mmol *i*-butyl bromide/LDA
 b) 71.0 μL , 89.5 mg, 0.65 mmol *i*-butyl bromide/LHMDS
 c) 71.0 μL , 89.5 mg, 0.65 mmol *i*-butyl iodide/LDA
 d) 71.0 μL , 89.5 mg, 0.65 mmol, *i*-butyl iodide/LHMDS
 Eluent: EtOAc

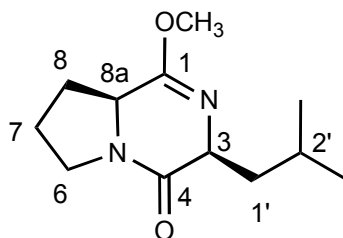
(3*S*,8*aS*)-isomer (*cis*-75d)

Yield: 29.0 mg, 130 μmol , 22% (*i*-butyl bromide/LDA)

Purity: >90% (GC, $^1\text{H-NMR}$)

$R_f = 0.35$ (EtOAc : PE = 1 : 1, Permanganate)

Pale yellow oil



$^1\text{H-NMR}$ (300 MHz, CDCl_3): $\delta = 0.93$ (*d*, $J = 6.4$ Hz, 3H, CH_3), 0.89 (*d*, $J = 6.5$ Hz, 3H, CH_3), 1.53-1.63 (*m*, 1H, 1'- H_b), 1.76-1.83 (*m*, 2H, 7- H_b , 2'-H), 1.86 (*m*, 1H, 1'- H_a), 1.90-2.04 (*m*, 2H, 7- H_a , 8- H_b), 2.13-2.33 (*m*, 1H, 8- H_a), 3.40-3.48 (*m*, 1H, 6- H_b), 3.54-

3.65 (*m*, 1H, 6-H_a), 3.73 (*s*, 3H, OCH₃), 3.87 (*dddd*, *J* = 9.9, 4.2, 4.2, 0.9, 0.9 Hz, 1H, 8a-H), 3.92-3.99 (*m*, 1H, 3-H) ppm.

¹³C-NMR (75 MHz, CDCl₃): δ = 20.6 (C-3'), 21.7 (C-4'), 22.5 (C-7), 23.8 (C-2'), 28.0 (C-8), 39.9 (C-1'), 43.4 (C-6), 52.2 (OCH₃), 55.8 (C-8a), 57.1 (C-3), 160.2 (C-4), 168.5 (C-1) ppm.

HRMS: calcd. for C₁₂H₂₀N₂O₂ 224.1525; found: 224.1525 [M⁺].

FT-IR (ATR): ν = 2952 (*s*), 2969 (*m*), 1660 (*vs*), 1434 (*s*), 1333 (*m*), 1259 (*s*), 1038 (*m*), 798 (*m*) cm⁻¹.

[α] = -59.7 (c = 1.0, CH₂Cl₂).

GC: t_R(*cis*-**75d**) = 13.71 min.

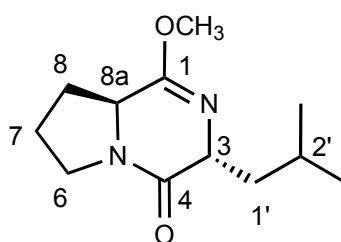
(3*R*, 8a*S*)-isomer (*trans*-**75d**)

Yield: 35.0 mg, 154 μmol, 26% (*i*-butyl bromide/LDA)

Purity: >90% (GC, ¹H-NMR)

R_f = 0.23 (EtOAc : PE = 1 : 1, Permanganate)

Pale yellow oil



$^1\text{H-NMR}$ (500 MHz, CDCl_3): δ = 0.97 (*d*, J = 6.7 Hz, 3H, CH_3), 0.98 (*d*, J = 6.7 Hz, 3H, CH_3), 1.43 (*ddd*, J = 13.3, 9.0, 6.5 Hz, 1H, $1'\text{-H}_b$), 1.57 (*ddd*, J = 13.3, 7.6, 6.0 Hz, 1H, $1'\text{-H}_a$), 1.72-1.91 (*m*, 3H, $2'\text{-H}$, 7-H), 1.99-2.05 (*m*, 1H, 8- H_b), 2.27-2.32 (*m*, 1H, 8- H_a), 3.43 (*ddd*, J = 11.4, 9.3, 2.4, 1H, 6- H_b), 3.64-3.70 (*m*, 1H, 6- H_a), 3.73 (*s*, 3H, OCH_3), 4.00 (*ddd*, J = 10.9, 5.9, 1.7 Hz, 1H, 8a-H), 4.19 (*ddd*, J = 9.0, 6.0, 1.7 Hz, 1H, 3-H) ppm.

$^{13}\text{C-NMR}$ (125 MHz, CDCl_3): δ = 22.1 (C-3'), 22.1 (C-4'), 23.0 (C-7), 24.7 (C-2'), 29.5 (C-8), 43.3 (C-1'), 44.5 (C-6), 53.2 (OCH_3), 56.1 (C-8a), 60.8 (C-3), 160.9 (C-4), 169.9 (C-1) ppm.

HRMS: calcd. for $\text{C}_{12}\text{H}_{20}\text{N}_2\text{O}_2$ 224.1525; found: 224.1524 [M^+].

FT-IR (ATR): ν = 2951 (*m*), 1679 (*vs*), 1654 (*vs*), 1435 (*s*), 1316 (*m*), 1252 (*s*), 1004 (*m*), 730 (*w*) cm^{-1} .

α = -56.5 (c = 1.0, CH_2Cl_2).

GC: $t_{\text{R}}(\text{trans-75d})$ = 13.88 min.

3-Isopropyl-1-methoxy-6,7,8,8a-tetrahydropyrrolo[1,2-a]pyrazin-4(3H)-one (75e)

Procedure	according to GP3
Stoichiometry:	a) 61.0 μL , 80.3 mg, 0.65 mmol <i>i</i> -propyl bromide/LDA b) 61.0 μL , 80.3 mg, 0.65 mmol <i>i</i> -propyl bromide/LHMDS c) 61.0 μL , 80.3 mg, 0.63 mmol <i>i</i> -propyl iodide/LDA d) 61.0 μL , 80.3 mg, 0.65 mmol <i>i</i> -propyl iodide/LHMDS
Eluent:	EtOAc

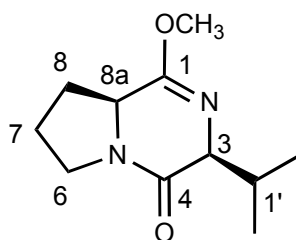
(3*S*,8*aS*)-isomer (*cis*-75e)

Yield: 54.0 mg, 0.25 mmol, 43%

Purity: >90% (GC, ¹H-NMR)

R_f = 0.47 (EtOAc : PE = 2 : 1, Permanganate)

Pale yellow oil



¹H-NMR (500 MHz, CDCl₃): δ = 0.73 (*d*, *J* = 6.7 Hz, 3H, CH₃), 1.12 (*d*, *J* = 6.7 Hz, 3H, CH₃), 1.82-1.96 (*m*, 2H, 7-H_b, 8-H_b), 1.99-2.07 (*m*, 1H, 7-H_a), 2.25-2.31 (*m*, 1H, 8-H_a), 2.60 (q_qd, *J* = 6.9, 6.7, 2.9 Hz, 1H, 1'-H), 3.39-3.44 (*m*, 1H, 6-H_b), 3.62-3.68 (*m*, 1H, 6-H_a), 3.74 (*s*, 3H, OCH₃), 3.79-3.81 (*m*, 1H, 8a-H), 3.95-4.01 (*m*, 1H, 3-H) ppm.

¹³C-NMR (125 MHz, CDCl₃): δ = 17.6 (C-3'), 19.4 (C-2'), 22.5 (C-7), 29.4 (C-8), 33.6 (C-1'), 44.0 (C-6), 53.0 (OCH₃), 56.6 (C-8a), 64.5 (C-3), 160.6 (C-4), 168.5 (C-1) ppm.

HRMS calcd. for C₁₁H₁₈N₂O₂ 210.1368; found: 210.1368 [M⁺].

MS (EI): *m/z* (%) = 210 (10) [M⁺], 168 (100) [M⁺ - C₃H₇], 140 (20), 112 (25), 70 (30).

FT-IR (ATR): ν = 3233 (*w*), 2958 (*m*), 2872 (*w*), 1635 (*vs*), 1435 (*s*), 1328 (*w*), 1239 (*w*), 997 (*w*), 772 (*w*) cm⁻¹.

$[\alpha] = -61.6$ ($c = 1.0$, CH_2Cl_2).

GC: $t_R(\text{cis-75e}) = 13.70$ min.

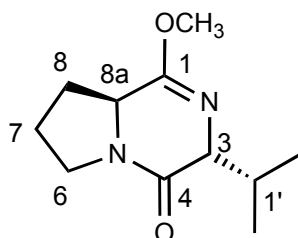
(3*R*, 8*aS*)-isomer (trans-75e)

Yield: 30.0 mg, 142 μmol , 24 % (*i*-propyl bromide/LDA)

Purity: >90% (GC, $^1\text{H-NMR}$)

$R_f = 0.35$ (EtOAc : PE = 2 : 1, Permanganate)

Pale yellow oil



$^1\text{H-NMR}$ (500 MHz, CDCl_3): $\delta = 0.73$ (*d*, $J = 6.6$ Hz, 3H, CH_3), 1.12 (*d*, $J = 6.9$ Hz, 3H, CH_3), 1.80-1.96 (*m*, 2H, 7-H), 2.00-2.06 (*m*, 1H, 8- H_b), 2.26-2.31 (*m*, 1H, 8- H_a), 2.38-2.42 (*m*, 1H, 1'-H), 3.42 (*ddd*, $J = 12.0, 9.2, 2.6$ Hz, 1H, 6- H_b), 3.65 (*dt*, $J = 12.0, 8.5$ Hz, 1H, 6- H_a), 3.49-3.54 (*m*, 1H, 6- H_a), 3.75 (*s*, 3H, OCH_3), 3.79 (*m*, 1H, 8a-H), 3.98 (*ddd*, $J = 10.5, 6.0, 4.3$ Hz, 1H, 3-H) ppm.

$^{13}\text{C-NMR}$ (125 MHz, CDCl_3): $\delta = 18.2$ (C-2'), 18.9 (C-3'), 21.5 (C-7), 28.9 (C-8), 33.1 (C-1'), 45.0 (C-6), 53.2 (OCH_3), 57.6 (C-8a), 58.3 (C-3), 160.7 (C-4), 169.0 (C-1) ppm.

FT-IR (ATR): $\nu = 3232$ (*w*), 2961 (*m*), 2873 (*w*), 1646 (*vs*), 1440 (*s*), 1327 (*w*), 1251 (*w*), 1021 (*w*), 780 (*w*) cm^{-1} .

MS (EI): m/z (%) = 210 (10) [M^+], 168 (100) [$\text{M}^+ - \text{C}_3\text{H}_7$], 154 (35), 140 (25), 112 (30), 70 (50).

HRMS calcd. for C₁₁H₁₈N₂O₂ 210.1368; found: 210.1368 [M⁺].

[α] = -22.6 (c = 0.5, CH₂Cl₂).

GC: t_R(*trans*-**75e**) = 13.86 min.

3-Allyl-1-methoxy-6,7,8,8a-tetrahydropyrrolo[1,2-a]pyrazin-4(3H)-one (**75f**).

Procedure according to GP3

Stoichiometry: a) 56.0 μL, 79.0 mg, 0.65 mmol allyl bromide/LDA
 b) 56.0 μL, 79.0 mg, 0.65 mmol allyl bromide/LHMDS
 c) 56.0 μL, 79.0 mg, 0.65 mmol allyl iodide/LDA
 d) 56.0 μL, 79.0 mg, 0.65 mmol allyl iodide/LHMDS

Eluent: EtOAc : PE = 5 : 1

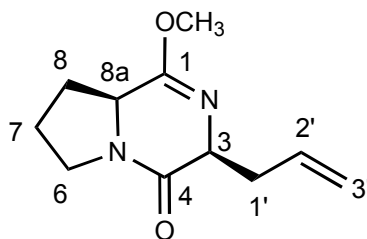
(*3S,8aS*)-isomer (*cis*-**75f**).

Yield: 7.00 mg, 39.1 μmol, 6% (allyl iodide/LDA)

Purity: >90% (GC, ¹H-NMR)

R_f = 0.56 (EtOAc : PE = 1 : 1, Permanganate)

Colorless oil



¹H-NMR (500 MHz, CDCl₃): δ = 1.73-1.92 (*m*, 2H, 7-H_b, 8-H_b), 1.94-2.08 (*m*, 1H, 7-H_a), 2.20-2.30 (*m*, 1H, 8-H_a), 2.55-2.65 (*dddd*, *J* = 14.1, 7.0, 6.5, 1.3, 1.2 Hz, 1H, 1'-H_b), 2.80 (*dddd*, *J* = 14.1, 7.2, 4.5, 1.3, 1.2 Hz, 1H, 1'-H_a), 3.38-3.49 (*m*, 1H, 6-H_b), 3.60-3.68 (*m*, 1H, 6-H_a), 3.73 (*s*, 3H, OCH₃), 3.95-4.05 (*m*, 2H, 3-H, 8a-H), 5.05 (*ddt*,

$J = 10.2, 2.2, 1.1, 1\text{H}, 3'\text{-H}_b$), 5.15 (ddt, $J = 17.2, 2.2, 1.4\text{ Hz}, 1\text{H}, 3'\text{-H}_a$), 5.92 (dddd, $J = 17.2, 10.2, 7.2, 6.5, 1\text{H}, 2'\text{-H}$) ppm.

^{13}C -NMR (125 MHz, CDCl_3): $\delta = 22.6$ (C-7), 29.2 (C-8), 36.6 (C-1'), 44.2 (C-6), 53.3 (OCH_3), 56.9 (C-8a), 60.0 (C-3), 116.9 (C-3'), 135.5 (C-2'), 161.3 (C-4), 168.2 (C-1) ppm.

HRMS calcd. for $\text{C}_{11}\text{H}_{16}\text{N}_2\text{O}_2$ 208.1212; found: 208.1211 [M^+].

MS (EI): m/z (%) = 208 (100) [M^+], 193 (46) [$\text{M}^+ - \text{CH}_3$], 167 (25) [$\text{M}^+ - \text{C}_3\text{H}_7$], 151 (12), 139 (60), 112 (35), 70 (40).

FT-IR (ATR): $\nu = 3231$ (*m*), 2949 (*m*), 1638 (*vs*), 1432 (*s*), 1305 (*m*), 1177 (*w*), 996 (*w*), 917 (*w*) cm^{-1} .

$[\alpha] = -15.0$ ($c = 0.5$, THF).

GC: $t_R(\text{cis-75f}) = 14.83$ min.

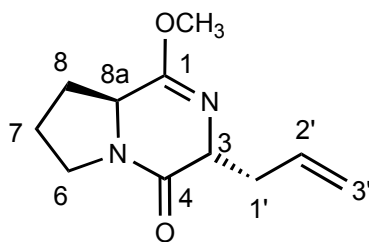
(3R,8aS)-isomer (trans-75f)

Yield: 33.0 mg, 172 μmol , 29%

Purity: >90% (GC, ^1H -NMR)

$R_f = 0.34$ (EtOAc : PE = 1 : 1, Permanganate)

Pale yellow oil



$^1\text{H-NMR}$ (500 MHz, CDCl_3): δ = 1.67-1.92 (*m*, 2H, 7- H_a , 8- H_a), 1.97-2.09 (*m*, 1H, 7 H_b), 2.21-2.31 (*m*, 1H, 8- H_b), 2.51-2.65 (*m*, 2H, 1'-H), 3.38-3.46 (*m*, 1H, 6- H_a), 3.57-3.69 (*m*, 1H, 6- H_b), 3.74 (*s*, 3H, OCH_3), 3.94-4.03 (*m*, 1H, 8a-H), 4.20-4.27 (*m*, 1H, 3-H), 5.02-5.18 (*m*, 2H, 3'-H), 5.71-5.98 (*m*, 1H, 2'-H) ppm.

$^{13}\text{C-NMR}$ (125 MHz, CDCl_3): δ = 22.0 (C-7), 29.0 (C-8), 36.2 (C-1'), 43.4 (C-6), 53.3 (OCH_3), 57.1 (C-8a), 61.8 (C-3), 116.3 (C-3'), 135.4 (C-2'), 161.8 (C-4), 168.5 (C-1) ppm.

HRMS calcd. for $\text{C}_{11}\text{H}_{16}\text{N}_2\text{O}_2$ 208.1212; found: 208.1211 [M^+].

MS (EI): m/z (%) = 208 (100) [M^+], 207 (15) [$\text{M}^+ - \text{H}$], 193 (12) [$\text{M}^+ - \text{CH}_3$], 167 (35) [$\text{M}^+ - \text{C}_3\text{H}_7$], 139 (60) [$\text{M}^+ - \text{CH}_3$], 112 (20).

FT-IR (ATR): ν = 3233 (*m*), 2947 (*m*), 2886 (*w*), 1637 (*vs*), 1433 (*s*), 1212 (*m*), 996 (*m*), 915 (*m*) cm^{-1} .

$[\alpha] = -17.4$ ($c = 1.0$, CH_2Cl_2).

GC: $t_R(\text{trans-75f}) = 15.08$ min.

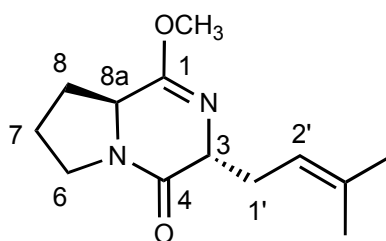
3-(Methylbut-2-enyl)-1-methoxy-3-6,7,8,8a-tetrahydropyrrolo[1,2-a]pyrazin-4(3H)-one (75g).

Procedure according to GP3
 Stoichiometry: 75.0 μ L, 97.0 mg, 0.65 mmol 3-methylbut-2-enyl bromide
 Base: LDA
 Eluent: Et₂O : MeOH = 8 : 1

(3*S*, 8*aS*)-isomer (cis-75g).

Yield: 10.0 mg, 41.6 μ mol, 7%
 Purity: >90% (GC, ¹H-NMR)
 R_f = 0.44 (Et₂O : MeOH = 8 : 1, Permanganate)

Yellow oil



¹H-NMR (300 MHz, CDCl₃): δ = 1.59-1.60 (*d*, *J* = 1.4 Hz, 3H, CH₃), 1.68-1.69 (*m*, 3H, CH₃), 1.62-1.76 (*m*, 1H, 8-H_b), 1.78-1.90 (*m*, 1H, 7-H_b), 1.96-2.05 (*m*, 1H, 7-H_a), 2.24-2.29 (*m*, 1H, 8-H_a), 2.50-2.53 (*m*, 2H, 1'-H), 3.41 (*ddd*, *J* = 11.9, 9.5, 2.4 Hz, 1H, 6-H_b), 3.66-3.71 (*m*, 1H, 6-H_a), 3.73 (*s*, 3H, OCH₃), 3.90 (*dd*, *J* = 11.3, 5.9, 1.9 Hz, 1H, 8a-H), 4.24 (*ddd*, *J* = 5.5, 5.5, 1.8 Hz, 1H, 3-H), 5.10-5.15 (*m*, *J* = 7.7, 1.4, 1.4 Hz, 1H, 2'-H) ppm.

^{13}C -NMR (125 MHz, CDCl_3): δ = 17.9 (C-3'), 22.0 (C-7), 26.0 (C-4'), 29.7 (C-8), 32.8 (C-1'), 44.4 (C-6), 53.3 (OCH_3), 56.7 (C-8a), 62.5 (C-3), 118.6 (C-2'), 135.7 (C-3'), 161.3 (C-4), 169.2 (C-1) ppm.

HRMS calc. for $\text{C}_{13}\text{H}_{20}\text{N}_2\text{O}_2$ 236.1525; found: 236.1525 [M^+].

MS (EI): m/z (%) = 236 (22) [M^+], 168 (28) [$\text{M}^+ - \text{C}_5\text{H}_9$], 70 (35).

FT-IR (ATR): ν = 3246 (*m*), 2970 (*m*), 1664 (*vs*), 1444 (*s*), 1305 (*w*), 1180 (*w*), 1117 (*w*), 801 (*w*) cm^{-1} .

$[\alpha] = -19$ ($c = 1.0$, CH_2Cl_2).

GC: $t_{\text{R}}(\text{cis-75g}) = 15.82$ min.

(A second fraction, a colorless solid, proved to be the diketopiperazine derivative of the second diastereoisomer, data are given under diketopiperazines.)

(3*R*,8*aS*)-3-Benzyl-1-methoxy-6,7,8,8*a*-tetrahydropyrrolo[1,2-*a*]pyrazin-4(3*H*)-one (trans-75h).

Procedure according to GP3

Stoichiometry: a) 78.0 μL , 112 mg, 0.65 mmol benzyl bromide/LDA

b) 78.0 μL , 112 mg, 0.65 mmol benzyl bromide/LHMDS

Eluent: EtOAc

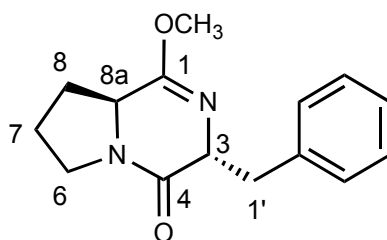
(3*R*, 8*aS*)-isomer (*trans*-**75h**)

Yield: 109 mg, 71% (benzyl bromide/LDA)

Purity: >90% (GC, ¹H-NMR)

R_f = 0.3 (EtOAc : PE = 1 : 20, Permanganate)

Yellow oil



¹H-NMR (500 MHz, CDCl₃): δ = 1.41-1.63 (*m*, 2H, 7-H_b, 8-H_b), 1.80-1.90 (*m*, 1H, 7-H_a), 1.92-1.99 (*m*, 1H, 8-H_a), 2.38-2.44 (*m*, 1H, 8a-H), 3.05 (*dd*, *J* = 13.2, 4.6 Hz, 2H, 1'-H_b), 3.22 (*ddd*, *J* = 11.8, 8.8, 2.9 Hz, 1H, 6-H_b), 3.27 (*dd*, *J* = 13.2, 4.6 Hz, 1'-H_a), 3.55-3.64 (*m*, 1H, 6-H_a), 3.67 (*s*, 3H, OCH₃), 4.50 (*dt*, *J* = 4.6, 1.9 Hz, 1H, 3-H), 7.08-7.13 (*m*, 2H, H_{aryl}), 7.19-7.25 (*m*, 3H, H_{aryl}) ppm.

¹³C-NMR (125 MHz, CDCl₃): δ = 21.4 (C-7), 29.0 (C-8), 39.6 (C-1'), 43.6 (C-6), 53.1 (OCH₃), 55.6 (C-8a), 62.8 (C-3), 126.1, 126.6, 127.7, 128.0, 130.1, 136.4 (CH_{aryl}), 160.9 (C-4), 167.0 (C-1) ppm.

HRMS calcd. for C₁₅H₁₈N₂O₂ 258.1368; found: 258.1369 [M⁺].

MS (EI): *m/z* (%) = 258 (30) [M⁺], 167 (35) [M⁺ - CH₂-C₆H₅], 139 (20) [M⁺ - OMe, CH₂-C₆H₅], 57 (100), 43 (70), 29 (30), 18 (50).

FT-IR (ATR): ν = 3438 (*w*), 3027 (*w*), 2945 (*m*), 1679 (*s*), 1639 (*s*), 1437 (*m*), 1318 (*m*), 1253 (*m*), 1027 (*m*), 700 (*s*) cm⁻¹.

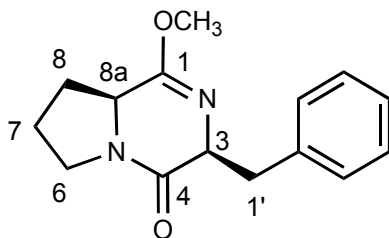
[α] = -31.1 (c = 1.0, CH₂Cl₂).

GC: t_R(*trans*-**75h**) = 24.97 min.

(3*S*,8*aS*)-isomer (cis-75h)

Yield: -

$R_f = 0.41$ (EtOAc : PE = 1 : 20, Permanganate)



GC: $t_R(\text{cis-75h}) = 23.94$ min.

**3-(3-Chlorobenzyl)-1-methoxy-6,7,8,8*a*-tetrahydropyrrolo[1,2-*a*]pyrazin-4(3*H*)
one (75i)**

Procedure: according to GP3

Stoichiometry: 86.0 μL , 134 mg, 0.65 mmol 3-chlorobenzyl chloride

Base LDA

Eluent: EtOAc

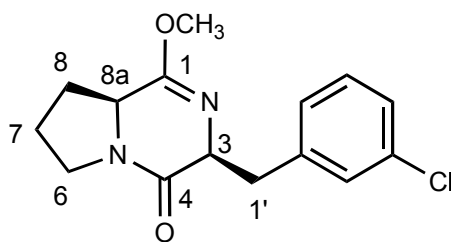
(3*S*,8*aS*)-isomer (cis-75i)

Yield: 10.5 mg, 35.6 μmol , 6%

Purity: >90% (GC, $^1\text{H-NMR}$)

$R_f = 0.31$ (EtOAc, Permanganate)

Pale yellow oil



$^1\text{H-NMR}$ (300 MHz, CDCl_3): δ = 1.21-1.32 (*m*, 1H, 8- H_b), 1.73-1.83 (*m*, 1H, 7- H_b), 1.89 (*dddd*, J = 12.8, 8.0, 7.9, 3.0, 1.7, 1H, 7- H_a), 2.07-2.13 (*m*, 1H, 8- H_a), 3.17 (*dd*, J = 13.3, 6.9 Hz, 1H, 1'- H_b), 3.30 (*dd*, J = 4.3, 13.3 Hz, 1H, 1'- H_a), 3.36 (*ddd*, J = 12.2, 9.6, 3.2 Hz, 1H, 6- H_b), 3.60 (*ddd*, J = 12.2, 8.6, 8.5 Hz, 1H, 6- H_a), 3.72 (*s*, 3H, OCH_3), 3.89 (*ddd*, J = 10.9, 6.0, 3.9 Hz, 1H, 8a-H), 4.21 (*dt*, J = 6.9, 4.3 Hz, 1H, 3-H), 7.15-7.17 (*m*, 3H, H_{aryl}), 7.30-7.31 (*m*, 1H, H_{aryl}) ppm.

$^{13}\text{C-NMR}$ (75 MHz, CDCl_3): δ = 22.4 (C-8), 29.0 (C-7), 38.2 (C-1'), 44.2 (C-6), 53.3 (OCH_3), 56.9 (C-3), 60.9 (C-8a), 126.2, 128.5, 128.9, 130.4, 133.4, 140.9 (CH_{aryl}), 160.9 (C-4), 167.7 (C-1) ppm.

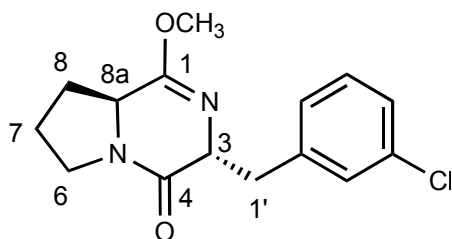
HRMS calcd. for $\text{C}_{15}\text{H}_{17}\text{ClN}_2\text{O}_2$ 292.0979; found: 292.0979 [M^+].

MS (EI): m/z (%) = 294 (32), 292 (98) [M^+], 167 (100), 139 (60), 112 (28), 70 (30), 70 (32), 43 (28), 28 (12).

$[\alpha] = -58.4$ (c = 1.0, CH_2Cl_2).

GC: $t_{\text{R}}(\text{cis-75i}) = 27.17$ min.

(3*R*, 8*aS*)-isomer (trans-75i)



$R_f = 0.18$ (EtOAc, Permanganate)

GC: $t_R(\text{trans-75i}) = 29.95$ min.

(A second fraction ($R_f = 0.09$), a colorless solid, that proved to be the diketopiperazine derivative of the second diastereoisomer, data are given under diketopiperazines.)

3-(3-methoxybenzyl)-1-methoxy--6,7,8,8*a*-tetrahydropyrrolo[1,2-*a*]pyrazin-4(3*H*)-one (75j)

Procedure	according to GP3
Stoichiometry:	91.0 μL , 131 mg, 0.65 mmol 3-methoxybenzyl bromide
Base:	LDA
Eluent:	EtOAc

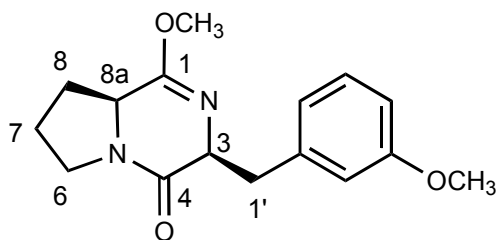
(3*S*, 8*aS*)-isomer (cis-75j)

Yield: 13.4 mg, 47.5 μmol , 8%

Purity: >90% (GC, $^1\text{H-NMR}$)

$R_f = 0.44$ (EtOAc, Permanganate)

Pale yellow oil



$^1\text{H-NMR}$ (300 MHz, CDCl_3): δ = 1.19 (*ddd*, J = 12.2, 11.0, 8.3 Hz, 1H, 7- H_b), 1.67-1.89 (*m*, 2H, 7- H_a , 8- H_b), 2.00-2.10 (*m*, 1H, 8- H_a), 3.16 (*dd*, J = 13.4, 7.0 Hz, 1H, 1'- H_b), 3.31 (*dd*, J = 13.4, 4.1 Hz, 1H, 1'- H_a), 3.32 (*ddd*, J = 12.0, 8.8, 3.5 Hz, 1H, 6- H_b), 3.62 (*dt*, J = 12.0, 8.6 Hz, 1H, 6- H_a), 3.72 (*s*, 3H, OCH_3), 3.76 (*s*, 3H, OCH_3), 3.85 (*ddd*, J = 11.0, 6.1, 3.9 Hz, 1H, 8a-H), 4.22 (*dt*, J = 7.0, 4.1 Hz, 1H, 3-H), 6.70-6.74 (*m*, 1H, H_{aryl}), 6.83-6.87 (*m*, 2H, H_{aryl}), 7.11-7.17 (*m*, 1H, H_{aryl}) ppm.

$^{13}\text{C-NMR}$ (75 MHz, CDCl_3): δ = 22.3 (C-8), 28.9 (C-7), 38.7 (C-1'), 44.1 (C-6), 53.1 (OCH_3), 55.1 (OCH_3), 56.8 (C-3), 61.2 (C-8a), 111.9, 115.5, 122.6, 128.6, 140.4, 159.1 (CH_{aryl}), 160.5 (C-4), 167.9 (C-1) ppm.

HRMS calcd. for $\text{C}_{16}\text{H}_{20}\text{N}_2\text{O}_3$ 288.1474; found: 288.1458 [M^+].

MS (CI): m/z (%) = 329 (1) [M^+ + C_3H_5], 317 (10) [M^+ + C_2H_5], 289 (100) [M^+ + H], 167 (15) [M^+ - $\text{CH}_2\text{-C}_6\text{H}_5\text{-OMe}$], 139 (15).

FT-IR (ATR): ν = 3229 (*m*), 2947 (*m*), 1655 (*vs*), 1600 (*m*), 1488 (*m*), 1434 (*vs*), 1294 (*w*), 1259 (*vs*), 1153 (*s*), 1109 (*w*), 1040 (*s*), 870 (*m*), 776 (*vs*), 730 (*vs*), 697 (*vs*) cm^{-1} .

$[\alpha] = -58.4$ ($c = 1.0$, CH_2Cl_2).

GC: $t_R(\text{cis-75j}) = 29.17$ min.

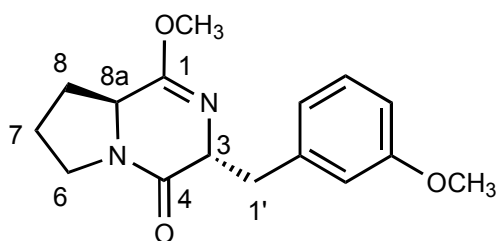
(3*R*,8*aS*)-isomer (*trans*-75j)

Yield: 99.0 mg, 0.344 mmol, 58%

Purity: >90% (GC, $^1\text{H-NMR}$)

$R_f = 0.32$ (EtOAc, Permanganate)

Pale yellow oil



$^1\text{H-NMR}$ (300 MHz, CDCl_3): $\delta = 1.44\text{-}1.67$ (*m*, 2H, 7- H_b , 8- H_b), 1.80-1.93 (*m*, 1H, 7- H_a), 1.94-2.01 (*m*, 1H, 8- H_b), 2.55-2.61 (*m*, 1H, 8a- H), 3.03 (*dd*, $J = 13.2, 4.6$ Hz, 1H, 1'- H_b), 3.23 (*dd*, $J = 13.2, 4.9$ Hz, 1H, 1'- H_a), 3.18-3.26 (*m*, 1H, 6- H_b), 3.57-3.69 (*m*, 1H, 6- H_a), 3.74 (*s*, 3H, OCH_3), 3.75 (*s*, 3H, OCH_3), 4.50 (*ddd*, $J = 4.9, 4.6, 1.9$ Hz, 1H, 3- H), 6.66 (*ddd*, $J = 2.6, 1.5, 0.5$ Hz, 1H, 2''- H), 6.69 (*ddd*, $J = 7.5, 1.5, 1.0$ Hz, 1H, 4''- H), 6.76 (*ddd*, $J = 8.4, 2.6, 1.0$ Hz, 1H, 6''- H), 7.12 (*ddd*, $J = 8.4, 7.5, 0.5$ Hz, 1H, 5''- H) ppm.

$^{13}\text{C-NMR}$ (75 MHz, CDCl_3): $\delta = 21.6$ (C-8), 29.3 (C-7), 40.0 (C-1'), 43.8 (C-6), 53.3 (OCH_3), 55.2 (OCH_3), 55.9 (C-3), 62.9 (C-8a), 112.9, 115.1, 122.6, 128.9, 138.1, 159.3 (CHaryl), 162.0 (C-4), 167.9 (C-1) ppm.

HRMS calcd. for $\text{C}_{16}\text{H}_{20}\text{N}_2\text{O}_2$ 288.1474; found: 288.1458 [M^+].

MS (EI): m/z (%) = 288 (68) [M^+], 167 (100) [$\text{M}^+ - \text{CH}_2\text{-C}_6\text{H}_5\text{-OCH}_3$], 139 (18), 83 (12).

FT-IR (ATR): $\nu = 2949$ (*m*), 1650 (*vs*), 1600 (*m*), 1487 (*w*), 1436 (*vs*), 1320 (*w*), 1256 (*vs*), 1152 (*s*), 1039 (*s*), 868 (*w*), 776 (*m*), 729 (*vs*), 697 (*vs*) cm^{-1} .

$\alpha = -21.9$ ($c = 1.0$, CH_2Cl_2).

GC: $t_{\text{R}}(\textit{trans}\text{-75j}) = 32.20$ min.

3-(Methylmethoxy)-1-methoxy-6,7,8,8a-tetrahydropyrrolo[1,2-a]pyrazin-4(3H)-one (75k)

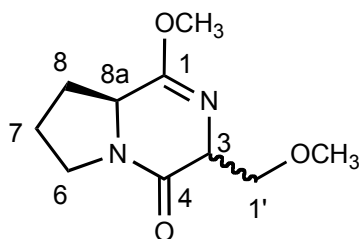
Procedure	according to GP3
Stoichiometry:	56.8 μL , 81.6 mg, 0.65 mmol 3-methoxymethyl bromide
Base	LDA
Eluent:	$\text{Et}_2\text{O} : \text{MeOH} = 4 : 1$

(3S, 8aS)-cis-75k

Yield: 45.0 mg, 0.20 mmol, 34%
Purity: >90% (GC, $^1\text{H-NMR}$)
 $R_{\text{f}} = 0.71$ ($\text{Et}_2\text{O} : \text{MeOH} = 4 : 1$, Permanganate)
GC: $t_{\text{R}}(\textit{cis}\text{-75k}) = 7.65$ min.
Pale yellow oil

(3R, 8aS)-trans-75k

Yield: 34.0 mg, 26%
Purity: >90% (GC, $^1\text{H NMR}$)
 $R_{\text{f}} = 0.52$ ($\text{Et}_2\text{O} : \text{MeOH} = 4 : 1$, Permanganate)
GC: $t_{\text{R}}(\textit{trans}\text{-75k}) = 7.78$ min.
Pale yellow oil



$^1\text{H-NMR}$ (500 MHz, CDCl_3): δ = 1.67-1.76 (*m*, 1H, 8- H_b), 1.81-1.91 (*m*, 3H, 7- H_b , 7*- H_b , 8*- H_b), 1.99-1.25 (*m*, 2H, 7- H_a , 7*- H_a), 2.25-2.30 (*m*, 2H, 8- H_a , 8*- H_a), 3.29 (*d*, J = 1.3 Hz, 3H, OMe), 3.42 (*d*, J = 1.3 Hz, 3H, OMe), 3.34-3.52 (*m*, 2H, 6- H_b , 6*- H_b), 3.61 (*ddd*, J = 9.5, 2.9, 1.4 Hz, 1H, 1'- H_b), 3.62-3.69 (*m*, 2H, 6- H_a , 6*- H_a), 3.76 (*d*, J = 1.3 Hz, OMe), 3.77 (*d*, J = 1.3 MHz, OMe*), 3.89 (*ddd*, J = 9.5, 2.9, 1.4 Hz, 1'- H_b *), 3.91-3.93 (*m*, 2H, 1'- H_a , 1'- H_a *), 4.00-4.07 (*m*, 2H, 3-H, 8a-H), 4.09-4.14 (*m*, 1H, 3*-H), 4.21-4.23 (*m*, 1H, 8a*-H) ppm.

$^{13}\text{C-NMR}$ (75 MHz, CDCl_3): δ = 22.1(C-7), 22.5 (C-7*), 29.1 (C-8*), 29.4 (C-8), 44.2 (C-6*), 44.4 (C-6), 52.4 (OCH₃), 53.4 (OCH₃*), 56.8 (C-3), 57.0 (C-3*), 59.3 (OCH₃), 59.6 (OCH₃*), 60.8 (C-8a), 63.5 (C-8a*), 74.6 (C-1'), 162.1 (C-1*), 163.0 (C-1), 166.6 (C-4*), 167.6 (C-4) ppm.

* the signals assigned to the minor diastereomer.

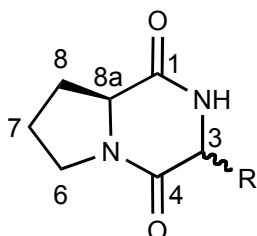
HRMS calcd. for $\text{C}_{10}\text{H}_{16}\text{N}_2\text{O}_3$ 212.1161; found: 212.1160 [M^+].

MS-EI: $m/z(\%)$ = 212 (100) [M^+], 197 (22), 181 (40), 167 (93), 153 (17), 139 (42), 112 (35).

FT-IR (ATR): ν = 2935 (*m*), 1708 (*vs*), 1651 (*vs*), 1434 (*s*), 1360 (*s*), 1220 (*s*), 1099 (*s*), 994 (*w*), 972 (*w*), 801 (*w*) cm^{-1} .

Hydrolysis of Lactim Ethers *cis*- and *trans*-75:

3-Alkyl-hexahydropyrrolo[1,2-a]pyrazine-1,4-dione (76)



76	R =				
a	CH ₃	d	C ₄ H ₉	g	C ₅ H ₉
b	C ₂ H ₅	e	i-C ₄ H ₉	h	CH ₂ -C ₆ H ₅
c	C ₃ H ₇	f	C ₃ H ₅	i	CH ₂ -C ₆ H ₄ -Cl

(3*S*,8*aS*)-3-Methylhexahydropyrrolo[1,2-a]pyrazine-1,4-dione (*cis*-76a)

Procedure according to GP6

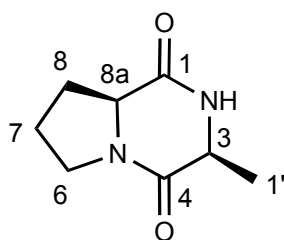
Stoichiometry: 182 mg, 1.00 mmol (3*S*,8*aS*)-1-Methoxy-3-methyl-6,7,8,8*a*-tetrahydropyrrolo [1,2-a]pyrazin-4(3*H*)-one (**75a**)

Yield: 136 mg, 0.81 mmol, 81%

Purity: >90% (GC, ¹H-NMR)

R_f = 0.31 (Et₂O : MeOH = 4 : 1, Permanganate)

Pale yellow oil



¹H-NMR (500 MHz, CDCl₃): δ = 1.50 (*d*, *J* = 7.2 Hz, 3H, CH₃), 1.87-1.94 (*m*, 1H, 7H_b), 1.96-2.08 (*m*, 2H, 7-H_a, 8-H_b), 2.32-2.45 (*m*, 1H, 8-H_b), 3.53 (*ddd*, *J* = 11.9, 9.3, 2.9 Hz, 1H, 6-H_b), 3.63-3.69 (*m*, 1H, 6-H_a), 4.03 (*dq*, *J* = 7.2, 4.2 Hz, 1H, 3-H), 4.10 (*dd*, *J* = 10.0, 6.5 Hz, 1H, 8*a*-H), 6.86 (*br s*, 1H, NH) ppm.

^{13}C -NMR (125 MHz, CDCl_3): δ = 16.0 (C-1'), 22.2 (C-7), 28.2 (C-8), 45.6 (C-6), 51.2 (C-3), 59.3 (C-8a), 166.6 (C-1), 169.3 (C-4) ppm.

HRMS calcd. for $\text{C}_8\text{H}_{12}\text{N}_2\text{O}_2$ 168.0899; found: 168.0899 [M^+].

FT-IR (ATR): ν = 3245 (*m*), 2929 (*m*), 1645 (*vs*), 1444 (*s*), 1260 (*w*), 1080 (*w*), 796 (*m*).

$[\alpha] = -84$ (*c* = 0.5, EtOH).

Experimental data are in accordance with the literature.^[80]

3-Butylhexahydropyrrolo[1,2-a]pyrazine-1,4-dione (*cis*-76c).

Procedure according to GP6

(3*S*, 8a*S*)-*cis*-76c

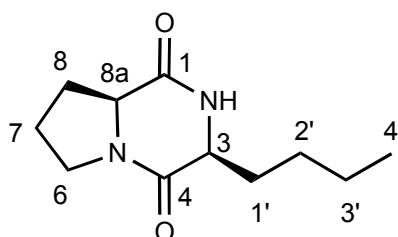
Stoichiometry: 224 mg, 1.00 mmol (3*S*,8a*S*)-1-Methoxy-3-*n*-butyl-6,7,8,8a-tetrahydropyrrolo [1,2-a]pyrazin-4(3*H*)-one (**75c**)

Yield: 170 mg, 810 μmol , 81%

Purity: >90% (GC, ^1H -NMR)

$R_f = 0.63$ ($\text{Et}_2\text{O} : \text{MeOH} = 8 : 1$, Permanganate)

Colorless solid



M.p. = 90–92°C.

$^1\text{H-NMR}$ (500 MHz, CDCl_3): δ = 0.93 (*t*, J = 7.0 Hz, 3H, CH_3), 1.33-1.48 (*m*, 4H, 2'-H, 3'-H), 1.72-1.81 (*m*, 1H, 1'-H_b), 1.87-1.96 (*m*, 1H, 1'-H_a), 1.99-2.13 (*m*, 3H, 7-H, 8-H_b), 2.32-2.37 (*m*, 1H, 8-H_a), 3.51-3.56 (*m*, 1H, 6-H_b), 3.59-3.64 (*m*, 1H, 6-H_a), 3.90 (*dddd*, J = 8.2, 4.0, 0.9 Hz, 1H, 3-H), 4.08 (*dd*, J = 10.0, 6.5, 0.9 Hz 1H, 8a-H), 7.25 (*br s*, *NH*) ppm.

$^{13}\text{C-NMR}$ (125 MHz, CDCl_3): δ = 13.9 (C-4'), 22.5 (C-3'), 22.6 (C-7), 27.3 (C-2'), 28.2 (C-8), 29.6 (C-1'), 45.3 (C-6), 55.4 (C-8a), 59.0 (C-3), 165.9 (C-1), 170.7 (C-4) ppm.

HRMS calcd. for $\text{C}_{11}\text{H}_{18}\text{N}_2\text{O}_2$ 210.1368; found: 210.1368 [M^+].

FT-IR (ATR): ν = 3228 (*m*), 2956 (*m*), 2870 (*m*), 1686 (*vs*), 1420 (*s*), 1297 (*w*), 1154 (*w*), 997 (*w*), 675 (*w*) cm^{-1} .

$[\alpha] = -58$ ($c = 1.0$, CH_2Cl_2).

(3*R*, 8*aS*)-trans-76c

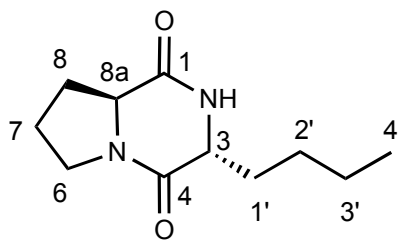
Stoichiometry: 224 mg, 1.00 mmol (3*R*,8*aS*)-1-Methoxy-3-*n*-butyl-6,7,8,8a-tetrahydropyrrolo [1,2-*a*]pyrazin-4(3*H*)-one (**75c**)

Yield: 210 mg, 1.00 mmol, quant.

Purity: >90% (GC, $^1\text{H-NMR}$)

$R_f = 0.59$ ($\text{Et}_2\text{O} : \text{MeOH} = 8 : 1$, Permanganate)

Pale yellow oil



$^1\text{H-NMR}$ (300 MHz, CDCl_3): δ = 0.91 (*t*, J = 6.9 Hz, 3H, CH_3), 1.28-1.49 (*m*, 4H, 2'-H, 3'-H), 1.68-2.09 (*m*, 5H, 1'-H, 7-H, 8- H_b), 2.36-2.44 (*m*, 1H, 8- H_a), 3.48-3.57 (*m*, 1H, 6- H_b), 3.62-3.70 (*m*, 1H, 6- H_a), 3.87-3.93 (*m*, 1H, 3-H), 4.06-4.12 (*m*, 1H, 8a-H), 7.15 (*br s*, 1H, NH) ppm.

$^{13}\text{C-NMR}$ (75 MHz, CDCl_3): δ = 13.8 (C-4'), 22.1 (C-3'), 22.2 (C-7), 27.4 (C-2'), 29.0 (C-8), 34.0 (C-1'), 45.5 (C-6), 58.0 (C-8a), 58.1 (C-3), 166.1 (C-1), 169.5 (C-4) ppm.

HRMS calcd. for $\text{C}_{11}\text{H}_{18}\text{N}_2\text{O}_2$ 210.1368; found: 210.1368 [M^+].

FT-IR (ATR): ν = 3228 (*m*), 2956 (*m*), 2870 (*m*), 1686 (*vs*), 1420 (*s*), 1297 (*w*), 1154 (*w*), 997 (*w*), 675 (*w*) cm^{-1} .

$[\alpha] = -58$ ($c = 1.0$, CH_2Cl_2).

3-Isobutylhexahydropyrrolo[1,2-a]pyrazine-1,4-dione. (76d)

Procedure according to GP6

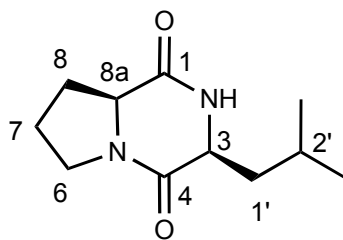
(3*S*, 8a*S*)-*cis*-76d

Stoichiometry: 224 mg, 1.00 mmol (3*S*,8a*S*)-1-Methoxy-3-*i*-butyl-6,7,8,8a-tetrahydropyrrolo [1,2-*a*]pyrazin-4(3*H*)-one (75d)

Yield: 210 mg, 1.00 mmol, quant.

R_f : 0.67 ($\text{Et}_2\text{O} : \text{MeOH} = 8 : 1$, Permanganate).

Colorless crystals



M.p. = 165°C.

$^1\text{H-NMR}$ (500 MHz, CDCl_3): δ = 0.95 (*d*, J = 6.6 Hz, 3H, CH_3), 1.00 (*d*, J = 6.6 Hz, 3H, CH_3), 1.53 (*ddd*, J = 14.3, 9.4, 5.0 Hz, 1H, 1'-H_b), 1.73-2.19 (*m*, 5H, 1'-H_a, 7-H, 8-H_b, 2'-H), 2.34 (*dtd*, J = 12.6, 7.0, 3.2 Hz, 1H, 8-H_a), 3.49-3.65 (*m*, 2H, 6-H), 4.01 (*dddd*, J = 9.4, 3.9, 1.6, 0.7 Hz, 1H, 3-H), 4.09-4.16 (*m*, 1H, 8a-H), 6.48 (*br s*, 1H, NH) ppm.

$^{13}\text{C-NMR}$ (125 MHz, CDCl_3): δ = 21.3 (C-3'), 22.8 (C-7), 23.3 (C-4'), 24.6 (C-2'), 28.1 (C-8), 38.6 (C-1'), 45.5 (C-6), 53.4 (C-8a), 59.0 (C-3), 166.3 (C-1), 170.4 (C-4) ppm.

CHN Analysis: $\text{C}_{11}\text{H}_{18}\text{N}_2\text{O}_2$ (210.27): calc: C 62.83, H 8.63, N 13.32;
found: C 62.71, H 8.58, N 13.29.

FT-IR (ATR): ν = 3221 (*m*), 2956 (*m*), 2871 (*m*), 1659 (*vs*), 1125 (*s*), 1302 (*w*), 1157 (*w*), 919 (*w*), 730 (*w*) cm^{-1} .

$[\alpha] = -137.5$ ($c = 0.4$, CH_2Cl_2).

Crystal data: $\text{C}_{11}\text{H}_{18}\text{N}_2\text{O}_2$, $M = 210.3$, orthorhombic, space group $P2(1)2(1)2(1)$; $a = 6.3429(4)$, $b = 9.466(3)$, $c = 19.5950(16)$ Å, $a = b = c = 90^\circ$; $V = 1176.5(4)$ Å³, $Z = 4$; $D_c = 1.187$ g cm⁻³. *Data collection*: crystal size 0.50 × 0.25 × 0.05 mm, 1592 reflections in the range $\theta = 4.51$ – 67.88° , 1434 unique reflections. *Structure refinement*: 1434 reflection data ($I > 2s(I)$), 141 parameters; the final R indices were $R = 0.0758$, $R_w = 0.2069$; residual electron density between 0.256 and -0.269 e Å⁻³.

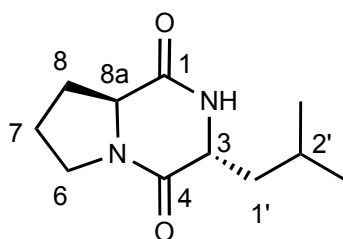
(3*R*, 8*aS*)-trans-76d

Stoichiometry: 224 mg, 1.00 mmol (3*R*, 8*aS*)-1-Methoxy-3-*i*-butyl-6,7,8,8*a*-tetrahydropyrrolo [1,2-*a*]pyrazin-4(3*H*)-one (**75d**)

Yield: 210 mg, 1.00 mmol, quant.

$R_f = 0.65$ (Et₂O : MeOH = 8 : 1, Permanganate)

Colorless crystals



M.p. = 150–152°C.

¹H-NMR (300 MHz, CDCl₃): $\delta = 0.95$ (*d*, $J = 6.4$ Hz, 3H, CH₃), 0.99 (*d*, $J = 6.4$ Hz, 3H, CH₃), 1.61 - 1.68 (*m*, 2H, 1'-H_b, 7-H_b), 1.70 - 1.80 (*m*, 1H, 2'-H), 1.82 - 2.09 (*m*, 3H, 7-H_a, 1'-H_a, 8-H_b), 2.36 - 2.44 (*m*, 1H, 8-H_a), 3.48 - 3.56 (*m*, 1H, 6-H_b), 3.61 - 3.70 (*m*, 1H, 6-H_a), 3.89 - 3.96 (*m*, 1H, 3-H), 3.98 - 4.13 (*m*, 1H, 8*a*-H), 6.49 (*br s*, 1H, NH) ppm.

¹³C-NMR (75 MHz, CDCl₃): $\delta = 21.4$ (C-4'), 22.2 (C-7), 23.0 (C-3'), 24.5 (C-2'), 29.0 (C-8), 42.6 (C-1'), 45.6 (C-6), 56.4 (C-8*a*), 58.0 (C-3), 166.3 (C-1), 169.4 (C-4) ppm.

CHN Analysis: C₁₁H₁₈N₂O₂ (210.27): calc: C 62.83, H 8.63, N 13.32;
found: C 62.62, H 8.54, N 13.18.

FT-IR (ATR): $\nu = 3230$ (*m*), 2955 (*m*), 2360 (*m*), 1649 (*vs*), 1433 (*s*), 1300 (*m*), 1144 (*w*), 918 (*w*), 729 (*m*) cm⁻¹.

$[\alpha] = -93.0$ ($c = 0.4$, CH₂Cl₂).

Crystal data: C₁₁H₁₈N₂O₂, $M = 210.3$, orthorhombic, space group P2(1)2(1)2(1); $a = 6.303(2)$, $b = 8.0267(14)$, $c = 23.146(4)$ Å, $a = b = g = 90^\circ$; $V = 1171.0(5)$ Å³, $Z = 4$;

$D_c = 1.193 \text{ g cm}^{-3}$. *Data collection*: crystal size $0.65 \times 0.2 \times 0.05 \text{ mm}$, 1103 reflections in the range $\theta = 3.82\text{--}62.50^\circ$, 1103 unique reflections. *Structure refinement*: 1103 reflection data ($I > 2s(I)$), 141 parameters; the final R indices were $R = 0.0775$, $R_w = 0.2084$; residual electron density between 0.217 and $-0.218 \text{ e \AA}^{-3}$.

3-Isopropylhexahydropyrrolo[1,2-a]pyrazine-1,4-dione (76e)

Procedure according to GP6

(3*S*, 8*aS*)-*cis*-76e

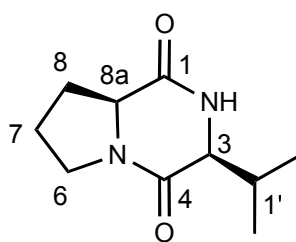
Stoichiometry: 210 mg, 1 mmol (3*S*,8*aS*)-1-Methoxy-3-*i*-propyl-6,7,8,8*a*-tetrahydropyrrolo [1,2-*a*]pyrazin-4(3*H*)-one (75e)

Yield: 195 mg, 1.00 mmol, quant.

Purity: >90% (GC, $^1\text{H-NMR}$)

$R_f = 0.60$ (CH_2Cl_2 : MeOH = 90 : 9, Permanganate)

Colorless solid



M.p. = $185\text{--}187^\circ\text{C}$.

$^1\text{H-NMR}$ (250 MHz, CDCl_3): δ = 0.91 (*d*, J = 6.8 Hz, 3H, CH_3), 1.07 (*d*, J = 7.2 Hz, 3H, CH_3), 1.84-2.13 (*m*, 3H, 7-H, 8- H_b), 2.33-2.43 (*m*, 1H, 8- H_a), 2.64 (*qqd*, J = 7.2, 6.8, 2.7 Hz, 1H, 1'-H), 3.49-3.71 (*m*, 2H, 6-H), 3.94 (*ddd*, J = 2.7, 1.8, 0.9 Hz, 1H, 3-H), 4.04-4.12 (*m*, 1H, 8a-H), 5.98 (*br s*, 1H, NH) ppm.

$^{13}\text{C-NMR}$ (63 MHz, CDCl_3): δ = 16.1 (C-2'), 19.3 (C-3'), 22.4 (C-7), 28.4 (C-8), 28.5 (C-1'), 45.2 (C-6), 58.8 (C-8a), 60.4 (C-3), 164.9 (C-1), 170.1 (C-4) ppm.

HRMS calcd. for $\text{C}_{10}\text{H}_{16}\text{N}_2\text{O}_2$ 194.1212; found: 194.1212 [M^+].

FT-IR (ATR): ν = 3393 (*s*), 2255 (*w*), 2128 (*w*), 1657 (*m*), 1050 (*s*), 1023 (*vs*), 1003 (*vs*), 823 (*m*), 761 (*m*) cm^{-1} .

$[\alpha] = -146.6$ ($c = 0.45$, CH_2Cl_2).

Experimental data are in accordance with the literature.^[81]

(3*R*, 8a*S*)-*trans*-76e

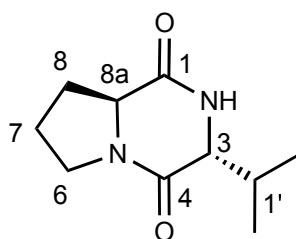
Stoichiometry: 210 mg, 1.00 mmol (3*R*,8a*S*)-1-Methoxy-3-*i*-butyl-6,7,8,8a-tetrahydropyrrolo [1,2-*a*]pyrazin-4(3*H*)-one (**75e**)

Yield: 184 mg, 0.94 mmol, 94%

Purity: >90% (GC, $^1\text{H-NMR}$)

$R_f = 0.56$ (CH_2Cl_2 : MeOH = 90 : 9, Permanganate)

Colorless solid



M.p. = 150°C.

¹H-NMR (500 MHz, DMSO): δ = 0.88 (*d*, *J* = 6.8 Hz, 3H, CH₃), 0.91 (*d*, *J* = 6.8 Hz, 3H, CH₃), 1.69-1.88 (*m*, 3H, 7-H, 8-H_b), 1.99 (*dqq*, *J* = 6.6, 6.6 Hz, 1H, 1'-H), 2.12-2.17 (*m*, 1H, 8-H_a), 3.38 (*dd*, *J* = 6.6, 4.2 Hz, 1H, 3-H), 3.25-3.30 (*m*, 1H, 6-H_b), 3.42-3.49 (*m*, 1H, 6-H_a), 4.11 (*dd*, *J* = 9.8, 6.8 Hz, 1H, 8a-H), 8.33 (*d*, *J* = 4.2 Hz, 1H, NH) ppm.

¹³C-NMR (125 MHz, CDCl₃): δ = 18.2 (C-2'), 19.0 (C-3'), 21.5 (C-7), 28.9 (C-8), 32.4 (C-1'), 45.1 (C-6), 57.6 (C-8a), 62.6 (C-3), 165.0 (C-1), 169.0 (C-4) ppm.

HRMS calcd. for C₁₀H₁₆N₂O₂ 194.1212; found: 194.1212 [M⁺].

FT-IR (ATR): ν = 3216 (*m*), 2962 (*m*), 1674 (*s*), 1648 (*vs*), 1447 (*s*), 1270 (*m*), 777 (*s*) cm⁻¹.

[α] = -20 (c = 0.45, CH₂Cl₂).

3-Allylhexahydropyrrolo[1,2-a]pyrazine-1,4-dione (76f).

Procedure according to GP6

(3*S*, 8a*S*)-*cis*-76f

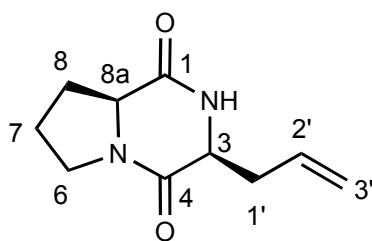
Stoichiometry: 208 mg, 1.00 mmol (3*S*,8a*S*)-1-Methoxy-3-allyl-6,7,8,8a-tetrahydropyrrolo [1,2-a]pyrazin-4(3*H*)-one (75f)

Yield: 136 mg, 700 μ mol, 70%

Purity: >90% (GC, ¹H-NMR)

R_f = 0.36 (Et₂O : MeOH = 8 : 1, Permanganate)

Pale yellow oil



$^1\text{H-NMR}$ (300 MHz, CDCl_3): δ = 1.83-2.17 (*m*, 3H, 7-H, 8- H_b), 2.31-2.47 (*m*, 2H, 8- H_a , 1'- H_b), 2.88-2.97 (*m*, 1H, 1'- H_a), 3.51-3.67 (*m*, 2H, 6-H), 4.03-4.17 (*m*, 2H, 3-H, 8a-H), 5.20-5.21 (*m*, 1-H, 3'- H_a), 5.24-5.28 (*m*, 1H, 3'- H_b), 5.72-5.87 (*m*, 1H, 2'-H), 6.19 (*br s*, 1H, NH) ppm.

$^{13}\text{C-NMR}$ (125 MHz, CDCl_3): δ = 22.6 (C-7), 28.1 (C-8), 34.7 (C-1'), 45.3 (C-6), 53.8 (C-3), 59.1 (C-8a), 120.0 (C-3'), 133.0 (C-2'), 165.0 (C-4), 169.6 (C-1) ppm.

HRMS calcd. for $\text{C}_{10}\text{H}_{14}\text{N}_2\text{O}_2$ 194.1055; found: 194.1056 [M^+].

FT-IR (ATR): ν = 3202 (*m*), 2981 (*w*), 2880 (*w*), 1664 (*vs*), 1420 (*s*), 1336 (*m*), 1241 (*w*), 996 (*w*), 916 (*m*), 678 (*w*).

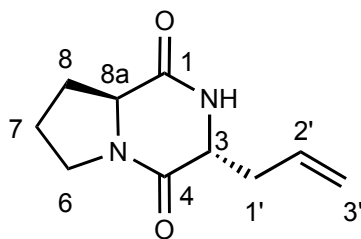
$[\alpha] = -89$ ($c = 0.1$, CH_2Cl_2).

(3R, 8aS)-trans-76f

Procedure	according to GP6
Stoichiometry:	208 mg, 1.00 mmol (3R,8aS)-1-Methoxy-3-allyl-6,7,8,8a-tetrahydropyrrolo [1,2-a]pyrazin-4(3H)-one (75f)
Yield:	116 g, 600 μmol , 60%
Purity:	>90% (GC, $^1\text{H-NMR}$)

$R_f = 0.34$ (Et₂O : MeOH = 8 : 1, Permanganate)

Yellow oil



¹H-NMR (500 MHz, CDCl₃): $\delta = 1.87$ - 1.97 (*m*, 1H, 7-H_b), 2.01 - 2.14 (*m*, 2H, 7-H_a, 8-H_b), 2.34 - 2.39 (*m*, 1H, 8-H_a), 2.39 - 2.46 (*m*, 1H, 1'-H_b), 2.91 (*dddd*, $J = 14.8, 5.7, 3.9, 1.6, 1.6$ Hz, 1H, 1'-H_a), 3.53 - 3.64 (*m*, 2H, 6-H), 4.06 (*dddd*, $J = 9.0, 3.9, 1.5, 0.7$ Hz, 1H, 3-H), 4.13 (*dddd*, $J = 9.2, 6.8, 1.8, 0.7$ Hz, 1H, 8a-H), 5.21 - 5.24 (*m*, 1H, 3'-H_a), 5.24 (*ddt*, $J = 17.0, 2.9, 1.5$, 1H, 3'-H_b), 5.79 (*dddd*, $J = 17.0, 10.2, 8.5, 5.7$ Hz, 2'-H), 6.33 (*br s*, 1H, NH) ppm.

¹³C-NMR (125 MHz, CDCl₃): $\delta = 22.5$ (C-7), 28.1 (C-8), 34.6 (C-1'), 45.3 (C-6), 53.8 (C-3), 59.0 (C-8a), 119.9 (C-3'), 133.0 (C-2'), 165.0 (C-4), 169.7 (C-1) ppm.

HRMS calcd. for C₁₀H₁₄N₂O₂ 194.1055; found: 194.1056 [M⁺].

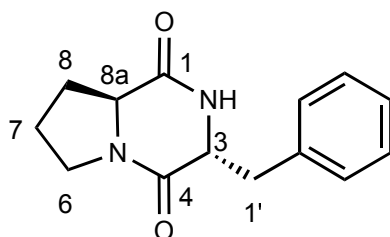
FT-IR (ATR): $\nu = 3220$ (*m*), 2981 (*w*), 2881 (*w*), 1663 (*vs*), 1416 (*s*), 1305 (*m*), 1002 (*m*), 921 (*m*), 708 (*w*) cm⁻¹.

$[\alpha] = -86$ ($c = 0.1$, CH₂Cl₂).

(3R,8aS)-3-Benzylhexahydropyrrolo[1,2-a]pyrazine-1,4-dione (*trans*-75h)

Procedure	according to GP6
Stoichiometry:	258 mg, 1.00 mmol (3R, 8aS)-1-Methoxy-3-benzyl-6,7,8,8a-tetrahydropyrrolo [1,2-a]pyrazin-4(3H)-one (75h)
Yield:	203 mg, 830 μ mol, 83%
Purity:	>90% (GC, ¹ H-NMR)

Colorless oil



$^1\text{H-NMR}$ (500 MHz, CDCl_3): δ = 1.84-2.04 (*m*, 3H, 7-H, 8- H_b), 2.29-2.34 (*m*, 1H, 8- H_a), 2.81 (*dd*, J = 14.5, 10.2 Hz, 1H, 1'- H_b), 3.53-3.67 (*m*, 3H, 1'- H_a , 6-H), 4.06 (*ddd*, J = 9.5, 6.5, 1.7 Hz, 1H, 8a-H), 4.28 (*ddd*, J = 10.2, 4.0, 1.6 Hz, 1H, 3-H), 5.89 (*br s*, 1H, NH), 5.89 (*br s*, 1H, NH), 7.22-7.24 (*m*, 2H, H_{aryl}), 7.25-7.30 (*m*, 1H, H_{aryl}), 7.32-7.36 (*m*, 2H, H_{aryl}) ppm.

$^{13}\text{C-NMR}$ (125 MHz, CDCl_3) δ = 21.7 (C-7), 29.0 (C-8), 40.7 (C-1'), 45.2 (C-6), 57.8 (C-3), 59.2 (C-8a), 127.5, 128.9, 134.3 (CH_{aryl}), 162.5 (C-1), 169.0 (C-4) ppm.

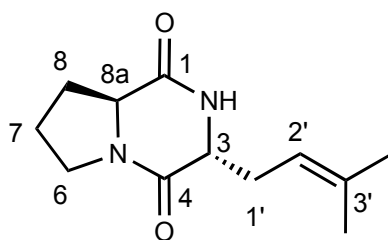
HRMS calcd. for $\text{C}_{14}\text{H}_{16}\text{N}_2\text{O}_2$ 244.1212; found: 244.1211 [M^+].

FT-IR (ATR): ν = 3245 (*m*), 2928 (*m*), 1661 (*vs*), 1453 (*s*), 1307 (*w*), 1184 (*w*), 1107 (*w*), 703 (*w*) cm^{-1} .

$[\alpha] = -14$ ($c = 1.0$, CH_2Cl_2).

Isolation of (3*R*, 8*aS*)-3-(3-Methylbut-2-enyl)hexahydropyrrolo[1,2-*a*]pyrazine-1,4-dione (*trans*-76*g*) and 3-(3-Chlorobenzyl)hexahydropyrrolo[1,2-*a*]pyrazine-1,4-dione (*trans*-76*i*) after chromatography of diastereomeric mixtures of 75*g* and 75*i*.

(3*S*, 8*aR*)-*trans*-76*g*



$R_f = 0.28$ (Et₂O : MeOH = 8:1, Permanganate)

¹H-NMR (300 MHz, CDCl₃): $\delta = 1.63$ (*d*, $J = 1.5$ Hz, 3H, CH₃), 1.73 (*dt*, $J = 1.3, 1.2$, 3H, CH₃), 1.83-1.98 (*m*, 2H, 7-H_b, 8-H_b), 2.00-2.07 (*m*, 1H, 7-H_a), 2.37-2.42 (*m*, 1H, 8-H_a), 2.5-2.54 (*m*, 2H, 1'-H), 3.49-3.54 (*m*, 1H, 6-H_b), 3.65-3.72 (*m*, 1H, 6-H_a), 3.94 (*dddd*, $J = 6.6, 5.7, 3.8, 0.9$ Hz, 1H, 3-H), 4.04 (*dd*, $J = 10.3, 6.4$, 1H, 8*a*-H), 5.15 (*tdq*, $J = 7.7, 1.5, 1.5$, 1H, 2'-H), 6.70 (*br s*, 1H, NH) ppm.

¹³C-NMR (125 MHz, CDCl₃): $\delta = 17.9$ (CH₃), 22.0 (C-7), 26.0 (CH₃), 29.3 (C-8), 33.0 (C-1'), 45.5 (C-6), 58.1 (C-3), 58.4 (C-8*a*), 117.5 (C-3'), 137.6 (C-2'), 165.7 (C-1), 169.3 (C-4) ppm.

HRMS calcd. for C₁₂H₁₈N₂O₂ 222.1368; found: 222.1352 [M⁺].

MS (EI): m/z (%) = 223 (45) [M⁺], 154 (100) [M⁺-C₅H₉], 125 (16), 70 (100).

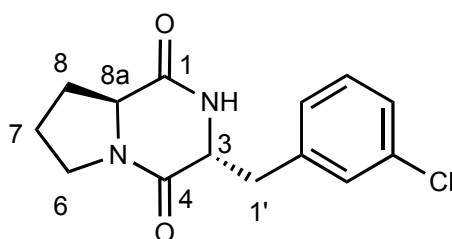
FT-IR (ATR): $\nu = 3235$ (*m*), 2927 (*m*), 1666 (*vs*), 1447 (*s*), 1304 (*w*), 1263 (*w*), 731 (*m*) cm^{-1} .

$[\alpha] = -2.7$ ($c = 1.0$, CH_2Cl_2).

GC: $t_{\text{R}}(\text{trans-76g}) = 19.80$ min.

Crystal data: $\text{C}_{12}\text{H}_{18}\text{N}_2\text{O}_2$, $M = 222.3$, orthorhombic, space group $\text{P}2(1)2(1)2(1)$; $a = 6.4274(8)$, $b = 7.8705(9)$, $c = 24.0198(19)$ Å, $a = b = c = 90^\circ$; $V = 1215.1(2)$ Å³, $Z = 4$; $D_{\text{c}} = 1.215$ g cm^{-3} . *Data collection*: crystal size $0.5 \times 0.3 \times 0.3$ mm, 2377 reflections in the range $\theta = 3.68\text{--}67.99^\circ$, 1992 unique reflections. *Structure refinement*: 1992 reflection data ($I > 2s(I)$), 150 parameters; the final R indices were $R = 0.0821$, $R_w = 0.1872$; residual electron density between 0.267 and -0.238 e \AA^{-3} .

(*3S*, *8aR*)-*trans*-**76i**



$R_f = 0.09$ (EtOAc, Permanganate).

M.p. = $135\text{--}137^\circ\text{C}$.

$^1\text{H-NMR}$ (500 MHz, CDCl_3): $\delta = 1.68\text{--}1.84$ (*m*, 2H, 7- H_b , 8- H_b), 1.96 (*dtd*, $J = 15.2$, 7.6 , 2.5 Hz, 1H, 7- H_a), $2.19\text{--}2.24$ (*m*, 1H, 8- H_a), 3.04 (*dd*, $J = 4.3$, 13.8 Hz, 1H, 1'- H_b), $3.05\text{--}3.08$ (*m*, 1H, 1'- H_a), 3.12 (*dd*, $J = 13.8$, 6.5 Hz, 1H, 8a-H), 3.43 (*ddd*, $J = 11.9$, 9.4 , 3.0 Hz, 1H, 6- H_b), 3.64 (*dt*, $J = 11.9$, 8.3 Hz, 1H, 6- H_a), 4.23 (*dtd*, $J = 6.0$, 4.3 , 0.9 Hz, 1H, 3-H), $7.01\text{--}7.12$ (*m*, 1H, H_{aryl}), $7.23\text{--}7.25$ (*m*, 2H, H_{aryl}), $7.26\text{--}7.28$ (*m*, 1H, H_{aryl}) ppm.

^{13}C -NMR (125 MHz, CDCl_3): δ = 21.7 (C-7), 29.0 (C-8), 40.1 (C-1'), 45.2 (C-6), 57.8 (C-3), 58.7 (C-8a), 127.6, 128.1, 129.9, 130.0, 134.5, 137.6 (CH_{aryl}), 164.6 (C-4), 169.4 (C-1) ppm.

CHN Analysis: $\text{C}_{16}\text{H}_{17}\text{ClN}_2\text{O}_2$ (292.10): calc: C 60.33, H 5.42, N 10.05, Cl 12.72;
found: C 60.17, H 5.45, N 20.01, Cl 12.81.

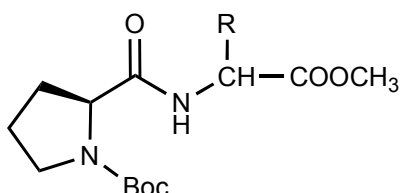
FT-IR (ATR): ν = 3226 (*m*), 2954 (*m*), 1646 (*vs*), 1439 (*vs*), 1305 (*vs*), 1305 (*s*), 1089 (*m*), 919 (*m*), 727 (*s*) cm^{-1} .

$[\alpha] = -20.6$ ($c = 1.0$, CH_2Cl_2).

GC: $t_{\text{R}}(\textit{trans}\text{-76i}) = 29.95$ min.

5.8 Experiments to chapter 4.3.2

The synthesis of the intermediate peptides (78)



78	R =		
a	CH ₃	c	<i>i</i> -C ₄ H ₉
b	<i>i</i> -C ₃ H ₇	d	CH ₂ -C ₆ H ₅

(S)-(-)-*N*-(*tert*-butoxycarbonyl)-prolylalanine methylester (78a)

Procedure according to GP5
 Stoichiometry: 3.20 g, 23.0 mmol alanine methylester hydrochloride
 Yield: 5.87 g, 19.5 mmol, 85%
 Purity: >90% (GC, ¹H-NMR)
 R_f : 0.60 (EtOAc, Permanganate)

M.p.= 75-77°C.

¹H-NMR (250 MHz, CDCl₃): δ = 1.39 (*d*, *J* = 7.2 Hz, 3H, CH₃), 1.47 [*s*, 9H, C(CH₃)₃], 1.77-2.00 (*m*, 2H, 3-H), 2.06-2.45 (*m*, 2H, 4-H), 3.43 (*br s*, 2H, 2-H), 3.74 (*s*, 3H, OCH₃), 4.28 (*br s*, 1H, CH), 4.56 (*br s*, 1H, CH), 7.33 (*br s*, 1 H, NH) ppm.

¹³C-NMR (125 MHz, CDCl₃): δ = 18.2 (C-1'), 24.5 (C-4), 28.2 [C(CH₃)₃, C-3], 52.3 (OCH₃), 60.9 (C-2), 80.3 [C(CH₃)₃], 155.6 (N-CO), 172.1 (CO-NH), 173.0 (COOCH₃) ppm.

FT-IR (ATR): ν = 3350 (*m*, NH), 2981 (*m*), 1745 (*s*, ester CO), 1661 (*vs*), 1539 (*s*), 1390 (*vs*), 1365 (*s*), 1157 (*vs*), 1120 (*s*), 1056 (*w*), 979 (*w*), 924 (*w*), 884 (*w*), 749 (*w*), 657 (*m*) cm⁻¹.

GC: $t_R = 9.155$ min.

Experimental data are in accordance with the literature.^[59]

(S)-(-)-N-(tert-butoxycarbonyl)-prolylvaline methylester (78b)

Procedure according to GP5
Stoichiometry: 3.85 g, 23.0 mmol valine methylester hydrochloride
Yield: 7.10 g, 21.6 mmol, 94%
Purity: >90% (GC, ¹H-NMR)
 $R_f = 0.64$ (EtOAc : PE = 1 : 1, Permanganate)

M.p. = 61-63°C.

¹H-NMR (500 MHz, CDCl₃): $\delta = 0.89$ (*d*, $J = 6.8$ Hz, 6H, 2'-CH₃, 2''-CH₃), 0.92 (*d*, $J = 6.8$ Hz, 6H, 3'-CH₃, 3''-CH₃), 1.48 [*s*, 18H, C(CH₃)₃, C(CH₃)₃*], 1.89 (*br s*, 4H, 3-H, 3-H*), 2.17 (*br s*, 4H, 4-H, 4-H*), 2.39 (*br s*, 1H, 2'-H), 3.30-3.56 (*m*, 4H, 5-H, 5*-H), 3.73 (*s*, 6H, OCH₃, OCH₃*), 4.27-4.37 (*m*, 1H, 2-H), 4.46-4.52 (*m*, 2H, 1'-H, 1-H*), 7.52 (*br s*, 1H, NH) ppm.

¹³C-NMR (125 MHz, CDCl₃): $\delta = 17.5$ (CH₃), 18.8 (CH₃), 24.5 (C-4), 28.2 [C(CH₃)₃], 30.9 (C-3), 46.8 (C-5, CH), 51.8 (OCH₃), 56.6 (C-1'), 60.4 (C-2), 80.2 [C(CH₃)₃], 155.7 (N-CO), 172.0 (CO-NH, COOCH₃) ppm.

*signals of the other rotamer

CHN Analysis: C₁₆H₂₈N₂O₅ (328.19): calc: C 58.52, H 8.59, N 8.53;
found: C 58.27, H 8.54, N 8.42.

FT-IR (ATR): $\nu = 3322$ (w), 2966 (m), 1742 (s), 1666 (vs), 1532 (s), 1391 (vs), 1365 (vs), 1256 (m), 1203 (m), 1159 (vs), 1119 (s), 982 (w), 886 (w), 772 (m).

GC: $t_R = 11.448$ min.

(S)-N-(tert-butoxycarbonyl)-prolylisoleucine methylester (78c)

Procedure according to GP6
Stoichiometry: 4.17 g, 23.0 mmol, isoleucine methylester hydrochloride
Yield: 5.8 g, 17.0 mmol, 74%
Purity: >90% (GC, ¹H-NMR)
R_f = 0.70 (EtOAc : PE = 1 : 1, Permanganate)

M.p. = 82-84°C.

FT-IR (ATR): ν = 3282 (m), 2953 (m), 1743 (s), 1695 (vs), 1656 (s), 1557 (s), 1389 (vs), 1212 (s), 1152 (s), 1117 (s), 988 (w), 771 (w), 680 (m).

¹H-NMR (500 MHz, CDCl₃): δ = 0.99 (s, 6H, 3'-CH₃, 4'-CH₃), 1.47 [s, 9H, C(CH₃)₃], 1.53-1.69 (m, 3H, 3-H_b, 3-H_a, 4-H_b), 1.77-2.01 (m, 3H, 4-H_a, 2'-H_b, 2'-H_a), 2.07-2.22 (m, 1H, 3'-H), 3.26-3.55 (m, 2H, 2'-H_b, 2'-H_a), 3.72 (s, 3H, OCH₃), 4.25-4.33 (m, 1H, CH), 4.52-4.63 (m, 1H, CH), 7.38 (br s, 0.5H, NH) ppm.

¹³C-NMR (125 MHz, CDCl₃): δ = 21.7 (CH₃), 22.8 (CH₃), 24.7 (C-4), 27.4 (C-1'), 28.2 (C(CH₃)₃, C-3), 41.6 (C-2'), 46.9 (C-1', C-5), 52.1 (OCH₃), 61.0 (C-2), 80.3 [C(CH₃)₃], 154.6, 155.8 (N-CO), 171.6 (CO-NH), 173.0 (COOCH₃) ppm.

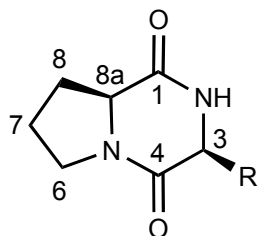
CHN Analysis: C₁₇H₃₀N₂O₅ (342.21): calcd: C 59.63, H 8.83, N 8.18;
found: C 59.60, H 8.64, N 8.26.

(S)-(-)-N-(tert-butoxycarbonyl)-prolylphenylalanine methylester (78d)

Procedure according to GP6
Stoichiometry: 5.00 g, 23.0 mmol phenylalanine methylester hydrochloride
Yield: 8.37 g, 22.3 mmol, 97%
Purity: >90% (GC, ¹H-NMR)

M.p. = 69-71°C.

Preparation of *cis*-diketopiperazines from (69) and L-amino acid esters (78)^[56]



6	R =		
a	CH ₃	e	<i>i</i> -C ₃ H ₇
d	<i>i</i> -C ₄ H ₉	h	CH ₂ -C ₆ H ₅

(3*S*, 8*aS*)-3-Methylhexahydropyrrolo[1,2-*a*]pyrazine-1,4-dione (*cis*-76*a*)

Procedure according to GP1

Stoichiometry: 2.70 g, 9.00 mmol N-(-)-(tert-butoxycarbonyl)-prolyl alanine methylester (**78a**)

Purity: >90% (GC, ¹H-NMR)

R_f = 0.27 (Et₂O : MeOH = 8 : 1, Permanganate)

M.p. = 173–175°C.

¹H-NMR (500 MHz, CDCl₃): δ = 1.48 (*d*, *J* = 6.8 Hz, 3H, CH₃), 1.86-1.95 (*m*, 1H, 7-H_b), 1.99-2.06 (*m*, 1H, 7-H_a), 2.07-2.15 (*m*, 1H, 8-H_b), 2.31-2.37 (*m*, 1H, 8-H_a), 3.53 (*dd*, *J* = 8.7, 3.5 Hz, 1H, 6-H_b), 3.58-3.63 (*m*, 1H, 6-H_a), 4.10-4.15 (*m*, 2H, 3-H_b, 8a-H), 7.27 (*br s*, 1H, NH) ppm.

¹³C-NMR (125 MHz, CDCl₃): δ = 15.9 (C-1'), 22.8 (C-7), 28.2 (C-8), 45.4 (C-6), 51.2 (C-3), 59.3 (C-8a), 166.6 (C-1), 170.7 (C-4) ppm.

MS (EI): *m/z* (%) = 169 (10) [M⁺ + H], 168 (62) [M⁺], 125 (30), 112 (10), 97 (50), 70 (100), 55 (12).

FT-IR (ATR): $\nu = 3228$ (*m*), 1661 (*vs*), 1429 (*m*), 1302 (*w*), 1202 (*w*), 1159 (*w*), 1127 (*w*), 658 (*w*) cm^{-1} .

$[\alpha] = -89$ ($c = 0.5$, EtOH).

GC: $t_R = 7.82$ min.

Crystal data: $\text{C}_8\text{H}_{12}\text{N}_2\text{O}_2$, $M = 168.2$, monoclinic, space group P2(1); $a = 7.2825(13)$, $b = 6.5604(13)$, $c = 9.2844(13)$ Å, $a = b = 90^\circ$, $b = 111.399(11)^\circ$; $V = 412.99(12)$ Å³, $Z = 2$; $D_c = 1.353$ g cm^{-3} . *Data collection*: crystal size 0.50 × 0.25 × 0.15 mm, 858 reflections in the range $\theta = 2.36$ – 24.99° , 795 unique reflections. *Structure refinement*: 795 reflection data ($I > 2s(I)$), 158 parameters; the final R indices were $R = 0.0352$, $R_w = 0.0719$; residual electron density between 0.131 and -0.128 e Å⁻³.

(3*S*, 8*aS*)-3-Isobutylhexahydropyrrolo[1,2-*a*]pyrazine-1,4-dione (cis-76d)

Procedure according to GP1
 Stoichiometry: 3.00 g, 9.00 mmol N-(*tert*-butoxycarbonyl)-Prolyl Isoleucine
 methylester (**78c**)
 Yield: 1.32 g, 6.30 mmol, 70%
 Purity: >90% (GC, ¹H-NMR)
 $R_f = 0.45$ (Et₂O : MeOH = 8 : 1, Permanganate).

M.p. = 157-159°C.

¹H-NMR (500 MHz, CDCl₃): $\delta = 0.95$ (*d*, $J = 6.5$ Hz, 3H, CH₃), 1.00 (*d*, $J = 6.5$ Hz, 3H, CH₃), 1.53 (*ddd*, $J = 14.4, 9.4, 4.9$ Hz, 1H, 1'-H_b), 1.75-1.84 (*m*, 1H, 1'-H_a), 1.86-1.95 (*m*, 1H, 7-H_b), 1.98–2.08 (*m*, 2H, 7-H_a, 2'-H_a), 2.09-2.16 (*m*, 1H, 8-H_b), 2.34 (*tdd*, $J = 12.8, 7.0, 3.1$, 1H, 8-H_a), 3.51-3.62 (*m*, 2H, 6-H), 4.01 (*dddd*, $J = 9.4, 3.9, 1.6, 0.8$ Hz, 1H, 3-H), 4.10-4.13 (*m*, 1H, 8a-H), 6.52 (*br s*, 1H, NH) ppm.

^{13}C -NMR (125 MHz, CDCl_3): δ = 21.3 (C-4'), 22.8 (C-3'), 24.6 (C-2'), 28.1 (C-8), 38.6 (C-1'), 45.5 (C-6), 53.4 (C-8a), 58.9 (C-3), 166.3 (C-1), 170.5 (C-4) ppm.

FT-IR (ATR): ν = 3262 (*m*), 2952 (*m*), 2871 (*w*), 1669 (*vs*), 1634 (*vs*), 1432 (*s*), 1301 (*m*), 1180 (*w*), 1157 (*w*), 916 (*m*), 710 (*w*) cm^{-1} .

$[\alpha] = -120$ ($c = 0.4$, CH_2Cl_2).

(3S, 8aS)-3-Isopropylhexahydropyrrolo[1,2-a]pyrazine-1,4-dione (cis-76e)

Procedure according to GP1
Stoichiometry: 3.00 g, 9.00 mmol *N*-(*tert*-butoxycarbonyl)-prolyl valine methylester (**78b**)
Purity: >90% (GC, ^1H -NMR)

M.p. = 181-183°C.

$R_f = 0.28$ ($\text{Et}_2\text{O} : \text{MeOH} = 4 : 1$, Permanganate).

^1H -NMR (500 MHz, CDCl_3): δ = 0.91 (*d*, $J = 6.8$ Hz, 3H, CH_3), 1.07 (*d*, $J = 7.2$ Hz, 3H, CH_3), 1.84–1.97 (*m*, 2H, 7- H_b , 8- H_b), 2.01-2.09 (*m*, 1H, 7- H_a), 2.34-2.41 (*m*, 1H, 8- H_a), 2.64 (*qqd*, $J = 7.2, 6.8, 2.7$ Hz, 1H, 1'-H), 3.54 (*dddd*, $J = 12.1, 9.2, 3.0, 0.7$, 1H, 6- H_b), 3.61–3.67 (*m*, 1H, 6- H_a), 3.94 (*ddd*, $J = 2.7, 1.8, 0.9$ Hz, 1H, 3-H), 4.06-4.14 (*m*, 1H, 8a-H), 5.96 (*br s*, 1H, NH) ppm.

^{13}C -NMR (125 MHz, CDCl_3): δ = 16.1 (C-2'), 19.3 (C-3'), 22.4 (C-7), 28.3 (C-1'), 28.5 (C-8), 45.2 (C-6), 58.8 (C-3), 60.4 (C-8a), 164.9 (C-1), 167.0 (C-4) ppm.

MS (EI): m/z (%) = 196 (5) [M^+], 154 (100) [$\text{M}^+ - \text{C}_3\text{H}_7$], 125 (35), 110 (10), 98 (12), 72 (32), 70 (98).

FT-IR (ATR): $\nu = 3210$ (*m*), 2962 (*m*), 1672 (*vs*), 1428 (*s*), 1298 (*m*), 1180 (*w*), 1121 (*w*), 916 (*m*), 735 (*w*) cm^{-1} .

$[\alpha] = -152$ ($c = 0.45$, CH_2Cl_2).

GC: $t_R = 8.51$ min.

(3S, 8aS)-3-Benzylhexahydropyrrolo[1,2-a]pyrazine-1,4-dione (cis-76h)

Procedure according to GP1

Stoichiometry: 3.40 g, 9.00 mmol *N*-(*tert*-butoxycarbonyl)-prolyl phenylalanil methylester (**78d**)

Yield: 1.62 g, 6.66 mmol, 74%

Purity: >90% (GC, $^1\text{H-NMR}$)

$R_f = 0.45$ ($\text{Et}_2\text{O} : \text{MeOH} = 4 : 1$, Permanganate).

$^1\text{H-NMR}$ (500 MHz, CDCl_3): $\delta = 1.86$ -2.04 (*m*, 3H, 8- H_b , 7-H), 2.29-2.34 (*m*, 1H, 8- H_a), 2.82 (*dd*, $J = 14.5, 10.2$ Hz, 1H, 1'- H_b), 3.53–3.67 (*m*, 3H, 1'- H_a , 6-H), 4.07 (*m*, 1H, 8a-H), 4.29 (*ddd*, $J = 10.2, 3.9, 1.6, 0.7$ Hz, 1H, 3-H), 6.00 (*br s*, 1H, NH), 7.23 (*m*, 1H, H_{aryl}), 7.28 (*m*, 1H, H_{aryl}), 7.34 (*m*, 1H, H_{aryl}) ppm.

$^{13}\text{C-NMR}$ (125 MHz, CDCl_3): $\delta = 22.5$ (C-7), 28.3 (C-8), 36.8 (C-1'), 45.4 (C-6), 56.2 (C-3), 59.1 (C-8a), 127.5, 129.2, 136.0 (CH_{aryl}), 165.1 (C-1), 169.4 (C-4) ppm.

CHN Analysis: $\text{C}_{14}\text{H}_{16}\text{N}_2\text{O}_2$ (244.12): calc: C 68.83, H 6.60, N 11.47;
found: C 68.30, H 6.55, N 11.43.

FT-IR (ATR): $\nu = 3228$ (*m*), 2881 (*m*), 1660 (*vs*), 1453 (*s*), 1421 (*s*), 1310 (*w*), 1204 (*w*), 1115 (*w*), 920 (*w*), 731 (*m*), 702 (*m*), 593 (*w*) cm^{-1} .

MS (EI): m/z (%) = 245 (12, $[\text{M}^+ + \text{H}]$), 244 (50, $[\text{M}^+]$), 153 (10, $[\text{M}^+ - \text{C}_6\text{H}_5\text{CH}_2]$), 125 (100), 104 (12), 91 (70), 70 (60), 64.9 (20).

$[\alpha] = -165$ ($c = 1.0$, CH_2Cl_2).

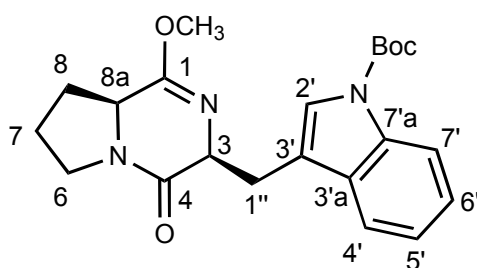
GC: $t_R = 11.67$ min.

5.9 Experiments to chapter 4.4

4.4.1 The Alkylation of the lactimether (**63**) with the indole derivate (**66**)

(3*S*,8*aS*)-3-(3-Methylindol)-methoxy-6,7,7,8,8*a*-tetrahydro-3*H*-[1,2-*a*]-pyrazine-4-one (**79**)

To a solution of LDA (6.36 mmol) in THF (10 mL), a solution of lactimether **63** (1.00 g, 6.00 mmol) in THF (10 mL) was added dropwise, at -78°C . LDA in THF was freshly prepared from *n*BuLi (4.00 mL solution 1.6 M in pentane, 6.36 mmol) and diisopropyl amine (0.90 mL, 643 mg, 6.36 mmol). After stirring for 4 h at -78°C , hexamethylphosphoramide (10.5 mL, 10.0 g, 63.6 mmol) was added as a co-solvent, and the stirring was maintained for 45 minutes under stirring, at the same temp., followed by the slow addition of the indole bromide **69** (2.00 g, 6.60 mmol) in THF (15 mL) and the reaction mixture was kept at -78°C overnight. Then it was warmed to room temp. and hydrolyzed with a saturated NaHCO_3 solution (250 mL). The layers were separated and the aqueous layer was extracted with CH_2Cl_2 (3×250 mL). The combined organic layers were dried (Na_2SO_4), evaporated and purified by flash chromatography on silica gel (EtOAc).



Yield: 320 mg, 0.78 mmol, 13%

Purity: >95% ($^1\text{H-NMR}$, GC)

M.p. = 63°C .

$R_f = 0.50$ (EtOAc, UV).

MS (EI): m/z (%) = 297 (25) [M^+ - Boc], 168 (60) [M^+ - $C_{14}H_{15}NO_2$], 167 (45) [M^+ - $C_{14}H_{16}NO_2$], 130 (100).

1H -NMR (300 MHz, $CDCl_3$): $\delta = 1.31$ - 1.45 (*m*, 1H, 7- H_b), 1.65 [*s*, 9H, $C(CH_3)_3$], 1.74- 1.88 (*m*, 2H, 7- H_a , 8- H_b), 2.11 (*dddd*, $J = 6.3, 6.3, 2.2$ Hz, 1H, 8- H_a), 3.22 (*ddd*, $J = 14.6, 7.3, 1.0$ Hz, 1H, 1''- H_b), 3.36 (*ddd*, $J = 12.1, 8.8, 3.5$ Hz, 1H, 6- H_b), 3.49 (*ddd*, $J = 14.6, 4.1, 1.0$ Hz, 1H, 1''- H_a), 3.59 (*dt*, $J = 12.1, 8.6$ Hz, 1H, 6- H_a), 3.68 (*s*, 3H, OCH_3), 3.92 (*ddd*, $J = 10.7, 6.3, 3.8$ Hz, 1H, 8a-H), 4.24 (*ddt*, $J = 7.3, 4.1, 0.9$ Hz, 1H, 3-H), 7.20 (*ddd*, $J = 7.7, 7.3, 1.2$ Hz, H_{aryl}), 7.24-7.29 (*m*, 1H, H_{aryl}), 7.50 (*br s*, 1H, H_{aryl}), 7.68-7.71 (*m*, 1H, H_{aryl}), 8.09 (*d*, $J = 8.3$ Hz, 1H, 2'-H) ppm.

^{13}C -NMR (75 MHz, $CDCl_3$): $\delta = 20.9$ (C-7), 22.3 (C-8), 28.1 ($C(CH_3)_3$), 28.8 (C-1''), 44.1 (C-6), 53.2 (OCH_3), 56.8 (C-3), 60.4 (C-8a), 83.0 [$C(CH_3)_3$], 114.8 (C-3'), 117.8 (C-2'), 119.9 (CH_{aryl}), 121.9 (CH_{aryl}), 123.1 (CH_{aryl}), 124.2 (CH_{aryl}), 131.3 (C-3'a), 135.0 (C-7'a), 149.7 (C=O), 161.0 (C-4), 167.9 (C-1) ppm.

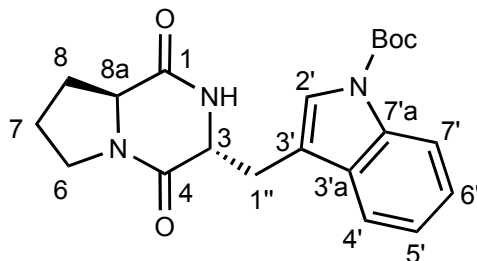
HRMS calcd. for $C_{22}H_{27}N_3O_4$ 397.2002; found: 397.2002 [M^+].

FT-IR (ATR): $\nu = 2978$ (*m*), 2944 (*w*), 1729 (*s*), 1672 (*s*), 1452 (*s*), 1370 (*vs*), 1255 (*s*), 1158 (*vs*), 1085 (*m*), 1016 (*w*), 855 (*w*), 764 (*w*), 748 (*w*), 592 (*w*), 563 (*w*) cm^{-1} .

$[\alpha] = -35$ ($c = 1$, CH_2Cl_2)

GC: $t_R = 13.687$ min.

(3S, 8aR)-3-(3-Methylindol)-6,7,7,8,8a-tetrahydro-3H-[1,2-a]pyrazine-2,4-dione (80)



M.p. = 182°C.

R_f = 0.64 (Et₂O : MeOH = 12 : 1, UV).

¹H-NMR (500 MHz, CDCl₃): δ = 1.53-1.63 (*m*, 1H, 7-H_b), 1.63 [s, 9H, C(CH₃)₃], 1.78 (*dtd*, *J* = 12.5, 11.3, 7.4 Hz, 1H, 8-H_b), 1.88-1.95 (*m*, 1H, 7-H_a), 2.17 (*dddd*, *J* = 12.5, 6.6, 6.6, 1.8 Hz, 1H, 8-H_a), 3.19 (*ddd*, *J* = 14.5, 4.4, 0.9 Hz, 1H, 1''-H_b), 3.24 (*ddd*, *J* = 14.5, 6.8, 0.4 Hz, 1H, 1''-H_a), 3.28-3.30 (*m*, 2H, 6-H_b, 3-H), 3.61 (*ddd*, 12.0, 9.2, 7.9 Hz, 6-H_a), 4.23-4.26 (*m*, 1H, 8a-H), 6.78 (*br s*, 1H, NH), 7.22-7.25 (*m*, 1H, H_{aryl}), 7.29-7.32 (*m*, 1H, H_{aryl}), 7.47 (*br s*, 1H, H_{aryl}), 7.54-7.56 (*m*, 1H, H_{aryl}), 8.11 (*d*, *J* = 8.0 Hz, 1H, 2'-H) ppm.

¹³C-NMR (125 MHz, CDCl₃): δ = 21.6 (C-7), 28.2 [C(CH₃)₃], 28.9 (C-8), 30.3 (C-1'), 45.3 (C-6), 57.9 (C-3), 58.0 (C-8a), 84.0 [C(CH₃)₃], 114.4 (C-3'), 115.3 (C-2'), 119.0 (CH_{aryl}), 122.7 (CH_{aryl}), 124.8 (CH_{aryl}), 125.2 (CH_{aryl}), 129.7 (C-3'a), 135.5 (C-7'a), 149.4 (C=O), 165.2 (C-4), 169.1 (C-1) ppm.

CHN Analysis: C₂₁H₂₅N₃O₄ (383.44): calc: C 65.78, H 6.57, N 10.96
found: C 65.14, H 6.58, N 10.55.

MS (EI): *m/z* (%) = 283 (10) [M⁺ - Boc], 130 (100).

FT-IR (ATR): ν = 2977 (*m*), 2932 (*w*), 1731 (*vs*), 1665 (*vs*), 1452 (*s*), 1369 (*s*), 1255 (*s*), 1157 (*s*), 1084 (*m*), 1017 (*m*), 854 (*w*), 747 (*w*) cm⁻¹.

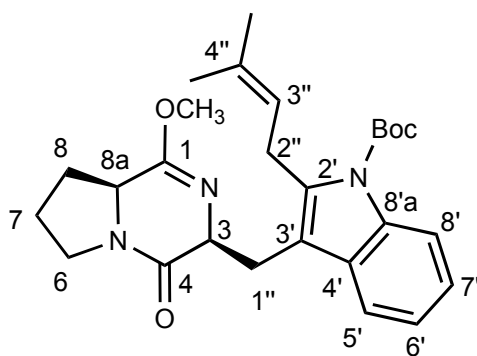
$[\alpha] = -17.5$ ($c = 0.5$, CH_2Cl_2).

GC: $t_R = 13.79$ min.

4.4.2 Alkylation of indole lactim ether *cis*-79 with isoprenyl derivative 46

(3*S*,8*aS*)-3-(3-Methyl-2-isoprenyl-indole)-1-methyl-6,7,7,8,8*a*-tetrahydro-3*H*-[1,2-*a*]-pyrazine-4-one (81)

To a solution of 3-(3-methylindol)-methoxy-6,7,7,8,8*a*-tetrahydro-3*H*-[1,2-*a*]-pyrazine-4-one **79** (100 mg, 0.25 mmol) in dry THF (2 mL), at -78°C under nitrogen, a solution of LDA (370 μmol) was added dropwise. The LDA was prepared from *n*BuLi (23.0 μL solution 1.6 M in pentane, 0.37 mmol) and diisopropyl amine (52.0 μL , 37.0 mg, 0.37 mmol). The mixture was stirred at -78°C for 1 h, then warmed to 0°C for 10 minutes. Then isoprenyl bromide (86.0 μL , 111 mg, 0.75 mmol) was quickly added at 0°C and the mixture was stirred at 0°C for 1 h and then warmed to room temp. overnight. The solvent was removed under reduced pressure. The residue was taken up in CH_2Cl_2 (5 mL) and washed with a 5% aqueous NaHCO_3 solution (3 mL). The aqueous layer was extracted with CH_2Cl_2 (4 x 5 mL) and the combined organic layers were dried over Na_2SO_4 . After the removal of the solvent under reduced pressure, the residue was purified on silica gel (EtOAc : PE = 1 : 1), to yield the product as a yellow oil (16.0 mg, 35.0 μmol , 14%).



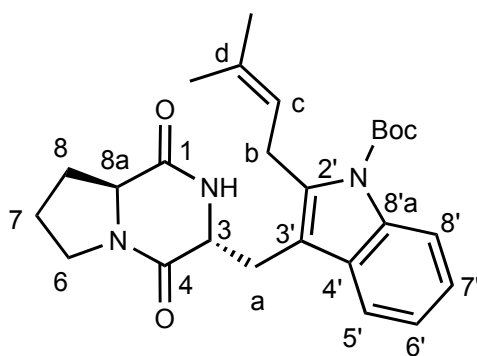
$R_f = 0.07$ (EtOAc : PE = 1 : 1, UV).

MS (EI): m/z (%) = 365 (15), $[M^+ - \text{Boc}]$, 281 (45), 236 (55), 207 (100), 192 (35), 181 (50), 161 (25), 156 (25), 130 (70), 105 (30), 95 (40), 82 (75), 70 (45).

(3*R*, 8*aS*)-*N*-(*tert*-butoxycarbonyl)-3-(3-methyl-2-isoprenyl-indole)-6,7,7,8,8*a*-tetrahydro-3*H*-[1,2-*a*]pyrazine-2,4-dione (82)

Procedure according to GP4

Stoichiometry 10.0 mg, 22.0 μmol (3*R*, 8*aS*)-3-(3-methyl-2-isoprenyl-indole)-1-methyl-6,7,7,8,8*a*-tetrahydro-3*H*-[1,2-*a*]pyrazine-4-one **81**
4.18 mg, 22.0 mmol, TsOH • H₂O

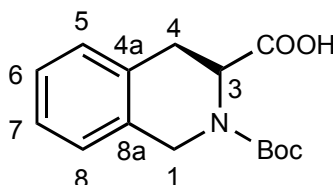


FT-IR (ATR): ν = 1719 (s), 1667 (s), 1451 (m), 1366 (s), 1252 (m), 1151 (vs), 911 (s), 731 (vs) cm^{-1} .

5.10 Experiments to chapter 4.6.1

(S)-(-)-N-(*tert*-butoxycarbonyl)-1,2,3,4-tetrahydroisoquinoline-3-carboxylic acid (131)

To a solution of (S)-1,2,3,4-tetrahydroisoquinoline-3-carboxylic acid **130** (16.1 g, 90.0 mmol) in an aqueous 1N NaOH solution (180 mL, 180 mmol) and *tert*-BuOH (110 mL), di-*tert*-butyl dicarbonate (19.6 g, 90.0 mmol) was added dropwise, while maintaining pH at 8.5 by further addition of NaOH. The resulting mixture was stirred at room temp. overnight. Then the mixture was extracted with hexanes (2 x 10 mL) and the combined organic layers were extracted with saturated NaHCO₃ solution (2 x 10 mL) and adjusted at pH = 1, by careful addition of KHSO₄ (23 g in 150 mL H₂O), under ice cooling. The resulted mixture was extracted with Et₂O (2 x 60 mL) and ethyl acetate (2 x 60 mL). The combined organic layers were washed with H₂O (10 mL) and brine (10 mL) and dried over Na₂SO₄. The removal of the solvent under reduced pressure yielded 21.0 g (75.6 mmol, 84%) of a colorless solid.



M.p. = 100-105°C.

R_f = 0.36 (EtOAc : PE = 1 : 2, UV).

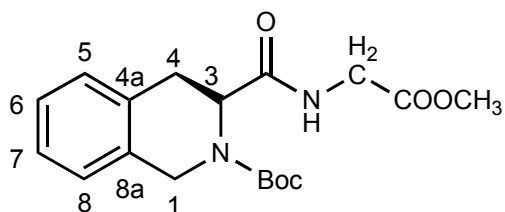
¹H-NMR (300 MHz, CDCl₃): δ = 1.39, 1.50 [2 x s, 9H, C(CH₃)₃], 3.09-3.27 (m, 2H, 1-H), 4.45 (dd, J = 12.4, 16.5 Hz, 1H, 4-H_a), 4.68 (dd, J = 6.0, 16.5 Hz, 1H, 4-H_b), 4.74 (d, J = 5.1 Hz, 0.5 H, 3-H), 5.11 (m, 0.5 H, 3-H), 7.09-7.17 (m, 4H, H_{aryl}), 10.38 (br s, 1H, COOH) ppm.

¹³C-NMR (75 MHz, CDCl₃): δ = 28.6 [C(CH₃)₃], 31.2 (C-4), 44.4 (C-1), 54.0 (C-3), 79.5 [C(CH₃)₃], 126.0, 126.6, 126.7, 127.6 (CH_{aryl}), 154.6 (C-4a), 155.5 (C-8a), 176.7 (COOH), 177.6 (C=O) ppm.

Experimental data are in accordance with the literature^[70].

(S)-(-)-N-(tert-butoxycarbonyl)-tetrahydroisoquinoline glycine methylester (133)

To a stirred mixture of (S)-N-Boc-1,2,3,4-tetrahydroisoquinoline-3-carboxylic acid **133** (4.43 g, 16.0 mmol), glycine methylester hydrochloride (2.00 g, 16.0 mmol), 1-[3-(dimethylamino)propyl]-3-ethylcarbodiimide hydrochloride (3.94 g, 2.00 mmol) and 4-hydroxybenzotriazole monohydrate (2.70 g, 20.0 mmol), triethylamine (4.50 mL, 3.23 mg, 32.0 mmol) was added and the reaction mixture was stirred for 24 h at room temp. The solvent was removed under reduced pressure and the residue was taken up in ethyl acetate (150 mL), and washed successively with H₂O (200 mL), 5 % aqueous citric acid solution (4 x 50 mL) and 10 % aqueous K₂CO₃ solution (2 x 70 mL) and the solvent was removed under reduced pressure, to give the product **133** as a colorless solid (3.52 g, 10 mmol, 63%).



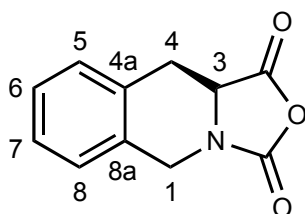
M.p. = 125-127°C.

¹H-NMR (300 MHz, CDCl₃): δ = 1.50 [s, 9H, C(CH₃)₃], 3.10-3.29 (m, 2H, 4-H), 3.68 (s, 3H, OCH₃), 3.85-4.00 (m, 2H, 1-H), 4.39-4.56 (m, 1H, 3-H), 4.65 (d, J = 16.7 Hz, 2H, CH₂), 6.52 (br s, 1H, NH), 7.17-7.23 (m, 4H, H_{aryl}) ppm.

¹³C-NMR (75 MHz, CDCl₃) = 28.3 [C(CH₃)₃], 31.6 (C-4), 41.1 (CH₂), 44.4 (C-1), 52.3 (OCH₃), 56.3 (C-3), 81.3 [C(CH₃)₃] 126.1, 126.5, 127.4, 128.0 (CH_{aryl}), 155.0 (C-4a), 156.4 (C-8a), 169.7 (CO-NH), 171.9 (COOCH₃) ppm.

(S)-(-)-N-carboxy-1,2,3,4-tetrahydroisoquinoline-3-carboxylic acid anhydride (132)

To a solution of (S)-(-)-N-(*tert*-butoxy-1,2,3,4-tetrahydroisoquinoline-3-carboxylic acid **52** (1.27 g, 4.50 mmol) in CH₂Cl₂, PCl₃ (741 mg, 0.50 mL, 5.40 mmol) was added drop wise at 0°C and the resulting mixture was stirred for 2 h at 0°C. The solvent was removed under reduced pressure and the residue was washed with *n*-hexane and crystallized from Et₂O, to yield the product as a colorless solid (900 mg, 4.45 mmol, 99%).



M.p. = 185°C.

¹H-NMR (300 MHz, D₂O): δ = 3.19-3.29 (*m*, 1H, 4-H_b), 3.47 (*dd*, *J* = 17.3, 5.4 Hz, 4-H_a), 4.32 (*dd*, *J* = 11.0, 5.4 Hz, 1H, 3-H), 4.44 (*d*, *J* = 16.0 Hz, 1H, 1-H_b), 4.51 (*d*, *J* = 16.0 Hz, 1-H_a), 7.25-7.41 (*m*, 4H, H_{aryl}) ppm.

Experimental data are in accordance with the literature.^[48]

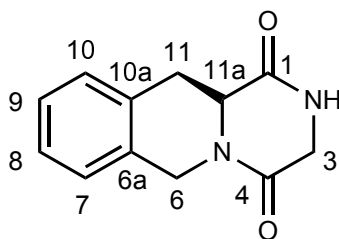
(S)-1,4-Dioxo-1,3,4,6,11,11a-hexahydro-pyrazino[1,2-*b*]isoquinoline (134)*Method A:*

The anhydride **132** (900 mg, 4.45 mmol) was added to a cooled solution of glycine methylester hydrochloride (614 mg, 4.90 mmol) and triethylamine (1.25 mL, 900 mg, 8.90 mmol), in CH₂Cl₂ (10 mL), at -78°C. The stirring was continued for 2 h, at -78°C. The mixture was kept overnight at -20°C. The precipitate was removed by filtration through Celite and the solvent was evaporated. The residual oil was redissolved in toluene (10 mL), refluxed for 24 h and the precipitate was collected, redissolved in

H₂O (15 mL), treated with charcoal and refluxed for 1 h. After filtration through Celite, the solvent was removed by azeotropic distillation with EtOH. Purification by crystallization from H₂O yielded 800 mg (3.70 mmol, 83%) of a colorless solid.

Method B:

The peptide **133** (1.00 g, 2.80 mmol) was dissolved in trifluoroacetic acid (3.00 mL, 4.60 g, 40.0 mmol) and the solution was stirred at room temp. for 1 h. The solvent was removed and the residue was dissolved in MeOH (10 mL) and treated with triethylamine (1.57 mL, 1.13 g, 11.2 mmol). The reaction mixture was kept under reflux overnight. The solvent was removed under reduced pressure and the oily residue was crystallized from isopropanol, to give the product as colorless crystals (526 mg, 2.44 mmol, 87%).



M.p. = 200°C.

R_f = 0.20 (EtOAc, UV).

¹H-NMR (500 MHz, DMSO): δ = 3.09 (*ddd*, *J* = 16.1, 11.9, 0.9 Hz, 1-H, 11-H_b), 3.17 (*dd*, *J* = 16.1, 4.1 Hz, 1H, 11-H_a), 3.87 (*dddd*, *J* = 17.4, 1.9, 1.1, 0.8 Hz, 1H, 3-H_b), 3.92 (*ddd*, *J* = 17.4, 2.1, 1.0, 1H, 3-H_a), 4.20 (*dddd*, *J* = 11.9, 4.1, 1.2, 1.1 Hz, 1-H, 11a-H), 4.28 (*d*, *J* = 16.8 Hz, 1H, 6-H_b), 5.12 (*d*, *J* = 16.8 Hz, 1-H, 6-H_a), 7.23-7.25 (*m*, 4H, H_{aryl}), 8.27 (*br s*, 1H, NH) ppm.

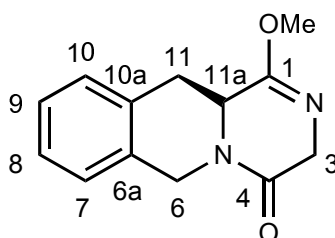
¹³C-NMR (125 MHz, DMSO): δ = 32.0 (C-11), 43.2 (C-6), 44.1 (C-3), 54.6 (C-11a), 126.2 (C-8), 126.5 (C-9), 126.6 (C-10), 128.5 (C-7), 132.3 (C-6_a), 133.1 (C-10a), 163.2 (C-1), 166.5 (C-4) ppm.

CHN Analysis: C₁₂H₁₂N₂O₂ (216.23): calc: C 66.65, H 5.59, N 12.96;
found: C 66.75, H 5.74, N 12.85.

Experimental data are in accordance with the literature.^[48]

1-Methoxy-3,6,11,11a-tetrahydro-4H-pyrazine-[1,2-b]-isoquinolin-4-one (129)

A mixture of diketopiperazine **134** (1.17 g, 5.40 mmol) and trimethyloxonium tetrafluoroborate (880 mg, 6.00 mmol) were ground together in a mortar, dissolved in CH₂Cl₂ (20 mL) and refluxed for 12 h. Trimethyloxonium tetrafluoroborate (440 mg, 3.00 mmol) was then added and refluxing was continued for another 12 h. Then, the solution was poured into an ice-cooled saturated NaHCO₃ solution (pH > 7.5), under vigorous stirring, the layers were separated and the aqueous layer was extracted with CH₂Cl₂ (4 x 30 mL). The combined organic layers were dried over Na₂SO₄ and the solvent removed under reduced pressure, to yield 653 mg (2.80 mmol, 52%) of a colorless solid.



M.p. = 135°C.

R_f = 0.18 (EtOAc, UV).

¹H-NMR (300 MHz, CDCl₃): δ = 2.96 (*dd*, *J* = 16.0, 11.8 Hz, 1H, 11-H_b), 3.27 (*dd*, *J* = 16.0, 3.3 Hz, 1H, 11-H_b), 3.78 (*s*, 3H, OCH₃), 4.16-4.25 (*m*, 4H, 3-H, 6-H), 5.48 (*d*, *J* = 17.4 Hz, 1H, 11a-H), 7.13-7.27 (*m*, 4H, H_{aryl}) ppm.

¹³C-NMR (75 MHz, CDCl₃): δ = 33.8 (C-11), 43.2 (C-6), 49.8 (C-3), 52.8 (OCH₃), 53.1 (C-11a), 126.5 (C-8), 126.7 (C-9), 127.0 (C-10), 128.8 (C-7), 131.5 (C-6_a), 131.8 (C-10a), 160.0 (C-1), 165.3 (C-4) ppm.

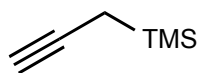
GC : $t_R = 10.39$ min.

Experimental data are in accordance with the literature.^[48]

5.11 Experiments to chapter 4.6.2

Propargyltrimethylsilane (136)

Magnesium turnings (45.0 g, 1.84 mol) were covered with dry Et₂O (200 mL), under nitrogen atmosphere. To this stirred mixture, HgCl₂ (610 mg, 2.24 mmol) was added, followed by propargyl bromide **135** (16.0 mL 80% solution in toluene, 17.8 g, 150 mmol), in a single portion. After few minutes the reaction started, the mixture was cooled to 20°C and propargyl bromide (184 mL 80% solution in toluene, 201 g, 1.69 mol) and Et₂O (1000 mL) were added at such a rate to maintain the temp. at 20°C. At the end of the addition, the stirring was continued for 20 min. The mixture was cooled at 0°C and chlorotrimethylsilane (235 mL, 200 g, 1.85 mol) was added during 30 min. The mixture was stirred at room temp. for 12 h and, after cooling at 0°C, saturated aqueous NH₄Cl solution (150 mL) was added, followed by Et₂O (300 mL). The organic layer was separated, dried (MgSO₄) and the solvent was removed under reduced pressure. Purification by fractioned distillation gave the product, as a light yellow oil (22.0 g, 202 mmol, 11%)



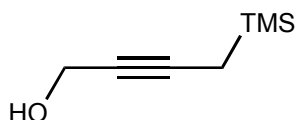
b.p. = 85-90°C.

¹H-NMR (300 MHz, CDCl₃): $\delta = 0.05$ (s, 9H, TMS), 1.39 (d, $J = 3.0$ Hz, 2H, 3-H), 1.74 (t, $J = 3.0$ Hz, 1H, 1-H) ppm.

Experimental data are in accordance with the literature.^[48]

1-(Trimethylsilyl)-2-butyne-4-ol (137)

To a solution of propargyltrimethylsilane **136** (4.48 g, 40 mmol) in dry THF (25 mL), at -78°C , *n*BuLi (25 mL solution 1.6 M in pentane, 40 mmol) was added dropwise. After 10 minutes, at this temp., gaseous formaldehyd, generated by depolymerization of paraformaldehyde (12.0 g, 400 mmol), at 180°C , was carried over into the mixture by a slow current of dry nitrogen. Then the mixture was allowed to warm at room temp. for 3 h and it was treated with saturated aqueous NH_4Cl solution (30 mL) and Et_2O (50 mL). The organic phase was separated, dried (NaSO_4) and the solvent removed under reduced pressure. Purification by fractioned distillation yielded the product **137** as a colorless oil (3.30 g, 23.2 mmol, 58%).



GC: $t_R = 3.56$ min.

$^1\text{H-NMR}$ (300 MHz, CDCl_3): $\delta = 0.04$ (s, 9H, TMS), 1.43 (t, $J = 2.5$ Hz, 2H, 4-H), 2.63 (s, 1H, OH), 4.16 (t, $J = 2.5$ Hz, 2H, 1-H)) ppm.

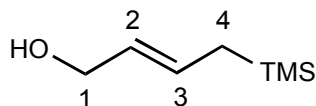
MS (EI): m/z (%) = 142 (50) [M^+], 125 (15) [$\text{M}^+ - \text{OH}$], 91 (35), 75 (100), 52 (85).

Experimental data are in accordance with the literature.^[72]

1-Trimethylsilyl-2-buten-4-ol (138)

Lithium aluminum hydride (2.28 g, 60.0 mmol) was suspended in dry THF (50 mL) and then 1-(trimethylsilyl)-2-butyne-4-ol **137** (4.25 g, 30.0 mmol) in dry THF (50 mL) was added slowly. The mixture was stirred under reflux for 1 h, was allowed to cool at room temp., was treated with ethyl acetate (25 mL) and poured on a saturated aqueous NaHSO_4 solution (300 mL). The solution was filtered and the organic layer

was separated. The aqueous layer was washed with ethyl acetate (2 x 70 mL) and the combined organic layers were dried (Na_2SO_4) and the solvent removed under reduced pressure. Purification by fractioned distillation yielded the product **138** as a colorless oil (2.51g, 34.8 mmol, 58%).



$^1\text{H-NMR}$ (300 MHz, CDCl_3): δ = 0.04 (s, 9H, TMS), 1.51 (*ddd*, J = 8.0, 1.1, 0.8 Hz, 2H, 4-H), 4.08 (*ddd*, J = 6.2, 1.0, 0.9 Hz, 2H, 1-H), 5.52 (*dt*, J = 15.1, 6.2, 1.1 Hz, 1H, 2-H), 5.71 (*dt*, J = 15.1, 8.0, 1.1 Hz, 1H, 3-H) ppm.

MS (EI): m/z (%) = 126 (20) [$\text{M}^+ - \text{OH}$], 111 (100), 95 (25), 83 (35), 73 (40).

Experimental data are in accordance with the literature.^[72]

6 X-Ray analysis data

6.1 X-Ray analysis data for (S)-Hexahydropyrrolo[1,2-a]pyrazine-1,4-dione 73

Table 5: Crystal data and structure refinement for **73**.

Wavelength[mm]		1.54178
Crystal system		orthorhombic
Space group		P2(1)2(1)2(1)
Unit cell dimensions [Å]	a	5.8631(3)
	b	9.6723(5)
	c	13.0583(12)
Angle	α	90°
	β	90°
	γ	90°
Volume[Å ³]		740.53(9)
Calculated density [g/cm ³]		1.383
Crystal size[mm]		0.4 x 0.25 x 0.10
θ - range for data collection		5.69 - 68.00°
Reflections collected		1082
Reflections unique		947
R[%]		4.29
Rw[%]		11.07
Absolute structure parameter		-0.7(6)
Extinction coefficient		0.038(4)
Identification code		s1124rc

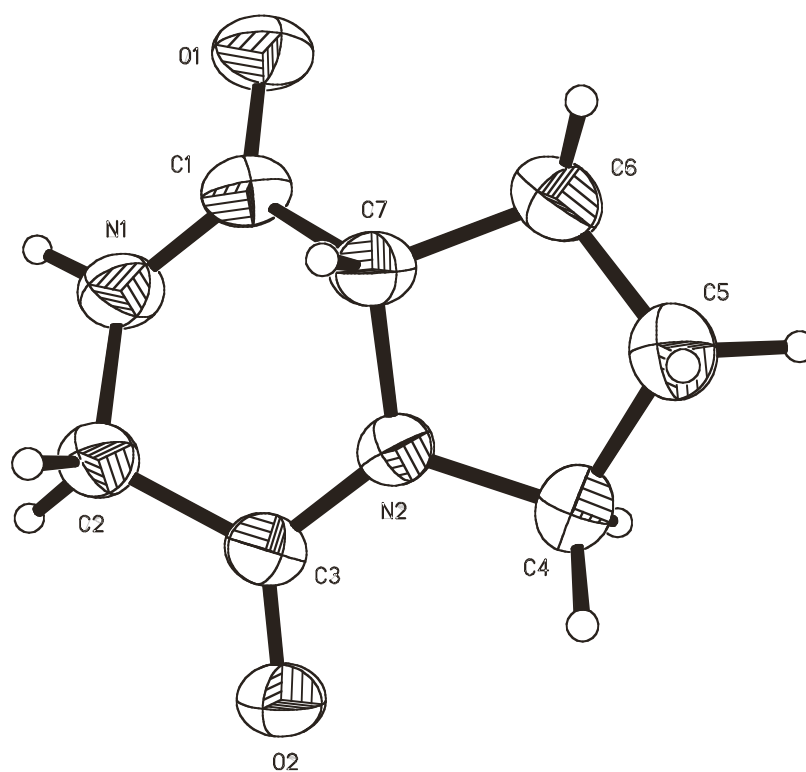


Fig. 6: X-Ray crystal structure of **73** (displacement parameters)

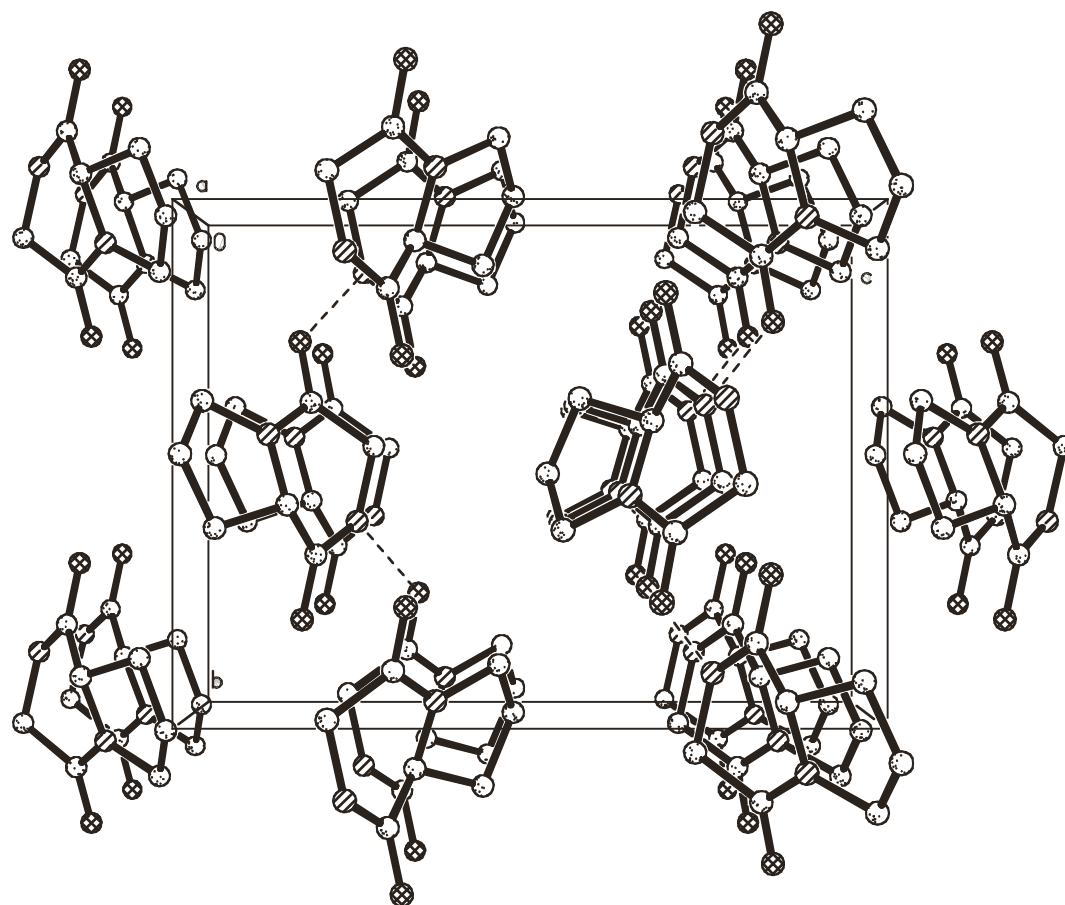


Fig. 7: Unit cell of **73**

Table 6: Atomic coordinates ($\times 10^4$) and equivalent isotropic displacement parameters $U(\text{eq})$ ($\text{\AA}^2 \times 10^3$) for **73**.

Atom	x	y	z	U(eq)
O(1)	6580(4)	2011(2)	6758(2)	57(1)
N(1)	8270(4)	3873(2)	7497(2)	49(1)
C(1)	6611(5)	3255(3)	6952(2)	44(1)
O(2)	7998(4)	7381(2)	6680(2)	53(1)
N(2)	5713(4)	5562(2)	6312(2)	41(1)
C(2)	8247(6)	5341(3)	7737(2)	47(1)
C(3)	7319(5)	6194(3)	6862(2)	40(1)
C(4)	4518(6)	6186(4)	5441(2)	55(1)
C(5)	2575(7)	5181(3)	5240(3)	57(1)
C(6)	3401(7)	3813(4)	5670(3)	57(1)
C(7)	4753(5)	4231(3)	6614(2)	42(1)

Table 7: Anisotropic displacement parameters $U_{ij}(\text{\AA}^2 \times 10^3)$ for **73**

Atom	U11	U22	U33	U23	U13	U12
O(1)	62(1)	34(1)	75(1)	-4(1)	1(1)	2(1)
N(1)	47(1)	37(1)	64(1)	3(1)	-10(1)	4(1)
C(1)	43(1)	34(1)	55(1)	2(1)	6(1)	1(1)
O(2)	57(1)	38(1)	63(1)	4(1)	-8(1)	-8(1)
N(2)	44(1)	34(1)	46(1)	5(1)	-7(1)	-2(1)
C(2)	51(2)	36(1)	54(2)	0(1)	-12(1)	2(1)
C(3)	39(1)	36(1)	47(1)	-3(1)	-1(1)	-1(1)
C(4)	61(2)	49(2)	53(2)	9(1)	-16(2)	-2(2)
C(5)	54(2)	56(2)	62(2)	1(2)	-13(2)	0(2)
C(6)	55(2)	48(2)	68(2)	-3(2)	-14(2)	-9(2)
C(7)	40(1)	35(1)	51(1)	3(1)	0(1)	-2(1)

Table 8: Hydrogen coordinates ($\times 10^4$) and isotropic displacement parameters ($\text{Å}^2 \times 10^3$) for **73**.

Atom	x	y	z	U(eq)
H(1)	9530(70)	3300(40)	7790(30)	68(11)
H(2A)	7140(80)	5540(40)	8410(30)	80(12)
H(2B)	9910(60)	5620(30)	7890(20)	49(9)
H(4A)	3970(80)	7190(40)	5650(30)	86(12)
H(4B)	5620(90)	6160(50)	4770(40)	99(15)
H(5A)	1230(70)	5530(30)	5660(30)	66(11)
H(5B)	2190(80)	5160(40)	4440(30)	83(12)
H(6A)	4530(80)	3440(40)	5150(30)	83(13)
H(6B)	2230(80)	3260(40)	5800(30)	80(13)
H(7)	3700(60)	4390(30)	7230(30)	51(8)

Table 9. Torsion angles [°] for **73**.

C(2)-N(1)-C(1)-O(1)	-178.6(3)
C(2)-N(1)-C(1)-C(7)	0.5(4)
C(1)-N(1)-C(2)-C(3)	-37.4(4)
C(7)-N(2)-C(3)-O(2)	-172.6(3)
C(4)-N(2)-C(3)-O(2)	-1.2(4)
C(7)-N(2)-C(3)-C(2)	7.2(4)
C(4)-N(2)-C(3)-C(2)	178.6(3)
N(1)-C(2)-C(3)-O(2)	-147.5(3)
N(1)-C(2)-C(3)-N(2)	32.7(4)
C(3)-N(2)-C(4)-C(5)	-168.5(3)
C(7)-N(2)-C(4)-C(5)	3.6(3)
N(2)-C(4)-C(5)-C(6)	-24.4(4)
C(4)-C(5)-C(6)-C(7)	36.0(4)
C(3)-N(2)-C(7)-C(1)	-44.1(3)
C(4)-N(2)-C(7)-C(1)	143.6(3)
C(3)-N(2)-C(7)-C(6)	-169.2(3)
C(4)-N(2)-C(7)-C(6)	18.5(3)
O(1)-C(1)-C(7)-N(2)	-142.3(3)
N(1)-C(1)-C(7)-N(2)	38.7(3)
O(1)-C(1)-C(7)-C(6)	-25.6(4)
N(1)-C(1)-C(7)-C(6)	155.3(3)
C(5)-C(6)-C(7)-N(2)	-32.8(3)
C(5)-C(6)-C(7)-C(1)	-153.9(3)

6.2 X-Ray analysis data for (3*S*,8*aS*)-3-Methylhexahydropyrrolo[1,2-*a*]pyrazine- 1,4-dione (*cis*-76a)

Table 10: Crystal data and structure refinement for *cis*-76a.

Wavelength[mm]		0.71073
Crystal system,		monoclinic
Space group		P2(1)
Unit cell dimensions[Å]	a	7.2825(13)
	b	6.5604(13)
	c	9.2844(13)
	α	90°
	β	111.399(11)°
	γ	90°
Volume (unit cell)[Å ³]		412.99(12)
Molecules per cell		2
Calculated density[g/cm ³]		1.353
Crystal size[mm]		0.50 x 0.25 x
0.15		
θ - range		2.36 to 24.99°
Reflections collected		858
Reflections unique		795
Refinement parameter		158
R[%]		0.0427,
Rw[%]		0.0749
Absolute structure parameter		0(3)
Identification code		s1225rm

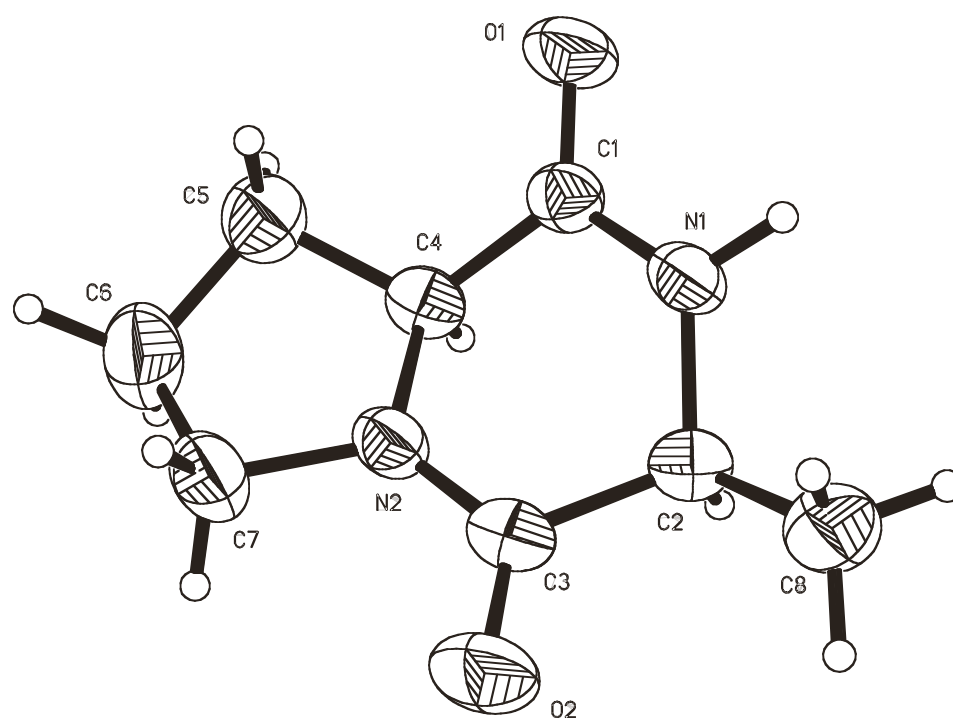


Fig. 8: X-Ray crystal structure of *cis*-76a (displacement parameters)

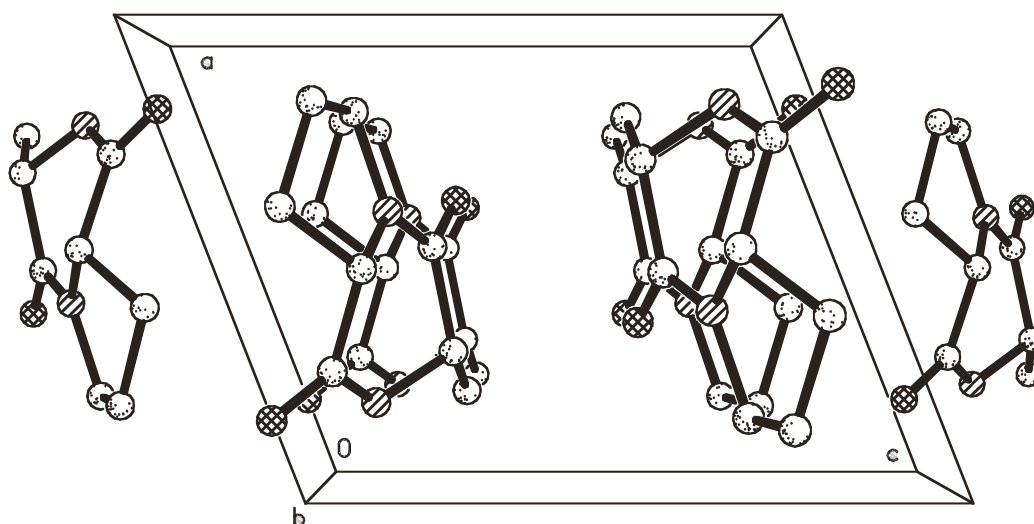


Fig. 9: Unit cell of *cis*-76a

Table 11: Atomic coordinates ($\times 10^4$) and equivalent isotropic displacement parameters ($\text{Å}^2 \times 10^3$) for *cis*-**76a**

Atom	x	y	z	U(eq)
O(1)	8214(3)	6948(4)	9872(2)	56(1)
N(1)	7975(4)	4133(4)	8392(3)	41(1)
C(1)	7278(4)	5855(5)	8775(3)	38(1)
N(2)	4019(3)	4578(4)	7069(3)	39(1)
O(2)	3737(3)	1429(4)	6023(3)	64(1)
C(2)	6946(4)	3018(5)	6945(3)	40(1)
C(3)	4737(4)	2909(5)	6638(3)	42(1)
C(4)	5198(4)	6393(5)	7727(3)	39(1)
C(5)	3967(5)	7487(6)	8509(5)	56(1)
C(6)	1859(6)	6960(7)	7475(6)	68(1)
C(7)	1977(5)	4783(6)	6988(5)	54(1)
C(8)	7854(6)	938(6)	7032(5)	56(1)

Table 12: Anisotropic displacement parameters ($\text{Å}^2 \times 10^3$) for *cis-76a*.

Atom	U11	U22	U33	U23	U13	U12
O(1)	49(1)	52(1)	52(1)	-17(1)	3(1)	-9(1)
N(1)	32(1)	43(2)	40(1)	-4(1)	4(1)	-2(1)
C(1)	37(2)	38(2)	38(2)	-3(1)	13(1)	-8(1)
N(2)	32(1)	42(2)	40(1)	-3(1)	10(1)	-7(1)
O(2)	56(1)	53(2)	71(2)	-22(1)	12(1)	-19(1)
C(2)	43(2)	40(2)	34(1)	-2(1)	12(1)	-2(2)
C(3)	41(2)	43(2)	35(2)	-1(2)	8(1)	-7(2)
C(4)	41(2)	35(2)	39(2)	3(1)	12(1)	-6(1)
C(5)	54(2)	48(3)	66(2)	-5(2)	20(2)	5(2)
C(6)	51(2)	69(3)	89(3)	-2(3)	31(2)	6(2)
C(7)	37(2)	67(3)	58(2)	-2(2)	16(2)	-7(2)
C(8)	57(2)	43(2)	62(2)	-10(2)	15(2)	1(2)

Table 13: Hydrogen coordinates ($\times 10^4$) and isotropic displacement parameters ($\text{Å}^2 \times 10^3$) for *cis-76a*

Atom	x	y	z	U(eq)
H(1)	9210(60)	3660(60)	9020(40)	65(11)
H(2)	7110(50)	3820(50)	6060(40)	44(9)
H(4)	5390(40)	7230(50)	6930(30)	35(7)
H(5A)	4290(50)	6830(70)	9560(40)	69(11)
H(5B)	4270(50)	8900(70)	8570(40)	65(11)
H(6A)	1520(60)	7950(80)	6420(50)	89(14)
H(6B)	960(60)	7240(90)	8080(50)	112(16)
H(7A)	1760(60)	3740(60)	7810(40)	76(12)
H(7B)	1160(60)	4570(70)	5950(40)	76(12)
H(8A)	7810(50)	200(60)	7970(40)	62(11)
H(8B)	7230(60)	130(70)	6150(50)	71(12)
H(8C)	9230(70)	1090(70)	7150(40)	89(13)

Table 14: Torsion angles [°] for *cis-76a*.

C(2)-N(1)-C(1)-O(1)	-170.5(3)
C(2)-N(1)-C(1)-C(4)	9.0(4)
C(1)-N(1)-C(2)-C(8)	-167.1(3)
C(1)-N(1)-C(2)-C(3)	-43.2(4)
C(4)-N(2)-C(3)-O(2)	-176.5(3)
C(7)-N(2)-C(3)-O(2)	5.8(5)
C(4)-N(2)-C(3)-C(2)	2.0(4)
C(7)-N(2)-C(3)-C(2)	-175.8(3)
N(1)-C(2)-C(3)-O(2)	-145.6(3)
C(8)-C(2)-C(3)-O(2)	-23.3(4)
N(1)-C(2)-C(3)-N(2)	35.9(4)
C(8)-C(2)-C(3)-N(2)	158.2(3)
C(3)-N(2)-C(4)-C(1)	-36.6(4)
C(7)-N(2)-C(4)-C(1)	141.4(3)
C(3)-N(2)-C(4)-C(5)	-161.2(3)
C(7)-N(2)-C(4)-C(5)	16.8(3)
O(1)-C(1)-C(4)-N(2)	-150.4(3)
N(1)-C(1)-C(4)-N(2)	30.0(3)
O(1)-C(1)-C(4)-C(5)	-33.0(4)
N(1)-C(1)-C(4)-C(5)	147.4(3)
N(2)-C(4)-C(5)-C(6)	-32.5(4)
C(1)-C(4)-C(5)-C(6)	-154.9(3)
C(4)-C(5)-C(6)-C(7)	37.2(4)
C(3)-N(2)-C(7)-C(6)	-175.8(3)
C(4)-N(2)-C(7)-C(6)	6.2(4)
C(5)-C(6)-C(7)-N(2)	-26.8(4)

6.3 X-Ray structure analysis for (3*S*,8*aS*)-3-Isopropyl hexahydropyrrolo[1,2*a*]pyrazine-1,4-dione (*cis*-76e)

Table 15: Crystal data and structure refinement for *cis*-76e.

Wavelength[mm]		1.54178
Crystal system		orthorhombic
Space group		P2(1)2(1)2(1)
Unit cell dimensions[Å]	a	5.7020(5)
	b	10.3692(8)
	c	34.776(3)
Angle	α	90°
	β	90°
	γ	90°
Volume (unit cell)[Å ³]		2056.1(3)
Calculated density [g/cm ³]		1.268
Crystal size [mm]		0.4 x 0.2 x 0.1
Θ - range for data collection		2.54 to 67.97°
Reflections collected		2878
Reflections unique		2643
R[%]		0.0713
R _w [%]		0.1593
Absolute structure parameter		-0.9(5)
Extinction coefficient		0.0045(5)
Identification code		s1317rc

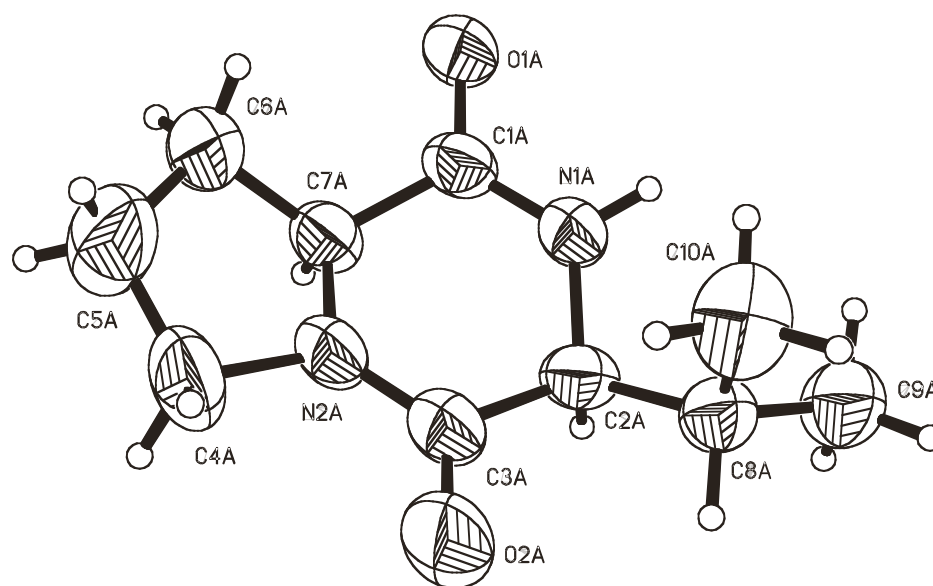


Fig 10: X-Ray crystal structure of *cis*-76e (displacement parameters)

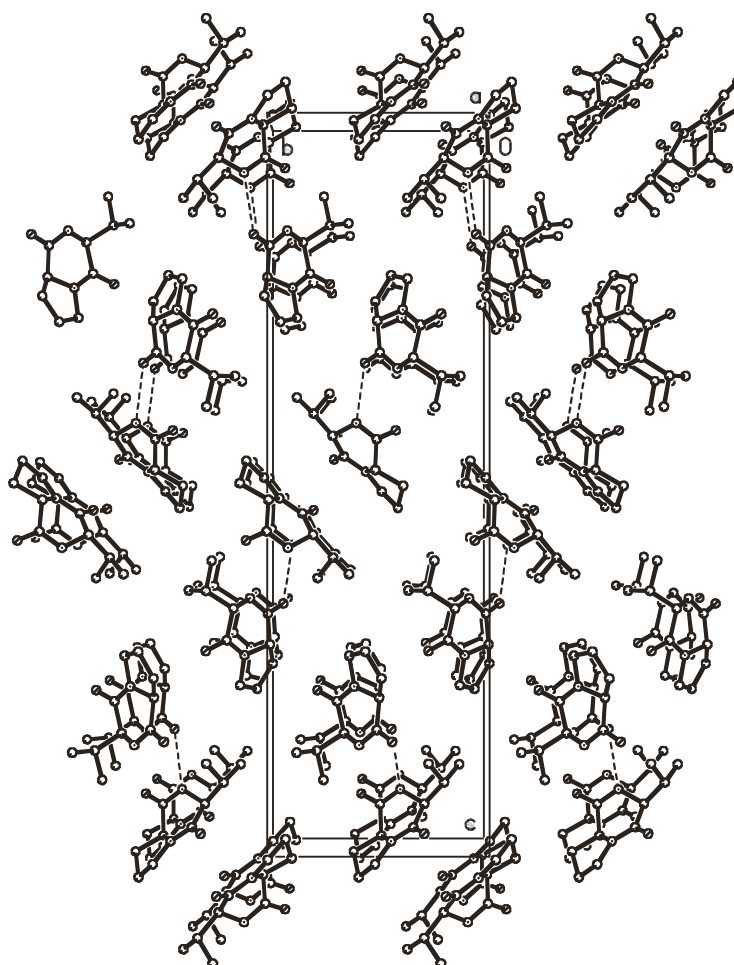


Fig. 11: Unit cell of *cis*-76e

Table 16. Atomic coordinates ($\times 10^4$) and equivalent isotropic displacement parameters ($\text{\AA}^2 \times 10^3$) for **cis-76e**.

Atom	x	y	z	U(eq)
N(1A)	-2479(7)	-851(3)	1546(1)	52(1)
O(1A)	413(6)	601(3)	1642(1)	65(1)
C(1A)	-1239(8)	-65(4)	1767(1)	51(1)
N(2A)	-3229(8)	-1077(4)	2313(1)	61(1)
C(2A)	-4579(8)	-1539(4)	1668(1)	52(1)
O(2A)	-5672(9)	-2752(4)	2226(1)	104(2)
C(3A)	-4512(10)	-1847(4)	2096(1)	62(1)
C(4A)	-2841(11)	-1288(5)	2725(1)	85(2)
C(5A)	-669(14)	-566(7)	2806(2)	115(3)
C(6A)	77(11)	125(7)	2464(1)	91(2)
C(7A)	-1932(8)	45(4)	2181(1)	54(1)
C(8A)	-4960(8)	-2770(4)	1429(1)	54(1)
C(9A)	-5689(10)	-2483(5)	1018(1)	74(1)
C(10A)	-2828(11)	-3638(5)	1439(2)	83(2)
N(1B)	1470(6)	1004(3)	832(1)	47(1)
O(1B)	-746(5)	-783(3)	727(1)	57(1)
C(1B)	584(7)	77(4)	612(1)	46(1)
N(2B)	3841(5)	582(3)	181(1)	44(1)
O(2B)	6584(5)	2059(3)	348(1)	60(1)
C(2B)	2770(7)	2093(3)	666(1)	43(1)
C(3B)	4614(8)	1584(4)	387(1)	44(1)
C(4B)	5244(8)	-150(4)	-94(1)	55(1)
C(5B)	3387(8)	-894(4)	-318(1)	54(1)
C(6B)	1495(8)	-1132(4)	-18(1)	53(1)
C(7B)	1398(7)	142(4)	198(1)	44(1)
C(8B)	3785(8)	2975(4)	974(1)	51(1)
C(9B)	1846(9)	3701(5)	1183(1)	68(1)
C(10B)	5372(9)	2259(5)	1257(1)	68(1)

Table 17: Anisotropic displacement parameters ($\text{\AA}^2 \times 10^3$) for **cis-76e**.

Atom	U11	U22	U33	U23	U13	U12
N(1A)	56(2)	58(2)	44(2)	-2(2)	9(2)	-9(2)
O(1A)	65(2)	77(2)	52(1)	3(1)	11(2)	-21(2)
C(1A)	50(3)	54(2)	49(2)	3(2)	11(2)	-6(2)
N(2A)	72(3)	70(2)	42(2)	0(2)	16(2)	-21(2)
C(2A)	45(2)	53(2)	58(2)	2(2)	9(2)	-6(2)
O(2A)	143(4)	109(3)	61(2)	5(2)	23(2)	-67(3)
C(3A)	68(3)	71(3)	48(2)	1(2)	13(2)	-15(3)
C(4A)	122(5)	91(3)	42(2)	2(2)	8(3)	-22(4)
C(5A)	136(6)	139(6)	69(3)	30(4)	-23(4)	-62(6)
C(6A)	80(4)	142(5)	50(2)	6(3)	0(2)	-31(4)
C(7A)	59(3)	53(2)	49(2)	-1(2)	12(2)	-5(2)
C(8A)	53(3)	57(2)	52(2)	2(2)	-1(2)	-7(2)
C(9A)	70(3)	94(3)	60(2)	5(2)	-10(3)	-9(3)
C(10A)	95(4)	64(3)	88(3)	-3(3)	-15(3)	23(3)
N(1B)	46(2)	50(2)	44(1)	0(1)	9(2)	-11(2)
O(1B)	56(2)	58(2)	57(1)	0(1)	11(1)	-17(2)
C(1B)	41(2)	48(2)	48(2)	0(2)	6(2)	-5(2)
N(2B)	37(2)	46(2)	47(2)	-6(1)	9(1)	-2(2)
O(2B)	50(2)	62(2)	67(2)	-2(1)	14(2)	-15(2)
C(2B)	41(2)	41(2)	47(2)	3(2)	2(2)	-1(2)
C(3B)	40(2)	48(2)	45(2)	3(2)	6(2)	-1(2)
C(4B)	53(3)	57(2)	54(2)	-6(2)	16(2)	-1(2)
C(5B)	55(3)	59(2)	48(2)	-6(2)	8(2)	1(2)
C(6B)	49(2)	54(2)	58(2)	-10(2)	4(2)	-5(2)
C(7B)	41(2)	47(2)	44(2)	-2(2)	1(2)	0(2)
C(8B)	54(3)	51(2)	47(2)	-5(2)	6(2)	-7(2)
C(9B)	77(4)	62(2)	65(2)	-16(2)	12(3)	3(3)
C(10B)	59(3)	82(3)	64(2)	-1(2)	-7(2)	-8(3)

Table 18. Hydrogen coordinates ($\times 10^4$) and isotropic displacement parameters ($\text{\AA}^2 \times 10^3$) for *cis-76e*.

Atom	x	y	z	U(eq)
H(1A)	-2011	-963	1313	63
H(2A)	-5924	-971	1623	62
H(4A1)	-2643	-2198	2782	102
H(4A2)	-4139	-956	2876	102
H(5A1)	-941	41	3013	138
H(5A2)	554	-1158	2886	138
H(6A1)	1476	-267	2357	109
H(6A2)	420	1018	2526	109
H(7A)	-2923	810	2212	64
H(8A)	-6252	-3247	1548	65
H(9A1)	-7045	-1935	1019	111
H(9A2)	-6055	3275	888	111
H(9A3)	-4426	-2058	886	111
H(10A)	-3135	-4406	1293	124
H(10B)	-2486	-3866	1701	124
H(10C)	-1510	-3193	1331	124
H(1B)	1278	967	1077	56
H(2B)	1652	2604	516	52
H(4B1)	6319	-729	36	66
H(4B2)	6128	419	-262	66
H(5B1)	2786	-389	-531	65
H(5B2)	4011	-1700	-416	65
H(6B1)	1924	-1836	152	64
H(6B2)	1	-1327	-138	64
H(7B)	403	748	56	53
H(8B)	4755	3619	842	61
H(9B1)	2526	4255	1374	102
H(9B2)	813	3095	1305	102
H(9B3)	976	4211	1002	102

X-Ray analysis data

H(10D)	5981	2857	1442	103
H(10E)	6648	1868	1119	103
H(10F)	4484	1603	1386	103

Table 19: Torsion angles [°] for *cis-76e*.

C(2A)-N(1A)-C(1A)-O(1A)	-172.9(4)
C(2A)-N(1A)-C(1A)-C(7A)	5.1(6)
C(1A)-N(1A)-C(2A)-C(3A)	-30.1(6)
C(1A)-N(1A)-C(2A)-C(8A)	-154.7(4)
C(7A)-N(2A)-C(3A)-O(2A)	-176.3(5)
C(4A)-N(2A)-C(3A)-O(2A)	6.6(9)
C(7A)-N(2A)-C(3A)-C(2A)	1.5(7)
C(4A)-N(2A)-C(3A)-C(2A)	-175.6(5)
N(1A)-C(2A)-C(3A)-O(2A)	-156.2(5)
C(8A)-C(2A)-C(3A)-O(2A)	-31.3(7)
N(1A)-C(2A)-C(3A)-N(2A)	26.0(6)
C(8A)-C(2A)-C(3A)-N(2A)	150.8(4)
C(3A)-N(2A)-C(4A)-C(5A)	158.0(5)
C(7A)-N(2A)-C(4A)-C(5A)	-19.5(6)
N(2A)-C(4A)-C(5A)-C(6A)	4.5(7)
C(4A)-C(5A)-C(6A)-C(7A)	11.0(8)
C(3A)-N(2A)-C(7A)-C(1A)	-26.7(6)
C(4A)-N(2A)-C(7A)-C(1A)	150.7(4)
C(3A)-N(2A)-C(7A)-C(6A)	-151.5(5)
C(4A)-N(2A)-C(7A)-C(6A)	25.9(5)
O(1A)-C(1A)-C(7A)-N(2A)	-159.1(4)
N(1A)-C(1A)-C(7A)-N(2A)	22.9(6)
O(1A)-C(1A)-C(7A)-C(6A)	-41.6(6)
N(1A)-C(1A)-C(7A)-C(6A)	140.4(5)
C(5A)-C(6A)-C(7A)-N(2A)	-22.0(6)
C(5A)-C(6A)-C(7A)-C(1A)	-144.5(5)
N(1A)-C(2A)-C(8A)-C(10A)	55.2(5)
C(3A)-C(2A)-C(8A)-C(10A)	-69.8(5)
N(1A)-C(2A)-C(8A)-C(9A)	-70.5(5)
C(3A)-C(2A)-C(8A)-C(9A)	164.5(4)
C(2B)-N(1B)-C(1B)-O(1B)	-171.4(4)
C(2B)-N(1B)-C(1B)-C(7B)	9.9(5)

C(1B)-N(1B)-C(2B)-C(8B)	-175.4(4)
C(1B)-N(1B)-C(2B)-C(3B)	-49.0(5)
C(4B)-N(2B)-C(3B)-O(2B)	5.0(6)
C(7B)-N(2B)-C(3B)-O(2B)	-172.0(4)
C(4B)-N(2B)-C(3B)-C(2B)	-176.7(3)
C(7B)-N(2B)-C(3B)-C(2B)	6.3(5)
N(1B)-C(2B)-C(3B)-O(2B)	-142.9(4)
C(8B)-C(2B)-C(3B)-O(2B)	-17.1(5)
N(1B)-C(2B)-C(3B)-N(2B)	38.8(4)
C(8B)-C(2B)-C(3B)-N(2B)	164.6(3)
C(3B)-N(2B)-C(4B)-C(5B)	-165.0(3)
C(7B)-N(2B)-C(4B)-C(5B)	12.3(4)
N(2B)-C(4B)-C(5B)-C(6B)	-32.4(4)
C(4B)-C(5B)-C(6B)-C(7B)	40.9(4)
C(3B)-N(2B)-C(7B)-C(1B)	-45.4(5)
C(4B)-N(2B)-C(7B)-C(1B)	137.2(3)
C(3B)-N(2B)-C(7B)-C(6B)	-169.7(3)
C(4B)-N(2B)-C(7B)-C(6B)	12.9(4)
O(1B)-C(1B)-C(7B)-N(2B)	-143.1(4)
N(1B)-C(1B)-C(7B)-N(2B)	35.6(5)
O(1B)-C(1B)-C(7B)-C(6B)	-27.2(6)
N(1B)-C(1B)-C(7B)-C(6B)	151.5(4)
C(5B)-C(6B)-C(7B)-N(2B)	-32.8(4)
C(5B)-C(6B)-C(7B)-C(1B)	-152.9(3)
N(1B)-C(2B)-C(8B)-C(9B)	-69.0(4)
C(3B)-C(2B)-C(8B)-C(9B)	166.6(3)
N(1B)-C(2B)-C(8B)-C(10B)	56.4(5)
C(3B)-C(2B)-C(8B)-C(10B)	-67.9(4)

6.4 X-Ray data analysis for (3*S*, 8*aS*)-3-Isobutyl hexahydropyrrolo[1,2-*a*]pyrazine-1,4-dione *cis*-76d

Table 20: Crystal data and structure refinement for *cis*-76d

Wavelength[mm]		1.54178
Crystal system		orthorhombic
Space group		P2(1)2(1)2(1)
Unit cell dimensions[Å]	a	6.3429(4)
	b	9.466(3)
	c	19.5950(16)
Angle	α	90°
	β	90°
	γ	90°
Volume (unit cell)[Å ³]		1176.5(4)
Calculated density [g/cm ³]		1.187
Crystal size [mm]		0.5 x 0.25 x 0.05
Θ - range for data collection		4.51 to 67.88°
Reflections collected		1592
Reflections unique		1434
R[%]		0.0958
R _w [%]		0.2506
Absolute structure parameter		0.5(10)
Extinction coefficient		0.016(4)
Identification code		s1179rc

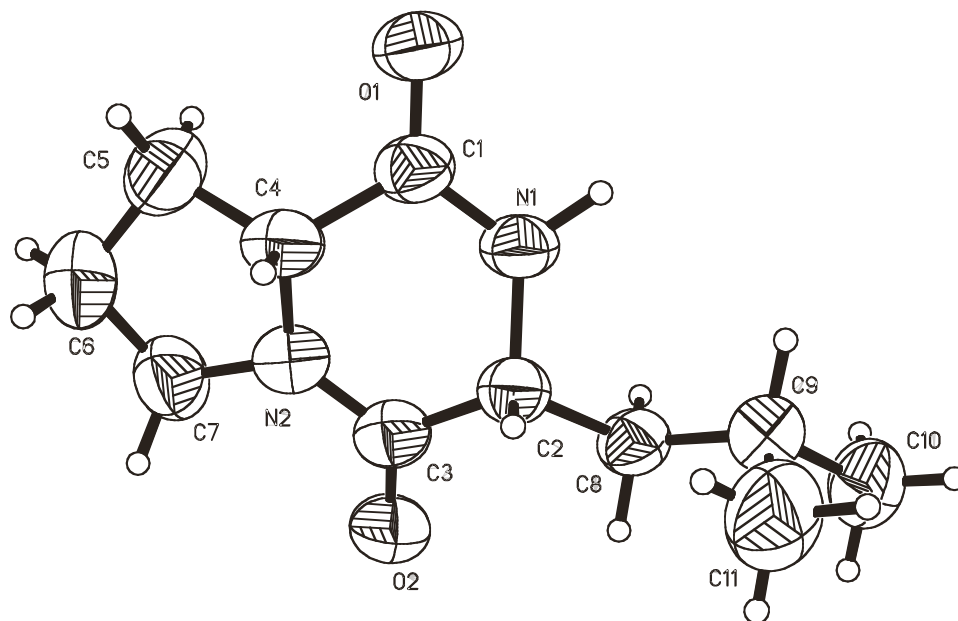


Fig. 12: X-Ray crystal structure of *cis*-76d (displacement parameters)

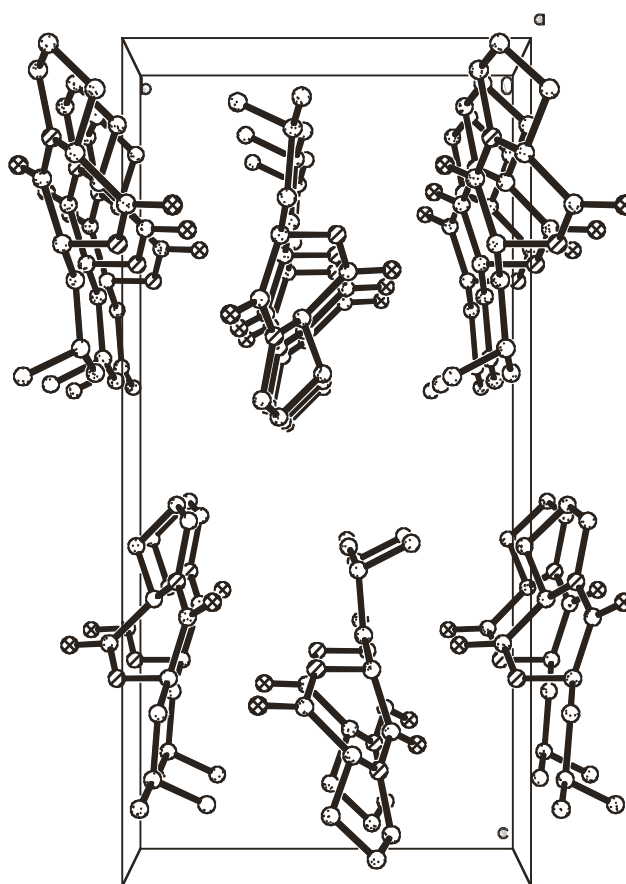


Fig. 13: Unit cell of *cis*-76d

Table 21: Atomic coordinates ($\times 10^4$) and equivalent isotropic displacement parameters ($\text{Å}^2 \times 10^3$) for **cis-76d**.

Atom	x	y	z	U(eq)
O(1)	15071(7)	6596(4)	7734(2)	78(1)
N(1)	12304(7)	5245(4)	7390(2)	59(1)
C(1)	13985(9)	5522(5)	7778(3)	61(1)
O(2)	9323(7)	2774(4)	8356(2)	72(1)
N(2)	12481(7)	3751(4)	8553(2)	62(1)
C(2)	11120(9)	3910(5)	7420(2)	54(1)
C(3)	10879(10)	3432(5)	8154(2)	58(1)
C(4)	14451(9)	4402(5)	8315(3)	60(1)
C(5)	15488(12)	4904(7)	8955(3)	87(2)
C(6)	14795(13)	3836(9)	9471(3)	107(3)
C(7)	12574(11)	3453(7)	9288(3)	80(2)
C(8)	8986(9)	4086(6)	7063(3)	58(1)
C(9)	9053(10)	4216(6)	6287(3)	67(1)
C(10)	6783(11)	4437(9)	6032(4)	94(2)
C(11)	10023(14)	2928(9)	5958(3)	109(3)

Table 22. Anisotropic displacement parameters ($\text{\AA}^2 \times 10^3$) for **cis-76d**.

Atom	U11	U22	U33	U23	U13	U12
O(1)	61(2)	60(2)	114(3)	8(2)	-14(3)	-13(2)
N(1)	50(2)	51(2)	77(2)	6(2)	-3(2)	-9(2)
C(1)	48(3)	51(2)	84(3)	2(2)	-6(3)	-1(2)
O(2)	69(3)	67(2)	79(2)	8(2)	1(2)	-14(2)
N(2)	62(3)	58(2)	66(2)	1(2)	-1(2)	-8(2)
C(2)	51(3)	48(2)	62(2)	1(2)	-3(3)	-1(2)
C(3)	57(3)	52(2)	67(2)	-4(2)	2(3)	-2(3)
C(4)	55(3)	49(2)	76(3)	-1(2)	2(3)	-4(2)
C(5)	80(5)	82(4)	100(4)	-5(3)	-27(4)	-1(4)
C(6)	129(7)	108(5)	85(4)	21(4)	-43(5)	-11(6)
C(7)	98(5)	78(4)	64(3)	10(3)	-5(3)	1(4)
C(8)	47(3)	58(2)	68(3)	2(2)	-6(2)	-6(3)
C(9)	69(4)	67(3)	65(3)	1(2)	-7(3)	-6(3)
C(10)	81(4)	108(5)	91(4)	17(4)	-30(4)	-14(4)
C(11)	144(7)	104(5)	81(3)	-21(4)	-7(5)	12(6)

Table 23. Hydrogen coordinates ($\times 10^4$) and isotropic displacement parameters ($\text{Å}^2 \times 10^3$) for **cis-76d**.

Atom	x	y	z	U(eq)
H(1)	12190(130)	5900(110)	7010(40)	130(30)
H(2)	11927	3190	7174	64
H(4)	15334	3668	8109	72
H(5A)	15011	5844	9078	105
H(5B)	17011	4911	8908	105
H(6A)	14854	4232	9927	129
H(6B)	15695	3008	9455	129
H(7A)	12294	2464	9380	96
H(7B)	11570	4028	9538	96
H(8A)	8109	3282	7180	69
H(8B)	8306	4923	7245	69
H(9)	9895	5046	6165	80
H(10A)	6209	5277	6234	140
H(10B)	5935	3639	6158	140
H(10C)	6789	4534	5544	140
H(11A)	10065	3055	5472	164
H(11B)	9190	2111	6066	164
H(11C)	11429	2800	6128	164

Table 24: Torsion angles [°] for *cis*-76d.

C(2)-N(1)-C(1)-O(1)	175.6(5)
C(2)-N(1)-C(1)-C(4)	-6.4(7)
C(1)-N(1)-C(2)-C(3)	40.7(7)
C(1)-N(1)-C(2)-C(8)	164.8(5)
C(7)-N(2)-C(3)-O(2)	-4.0(9)
C(4)-N(2)-C(3)-O(2)	173.4(4)
C(7)-N(2)-C(3)-C(2)	177.3(5)
C(4)-N(2)-C(3)-C(2)	-5.4(7)
N(1)-C(2)-C(3)-O(2)	147.8(5)
C(8)-C(2)-C(3)-O(2)	25.1(6)
N(1)-C(2)-C(3)-N(2)	-33.4(6)
C(8)-C(2)-C(3)-N(2)	-156.1(4)
C(3)-N(2)-C(4)-C(5)	165.3(5)
C(7)-N(2)-C(4)-C(5)	-17.1(6)
C(3)-N(2)-C(4)-C(1)	39.8(7)
C(7)-N(2)-C(4)-C(1)	-142.6(5)
O(1)-C(1)-C(4)-N(2)	145.9(5)
N(1)-C(1)-C(4)-N(2)	-32.2(6)
O(1)-C(1)-C(4)-C(5)	27.8(8)
N(1)-C(1)-C(4)-C(5)	-150.3(5)
N(2)-C(4)-C(5)-C(6)	32.0(6)
C(1)-C(4)-C(5)-C(6)	153.5(6)
C(4)-C(5)-C(6)-C(7)	-36.3(8)
C(3)-N(2)-C(7)-C(6)	172.5(6)
C(4)-N(2)-C(7)-C(6)	-5.2(7)
C(5)-C(6)-C(7)-N(2)	25.6(8)
N(1)-C(2)-C(8)-C(9)	71.2(6)
C(3)-C(2)-C(8)-C(9)	-165.8(4)
C(2)-C(8)-C(9)-C(11)	60.1(7)
C(2)-C(8)-C(9)-C(10)	-178.0(5)

6.4 X-Ray data analysis for (3*S*, 8*aR*)-3-Isobutylhexahydropyrrolo[1,2-*a*]pyrazine-1,4-dione *trans*-76d

Table 25: Crystal data and structure refinement for *trans*-76d

Wavelength[mm]		1.54178
Crystal system		orthorhombic
Space group		P2(1)2(1)2(1)
Unit cell dimensions[Å]	a	6.303(2)
	b	8.0267(14)
	c	23.146(4)
Angle	α	90°
	β	90°
	γ	90°
Volume (unit cell)[Å ³]		1171.0(5)
Calculated density [g/cm ³]		1.193
Crystal size [mm]		0.65 x 0.2 x 0.05
Θ - range for data collection		3.82 to 62.50 °
Reflections collected		1103
Reflections unique		1103
R[%]		0.1165
R _w [%]		0.2756
Absolute structure parameter		-1.3(16)
Extinction coefficient		0.041(6)
Identification code		s1209rc

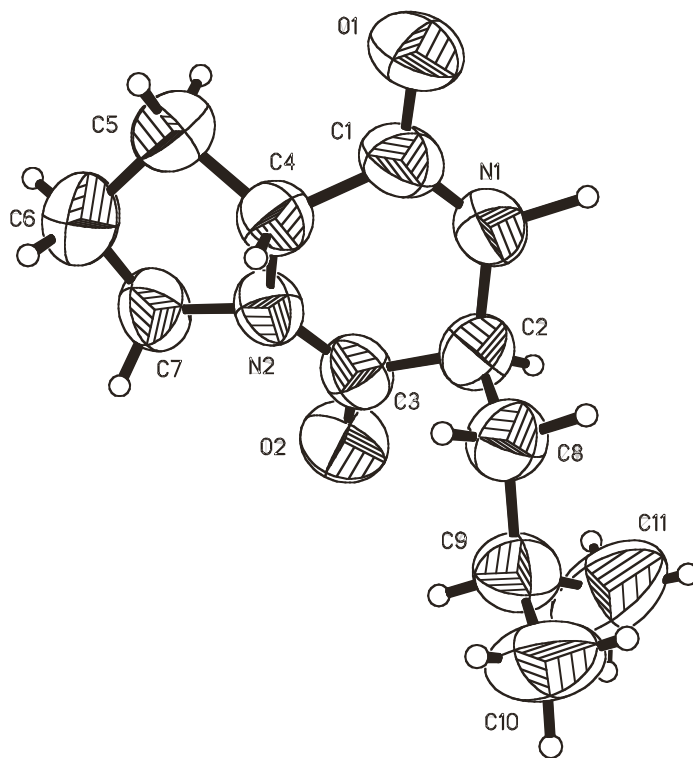


Fig. 14: X-Ray crystal structure of *trans*-76d (displacement parameters)

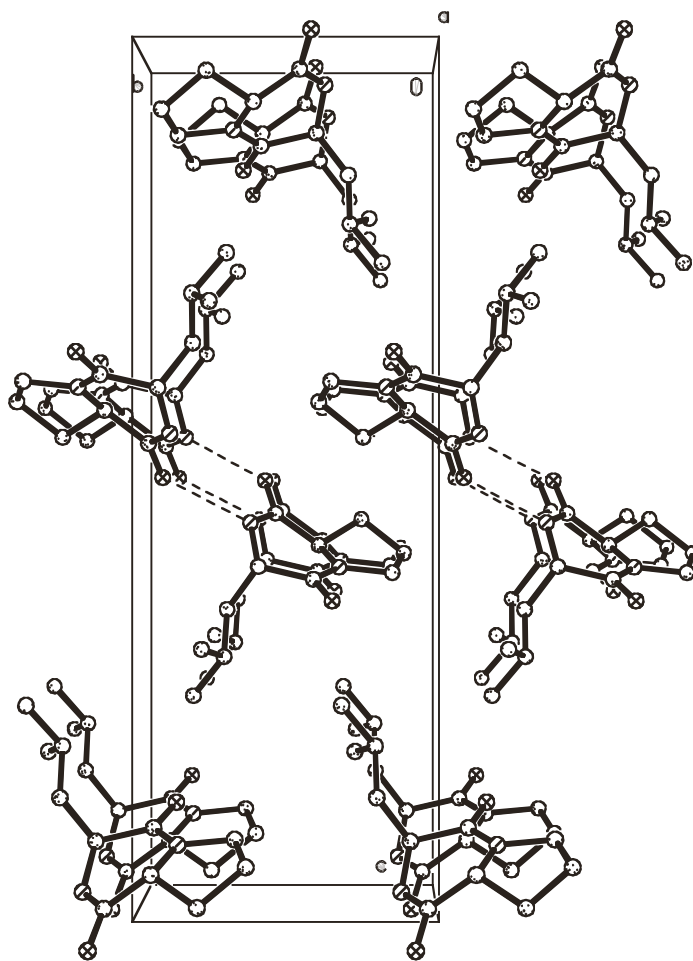


Fig. 15: Unit cell of *trans*-76d

Table 26: Atomic coordinates ($\times 10^4$) and equivalent isotropic displacement parameters ($\text{Å}^2 \times 10^3$) for ***trans*-76d**.

Atom	x	y	z	U(eq)
N(1)	9093(12)	3722(8)	510(3)	82(2)
O(1)	12179(11)	4132(8)	17(2)	115(2)
C(1)	10911(16)	4526(10)	407(3)	84(2)
N(2)	9467(10)	6715(7)	1035(2)	69(2)
O(2)	6133(10)	6507(7)	1389(2)	99(2)
C(2)	7740(13)	4030(9)	1011(3)	76(2)
C(3)	7698(14)	5868(9)	1158(3)	75(2)
C(4)	11396(12)	6004(8)	789(3)	72(2)
C(5)	12403(15)	7473(9)	482(3)	91(2)
C(6)	11806(17)	8935(11)	886(4)	107(3)
C(7)	9626(16)	8519(9)	1101(4)	88(2)
C(8)	8486(14)	2960(9)	1518(3)	84(2)
C(9)	7055(14)	2914(11)	2042(4)	92(3)
C(10)	8060(20)	1847(14)	2513(3)	130(4)
C(11)	4848(18)	2265(17)	1920(5)	154(5)

Table 27: Anisotropic displacement parameters ($\text{Å}^2 \times 10^3$) for *trans*-76d

Atom	U11	U22	U33	U23	U13	U12
N(1)	101(5)	69(4)	75(4)	-6(3)	3(4)	-2(4)
O(1)	142(6)	96(4)	108(4)	-22(3)	49(4)	7(4)
C(1)	100(6)	76(4)	75(4)	-7(4)	15(5)	14(5)
N(2)	71(4)	59(3)	78(4)	-10(3)	2(3)	9(3)
O(2)	84(4)	107(4)	105(4)	-9(3)	8(3)	23(4)
C(2)	71(4)	78(4)	80(4)	3(4)	1(4)	-3(4)
C(3)	81(5)	72(4)	71(4)	-3(4)	-9(4)	5(4)
C(4)	73(5)	69(4)	74(4)	-1(4)	4(4)	4(4)
C(5)	85(5)	96(5)	93(5)	4(4)	9(5)	-10(5)
C(6)	119(8)	82(5)	120(7)	-1(5)	5(6)	-18(6)
C(7)	112(7)	59(4)	93(5)	-5(3)	-2(5)	4(4)
C(8)	93(6)	75(4)	84(4)	6(4)	2(5)	4(4)
C(9)	89(6)	100(6)	87(5)	-7(5)	14(5)	2(5)
C(10)	150(10)	164(9)	77(5)	38(6)	0(6)	-7(9)
C(11)	101(8)	197(14)	163(10)	61(9)	1(7)	-36(9)

Table 28: Hydrogen coordinates ($\times 10^4$) and isotropic displacement parameters ($\text{Å}^2 \times 10^3$) for *trans*-76d.

Atom	x	y	z	U(eq)
H(1)	8610(130)	2560(100)	270(30)	90(20)
H(2)	6292	3688	912	92
H(4)	12330	5645	1104	86
H(5A)	11814	7624	99	109
H(5B)	13930	7343	453	109
H(6A)	12799	9020	1205	128
H(6B)	11799	9981	676	128
H(7A)	9462	8840	1502	106
H(7B)	8552	9080	872	106
H(8A)	8671	1828	1381	101
H(8B)	9867	3362	1639	101
H(9)	6922	4052	2190	111
H(10A)	7151	1827	2846	195
H(10B)	9412	2309	2619	195
H(10C)	8256	732	2372	195
H(11A)	4201	2930	1623	230
H(11B)	4008	2325	2265	230
H(11C)	4933	1128	1793	230

Table 29: Torsion angles [°] for *trans*-76d.

C(2)-N(1)-C(1)-O(1)	171.5(7)
C(2)-N(1)-C(1)-C(4)	-9.3(11)
C(1)-N(1)-C(2)-C(3)	37.7(10)
C(1)-N(1)-C(2)-C(8)	-86.8(9)
C(7)-N(2)-C(3)-O(2)	-7.5(11)
C(4)-N(2)-C(3)-O(2)	176.8(7)
C(7)-N(2)-C(3)-C(2)	174.3(7)
C(4)-N(2)-C(3)-C(2)	-1.4(10)
N(1)-C(2)-C(3)-O(2)	150.8(7)
C(8)-C(2)-C(3)-O(2)	-86.3(9)
N(1)-C(2)-C(3)-N(2)	-31.0(9)
C(8)-C(2)-C(3)-N(2)	91.9(8)
C(3)-N(2)-C(4)-C(1)	29.9(10)
C(7)-N(2)-C(4)-C(1)	-146.2(6)
C(3)-N(2)-C(4)-C(5)	153.9(7)
C(7)-N(2)-C(4)-C(5)	-22.2(8)
O(1)-C(1)-C(4)-N(2)	155.4(7)
N(1)-C(1)-C(4)-N(2)	-23.9(9)
O(1)-C(1)-C(4)-C(5)	38.4(11)
N(1)-C(1)-C(4)-C(5)	-140.9(7)
N(2)-C(4)-C(5)-C(6)	34.8(8)
C(1)-C(4)-C(5)-C(6)	156.5(8)
C(4)-C(5)-C(6)-C(7)	-36.1(9)
C(3)-N(2)-C(7)-C(6)	-176.9(7)
C(4)-N(2)-C(7)-C(6)	-0.7(9)
C(5)-C(6)-C(7)-N(2)	22.9(9)
N(1)-C(2)-C(8)-C(9)	-170.5(7)
C(3)-C(2)-C(8)-C(9)	66.0(10)
C(2)-C(8)-C(9)-C(11)	59.5(11)
C(2)-C(8)-C(9)-C(10)	-178.0(8)

6.5 X-Ray data analysis for (3*S*, 8*aS*)-3-Allylhexahydropyrrolo[1,2-*a*]pyrazine-1,4-dione *cis*-76f

Table 30. Crystal data and structure refinement for *cis*-76f

Wavelength[mm]		0.71073
Crystal system		orthorhombic
Space group		P2(1)2(1)2(1)
Unit cell dimensions[Å]	a	8.2459(16)
	b	10.979(2)
	c	11.0314(18)
Angle	α	90°
	β	90°
	γ	90°
Volume (unit cell)[Å ³]		998.7(3)
Calculated density [g/cm ³]		1.292
Crystal size [mm]		0.8 x 0.5 x 0.3
Θ - range for data collection		2.62 to 27.49°
Reflections collected		1805
Reflections unique		1665
R[%]		0.0701
R _w [%]		0.1021
Absolute structure parameter		1(2)
Extinction coefficient		0.055(4)
Identification code		s1209rc

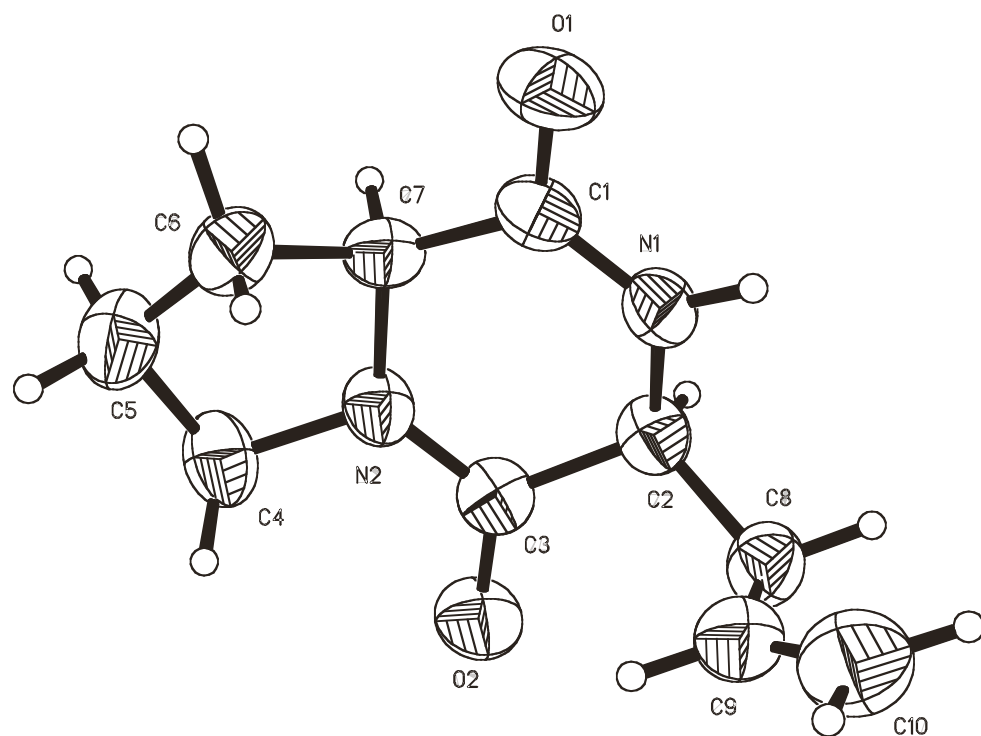


Fig. 16: X-Ray crystal structure of *cis-76f* (displacement parameters)

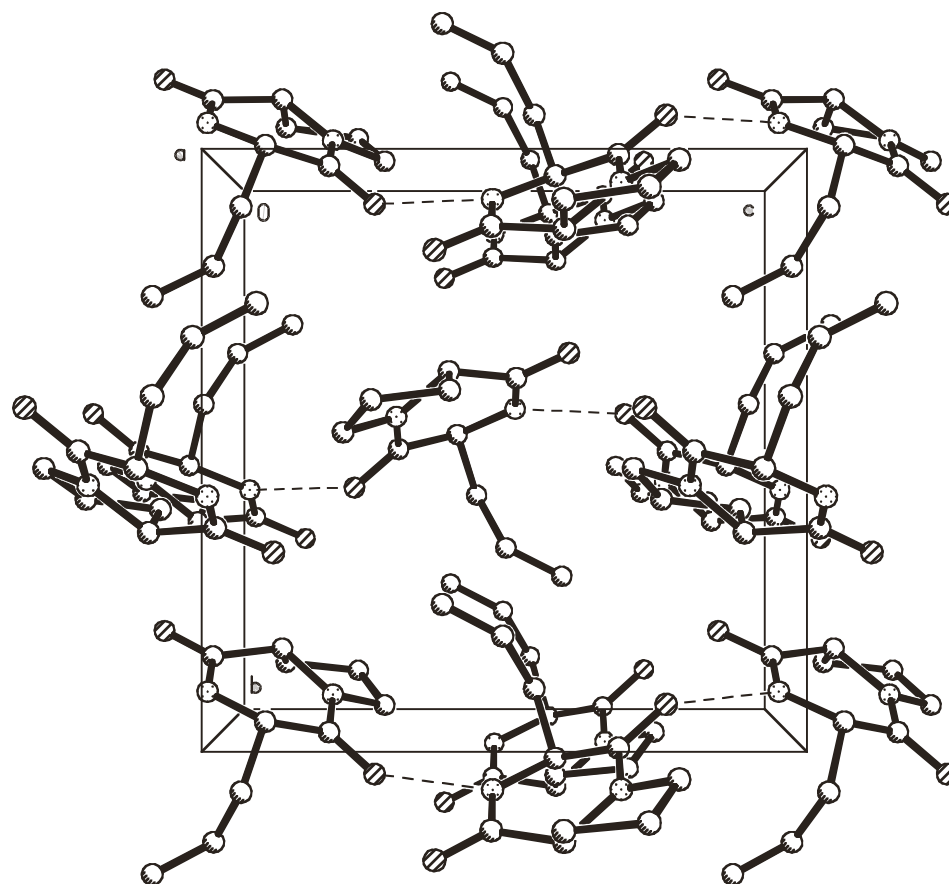


Fig. 17: Unit cell for *cis-76f*.

Table 31: Atomic coordinates ($\times 10^4$) and equivalent isotropic displacement parameters ($\text{Å}^2 \times 10^3$) for **cis-76f**.

Atom	x	y	z	U(eq)
N(1)	1311(3)	5754(2)	197(2)	48(1)
O(1)	-741(3)	6720(2)	1139(2)	61(1)
C(1)	-131(3)	6293(2)	215(2)	44(1)
N(2)	-392(3)	5590(2)	-1917(2)	44(1)
O(2)	1438(2)	4315(2)	-2735(2)	60(1)
C(2)	2166(3)	5289(2)	-869(2)	45(1)
C(3)	1033(3)	5020(2)	-1917(2)	44(1)
C(4)	-1666(3)	5312(3)	-2809(2)	57(1)
C(5)	-3193(4)	5860(3)	-2268(3)	67(1)
C(6)	-2789(3)	6031(3)	-939(3)	61(1)
C(7)	-1007(3)	6391(2)	-972(2)	45(1)
C(8)	3125(3)	4155(3)	-518(3)	55(1)
C(9)	2095(4)	3191(3)	27(3)	63(1)
C(10)	2342(5)	2658(3)	1065(3)	80(1)

Table 32. Anisotropic displacement parameters ($\text{Å}^2 \times 10^3$) for **cis-76f**.

Atom	U11	U22	U33	U23	U13	U12
N(1)	52(1)	57(1)	35(1)	-6(1)	-5(1)	4(1)
O(1)	67(1)	68(1)	50(1)	-18(1)	14(1)	-4(1)
C(1)	51(2)	39(1)	42(1)	-1(1)	4(1)	-9(1)
N(2)	43(1)	58(1)	31(1)	-2(1)	2(1)	-1(1)
O(2)	62(1)	76(1)	41(1)	-14(1)	11(1)	4(1)
C(2)	39(1)	53(2)	43(1)	0(1)	4(1)	-5(1)
C(3)	46(1)	50(1)	35(1)	3(1)	8(1)	-3(1)
C(4)	55(2)	78(2)	39(1)	2(1)	-7(1)	-7(2)
C(5)	56(2)	79(2)	66(2)	4(2)	-10(2)	6(2)
C(6)	44(2)	72(2)	67(2)	-12(2)	4(2)	8(2)
C(7)	52(2)	38(1)	46(1)	-1(1)	3(1)	1(1)
C(8)	45(1)	65(2)	55(2)	-6(1)	-1(1)	6(2)
C(9)	62(2)	48(2)	79(2)	-4(2)	-12(2)	2(2)
C(10)	93(3)	60(2)	87(2)	9(2)	-5(3)	-7(2)

Table 33: Anisotropic displacement parameters ($\text{Å}^2 \times 10^3$) for **cis-76f**.

Atom	U11	U22	U33	U23	U13	U12
N(1)	52(1)	57(1)	35(1)	-6(1)	-5(1)	4(1)
O(1)	67(1)	68(1)	50(1)	-18(1)	14(1)	-4(1)
C(1)	51(2)	39(1)	42(1)	-1(1)	4(1)	-9(1)
N(2)	43(1)	58(1)	31(1)	-2(1)	2(1)	-1(1)
O(2)	62(1)	76(1)	41(1)	-14(1)	11(1)	4(1)
C(2)	39(1)	53(2)	43(1)	0(1)	4(1)	-5(1)
C(3)	46(1)	50(1)	35(1)	3(1)	8(1)	-3(1)
C(4)	55(2)	78(2)	39(1)	2(1)	-7(1)	-7(2)
C(5)	56(2)	79(2)	66(2)	4(2)	-10(2)	6(2)
C(6)	44(2)	72(2)	67(2)	-12(2)	4(2)	8(2)
C(7)	52(2)	38(1)	46(1)	-1(1)	3(1)	1(1)
C(8)	45(1)	65(2)	55(2)	-6(1)	-1(1)	6(2)
C(9)	62(2)	48(2)	79(2)	-4(2)	-12(2)	2(2)
C(10)	93(3)	60(2)	87(2)	9(2)	-5(3)	-7(2)

Table 34: Hydrogen coordinates ($\times 10^4$) and isotropic displacement parameters ($\text{Å}^2 \times 10^3$) for *cis*-76f.

Atom	x	y	z	U(eq)
H(1)	1792	5670	883	58
H(2)	2939	5913	-1134	54
H(4A)	-1783	4440	-2916	69
H(4B)	-1420	5680	-3588	69
H(5A)	-3447	6634	-2648	80
H(5B)	-4108	5314	-2368	80
H(6A)	-2947	5282	-488	73
H(6B)	-3447	6669	-580	73
H(7)	-928	7234	-1258	54
H(8A)	3654	3831	-1235	66
H(8B)	3963	4382	56	66
H(9)	1190	2946	-413	75
H(10A)	3232	2874	1536	96
H(10B)	1629	2060	1335	96

Table 35: Torsion angles [°] for *cis-76f*.

C(2)-N(1)-C(1)-O(1)	-176.0(2)
C(2)-N(1)-C(1)-C(7)	2.7(4)
C(1)-N(1)-C(2)-C(3)	-22.4(4)
C(1)-N(1)-C(2)-C(8)	-145.9(2)
C(7)-N(2)-C(3)-O(2)	177.1(2)
C(4)-N(2)-C(3)-O(2)	7.5(4)
C(7)-N(2)-C(3)-C(2)	-3.9(4)
C(4)-N(2)-C(3)-C(2)	-173.4(2)
N(1)-C(2)-C(3)-O(2)	-158.9(2)
C(8)-C(2)-C(3)-O(2)	-36.2(3)
N(1)-C(2)-C(3)-N(2)	22.0(3)
C(8)-C(2)-C(3)-N(2)	144.8(2)
C(3)-N(2)-C(4)-C(5)	163.7(2)
C(7)-N(2)-C(4)-C(5)	-7.3(3)
N(2)-C(4)-C(5)-C(6)	-18.4(3)
C(4)-C(5)-C(6)-C(7)	36.2(3)
C(3)-N(2)-C(7)-C(1)	-16.3(4)
C(4)-N(2)-C(7)-C(1)	154.2(2)
C(3)-N(2)-C(7)-C(6)	-140.9(3)
C(4)-N(2)-C(7)-C(6)	29.6(3)
O(1)-C(1)-C(7)-N(2)	-164.5(2)
N(1)-C(1)-C(7)-N(2)	16.7(3)
O(1)-C(1)-C(7)-C(6)	-47.6(4)
N(1)-C(1)-C(7)-C(6)	133.6(2)
C(5)-C(6)-C(7)-N(2)	-39.8(3)
C(5)-C(6)-C(7)-C(1)	-163.9(2)
N(1)-C(2)-C(8)-C(9)	56.4(3)
C(3)-C(2)-C(8)-C(9)	-68.2(3)
C(2)-C(8)-C(9)-C(10)	-126.5(3)

6.6 X-Ray data analysis for (3*S*, 8*aR*)-3-Prenylhexahydropyrrolo[1,2-*a*]pyrazine-1,4-dione *trans*-76g

Table 36: Crystal data and structure refinement for *trans*-76g

Wavelength[mm]		1.54178
Crystal system		orthorhombic
Space group		P2(1)2(1)2(1)
Unit cell dimensions[Å]	a	6.4274(8)(4)
	b	7.8705(9)
	c	24.0198(19)
Angle	α	90°
	β	90°
	γ	90°
Volume (unit cell)[Å ³]		1215.1(2)
Calculated density [g/cm ³]		1.215
Crystal size [mm]		0.5 x 0.3 x 0.3
Θ - range for data collection		3.68 to 67.99°
Reflections collected		2377
Reflections unique		1992
R[%]		0.1041
R _w [%]		0.2059
Absolute structure parameter		-0.3(9)
Extinction coefficient		0.0121(15)
Identification code		s1267rc

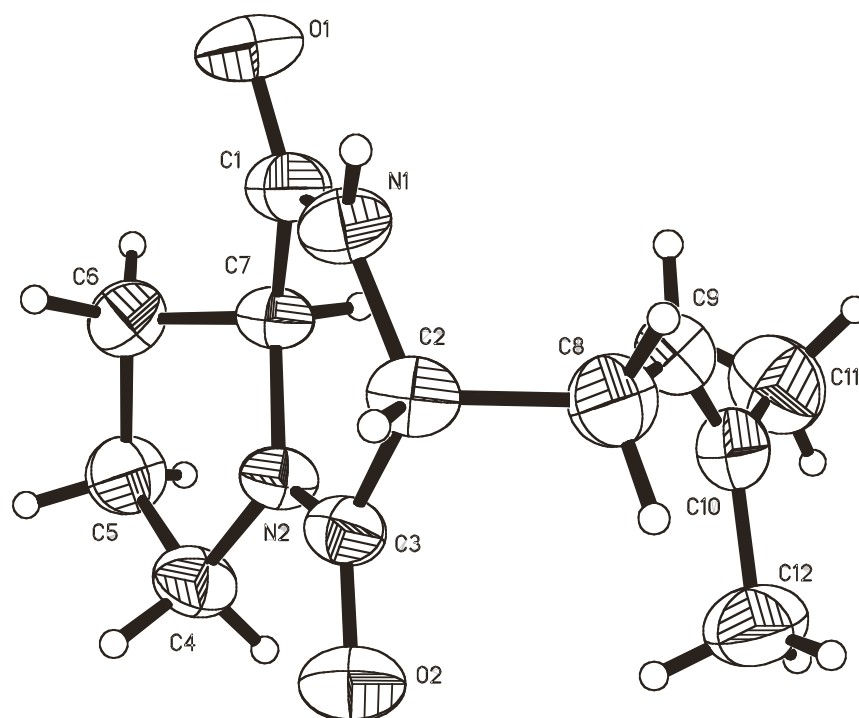


Fig. 18: X-Ray crystal structure of *trans*-76g (displacement parameters)

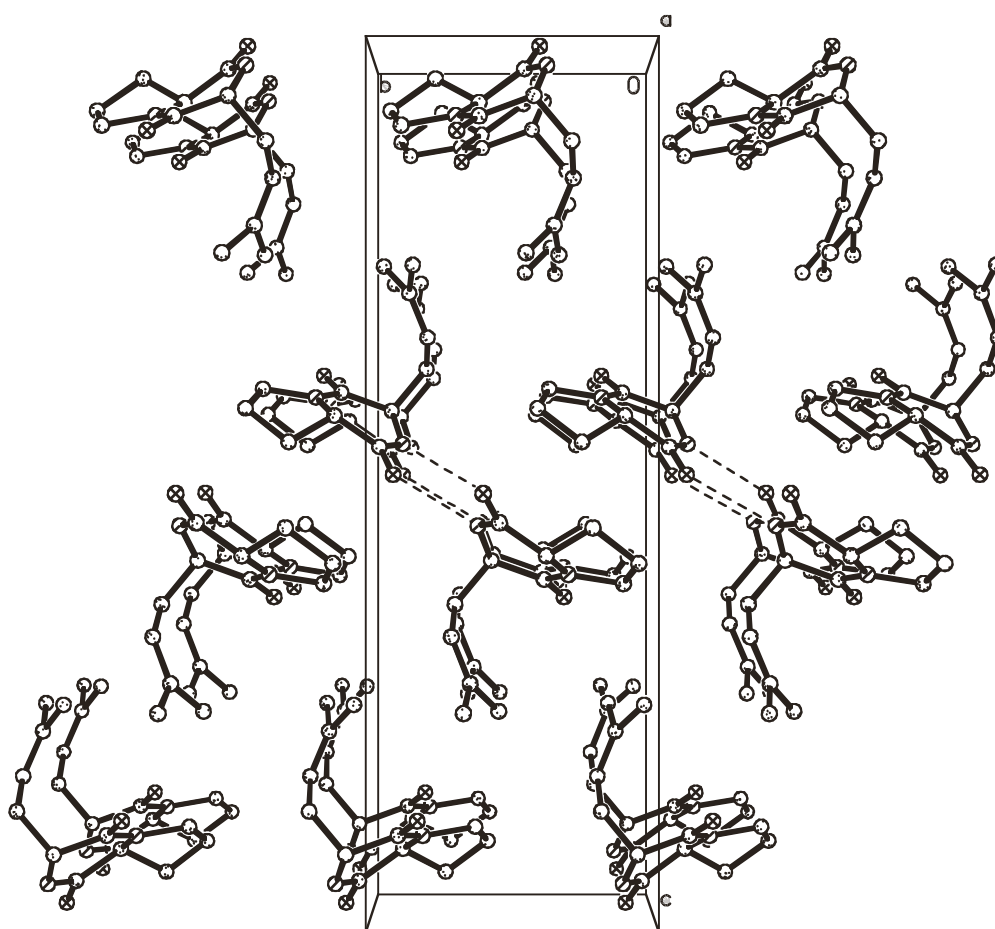


Fig. 19: Unit cell of *trans*-76g

Table 37. Atomic coordinates ($\times 10^4$) and equivalent isotropic displacement parameters ($\text{Å}^2 \times 10^3$) for *trans*-76g.

Atom	x	y	z	U(eq)
O(1)	-202(6)	4057(6)	104(2)	80(1)
N(1)	3031(7)	3851(6)	456(2)	56(1)
C(1)	1190(9)	4582(7)	418(2)	57(1)
N(2)	2694(6)	6878(5)	990(2)	48(1)
O(2)	6026(6)	6787(5)	1274(2)	67(1)
C(2)	4687(8)	4290(6)	851(2)	54(1)
C(3)	4507(8)	6083(6)	1061(2)	49(1)
C(4)	2453(8)	8708(6)	1086(2)	60(1)
C(5)	311(9)	9131(7)	848(3)	68(2)
C(6)	-202(9)	7623(7)	468(2)	60(1)
C(7)	804(8)	6121(6)	770(2)	49(1)
C(8)	4798(9)	3053(7)	1339(2)	65(2)
C(9)	2848(9)	2966(7)	1675(2)	63(1)
C(10)	2490(10)	3601(7)	2178(2)	64(2)
C(11)	406(12)	3409(10)	2453(3)	95(2)
C(12)	4074(12)	4543(10)	2515(3)	91(2)

Table 38: Anisotropic displacement parameters ($\text{Å}^2 \times 10^3$) for *trans*-76g.

Atom	U11	U22	U33	U23	U13	U12
O(1)	75(3)	86(3)	78(3)	-27(2)	-23(2)	-12(2)
N(1)	58(3)	60(3)	52(2)	-16(2)	0(2)	1(2)
C(1)	57(3)	60(3)	54(3)	-10(2)	0(3)	-12(3)
N(2)	45(2)	42(2)	56(2)	-9(2)	-3(2)	-3(2)
O(2)	50(2)	75(2)	78(2)	-18(2)	-2(2)	-9(2)
C(2)	45(3)	56(3)	60(3)	-10(2)	6(2)	0(2)
C(3)	47(3)	51(3)	49(2)	-7(2)	5(2)	-9(2)
C(4)	64(3)	42(2)	73(3)	-10(2)	-2(3)	0(2)
C(5)	72(4)	58(3)	75(4)	-2(3)	-8(3)	8(3)
C(6)	54(3)	67(3)	58(3)	-2(3)	-2(2)	5(3)
C(7)	45(3)	48(2)	52(3)	-11(2)	2(2)	-6(2)
C(8)	68(4)	54(3)	74(3)	-2(3)	-7(3)	13(3)
C(9)	69(4)	57(3)	64(3)	4(3)	-4(3)	-7(3)
C(10)	73(4)	56(3)	64(3)	7(2)	-7(3)	1(3)
C(11)	101(6)	96(5)	89(5)	0(4)	25(4)	-9(4)
C(12)	97(5)	101(5)	76(4)	-16(4)	-15(4)	-18(5)

Table 39: Hydrogen coordinates ($\times 10^4$) and isotropic displacement parameters ($\text{Å}^2 \times 10^3$) for *trans*-76g.

Atom	x	y	z	U(eq)
H(1)	3470(110)	2960(90)	250(30)	100(20)
H(2)	6009	4207	650	65
H(4A)	3533	9342	895	72
H(4B)	2514	8967	1480	72
H(5A)	351	10183	638	82
H(5B)	-712	9238	1143	82
H(6A)	-1693	7468	433	72
H(6B)	394	7776	100	72
H(7)	-90	5796	1083	58
H(8A)	5110	1928	1197	78
H(8B)	5934	3388	1581	78
H(9)	1741	2394	1510	76
H(11A)	445	3923	2815	143
H(11B)	78	2224	2489	143
H(11C)	-637	3957	2231	143
H(12A)	3476	4865	2866	137
H(12B)	4502	5544	2317	137
H(12C)	5259	3826	2579	137

Table 40: Torsion angles [°] for *trans*-76g.

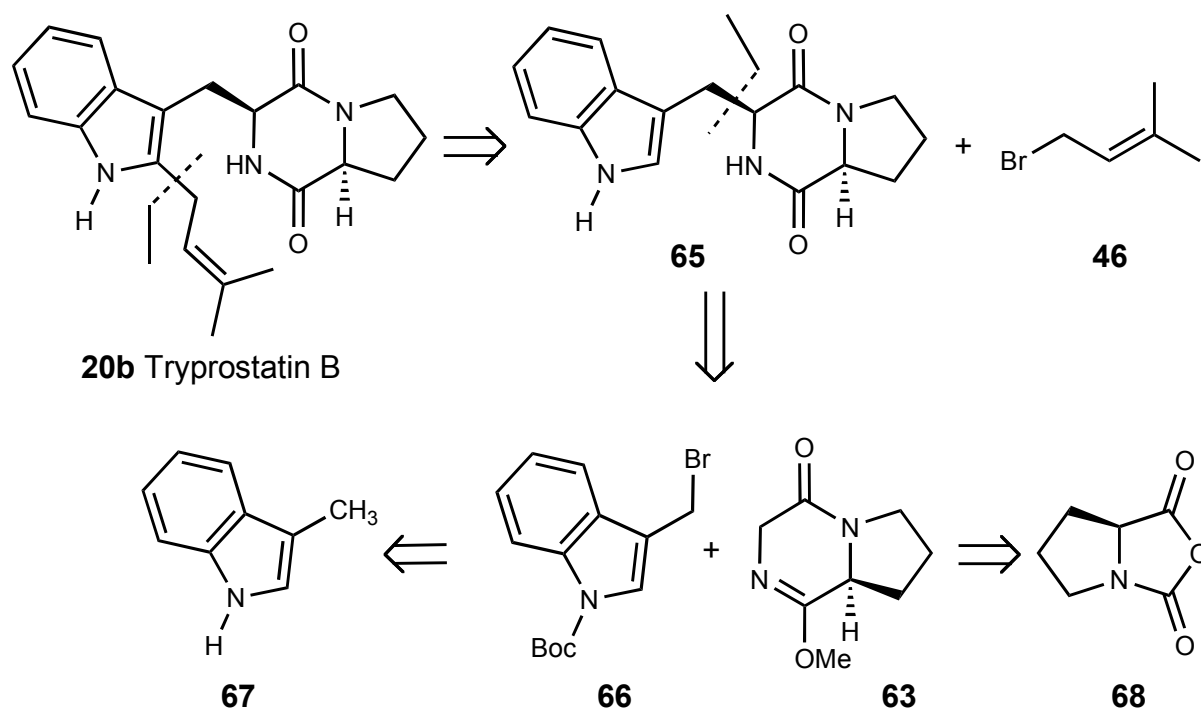
C(2)-N(1)-C(1)-O(1)	-174.0(5)
C(2)-N(1)-C(1)-C(7)	6.6(8)
C(1)-N(1)-C(2)-C(3)	-23.6(7)
C(1)-N(1)-C(2)-C(8)	101.5(6)
C(7)-N(2)-C(3)-O(2)	-176.7(5)
C(4)-N(2)-C(3)-O(2)	8.8(7)
C(7)-N(2)-C(3)-C(2)	5.6(7)
C(4)-N(2)-C(3)-C(2)	-168.8(5)
N(1)-C(2)-C(3)-O(2)	-161.1(5)
C(8)-C(2)-C(3)-O(2)	72.7(6)
N(1)-C(2)-C(3)-N(2)	16.7(6)
C(8)-C(2)-C(3)-N(2)	-109.6(5)
C(3)-N(2)-C(4)-C(5)	169.0(5)
C(7)-N(2)-C(4)-C(5)	-6.2(6)
N(2)-C(4)-C(5)-C(6)	-17.8(6)
C(4)-C(5)-C(6)-C(7)	34.1(6)
C(3)-N(2)-C(7)-C(1)	-22.9(7)
C(4)-N(2)-C(7)-C(1)	152.1(4)
C(3)-N(2)-C(7)-C(6)	-147.6(5)
C(4)-N(2)-C(7)-C(6)	27.4(5)
O(1)-C(1)-C(7)-N(2)	-163.2(5)
N(1)-C(1)-C(7)-N(2)	16.2(7)
O(1)-C(1)-C(7)-C(6)	-46.0(7)
N(1)-C(1)-C(7)-C(6)	133.4(5)
C(5)-C(6)-C(7)-N(2)	-37.0(5)
C(5)-C(6)-C(7)-C(1)	-160.5(4)
N(1)-C(2)-C(8)-C(9)	-59.8(6)
C(3)-C(2)-C(8)-C(9)	66.5(6)
C(2)-C(8)-C(9)-C(10)	-106.2(7)
C(8)-C(9)-C(10)-C(12)	-0.8(10)
C(8)-C(9)-C(10)-C(11)	179.3(6)

7 Summary

The summary of the present Ph.D. thesis consists of two major parts: In part one the synthesis of bicyclic lactim ether **63** and its alkylation with various electrophiles has been studied, as a pathway to the synthesis of the antitumor natural compound tryprostatin B (**20b**). In part two, the alkylation strategy has been attempted toward the synthesis of the quinocarcin ring system **83**.

Among the biologically relevant bicyclic diketopiperazines, tryprostatin A **20a** and B **20b** have been isolated as secondary metabolites from the fermentation broth of a marine fungal strain of *Aspergillus fumigatus* BM939. They completely inhibit cell cycle progression at a final concentration of 50 $\mu\text{g/mL}$ of **20a** and 12.5 $\mu\text{g/mL}$ of **20b**, respectively. Structurally, the tryprostatins **20a**, **20b** contain a 2-isoprenyltryptophan moiety and a proline residue, the latter of which is fused to the diketopiperazine unit.

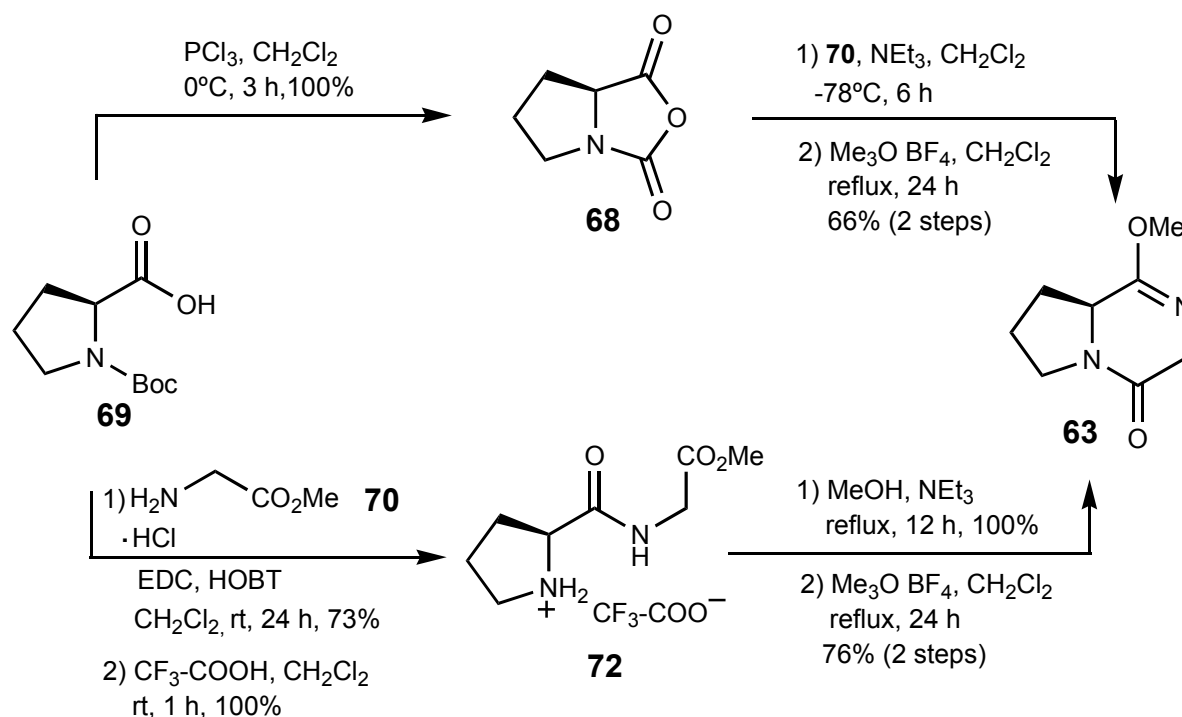
The synthetic strategy described in this work (Scheme 44) is based on the degradation of tryprostatin B **20b** into two fragments **63** and **66**.



Scheme 44

The lactim ether **63** can be obtained from the anhydride **68**, by treatment with glycine methyl ester hydrochloride **70** (Scheme 45). The bromoindole derivative **66** resulted from 3-methylindole **67**, by regiospecific bromination under free radical conditions. The key step is the diastereoselective alkylation of fragment **63** with bromoindole derivative **66**, followed by prenylation of the alkylated product **65**.

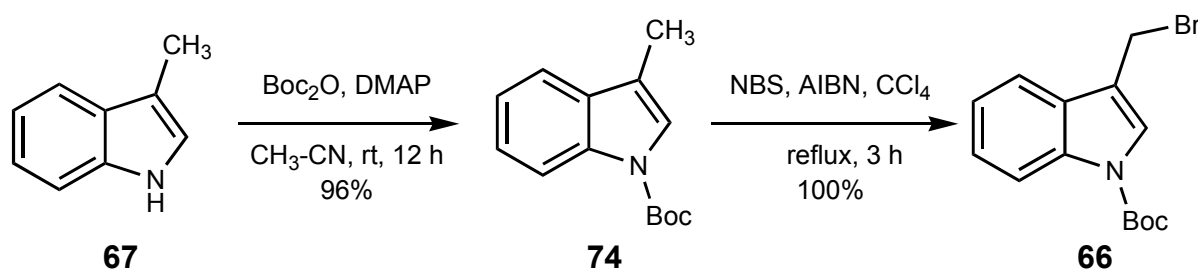
The synthesis of the lactim ether **63** was achieved by treatment of L-(*tert*-butoxycarbonyl)-proline **69** with phosphorus trichloride, providing the anhydride **68** in quantitative yield (Scheme 45). Reaction of anhydride **68** with hydrochloride **70** in the presence of NEt_3 provided the ring closure and treatment with Meerwein's salt afforded the lactim ether **63** in 66% total yield.



Scheme 45

As an alternative to the previous method, L-proline **69** was coupled with glycine methyl ester hydrochloride **70** in the presence of HOBT and EDC (Scheme 45). Boc-deprotection with $\text{F}_3\text{C-COOH}$ followed by evaporation of the solvent gave the corresponding salt **72** in quantitative yield. Neutralization of salt **72** with excess NEt_3 in MeOH at reflux, followed by treatment with Meerwein's salt afforded the lactim ether **63** in 76% total yield. Both methods were performed in parallel, because the

classic method involving the salt **72** allowed a secure synthesis of the lactim ether **63** in a good yield, although the reagents were expensive, while the method via the anhydride **68**, using affordable starting material and less reaction steps, was optimized.

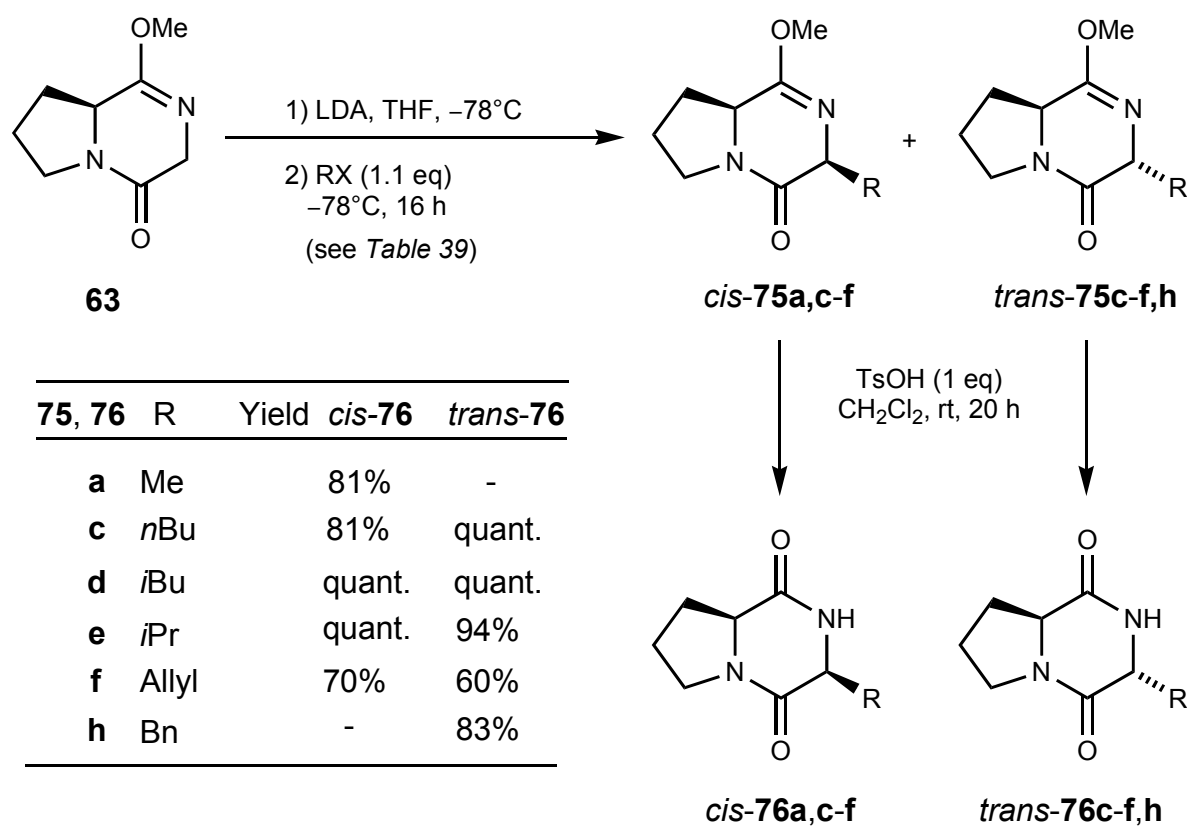


Scheme 46

The preparation of the desired N -(*tert*-butoxycarbonyl)-3-bromomethylindole **66** was based on the regiospecific bromination at C-3 of the N -Boc-protected derivative of 3-methylindole **74**. When 3-methylindole **67** was stirred with di-*tert*-butyl dicarbonate in the presence of DMAP, N -Boc protected indole **74** was obtained in 96% yield. The compound **74** was treated with N -bromosuccinimide in the presence of azobisisobutyronitrile to provide the 3-(bromomethyl) indole **66**, in quantitative yield (Scheme 46).

To determine the optimal reaction conditions for the alkylation toward the synthesis of tryprostatin B, the alkylation of lactim ether **63** with different electrophiles was investigated first (Scheme 47, Table 39). Since LDA was previously found to be most promising with regard to yields and diastereoselectivities for a similar lactim ether system, it was the base of choice for the deprotonation step.

Scheme 47 and Table 39 summarize some characteristic results.



Scheme 47

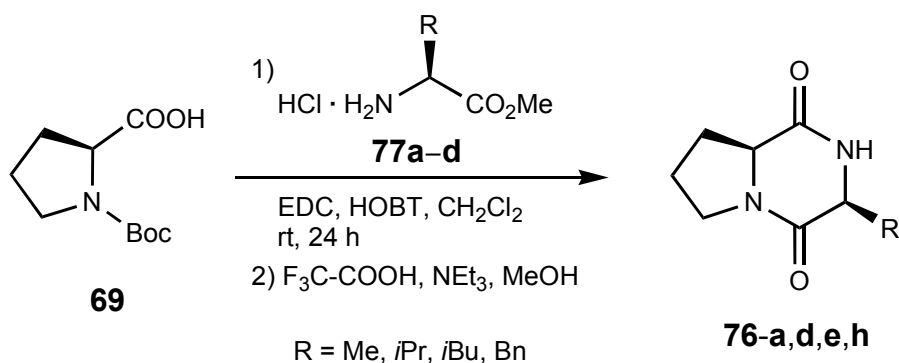
Table 39. Selected alkylations of lactim ether **63** to compounds **75**

Electrophile R	X	Product 75	Conv. ^{a)} [%]	Yield ^{b)} [%]	Ratio ^{a)} <i>cis</i> : <i>trans</i>
Me	I	75a	100	94	98 : 2
<i>n</i> Bu	I	75c	81	33 ^{c)}	50 : 50
<i>i</i> Bu	Br	75d	65	48	30 : 70
<i>i</i> Pr	Br	75e	86	67	60 : 40
Allyl	I	75f	90	35 ^{c)}	33 : 67
Bn	Br	75h	77	71	4 : 96

^{a)} Conversion and diastereomeric ratios were determined by capillary GC of the crude products. ^{b)} Yields refer to isolated yields. ^{c)} Difficult chromatographic purification caused loss of yields.

Finally, the isolated pure *cis*- and *trans*-lactim ethers **75** were treated with TsOH at room temperature in CH_2Cl_2 to give the corresponding diketopiperazines *cis*- and *trans*-**76** (Scheme 47).

In order to confirm the preliminary stereochemical assignment of the lactim ethers **75** and the corresponding diketopiperazines **76** based on NMR and NOE experiments, the diketopiperazines *cis*-**76a,d,e,h** were prepared from methyl L-alaninate (**77a**), L-leucinate (**77b**), L-valinate (**77c**) and L-phenylalaninate (**77d**), as outlined in Scheme 48. L-proline derivative **69** was condensed with the amino acid esters **77** in the presence of EDC and HOBT to give intermediate dipeptides which were immediately cyclized to the diketopiperazines *cis*-**76** (Scheme 48).

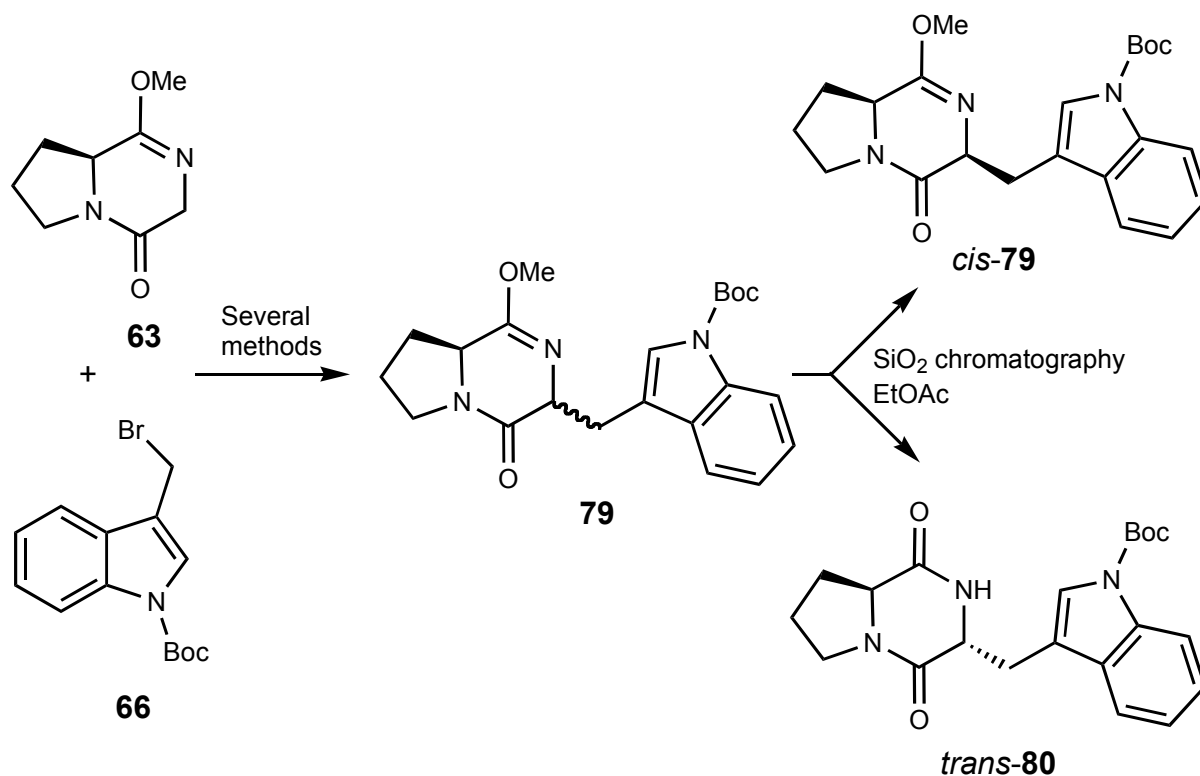


Scheme 48

The *cis*-diketopiperazines resulted by cyclization were compared by ^1H , ^{13}C -NMR, optical rotation $[\alpha]$ and X-ray crystal structures with the corresponding diketopiperazines obtained by alkylation, leading to the correct assignment of the diastereomers **76**.

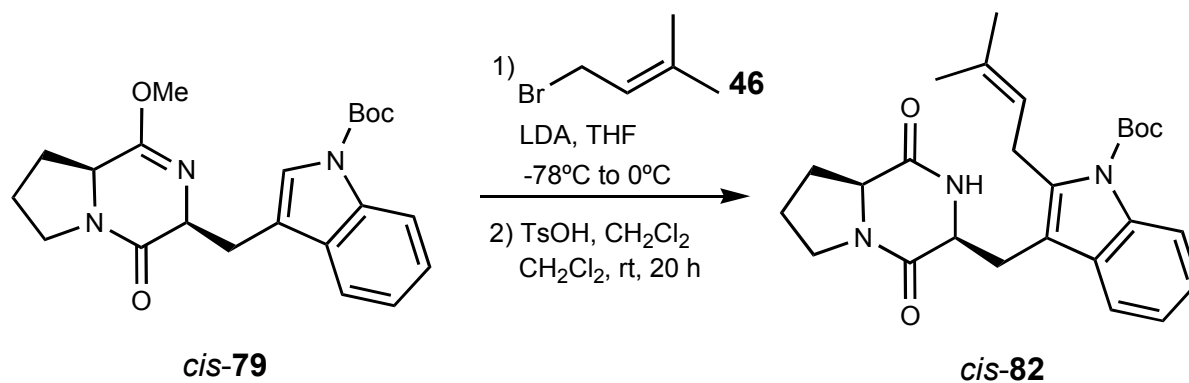
Based on these alkylation experiments, the alkylation reaction of the lactim ether **63** with the bromoindole derivative **66** was carried out under similar reaction conditions (Scheme 49).

The lactim ether **63** was deprotonated with LDA at -78°C and HMPA was added as a co-solvent. A solution of the indole derivative **66** in THF was added and the reaction mixture was kept over night at -78°C , leading to a mixture of diastereomers in 13% yield and a ratio of *cis* : *trans* = 32 : 68 (Scheme 49). During purification by flash chromatography on silica gel with ethyl acetate as eluent, the diastereomer *trans*-**79** hydrolysed to the corresponding diketopiperazine **80**.



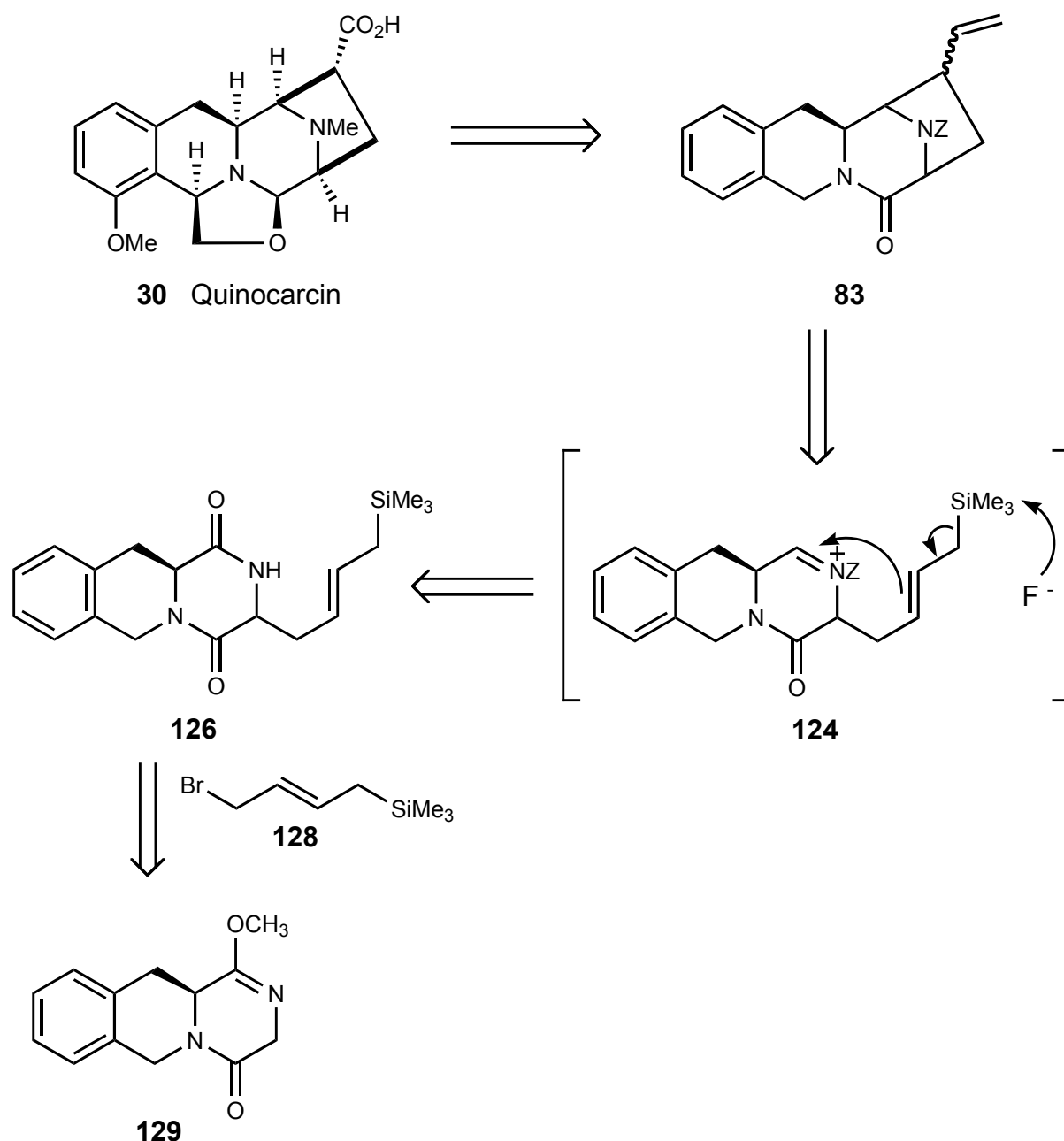
Scheme 49

For tryprostatin B **20b** the 2-isoprenyltryptophan precursor **82** was required. To introduce the isoprenyl group at the indole C-2 position, the substrate *cis*-79 was deprotonated, using LDA as a base, in THF at -78°C , to form the corresponding anion. This step was followed by addition of pure isoprenyl bromide **46**, to yield the alkylated product, which was treated with TsOH (1 eq) at room temperature in CH₂Cl₂ to give the corresponding diketopiperazine *cis*-82 (Scheme 50).



Scheme 50

Quinocarcin **30**, a tetrahydroisoquinoline antitumor antibiotic, that represents the focus of the second part of this work, was originally isolated from *Streptomyces melanovinaceus* and has shown potent antitumor activity against several human tumor cell lines.



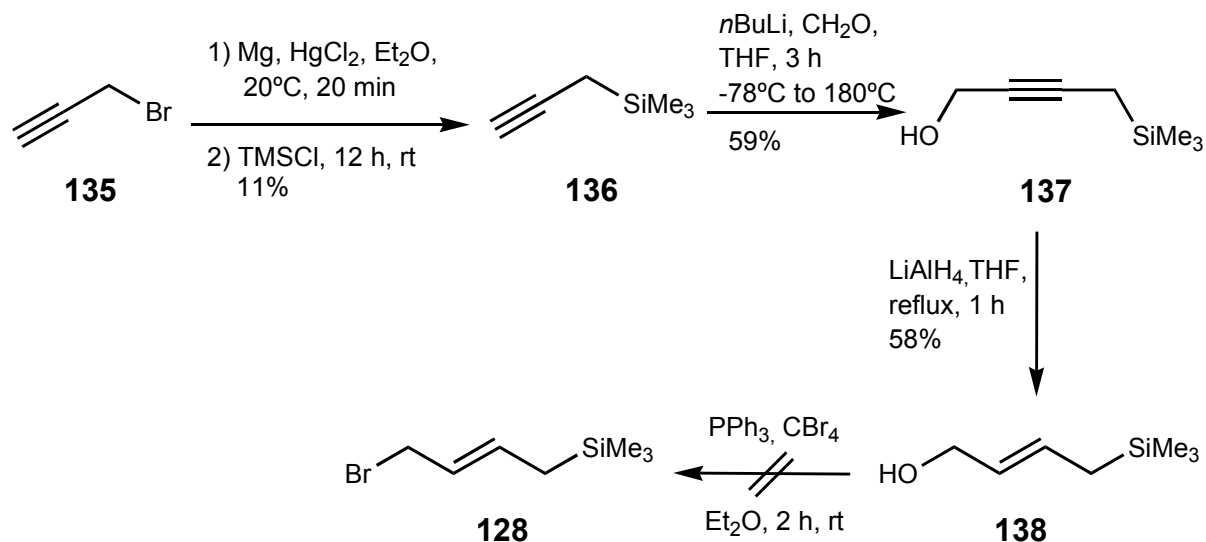
Scheme 51

The quinocarcin ring system **83** should be divided in two major fragments. The first fragment is represented by the isoquinoline structural motif which by transformation into tricyclic diketopiperazine, provides the first three rings of the quinocarcin

precursor molecule, which may be critical for the biological activity. The fourth ring is formed by introduction of a side chain in the tricyclic diketopiperazine fragment, followed by cyclization.

The synthetic strategy may start from the tricyclic lactim ether **129** which is alkylated at C-3 with bromo olefine **128**. In a four-step sequence, the piperazine **124** may be accessible (Scheme 51). Fluoride-initiated allylsilane addition to the iminium ion in the derivative **124** should accomplish the synthesis to quinocarcin precursor **83** (Scheme 51).

The bromo olefine **128** synthesis followed a procedure starting from propargyl bromide **135** that was transformed in a Grignard reagent with Mg in diethyl ether, followed by treatment with trimethylsilyl chloride, affording propargyltrimethylsilane **136** in 11% yield (Scheme 52). Compound **136** was treated with gaseous formaldehyde, leading to 1-(trimethylsilyl)-2-butyn-4-ol **137** in 59%. The reduction of the triple bond in **137** was performed by reduction with LiAlH_4 , affording the corresponding alkene **138** in 58% yield. The synthesis of the brominated alkene **128** was unsuccessful when PPh_3 and CBr_4 were used as reagents.



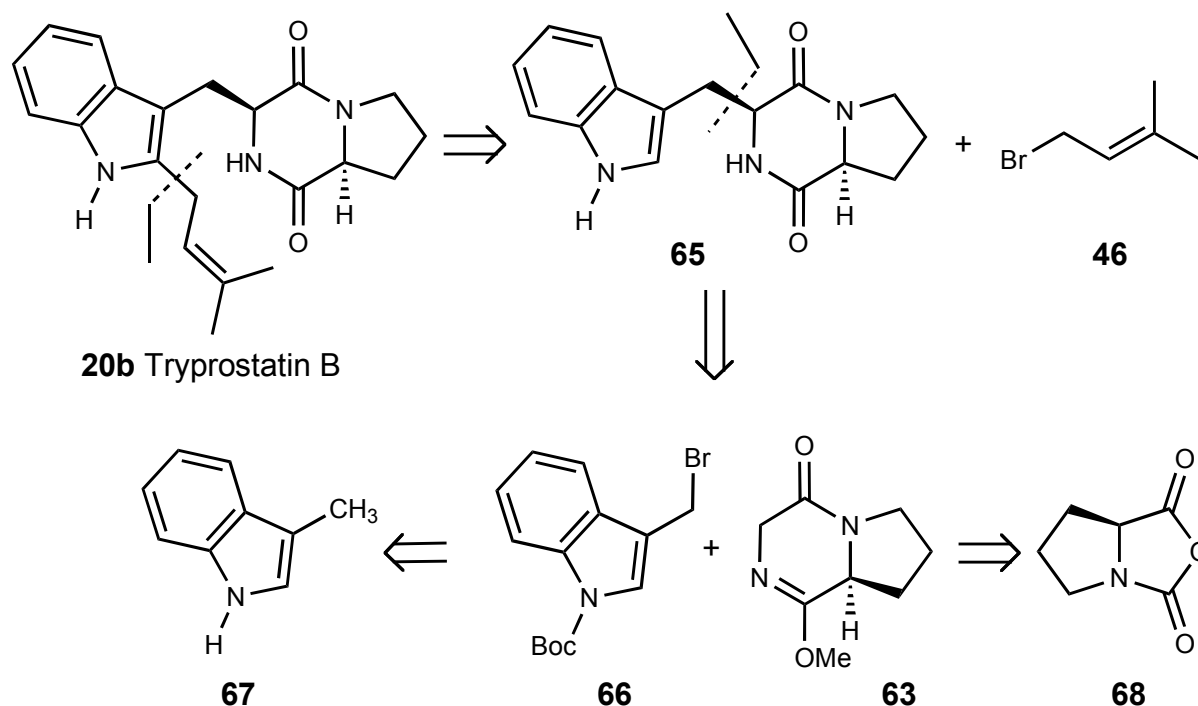
Scheme 52

8 Zusammenfassung

Im Rahmen dieser Arbeit wurden zwei Themengebiete bearbeitet. Im ersten Teil wurde die Synthese des bicyclischen Lactimethers **63** und dessen Alkylierung mit verschiedenen Elektrophilen untersucht. Auf diese Weise sollte ein Zugang zu Tryprostatin B (**20b**), einem Naturstoff mit Antitumoreigenschaften, gefunden werden.

Die biologisch relevanten Diketopiperazine Tryprostatin A **20a** und B **20b** wurden als sekundäre Metabolite aus der Fermentationsbrühe eines marinen Pilzstammes, *Aspergillus fumigatus* BM939, isoliert. Sie inhibieren vollständig die Zellzyklusprogression mit Konzentrationen von 50 µg/mL für **20a** bzw. 25 µg/mL für **20b**. Die Tryprostatine **20a**, **20b** enthalten einen 2-Isoprenyltryptophan- und einen Prolin-Rest, die in die Diketopiperazin-Einheit eingebaut sind.

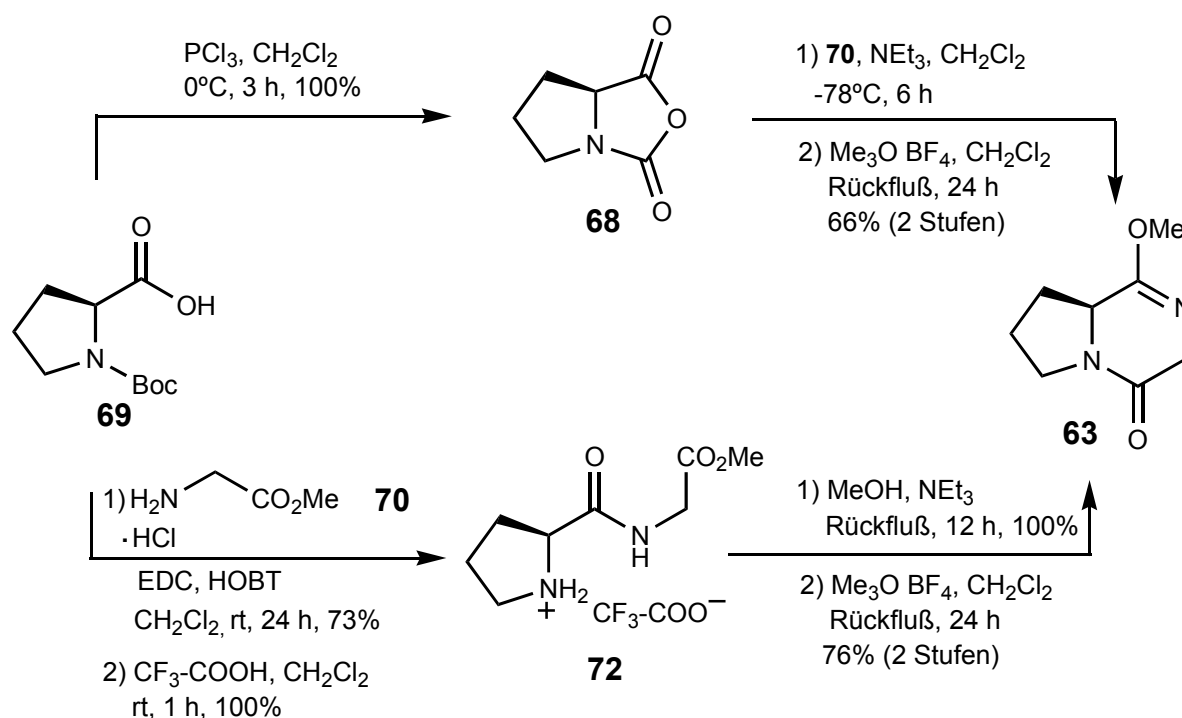
Die in dieser Arbeit beschriebene Synthesestrategie (Schema 1) basiert auf dem Aufbau von Tryprostatin **20b** aus den zwei Fragmenten **63** und **66**.



Schema 1

Der Lactimether **63** sollte über die Reaktion des Anhydrid **68** mit Glycinmethylesterhydrochlorid **43** zugänglich sein. Das Bromindolderivat **66** sollte durch regiospezifische Bromierung von 3-Methylindol **67** unter radikalischen Bedingungen erhältlich sein. Die Schlüsselstufe der Synthese ist die diastereoselektive Alkylierung des Fragmentes **63** mit Bromindolderivat **66**. Die anschließende Prenylierung des alkylierten Produkts **65** sollte zum Tryprostatin B **20b** führen.

Die Synthese des Lactimethers **63** begann mit der Reaktion von L-(*tert*-Butoxycarbonyl)prolin **69** mit Phosphortrichlorid, wobei das Anhydrid **68** in quantitativer Ausbeute isoliert wurde (Schema 2). Die Reaktion des Anhydrids **68** mit dem Hydrochlorid **70** in Gegenwart von NEt_3 führte zum Ringschluss, und nachfolgende O-Methylierung mit Meerwein's Salz ergab den Lactimether **63** in 66% Gesamtausbeute.

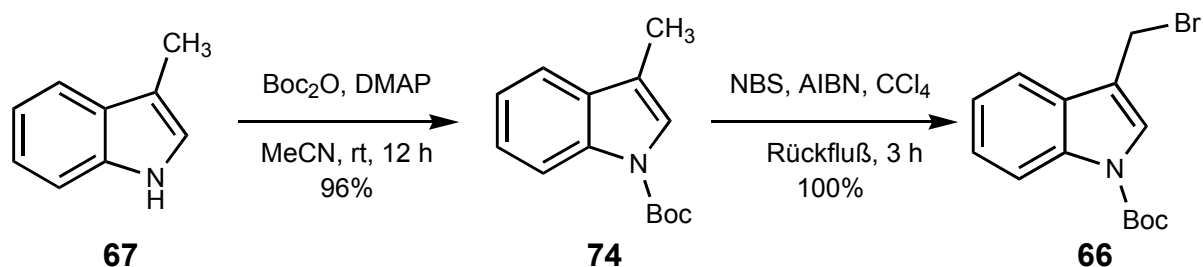


Schema 2

Alternativ dazu wurde das L-Prolin-Derivat **69** mit Glycinmethylesterhydrochlorid **70** in Gegenwart von HOBT und EDC umgesetzt (Schema 2). Die Boc-Entschützung mit Trifluoressigsäure ergab das entsprechende Salz **72** in quantitativer Ausbeute.

Neutralisation des Salzes **72** mit überschüssigem NEt_3 in MeOH unter Rückfluß und O-Methylierung mit Meerwein's Salz lieferte den Lactimether **63** in einer Gesamtausbeute von 76%.

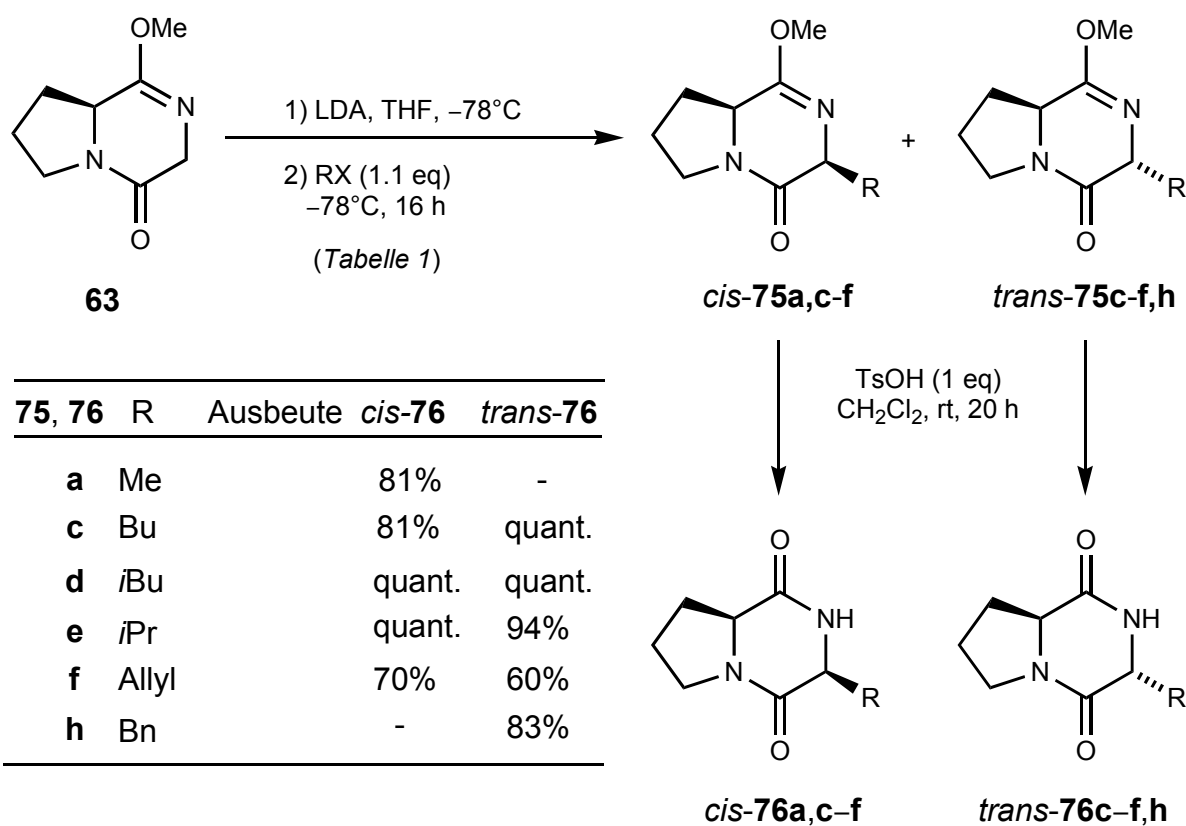
Die Darstellung des gewünschten *N*-(*tert*-Butoxycarbonyl)-3-brommethylindols **66** basiert auf einer regiospezifischen Bromierung der Methylgruppe im *N*-Boc-geschützten 3-Methylindol-Derivat **74** (Schema 3). 3-Methylindol **67** wurde mit Boc_2O in Gegenwart von DMAP zum *N*-Boc-geschützten Indol **74** umgesetzt. Das Derivat **74** wurde anschließend mit NBS in Gegenwart von AIBN bromiert und das 3-Brommethylindol **66** in quantitativer Ausbeute isoliert (Schema 3).



Schema 3

Um die optimalen Bedingungen für die Alkylierung des Tryprostatin B-Vorläufers zu bestimmen, wurde zuerst die Alkylierung des Lactimethers **63** mit verschiedenen Elektrophilen untersucht (Schema 4, Tabelle 1).

Schema 4 und Tabelle 1 fassen einige charakteristische Ergebnisse zusammen.



Schema 4

Tabelle 1. Ausgesuchte Alkylierungen des Lactimethers **63** zu Verbindungen **75**

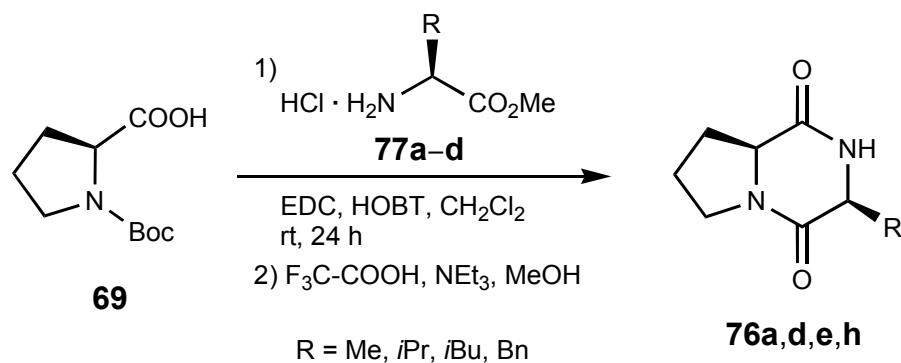
Elektrophil		Produkt	Umsatz ^{a)}	Ausbeute ^{b)}	D.v. ^{a)}
R	X	75	[%]	[%]	<i>cis</i> : <i>trans</i>
Me	I	75a	100	94	98 : 2
<i>n</i> Bu	I	75c	81	33 ^{c)}	50 : 50
<i>i</i> Br	Br	75d	65	48	30 : 70
<i>i</i> Pr	Br	75e	86	67	60 : 40
Allyl	I	75f	90	35 ^{c)}	33 : 67
Bn	Br	75h	77	71	4 : 96

^{a)} Umsatz und Diastereomerenverhältnis wurden mittels Kapillar-GC aus dem Rohprodukt bestimmt. ^{b)} Ausbeuten beziehen sich auf isolierte Ausbeute.

^{c)} Schwierige chromatographische Trennung führte zum Verlust der Ausbeute.

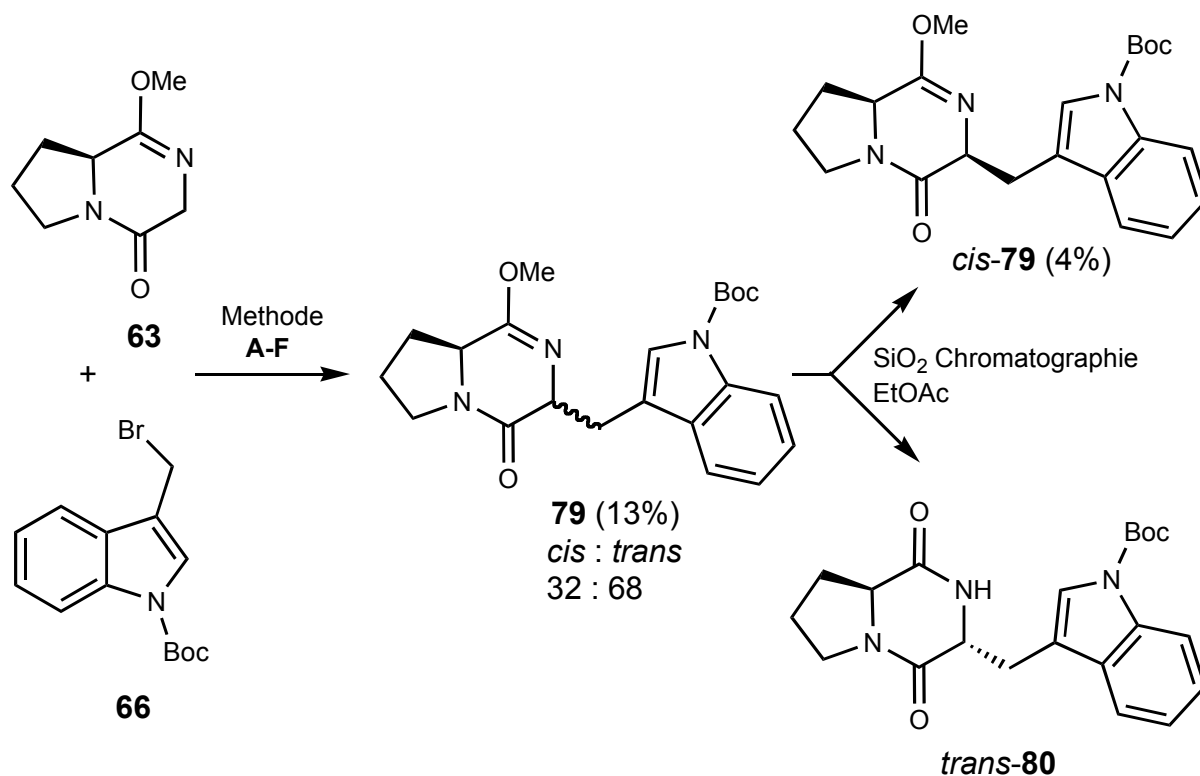
Schließlich wurden die isolierten reinen *cis*- und *trans*-Lactimether **75** bei niedriger Temperatur in die entsprechenden *cis*- und *trans*- Diketopiperazine **76** überführt (Schema 4).

Um die NMR-Zuordnung der Signale der Lactimether **75** und der entsprechenden Diketopiperazine **76** aus NMR- und NOE-Experimenten zu bestätigen, wurden die Diketopiperazine *cis*-**76a,d,e,h** aus Methylestern von L-Alanin (**77a**), L-Leucin (**77b**), L-Valin (**77c**) und L-Phenylalanin (**77d**) dargestellt (Schema 5). Das L-Prolin-Derivat **69** wurde mit den entsprechenden Aminosäureestern **77** in Gegenwart von EDC und HOBT kondensiert und die gewünschten Dipeptide erhalten, die sofort zu den entsprechenden Diketopiperazinen *cis*-**76** cyclisierten (Schema 5).



Schema 5

Die ^1H - und ^{13}C -NMR-Spektren, Drehwerte und Röntgenstrukturanalysen wurden mit entsprechenden Werten der Diketopiperazine, die durch Alkylierung erhalten wurden, verglichen.

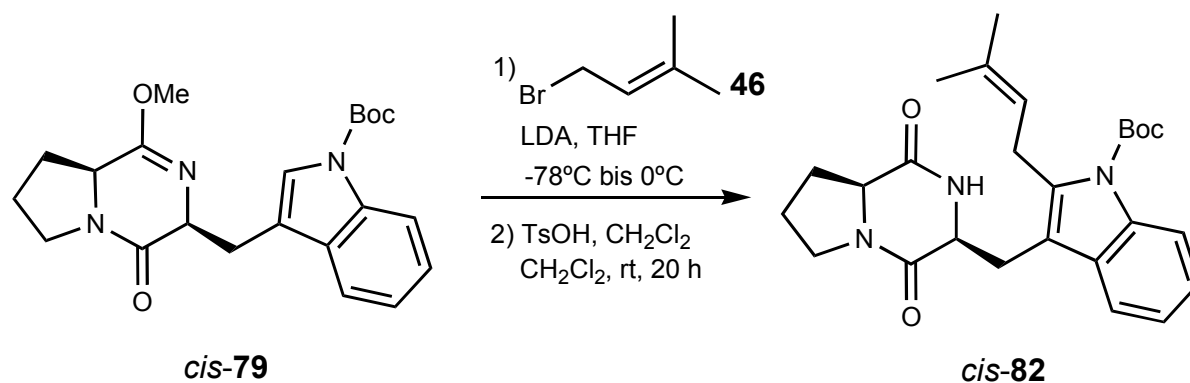


Schema 6

Auf der Grundlage von diesen Alkylierungsexperimenten wurde die Alkylierungsreaktion des Lactimethers **63** mit dem Bromoindol-Derivat **66** unter ähnlichen Reaktionsbedingungen durchgeführt (Schema 6).

Der Lactimether **63** wurde mit LDA deprotoniert, in Gegenwart von HMPA als Co-Solvens. Eine Lösung des Bromoindol-Derivates **66** in THF wurde dazu gegeben, und die Reaktionsmischung wurde über Nacht bei tiefer Temperatur gerührt, wobei Verbindung **79** als Diastereomergemisch in 13% Ausbeute mit einem Diastereomerenverhältnis von *cis* : *trans* = 32 : 68 entstand (Schema 6). Während der Reinigung durch Flash-Säulenchromatographie auf Kieselgel mit Essigsäureethylester als Laufmittel wurde das *trans*-Diastereomer **79** zu dem entsprechenden Diketopiperazin **80** hydrolysiert.

Um die Isoprenyl-Gruppe in der 2-Position des Indols einzuführen, wurde das Substrat *cis*-**79** mit LDA in THF bei -78°C deprotoniert, gefolgt von der Addition des Isoprenylbromids **46**. Das alkylierte Produkt wurde mit TsOH umgesetzt, um das entsprechende Diketopiperazin *cis*-**83** zu erhalten (Schema 7).

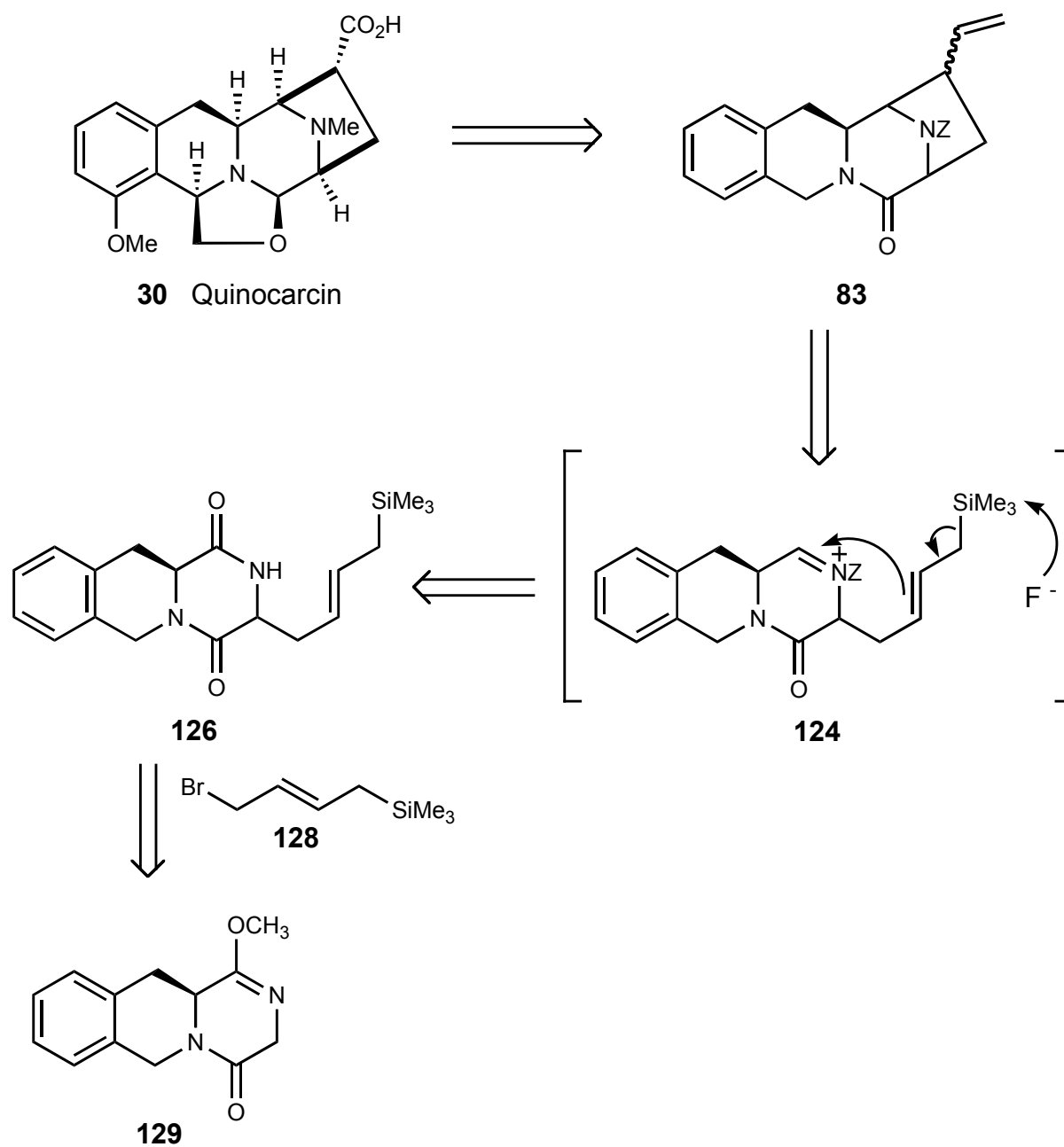


Schema 7

Der zweite Teil dieser Arbeit beschäftigte sich mit der Darstellung von Quinocarcin, einem Tetrahydroisochinolin-Alkaloid, welches ursprünglich aus *Streptomyces melanovinaceus* isoliert wurde und potentielle Anti-Tumoraktivität gegen verschiedene menschliche Tumorzellenlinien aufweist.

Die Retrosynthese, die in dieser Arbeit vorgesehen war, ist in Schema 8 angezeigt.

Das Quinocarcinsystem **83** wurde in zwei Hauptfragmente geteilt. Das erste Fragment **129** ist auf der Basis von Isochinolin aufgebaut. Die Synthese zu dem tricyclischen Lactimether **129** kann mit der Alkylierung in C-3 Position mit dem Bromolefine **128** beginnen. Piperazin **124** kann in einer vierstufigen Sequenz synthetisiert werden. Fluorid-vermittelte Allylsilan-Addition an das Derivat **124** liefert den Quinocarcinvorläufer **83** (Schema 8).



Schema 8

9 References

- [1] N. Neuss, M. Gormann, W. Hargrove, N. J. Cone, K. Biemann, G. Büchi, R. E. Manning, *J. Am. Chem. Soc.* **1964**, *86*, 1440-1442.
- [2] J. W. Moncrief, W. N. Lipscomb, *J. Am. Chem. Soc.* **1965**, *86*, 4963-4964.
- [3] I. Ojima, *J. Med. Chem.* (Book Review) **1996**, *39*, 807-807.
- [4] C. Kaiser, *J. Med. Chem.* (Book Review) **2001**, *44*, 3335-3336.
- [5] A. L. Demain, *J. Ind. Microbiol. Biotechnol.* **2006**, *33*, 486-495.
- [6] Y. Chin, M. J. Balunas, H. B. Chai, A. D. Kinghorn, *The AAPS Journal* **2006**, *8*, 239-253.
- [7] R. K. Pettit, *Cancer Chemother. Pharmacol.* **2004**, *54*, 1-6.
- [8] M. A. Farooq Biabani, H. Laatsch, *J. prakt. Chem.* **1998**, *340*, 589-607.
- [9] D. J. Faulker, *Nat. Prod. Rep.* **2001**, *18*, 1-49.
- [10] M. H. G. Munro, J. W. Blunt, E. J. Dumdei, S. J. H. Hickfort, R. E. Lill, L. Shangxiao, C. N. Battershill, A. R. Duckworth, *J. Biotechnol.* **1999**, *70*, 15-25.
- [11] L. H. O'Hanlon, *Journal of National Cancer Institute* **2006**, *98*, 662-663.
- [12] N. Cramer, Dissertation, Universität Stuttgart, **2005**.
- [13] D. J. Newman, G. M. Craigg, *Curr. Med. Chem.* **2004**, *11*, 1693-1713.
- [14] D. J. Newman, G. M. Craigg, *J. Nat. Prod.* **2004**, *11*, 1693-1713.
- [15] R. J. Carpon, *Eur. J. Org. Chem.* **2001**, 633-645.
- [16] M. S. Butler, *Nat. Prod. Rep.* **2005**, *22*, 162-195.
- [17] J. Jou, J. Gonzáles, F. Albericio, P. L. Williams, E. Giralt, *J. Org. Chem.* **1996**, *62*, 354-366.
- [18] www.lclabs.com
- [19] D. Mendola in *Drugs from the Sea* (Hrsg.: N. Fusetani), Karger, Basel, **2000**, 120-133.
- [20] G. R. Pettit in *Progress in the Chemistry of Organic Natural Products*, (Hrsg.: W. Hertz), Springer-Verlag, New York, **1991**.
- [21] K. L. Rinehart, T. G. Holt, N. L. Fregeau, P. A. Kiefer, G. R. Wilson, T. J. Perun Jr., R. Sakai, A. G. Thompson, J. G. Stroh, L. S. Shield, D. S. Seigler, L. H. Li, D. G. Martin, C. J. P. Grimmelikhuijzen, G. J. Gäde, *J. Nat. Prod.* **1990**, *53*, 771-792.
- [22] a) N. Cramer, M. Buchweitz, S. Laschat, W. Frey, A. Baro, D. Mathieu, C. Richter, H. Schwalbe, *Chem. Eur. J.* **2006**, *12*, 2488-2503; b) N. Cramer, S.

- Laschat, A. Baro, H. Schwalbe, C. Richter, *Angew. Chem.* **2005**, *117*, 831–833; c) N. Cramer, S. Laschat, A. Baro, H. Schwalbe, C. Richter, *Angew. Chem. Int. Ed.* **2005**, *44*, 820–822.
- [23] U. Schöllkopf, U. Groth, K.-O. Westphalen, C. Deng, *Synthesis* **1981**, *12*, 969–971.
- [24] S. D. Bull, S. G. Davies, R. M. Parkin, F. Sánchez-Sancho, *J. Chem. Soc., Perkin Trans. 1* **1998**, 2313–2320.
- [25] R. M. Williams, E. M. Stocking, J. F. Sanz-Cervera, *Top. Curr. Chem.* **2000**, *209*, 98–173.
- [26] B. J. Wilson, D. T. C. Yang, T. M. Harris, *Appl. Microbiol.* **1973**, 633–635.
- [27] J. E. Roberts, J. W. Strauss, *Lloydia* **1975**, *38*, 355–356.
- [28] A. J. Birch, J.J. Wright, *Tetrahedron* **1970**, *26*, 2329–2344.
- [29] M. Yamazaki, S. Suzuki, K. Miyaki, *Chem. Pharm. Bull.* **1971**, *19*, 1739–1740.
- [30] J. B. Day, P. G. Mantle, *Appl. Environ. Microbiol.* **1982**, *43*, 514–516.
- [31] (a) C. Cui, H. Kakeya, H. Osada, *J. Antibiot.* **1996**, *49*, 527–533; (b) C. Cui, H. Kakeya, H. Osada, *Tetrahedron* **1996**, *52*, 12651–12666.
- [32] (a) C. Cui, H. Kakeya, H. Osada, *Tetrahedron* **1997**, *53*, 59–72; (b) a) M. Kondoh, T. Usui, T. Mayumi, H. Osada, *J. Antibiot.* **1998**, *51*, 801–804.
- [33] H. Osada, *J. Antibiot.* **1998**, *51*, 973–982.
- [34] S. Zhao, K. S. Smith, A. M. Deveau, C. M. Dieckhaus, M. A. Johnson, T. L. MacDonald, J. M. Cook, *J. Med. Chem.* **2002**, *45*, 1559–1562.
- [35] R. M. Williams, E. M. Stocking, J. F. Sanz-Cervera, *Top. Curr. Chem.* **2000**, *209*, 98–173.
- [36] J. D. Scott, R. M. Williams, *Chem. Rev.* **2002**, *102*, 1669–1730.
- [37] S. Zhao, K. S. Smith, A. M. Deveau, C. M. Dieckhaus, M. A. Johnson, T. L. MacDonald, J. M. Cook, *J. Med. Chem.* **2002**, *45*, 1559–1562.
- [38] (a) K. M. Depew, S. J. Danishefsky, N. Rosen, L. Sepp-Lorenzino, *J. Am. Chem. Soc.* **1996**, *118*, 12463–12464; (b) J. M., Schkeryantz, J. C. G. Woo, P. Siliphaivanh, K. M. Depew, S. J. Danishefsky, *J. Am. Chem. Soc.* **1999**, *121*, 11964–11975.
- [39] (a) T. Gan, J. M. Cook, *Tetrahedron Lett.* **1997**, *38*, 1301–1304; (b) T. Gan, R. Liu, P. Yu, S., Zhao, J. M. Cook, *J. Org. Chem.* **1997**, *62*, 9298–9304; c) S. Zhao, T. Gan, P. Yu, J. M. Cook, *Tetrahedron Lett.* **1998**, *39*, 7009–7012; d) C. Ma, X. Liu, X. Li, J. Flippen-Anderson, S., Yu, J. M., Cook, *J. Org. Chem.*

- 2001**, 66, 4525-4542.
- [40] G. A. Molander, C. R. Harris, *Encyclopedia of Reagents for Organic Synthesis*; Paquette, L. A., Ed.; John Wiley and Sons: New York, **1995**; Vol. 8, p. 5522-5523.
- [41] G. V. M. Sharma, A. Ilangovan, A. K. Mahalingam, *J. Org. Chem.* **1998**, 63, 9103-9104.
- [42] U. Schöllkopf, U. Groth, C. Deng, *Angew. Chem.* **1981**, 93, 793-795; *Angew. Chem., Int. Ed. Engl.* **1981**, 20, 798-799.
- [43] Reviews: a) C. J. Dinsmore, D. C. Beshore, *Tetrahedron* **2002**, 58, 3297-3312; b) R. M. Williams, *Synthesis of Optically Active α -Amino Acids*, Pergamon Press, Oxford, **1989**; c) U. Schöllkopf, *Pure Appl. Chem.* **1983**, 55, 1799-1806; d) U. Schöllkopf, *Top. Curr. Chem.* **1983**, 109, 65-84.
- [44] Recent examples: a) S. D. Bull, S. G. Davies, W. O. Moss, *Tetrahedron: Asymmetry* **1998**, 9, 321-327; b) V. Ojea, C. Fernández, M. Ruiz, J. M. Quintela, *Tetrahedron Lett.* **1996**, 37, 5801-5804; c) A. J. Pearson, H. Shin, *J. Org. Chem.* **1994**, 59, 2314-2323; d) R. Mueller, L. Revesz, *Tetrahedron Lett.* **1994**, 35, 4091; e) M. Ohba, T. Mukaihira, T. Fujii, *Chem. Pharm. Bull.* **1994**, 42, 1784; f) J. Paladino, C. Guyard, C. Thurieau, J. Fanchere, *Helv. Chim. Acta* **1993**, 76, 2465-2472; g) J. E. Baldwin, R. M. Adlington, M. B. Mitchell, *J. Chem. Soc., Chem. Commun.* **1993**, 1332-1335.
- [45] a) I. M. Dawson, J. A. Gregory, R. B. Herbert, P. G. Sammes, *J. Chem. Soc., Perkin Trans. 1* **1988**, 2585-2593; b) I. M. Dawson, J. A. Gregory, R. B. Herbert, P. G. Sammes, *J. Chem. Soc., Chem. Commun.* **1986**, 620-621.
- [46] a) P. Di Felice, G. Porzi, S. Sandri, *Tetrahedron: Asymmetry* **1999**, 10, 2191-2201; b) G. Porzi, S. Sandri, P. Verrocchio, *Tetrahedron: Asymmetry* **1998**, 9, 119-132; c) V. Favero, G. Porzi, S. Sandri, *Tetrahedron: Asymmetry* **1997**, 8, 599-612; d) R. Galeazzi, M. Garavelli, A. Grandi, M. Monari, G. Porzi, S. Sandri, *Tetrahedron: Asymmetry* **2003**, 14, 2639-2649.
- [47] T. Fukuyama, R. K. Frank, A. A. Laird, *Tetrahedron Lett.* **1985**, 26, 2955-2958.
- [48] A. Hätzelt, S. Laschat, P. G. Jones, J. Grunenberg, *Eur. J. Org. Chem.* **2002**, 3936-3943.
- [49] a) F. von Nußbaum, *Angew. Chem.* **2003**, 115, 3176-3179; *Angew. Chem., Int. Ed.* **2003**, 42, 3068-3071; b) S. Jin, P. Wessig, J. Liebscher, *J. Org. Chem.* **2001**, 66, 3984-3997; c) E. M. Stocking, J. F. Sanz-Cervera, R. M. Williams, *J.*

- Am. Chem. Soc.* **2000**, *122*, 1675-1683; d) R. M. Williams, J. F. Sanz-Cervera, F. Sancenón, J. A. Marco, K. Halligan, *J. Am. Chem. Soc.* **1998**, *120*, 1090-1091; e) T. Kametani, N. Kanaya, M. Ihara, *J. Chem. Soc., Perkin Trans. 1* **1981**, 959; f) 5-Acyloxy-2(1*H*)-pyrazinones, structurally related to **109** (Schema 29), were used as key intermediates for brevianamide A: S. Jin, P. Wessig, J. Liebscher, *J. Org. Chem.* **2001**, *66*, 3984-3997.
- [50] E. Caballero, C. Avendano, J. C. Menéndez, *J. Org. Chem.* **2003**, *68*, 6944-6951.
- [51] a) T. Onishi, P. R. Sebahar, R. M. Williams, *Org. Lett.* **2003**, *5*, 3135-3137; b) P. R. Sebahar, H. Osada, T. Usui, R. M. Williams, *Tetrahedron* **2002**, *58*, 6311-6322; c) T. D. Bagul, G. Lakshmaiah, T. Kawabata, K. Fuji, *Org. Lett.* **2002**, *4*, 249-251; d) L. E. Overman, M. D. Rosen, *Angew. Chem.* **2000**, *112*, 4768-4771; *Angew. Chem., Int. Ed.* **2000**, *39*, 4596-4599.
- [52] L. Alberch, P. D. Bailey, P. D. Clingan, T. J. Mills, R. A. Price, R. G. Pritchard, *Eur. J. Org. Chem.* **2004**, 1887-1890.
- [53] M. Ginz, K. H. Engelhardt, *Eur. Food Res. Technol.* **2001**, *213*, 8-11.
- [54] For other synthetic studies dealing with proline-derived diketopiperazines see: A. Bartels, P. G. Jones, J. Liebscher, *Synthesis* **2003**, 67-72.
- [55] a) K. G. Poullennec, D. Romo, *J. Am. Chem. Soc.* **2003**, *125*, 6344-6345; b) A. Zawadzka, A. Leniewski, J. K. Maurin, K. Wojtasiewicz, A. Siwicka, D. Blachut, Z. Czarnocki, *Eur. J. Org. Chem.* **2003**, 2443-2453; c) F. Hernández, C. Avendano, M. Söllhuber, *Tetrahedron Lett.* **2003**, *44*, 3367-3369; d) P. S. Baran, C. A. Guerrero, E. J. Corey, *J. Am. Chem. Soc.* **2003**, *125*, 5628-6529.
- [56] B. R. de Costa, X. He, J. T. M. Linders, C. Dominguez, Z. Q. Gu, W. Williams, W. D. Bowen, *J. Med. Chem.* **1993**, *36*, 2311-2320.
- [57] D. Hendea, S. Laschat, A. Baro, W. Frey, *Helv. Chim. Acta* **2006**, *89*, 1894-1909.
- [58] G. B. Borowitz, I. J. Borowitz, Y. Wang, D. Yang, R. Toupençe, N. A. Persaud *J. Inclusion Phenom. Macrocyclic Chem.* **2000**, *38*, 207-219.
- [59] A. Lewis, M. D. Ryan, D. Gani, *J. Chem. Soc., Perkin Trans. 1* **1998**, 3767-3775.
- [60] K. M. Thomas, D. Naduthambi, N. J. Zondlo, *J. Am. Chem. Soc.*, **2006** *128*, 2216-2217.

- [61] F. Hernández, V. Morales, F. L. Buenadicha, M. Söllhuber, C. Avendaño, *Tetrahedron: Asymmetry* **2004**, *15*, 3045-3058.
- [62] C. Nájera, T. Abellán, J. M. Sansano, *Eur. J. Org. Chem.* **2000**, 2809-2820.
- [63] S. J. Danishefsky, P. J. Harrison, R. R. Webb II, B. T. O'Neill, *J. Am. Chem. Soc.* **1985**, *107*, 1421-1423.
- [64] T. Fukuyama, J. J. Nunes, *J. Am. Chem. Soc.* **1988**, *110*, 5196-5198.
- [65] P. Garner, K. Sunitha, W. B. Ho, W. J. Young, V. O. Kennedy, A. Djebli, *J. Org. Chem.* **1989**, *54*, 2041-2042.
- [66] P. Garner, W. B. Ho, H. Shin, *J. Am. Chem. Soc.* **1992**, *114*, 2767-2768.
- [67] P. Garner, W. B. Ho, H. Shin, *J. Am. Chem. Soc.* **1993**, *115*, 10742-10753.
- [68] M. E. Flanagan, R. M. Williams, *J. Org. Chem.* **1995**, *60*, 6791-6797.
- [69] S. Kwon, A. G. Myers, *J. Am. Chem. Soc.* **2005**, *127*, 16796-16797.
- [70] A. Monsees, S. Laschat, S. Kotila, T. Fox, E.-U. Würthwein, *Liebigs Ann./Recueil* **1997**, 533-540.
- [71] a) M. C. Mc Mills, D. L. Wright, J. D. Zubkowsky, E. J. Valente, *Tetrahedron Lett.* **1996**, *37*, 7205-7208; b) S. E. Gibson, N. Guillo, B. S. Kalindjian, J. M. Tozer, *Bioorg. Med. Chem. Lett.* **1997**, *7*, 1289-1292; c) J. R. Harrison, P. O'Brien, D. W. Porter, N. M. Smith, *J. Chem. Soc., Perkin Trans. 1* **1999**, 3623-3631.
- [72] C. Nativi, M. Taddei, *Tetrahedron* **1989**, *45*, 1131-1144.
- [73] H. Mastalerz, *J. Org. Chem.* **1984**, *49*, 4092-4094.
- [74] B. Lesur, J.-B. Ducep, C. Danzin, *Bioorg. Med. Chem. Lett.* **1997**, *7*, 355-360.
- [75] S. Zhao, X. Liao, T. Wang, J. Flippen-Anderson, J. M. Cook, *J. Org. Chem.*, **2003**, *68*, 6279-6295.
- [76] A. K. Beck, S. Blank, K. Job, D. Seebach, T. Sommerfeld *Org. Synth., Coll. Vol. IX*, **1998**, 626.
- [77] M. W. Rathke, *Org. Synth., Coll. Vol. VI*, **1988**, 598.
- [78] D. J. Mathre, T. K. Jones, L. C. Xavier, T. J. Blacklock, R. A. Reamer, J. J. Mohan, E. T. Turner Jones, K. Hoogsteen, M. W. Baum, E. J. J. Grabowski, *J. Org. Chem.* **1991**, *56*, 751-762.
- [79] T. Shioiri, Y. Yokoyama, Y. Kasai, S. Yamada, *Tetrahedron*, **1976**, *32*, 2211-2217.
- [80] M. M. Lenman, A. Lewis, D. Gani, *J. Chem. Soc., Perkin Trans. 1* **1997**, 2297-2311.

- [81] E. Giralt, R. Eritja, J. Josa, C. Kuklinski, E. Pedroso, *Synthesis* **1985**, 181-184.
- [82] D. K. Mohapatra, A. Datta, *J. Org. Chem.* **1999**, *64*, 6879-6880.